THE UNIVERSITY *of* EDINBURGH

Investigating the roles of Translation Elongation Factor 1B in mammalian cells

Yuan Cao

Thesis submitted for the degree of Doctor of Philosophy

The University of Edinburgh

2012

Declaration

I here declare that this thesis has been composed by me and that all the work presented within is my own, unless clearly indicated otherwise. This work has not been submitted for any other degree or professional qualification.

Yuan Cao

Acknowledgements

First of all I wish to express my deepest gratitude to my supervisor Professor Cathy Abbott who has been so patient and understanding in the last four years. I appreciate her scientific guidance throughout my research, her encouragement when I was being negative, as well as her support and help in both my work and life. I would also like to thank my second supervisor Rebecca Barnetson, and Ian Jackson and Elaine Nimmo of my thesis committee for their helpful advices for my project. I am also very grateful for the scholarship offered by the Chinese Scholarship Counsel and the College of Medicine and Veterinary Medicine and the opportunity to be a student of the University of Edinburgh.

Thanks to all those who have kindly offered technical support for my lab work. I thank Abby, Barbie for their help with microscope training, cell culture and lending me the humidity chamber for the PLA, Liang for his advice of the GelQuant software, and Shaun for the antibody. Thanks to Paul Perry in the MRC for his tutorial on the multi-purpose microscope and data analysis using the IPLab software. I also thank David and Chris at the BRF of the Western General Hospital for helping out with the mice.

A big thank you to all the past and present members of the Abbott group: to Helen for her guidance with lab techniques especially when I first started my PhD, to Jennifer for her help especially with the transgenic mice, and to Miriam from whom I took over this project. Thanks also to Justyna, Lowri and Mariam for all the experimental tips and the time we spent together in the lab as well as in the cinema and restaurants. I wish Yan and Faith, the current PhD students in the Abbott group, further success with their PhDs. I would also like to thank all other fellow PhD students in the MMC for organizing activities and wish them a bright future ahead.

I could not forget to thank my friends outside the lab, particularly Ling for her love and kindness, Lucy for being an inspiring, positive and trustworthy friend, and Yewen for all the fun (and silly) times as well as her encouragement and comfort in sad times. I also wish to thank Dr Linda Watson and David Purves for their patient

proofreading of the manuscript of this thesis, and Nelly for her help with the diagram drawing in this thesis and my other reports.

Last but by no means least, I would like to thank the brothers and sisters in the Bristo Baptist Church, in the Mandarin Fellowship of the Chinese Evangelical Church in Edinburgh, as well as those who are from other churches: Eleanor, Lindsey, Paul and Pete. They have been a great blessing and, in many ways, my family in Edinburgh. I appreciate so much their prayers, love, friendship and encouragement that supported me through difficult times.

Table of contents

List of figures

List of tables

Abbreviations and symbols

aa-tRNA	aminoacyl-tRNA
AD	Alzheimer's disease
ALDH1L1	aldehyde dehydrogenase 1 family, member L1
ALS	amyotrophic lateral sclerosis
ATP	adenosine triphosphate
BDNF	brain-derived neurotrophic factor
BRF	biomedical research facility
CACH	childhood ataxia with central nervous system hypomyelination
CDK	cyclin-dependent kinase
cDNA	complementary DNA
CF	cleavage furrow
CKII	casein kinase
CNS	central nerve system
CNV	copy number variation
co-IP	co-immunoprecipitation
DMEM	Dulbecco’s Modified Eagle Medium
DMSO	dimethyl sulphoxide
DNA	deoxyribonucleic acid
dNTPs	deoxynucleotides
DOA	Darkener of apricot
DPBS	Dulbecco's phosphate buffered saline
DTT	dithiothreitol
EBV	Epstein-Barr virus
EDTA	ethylenediaminetetraacetic acid
eEF1A	eukaryotic translation elongation factor 1A
eEF1A1	eukaryotic translation elongation factor 1A1
eEF1A2	eukaryotic translation elongation factor 1A2
eEF1B	eukaryotic translation elongation factor 1B
eEF1Bα	eukaryotic translation elongation factor 1B alpha
eEF1Bγ	eukaryotic translation elongation factor 1B gamma
eEF1Bδ	eukaryotic translation elongation factor 1B delta
eEF1H	‘heavy’ complex assembled by eEF1A and eEF1B
eEF2	eukaryotic translation elongation factor 2
EF-Ts	elongation factor thermo stable
EF-Tu	elongation factor thermo unstable
eIF1	eukaryotic translation initiation factor 1

eIF1A	eukaryotic translation initiation factor 1A
eIF2	eukaryotic translation initiation factor 2
eIF2α	eukaryotic translation initiation factor 2 alpha
eIF2B	eukaryotic translation initiation factor 2B
eIF3	eukaryotic translation initiation factor 3
eIF3a	eukaryotic translation initiation factor 3a
eIF3b	eukaryotic translation initiation factor 3b
eIF3c	eukaryotic translation initiation factor 3c
eIF3e	eukaryotic translation initiation factor 3e
eIF3f	eukaryotic translation initiation factor 3f
eIF3h	eukaryotic translation initiation factor 3h
eIF3i	eukaryotic translation initiation factor 3i
eIF4A	eukaryotic translation initiation factor 4A
eIF4B	eukaryotic translation initiation factor 4B
eIF4E	eukaryotic translation initiation factor 4E
eIF4F	eukaryotic translation initiation factor 4F
eIF4G	eukaryotic translation initiation factor 4G
eIF5	eukaryotic translation initiation factor 5
ER	endoplasmic reticulum
eRF1	eukaryotic release factor 1
eRF3	eukaryotic release factor 3
FACS	fluorescence-activated cell sorting
FBS	foetal bovine serum
FTLD	frontotemporal lobar degeneration
G418	geneticin
GAPDH	glyceraldehyde-3-phosphate dehydrogenase
GDP	guanosine diphosphate
GEF	guanine nucleotide exchange factor
GFAP	glial fibrillary acid protein
GST	glutathione S-transferase
GTP	guanosine triphosphate
H_2O_2	hydrogen peroxide
HChr21	human chromosome 21
HCl	hydrochloric acid
HAS	human specific actin
HSE	heat shock elements
HSF-1	heat shock transcription factor-1
HSP	heat shock protein
Hsp70	heat shock protein 70

HSR	heat shock RNA
HSV-1	herpes simplex virus 1
HPLC	high-performance liquid chromatography
Iba1	ionized calcium-binding adapter molecule 1
ICC	immunocytochemistry
IF	immunofluorecense
IHC	immunohistochemistry
IR	ionizing radiation
IRES	internal ribosome entry site
Kb	kilobase pairs
kD	kilodaltons
MAPK1	mitogen activated protein kinase 1
Met	methionine
Met-tRNAi	initiating methionine-tRNA
microRNA	micro ribonucleic acid
MN	motor neuron
MND	motor neuron disease
mRNA	messenger ribonucleic acid
msrA	methionine sulfoxide reductase A
NBCS	newborn calf serum
Nt	nucleotide
NE	nuclear envelope
NP-40	nonyl phenoxylpolyethoxylethanol
ORF	open reading frame
OTA	ochratoxin A
PABP	poly (A) binding protein
PBS	phosphate buffered saline
PCR	polymerase chain reaction
Pi	phosphate
PKC	protein kinase C
PLA	proximity ligation assay
PMA	4P-phorbol 12-myristate 13-acetate
qPCR	Real-Time quantitative PCR
RCA	rolling-circle amplification
RF	release factor
RIPA	radioimmuno-precipitation assay
RNA	ribonucleic acid
RNAi	ribonucleic acid interference
ROS	reactive oxygen species

RT	reverse transcriptase
SD	standard deviation
SDS	sodium dodecyl sulphate
SEM	standard error of the mean
siRNA	small interfering RNA
TDLU	terminal duct lobular unit
TEMED	tetramethylethylenediamine
Thr	threonine
TMA	tumour microarray
5'TOP	5'terminal oligopyrimidine tract
tRNA	transfer ribonucleic acid
uORF	upstream reading frame
UTR	untranslated region
UV	ultraviolet
UVC	ultraviolet c, short wave
VWM	vanishing white matter
wst	wasted
Y2H	yeast two-hybrid

Amino acids

A	alanine
C	cysteine
D	aspartic acid
E	glutamic acid
F	phenylalanine
G	glycine
H	histidine
I	isoleucine
K	lysine
L	leucine
M	methionine
N	asparagine
P	proline
Q	glutamine
R	arginine
S	serine
T	threonine
U	valine

W	tryptophan
Y	tyrosine

Nucleotides

A	adenine
C	cytosine
G	guanine
T	thymidine

Units

°C	degrees centrigrade
A	ampere
bp	nucleic acid base pair
g	gram
l	litre
M	molar
rpm	revolutions per minute
V	volt

Abstract

Eukaryotic protein translation elongation is tightly controlled by several regulation factors. Eukaryotic translation elongation factor 1B (eEF1B) is the GTP exchange factor for eukaryotic translation elongation factor 1A (eEF1A), which is a G-protein transporting aminoacyl-tRNA to the A site of the ribosome in a GTP dependent manner. The structure of the heavy complex composed of eEF1B and eEF1A (eEF1H) has been widely studied and several models have been proposed, but it is yet not clear how the subunits of the two proteins interact with each other. eEF1B is made up of three subunits, eEF1Bα, eEF1Bδ and eEF1Bγ, and each subunit has been found to be over expressed in different types of cancer. A copy number variant near the eEF1Bδ gene is associated with amyotrophic lateral sclerosis. The two isoforms of eEF1A, eEF1A1 and eEF1A2, are 92% identical, but only eEF1A1 was found to interact with eEF1B subunits in yeast two hybrid (Y2H) experiments. The aims of this PhD project are to investigate the potential involvement of eEF1B in disease, as well as the relationship between eEF1B and eEF1A2.

All three eEF1B subunits were present in almost all the cell types and mouse tissues tested. eEF1Bδ showed different variants, the heaviest of which is tissue specific and expressed only in brain and spinal cord. eEF1Bα and eEF1Bδ showed certain abnormalities in transformed cell lines, although in the breast cancer tissues tested no apparent change in eEF1B expression was found. Knockdown of eEF1B did not significantly affect NSC34 cell viability over short periods. In spinal cord sections from motor neurone disease (MND) patients, half of the cases showed a change of eEF1B protein expression compared to normal spinal cord, with either a higher level in glial cells, or a lower level in motor neurones.

eEF1B and eEF1A2 were found to be co-expressed in mouse motor neurones, and proximity ligation assay also detected physical interactions between both eEF1A isoforms and eEF1B subunits in mammalian cells, contrary to the previous Y2H study. Experiments in a mouse model with no eEF1A2 expression also support this finding. In heart and skeletal muscle from wasted mice where eEF1A is absent the expression of eEF1Bα and eEF1Bδ was down regulated at both protein and mRNA

level, suggesting that eEF1A2 and eEF1B not only physically interact, but also show an interdependence in expression.

Overall the results from cultured cells, mouse and human tissues in this study demonstrate the potential involvement of eEF1B in MND, and its interaction with eEF1A, which contributes to the understanding of the non-canonical functions of eEF1B and the structure of eEF1H.

Chapter 1 Introduction

1. 1 Protein translation

Protein translation is a stage in gene expression when messenger RNA (mRNA) is decoded on the ribosome into specific polypeptides. Protein translation contains three steps: initiation, elongation and termination, each of which is precisely regulated by a number of factors.

1.1.1 Initiation

Eukaryotic translation begins with recognition of the initiation site and formation of the 48S initiation complex, which is a stepwise process and regulated by many initiation factors (eIFs). The first step of initiation is the formation of the 43S preinitiation complex consisting of the small (40S) ribosomal subunit, initiator tRNA (Met-tRNA$_i^{Met}$), eIF2 and GTP. To make the 40S ribosomal subunit vacant, the ribosome must be dissociated, which is thought to be promoted by eIF3 and eIF1A. eIF2, with eIF2B as the guanine nucleotide exchange factor (GEF), binds Met-tRNA$_i^{Met}$ and GTP jointly to form a ternary complex, which then binds the 40S subunit aided by eIF1, eIF1A and eIF3, thus the 43S preinitiation complex is formed.

The next step is the preinitiation complex binding to the 5' cap of the mRNA, which is mediated by eIF4F, eIF4B, eIF3. eIF4F is a heterotrimeric complex comprising three subunits: eIF4E, which is a cap binding protein; eIF4G, which serves as a scaffold for other components and contains binding sites for eIF4E, PABP, and, at least in mammalian cells, for eIF4A, RNA and eIF3; and eIF4A, the ATP-dependent RNA helicase. The eIF4F/4A/4B complex cooperatively unwinds the cap-proximal region of mRNA, to allow the 43S complex to bind.

After binding to the 5' end of the mRNA, the 43S preinitiation complex starts to scan downstream along the mRNA to identify the initiation codon in the presence

of eIF1. eIF1 also induces conformational change of the 43S complex, from 'closed' to 'open' state, as suggested by Pestova and Kolupaeva (Pestova and Kolupaeva 2002). Other factors including eIFA, eIF4A, eIF4B and eIF4F are also involved in the scanning, although they may have complementary roles. This "scanning mode" is the most common approach to recognise initiation sites in eukaryotic cells.

In rare cases, a 5' cap-independent mechanism is used whereby the 40S ribosomal subunit binds to an internal ribosome entry site (IRES) on the mRNA at or just upstream of the initiation codon directly without scanning from the 5' end cap, independent of eIF4E.

Once the initiation codon on the mRNA is recognised and its codon/anticodon interaction with the Met-$tRNA_i^{Met}$ is established, another initiation factor, eIF5, activates the GTPase centre in eIF2. The GTP hydrolysis on eIF2 induces the release of eIF2 and possibly other initiation factors off the ribosomal complex, so that the large (60S) ribosomal subunit can bind the 40S to assemble a complete (80S) ribosome. A different GTPase initiation factor, eIF5B, is required for this last step in initiation, but the GTP hydrolysis occurs after the formation of the 80S ribosome, indicating that it serves as a final checkpoint for correct 80S ribosome assembly rather than having a mechanical role.

1.1.2 Elongation

During translation elongation, the aminoacyl-tRNA (aa-tRNA) is delivered to the A-site of the ribosome to join the peptide under formation. In eukaryotic cells, protein translation elongation is mediated by elongation factors (EFs), eEF1 and eEF2. eEF1 includes eEF1A, the GTP-binding protein, and eEF1B, the GEF for eEF1A, which will be discussed in detail in the following sections. eEF1 transports aa-tRNA and eEF2 promotes the GTP-dependent translocation of the peptide chain synthesized from the A-site to the P-site of the ribosome.

eEF1A, together with GTP as a complex, carries an aa-tRNA to the A-site of the ribosome. After decoding between the mRNA and the tRNA and conformational change in the decoding centre of the ribosome, only the cognate tRNA is permitted to enter the following steps and the GTP hydrolysis is activated. eEF1A•GDP is released and recycled to the GTP-binding form, and the cognate aa-tRNA is located in the A-site of the ribosome. The next step is to form a peptide bond between the amino acid and the peptidyl-tRNA, catalyzed by the peptidyl transferase center in the ribosome. The previous peptidyl-tRNA is deacylated and the previous aa-tRNA is bound to the nascent peptide chain, then both the deacylated tRNA and the peptidyl-tRNA are translocated by eEF2 to the E-site and the P-site of the ribosome respectively, and the mRNA is also moved by three amino acid so that the next codon is presented near the A-site of the ribosome for the next cycle of the above process (Figure 1.1).

Elongation factors are highly conserved among different species and may be involved in other cellular activities apart from protein synthesis, such as the cell cycle control, signal transduction, cytoskeleton regulation and stress response.

1.1.3 Termination

When the ribosome reaches a stop codon, translation termination is triggered. The completion of termination requires release factors (RFs). There exist two classes of RFs in both prokaryotes and eukaryotes. Class I are codon specific RFs which recognize a stop codon and promote peptide chain release; class II are non-specific RFs which stimulate the activity of class I RFs. In eukaryotic cells, each class of RFs contains only one eukaryotic RF (eRF): eRF1 belongs to class I, and eRF3, class II. eRF1 has an omnipotent decoding capacity of all three termination codons, UAA, UAG and UGA.

Once a stop codon presented in the A site of the ribosome is decoded by eRF1, in response, the hydrolysis of the peptidyl-tRNA is catalyzed by eRF1 and the

peptidyl transferase center of the ribosome, and the consequent release of the nascent peptide chain is triggered. eRF1 and eRF3 function as a complex, with eRF1 as a GTP-dissociation inhibitor, which promotes the GTP-binding to eRF3, and eRF3 stimulates the activity of eRF1 and enhances the peptide release by eRF1 in the presence of GTP.

Ultimately the completed polypeptide is released from the tRNA and the tRNA is released from the ribosome.

1.1.4 Regulation of protein translation

In eukaryotic cells, gene expression is strictly regulated at several different levels, such as modification of DNA, transcriptional regulation controlling the transcription of DNA to RNA, posttranscriptional regulation modulating the modification of the mRNA, and translational regulation monitoring the translation process of mRNA to protein.

The regulation of protein translation steps is usually mediated by modifying translation factors. For example, eIF4E can be bound by inhibitory proteins and therefore hinders the binding of mRNA. Phosphorylation of eEF1 (discussed in detail in section 1.3.5) or eEF2 (Sivan, Kedersha et al. 2007) by certain kinases could upregulate or downregulate protein translation. Protein translation could also be regulated through modifications, including phosphorylation, ubiquitination and methylation, of certain protein components of the ribosome.

The structure of the mRNA could affect translation efficiency as well. For example, mRNA with high secondary structures and thermal stability at the 5' untranslated region (UTR) showed more dependence on initiation factors, therefore affected the ribosome recruitment as well as the scanning (De Benedetti and Graff, 2004). The initiation factor dependence of the mRNA could also be affected by the 3' UTR.

Micro RNAs (miRNAs) are a group of shortRNA molecules found in eukaryotic cells. miRNAs have been identified to act as regulators of mRNA stability and translation, by repressing translation at the initiation or postinitiation step, or triggering the deadenylation and subsequent degradation of the mRNA (reviewed in Fabian, Sonenberg, et al. 2010).

After translation, the nascent polypeptide is under posttranslational regulation. Proteins need to undergo certain modifications to be functionally activated, including addition of other proteins, methylation, glycosylation, removal of certain amino acids, or conformational change. Lipidation is crucial for locating the membrane proteins. Phosphorylation is a common mechanism to active or inactive a protein instantly, while ubiquitination is a major way of protein degradation.

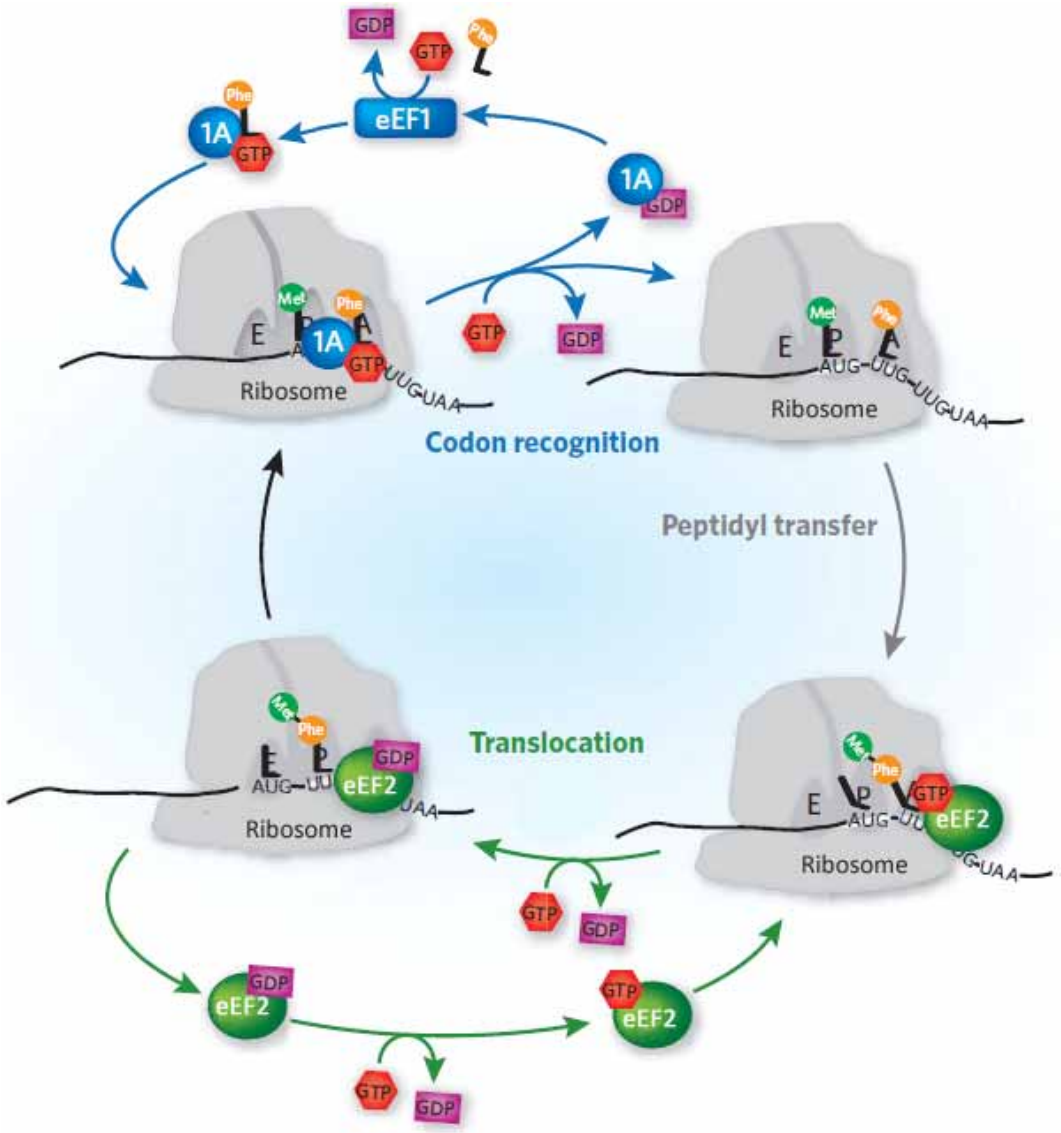

Figure 1.1 A schematic diagram of protein translation elongation in eukaryotic cells (adapted from Schneider-Poetsch, Usui et al. 2010). E, P and A. The E-, P- and A-site on the ribosome. Phe- and Met-. Two examples of aminoacyl-tRNA. eEF1A (1A) delivers aminoacyl-tRNA to the A-site of the ribosome based on the interaction between the mRNA codon exposed on the A-site and the anticodon on the tRNA, and is then released from the ribosome. eEF2 translocates the peptidyl-tRNA to the P-site and the deacylated tRNA to the E-site, so that the A-site of the ribosome is vacated for another round of elongation.

1. 2 Eukaryotic translation elongation factor 1A

eEF1A is equivalent to the bacterial elongation factor thermo unstable (EF-Tu) (Amons, Pluijms et al. 1983). eEF1A is a GTP binding protein, which transports aminoacyl-tRNA to the A site of ribosome in a GTP-dependent manner, catalysed by its GEF, eEF1B.

eEF1A is encoded by various genes in different species. Lower eukaryotes such as S. *cerevisiae* contain at least two genes encoding for the same eEF1A protein, while mammals have two isoforms for eEF1A encoded by separate genes, eEF1A1 and eEF1A2. The two eEF1A isoforms are 92% identical and share the same function in translation elongation (Ann, Moutsatsos et al. 1991), but they have very different expression patterns. It has been observed in mice that during early development eEF1A1 is expressed ubiquitously but starts to decrease in skeletal muscle, heart and neurons postnatally until eEF1A2 takes its place in these tissues and cells. As a result, in adult tissues eEF1A1 and eEF1A2 are exclusively expressed, and the tissues where eEF1A2 is expressed contains mostly cells fully differentiated and characterised by very little or no cell division (Lee, Francoeur et al. 1992; Khalyfa, Bourbeau et al. 2001; Newbery, Loh et al. 2007).

eEF1A1 and eEF1A2 showed equal activities and GTP hydrolysis rates in translation assays *in vivo* and *in vitro*. Interestingly, when their affinities to GDP and GTP were examined, eEF1A1 bound GDP and GTP with about equal affinity, while eEF1A2 showed stronger affinity for GDP than to GTP (Kahns, Lund et al. 1998), hence eEF1A2 was thought to be more dependent on a GEF than eEF1A1 was. However a Y2H study found no interaction between eEF1A2 and any of the eEF1B subunit (Mansilla, Friis et al. 2002).

eEF1A has non-canonical functions other than its roles in translation, including roles in cytoskeleton regulation, apoptosis, stress response and protein degradation (reviewed in Mateyak and Kinzy 2010). Moreover, eEF1A2 has been found to be an

oncogene as it is overexpressed inappropriately in a number of cancers (reviewed in Lee and Surh 2009). On the other hand, loss of eEF1A2 expression in the motor neuron leads to a dramatic neuronal defect in mice (Abbott, Newbery et al. 2009).

1.3 Eukaryotic Translation elongation factor 1B

eEF1B is a macromolecular complex stimulating the GDP-GTP exchange on eEF1A. In lower eukaryotes eEF1B contains a guanine nucleotide exchange subunit eEF1Bα and a structural subunit eEF1Bγ, while higher eukaryotic cells have another guanine nucleotide exchange subunit eEF1Bδ. Other nomenclatures have been used for eEF1B components during a long period of research, and the nomenclature used in this thesis is the one proposed by Le Sourd et al in 2006 (Le Sourd, Boulben et al. 2006), as listed in Table 1.1.

Table 1.1 Nomenclature of eEF1B subunits in human.

Gene symbol	Current protein nomenclature	Former protein nomenclature	Molecular weight (MW)
EEF1B2	eEF1Bα	eEF1β	24-28kD
EEF1D	eEF1Bδ	eEF1Bβ, eEF1δ	32-36kD
EEF1G	eEF1Bγ	eEF1γ	47-52kD

1.3.1 eEF1Bα

eEF1Bα is the lightest subunit of eEF1B complex, which is equivalent of bacterial elongation factor thermo stable (EF-Ts), and has guanine nucleotide exchange activity. The gene encoding eEF1Bα was mapped to human chromosome 2 (EEF1B2). Other loci for eEF1Bα mapped to human chromosome 15 (EEF1B1), 5 (EEF1B3) and X (EEF1B4) are most probably correspond to tissue specific intronless paralogues or pseudogenes (Chambers, Rouleau et al. 2001).

eEF1Bα is conserved among eukaryotic species. The C-terminal domain of eEF1Bα is considered to be necessary and sufficient for its GEF activity (Perez, Kriek et al. 1998), and responsible for the interaction between eEF1Bα and eEF1A, while the N-terminal domain is involved in its binding to the N-terminal domain of eEF1Bγ (van Damme, Amons et al. 1991).

The main function of eEF1Bα is to mediate the nucleotide exchange for eEF1A. It has been found essential for cell growth in yeast (Hiraga, Suzuki et al. 1993), and mutation of yeast eEF1Bα enhances translation fidelity with a lower translational efficiency (Carr-Schmid, Valente et al. 1999). It is assumed that eEF1Bα helps nucleotide exchange in eEF1A by disrupting interactions between GDP with the P-loop and switch regions of eEF1A (Pittman, Valente et al. 2006).

1.3.2 eEF1Bδ

eEF1Bδ is the metazoan-specific subunit of eEF1B. The human eEF1Bδ gene is mapped to chromosome 8 which is transcribed to into two mRNAs by alternative splicing.

The C-terminus of eEF1Bδ is homologous with eEF1Bα (Guerrucci, Monnier et al. 1999) and contains the nucleotide exchange activity. However, a study found that eEF1Bδ dissociated GDP from eEF1A•[^{3}H]GDP *in vitro* at the same rate as eEF1Bα did only in the first minute of the reaction, then the nucleotide exchange rate in the system with eEF1Bδ became the same as the one without any GEF. In addition, while the presence of eEF1Bγ stimulated the nucleotide exchange activity of eEF1Bα, it did not affect the GDP dissociation catalyzed by eEF1Bδ (Bec, Kerjan et al. 1994).

The N-terminal domain of eEF1Bδ has a leucine zipper motif (Morales, Cormier et al. 1992), indicating possible binding of other proteins, but this motif is not involved in the polymerization of eEF1Bδ monomers (Sheu and Traugh 1997), and the N-terminal domain is not sufficient for the dimerization of eEF1Bδ (Mansilla, Friis et al. 2002).

eEF1Bδ has been found to exist as different isoforms resulting from alternative splicing. Two isoforms with close MW have been discovered in *Xenopus laevis* oocytes (Mulner-Lorillon, Minella et al. 1994; Minella, Mulner-Lorillon et al. 1996), sea urchin embryo (Boulben, Monnier et al. 2003), which are encoded by two

mRNAs, differing by the existence of a 78-base stretch inserted in the open reading frame (ORF), in front of the leucine zipper-encoding sequence. As a result, the two isoforms of eEF1Bδ protein have similar MWs and migration patterns on SDS-PAGE, showing two bands on Western blots that are close to each other.

Recent studies have identified another isoform for eEF1Bδ protein, which is around 70-80kD, namely eEF1BδL. The mRNA encoding eEF1BδL contains an extra exon, exon 3, which is skipped in the mRNA transcripts of other isoforms. Up to now little is known about the significance of eEF1BδL, except that it is tissue specific, expressed only in brain, spinal cord and testis (Kaitsuka, Tomizawa et al. 2011), which is in line with the results obtained by our lab (Miriam Portela, PhD thesis, 2008). It was also demonstrated that the expression of eEF1BδL in brain started from embryonic day 15 (Kaitsuka, Tomizawa et al. 2011). However, when the expression pattern of eEF1Bδ protein was examined in different cell lines, Kaitsuka and colleagues reported the expression of eEF1BδL in HeLa and Hek293 cell lines, while in our lab the same antibody detected eEF1BδL expression only in neuronal cell lines such as NSC34, SHSy5Y and Lan5, but not HeLa or Hek293 (Miriam Portela, PhD thesis, 2008).

1.3.3 eEF1Bγ

eEF1Bγ is the eukaryotic specific subunit of eEF1B, the gene of which has been mapped to human chromosome 11. The N-terminal domain of eEF1Bγ contains a homologue to the theta class of glutathione S-transferases (GSTs) (Jeppesen, Ortiz et al. 2003), which will be discussed later.

The role of eEF1Bγ in translation elongation is not well understood yet. eEF1Bγ is usually found tightly associated with eEF1Bα and it can be isolated from eEF1Bα only under strong denaturing conditions. Research on *Artemia* showed that the nucleotide exchange rate of eEF1Bα is higher in the presence of eEF1Bγ than

eEF1Bα alone, indicating that eEF1Bγ is possibly a catalyst for eEF1Bα. eEF1Bγ is also likely to be involved in directing other subunits in the eEF1B complex (Janssen and Moller 1988) and to play a role in scaffolding for the eEF1B complex (Le Sourd, Boulben et al. 2006) as it is highly associated with membrane and cytoskeleton structures which is further discussed in section 1.4.2 of this thesis.

1.3.4 The eEF1B Complex

Although the components of eEF1B are now clear, and eEF1B is considered to form a reversible macro complex with eEF1A (eEF1H) to mediate the guanine nucleotide exchange on eEF1A, yet how the three subunits of eEF1B combine together and how they interact with eEF1A remain unknown. The components of eEF1H have been studied in various species by different groups and several structural models have been proposed, as shown in Figure 1.2. However, there is much inconsistency among these models.

The first structure model proposed was by G Bec and colleagues, based on *in vitro* reconstitution experiments using different combinations of the subunits purified from rabbit liver, as well as published information about eEF1H subunits from *Artemia* by other groups (Bec, Kerjan et al. 1994). They suggested a protomer composed of valyl-tRNA and eEF1H, which were associated through eEF1Bδ. Two such protomers could bind to each other via the leucine zipper motif on the N-terminus of two eEF1Bδ subunits (Figure 1.2 A).

Later in the same year a paper studying *Artemia* had different findings (Janssen, van Damme et al. 1994), and suggested a structure model wherein eEF1Bγ binds to both eEF1Bα and eEF1Bδ, each of which binds to a eEF1A subunit (Figure 1.2 B).

O Minella et al. proposed a model (Figure 1.2 C) for *Xenopus* eEF1H based on results from the analysis of native complexes instead of reconstitution experiments (Minella, Mulner-Lorillon et al. 1998).

The model proposed by GT Sheu and colleagues suggests the existence of eEF1Bγ dimers (Sheu and Traugh 1999). The major difference between this model and others is that each eEF1Bγ subunit binds to one eEF1Bα or eEF1Bδ subunit, not both (Figure 1.2 D).

Another model (Figure 1.2 F) was proposed by Jiang et al (Jiang, Wolfe et al. 2005) according to three-dimensional research. This model, without information of the binding regions on each subunit, is in line with the one proposed by Bec et al in 1994, supporting the hypothesis of eEF1Bδ dimer being a core in the complex.

While eEF1A has two isoforms, none of the models above has taken the two isoforms of eEF1A into account. Mansilla and colleagues identified an interaction between eEF1B and eEF1A1 but not eEF1A2 based on a series of Y2H experiments, and therefore suggested a model of eEF1H containing eEF1A1 but not eEF1A2 (Mansilla, Friis et al. 2002). The model (Figure 1.2 E) is similar to the one proposed by Janssen et al, except that it suggests the potential of dimerizing of eEF1B via the eFE1Bδ subunit.

Although the above models are different from each other, which is very likely to be caused by the different techniques used in different groups, there are some points that seem to be less controversial among all the models. Firstly, it is believed that eEF1Bα and eEF1Bγ are tightly associated and can only be separated under denaturing conditions (Bec and Waller 1989). Secondly, eEF1Bα and eEF1Bδ showed no affinity for each other. Finally, the binding sites of eEF1Bα and eEF1Bδ to eEF1Bγ locate on the N-terminus of the three proteins, while the C-terminus of eEF1Bα and eEF1Bδ harbors the binding sites for eEF1A.

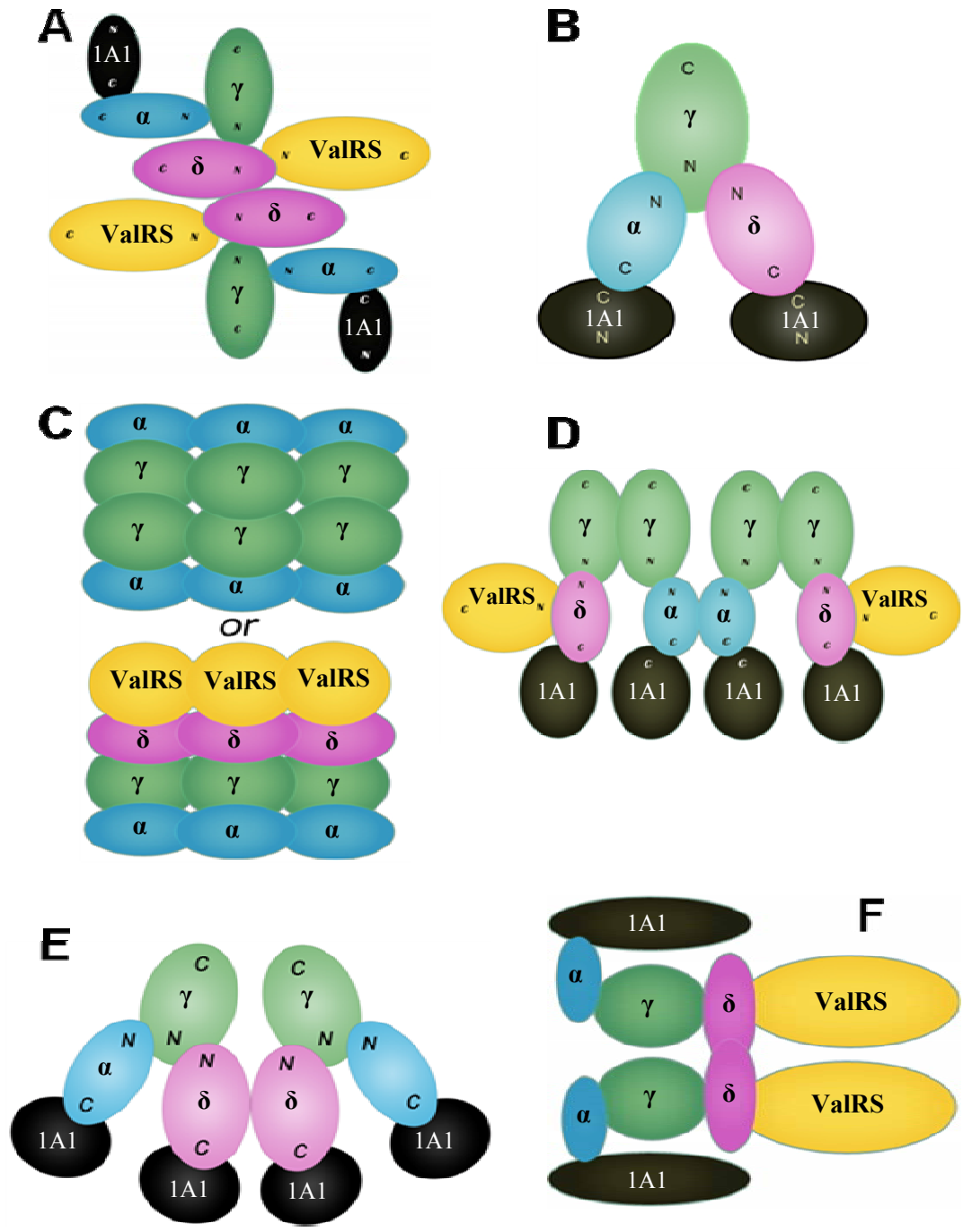

Figure 1.2 Schematic models of eEF1B interacting with eEF1A and/or ValRS proposed by Bec, Kerjan et al. 1994 (A), Janssen, van Damme et al. 1994 (B), Minella, Mulner-Lorillon et al. 1998 (C), Sheu and Traugh 1999 (D), Mansilla, Friis et al. 2002 (E) and Jiang, Wolfe et al. 2005 (F). α, δ, γ, 1A1 and ValRS represent eEF1Bα, eEF1Bδ, eEF1Bγ, eEF1A1 and ValRS respectively. N and C represent N-terminus and C-terminus of the subunit respectively.

1.3.5 Regulation of eEF1B by phosphorylation

Phosphorylation by protein kinases is a major way to modulate protein and cellular activities, and eEF1B subunits have been shown to be phosphorylated *in vivo* and *in vitro* by different protein kinases, mainly on the serine or threonine residues.

eEF1Bα and eEF1Bδ, together with ValRS and eEF1A, are phosphorylated by protein kinase C (PKC) in response to the stimulation of hormones such as 4P-phorbol 12-myristate 13-acetate (PMA) in rabbit reticulocytes; this stimulated elongation activity up to threefold both *in vitro* and *in vivo* (Venema, Peters et al. 1991). It is then found that this phosphorylation by PKC of eEF1Bα and eEF1Bδ increased the rate of nucleotide exchange and of Phe-tRNA binding to ribosomes, and thus stimulated elongation activity (Peters, Chang et al. 1995).

Insulin stimulation resulted in phosphorylation of eEF1A, eEF1Bα and eEF1Bδ, but not eEF1Bγ, by multipotential S6 kinase, leading to 2 to 2.5 fold stimulation of elongation activity in 3T3 cells (Chang and Traugh 1997; Chang and Traugh 1998). Furthermore, HeLa cells treated with paclitaxel showed an elevated phosphorylation on eEF1Bγ while the protein level was not affected (Prado, Casado et al. 2007).

eEF1Bγ can be phosphorylated *in vitro* by Darkener of apricot (DOA) kinase in Drosophila. DOA is a member of the LAMMER family, a protein kinase family in higher eukaryotes characterized by a EHLAMMERILG motif (Yun, Farkas et al. 1994), which is essential for their kinase activity (Savaldi-Goldstein, Sessa et al. 2000). The phosphorylation site for DOA is located on S294 in the C-terminus of eEF1Bγ, which is considered essential for its activity (Fan, Schlierf et al. 2010).

eEF1Bδ and eEF1Bγ have been found to be substrates for cyclin-dependent kinases (CDK) 1 during the maturation of *Xenopus* oocytes (Belle, Derancourt et al. 1989; Mulner-Lorillon, Poulhe et al. 1989; Janssen, Morales et al. 1991). *In vitro* studies revealed the CDK1 phosphorylation sites for eEF1Bδ and eEF1Bγ are S133

(Kawaguchi, Kato et al. 2003) and T230 (Mulner-Lorillon, Cormier et al. 1992) respectively. This phosphorylation does not affect the guanine nucleotide exchange rate for the complex, but decreases the elongation rate of valine while increasing the synthesis rate of serine and phenylalanine (Monnier, Belle et al. 2001). The phosophorylation of S133 of eEF1Bδ by CDK1 during mitosis in HeLa cells, however, results in induction of the affinity of eEF1Bδ to eEF1A, leading to a lower guanine nucleotide change activity and subsequently slower translation (Sivan, Aviner et al. 2011).

eEF1Bα from *Artemia* can be phosphorylated on S89 by a casein kinase (CKII) -like protein kinase, and the phosphorylation inhibits the guanine nucleotide exchange activity of eEF1Bα (Janssen, Maessen et al. 1988).

eEF1Bα from *Artemia*, wheat germ embryos and rabbit is phosphorylated by CKII (Palen, Huang et al. 1990; Palen, Venema et al. 1994; Chen and Traugh 1995). The sites for CKII phosphorylation of recombinant rabbit eEF1Bα expressed in *E. coli* have been identified as S106 and S112 (Chen and Traugh 1995). CKII also phosphorylates eEF1Bδ (Palen, Venema et al. 1994), on S162 of tagged eEF1Bδ in HeLa cells, and phosphorylation of endogenous eEF1Bδ was also detected by the phosphor-specific S162 antibody (Gyenis, Duncan et al. 2011). In the native eEF1H complex eEF1Bα and eEF1Bδ are phosphorylated by CKII only in the presence of GDP (Palen, Venema et al. 1994), suggesting that the phosphorylation of eEF1Bα and eEF1Bδ by CKII happens when eEF1A•GDP is associated with eEF1B complex.

In cells infected with viruses, eEF1Bδ can be phosphorylated by viral protein kinases, suggesting that the modification of eEF1Bδ by viral protein kinases may be a way for viruses to regulate their protein synthesis and replication. The viral proteins kinases leading to eEF1Bδ phosphorylation include U_L13 encoded by herpes simplex virus 1 (HSV-1) (Kawaguchi, Van Sant et al. 1998), U_L97 of human cytomegalovirus (Kawaguchi, Matsumura et al. 1999), and BGLF4 of Epstein-Barr virus (EBV) (Kato, Kawaguchi et al. 2001). *In vitro* experiments found that these

viral protein kinases share the same phosphorylation site with cellular kinase CDK1 (Kawaguchi and Kato 2003).

Table 1.2. Phosphorylation of eEF1B subunits by cellular protein kinases and their affects on protein translation.

Kinases	Effect on translation	Subunits phosphorylated (sites if known)
PKC	Upregulation	eEF1Bα eEF1Bδ
CDK1	Possible downregulation	eEF1Bδ (S133) eEF1Bγ (T230)
CKII	No effect	eEF1Bα (S106, S112) eEF1Bδ (S162)
CKII-like kinase	Downregulation	eEF1Bα (S89)
Multipotential S6 kinase	Upregulation	eEF1Bα eEF1Bδ
DOA kinase	Unknown	eEF1Bγ (S294)

1.4 The functions of eEF1B

1.4.1 eEF1B and the cell cycle control

The cell cycle is controlled mainly through CDKs (reviewed in Murray 2004), which are regulated by cyclical proteolysis of cyclins by phosphorylation cascades. As discussed in section 1.3.5 eEF1B subunits are regulated by kinases that are involved in the cell cycle, including CDK1 and PKC, and the phosphorylation of eEF1B subunits by some kinases coincide with the reduced protein synthesis activity during mitosis. In addition, other lines of evidences also suggest that eEF1B plays a role in cell cycle control.

The two proteins, CF51 and CF32, which were found to be enriched in the cleavage furrow (CF) isolated from dividing sea urchin eggs have been identified as eEF1A and eEF1Bα respectively, and eEF1Bα regulates the actin bundling activity of eEF1A, which is important to maintain the structure of the contractile ring during cytokinesis (Fujimoto and Mabuchi 2010).

During the first mitotic cell cycle in sea urchin embryos, the subcellular location of eEF1Bδ changes in a cell cycle specific manner although the total expression level does not change. At the time of nuclear envelope breakdown during mitosis, a fraction of eEF1Bδ concentrates around the nucleus and later forms two large spheres around the mitotic spindle poles, suggesting a link between eEF1Bδ and cell cycle regulation (Boulben, Monnier et al. 2003). In HeLa cells undergoing mitosis, the two shorter isoforms of endogenous eEF1Bδ protein change their intensities around the M-phase, with a shift of the lower to the upper band (Sivan, Aviner et al. 2011), indicating a cell cycle dependent alternative splicing of eEF1Bδ mRNA.

Human squamous carcinoma cells SCC-35 exposed to ionizing radiation express an elevated level of eEF1Bδ and are arrested at G2/M transition, indicating a

role of eEF1Bδ in cell cycle dependent response to DNA damage (Jung, Kondratyev et al. 1994).

1.4.2 eEF1B and the cytoskeleton

The cytoskeleton in eukaryotic cells includes actin filaments, microtubules and intermediate filaments, each of which has been found to be associated with different subunits of eEF1B, suggesting the roles of eEF1B and the regulation of cytoskeleton may be closely related.

A 17 kD fragment of *Dictyostelium discoideum* eEF1Bα was found to associate with actin *in vitro*, and recombinant *Dictyostelium discoideum* eEF1Bα expressed in *E. coli* stimulates the assembly of actin (Furukawa, Jinks et al. 2001), whereas eEF1Bα and actin extracted from sea urchin eggs show no affinity to each other (Fujimoto and Mabuchi 2010). One group suggested that eEF1Bα balances the roles of eEF1A between translation and actin organization by competing with actin for the binding site on eEF1A (Pittman, Kandl et al. 2009), while another group found that eEF1Bα disrupts the eEF1A-induced actin bundling by promoting guanine nucleotide change on eEF1A (Fujimoto and Mabuchi 2010). Nevertheless, the observation that eEF1Bα disrupts eFE1A-induced actin bundling may to some extent explain the observation that eEF1Bα stimulates the rate of actin assembly in a concentration dependent negative manner (Furukawa, Jinks et al. 2001). However, the same report found that unlike eEF1Bα alone, the intact eEF1Bα:eEF1Bγ complex stimulated actin assembly in a concentration dependent manner (Furukawa, Jinks et al. 2001), indicating eEF1Bγ is likely to play a role in actin assembly.

Microtubules are also found associated with eEF1B. eEF1Bα and eEF1Bγ are often associated with tubulin in *Artemia*, and under non-denaturing conditions eEF1Bγ coprecipitated with tubulin (Janssen and Moller 1988).

Kinectin is a microtubule-dependent membrane anchor, and eEF1Bδ has been found to interact with kinectin both *in vivo* and *in vitro*. Overexpression of kinectin fragments *in vivo* disrupts the subcellular localization of eEF1Bδ but not the ER network, indicating its potential role as the anchor for eEF1B complex to the ER

(Ong, Er et al. 2003). Interruption of kinectin binding to eEF1Bδ decreases the expression of membrane protein but enhances cytosolic protein expression, showing that the binding of eEF1B to certain cytoskeleton components regulates protein synthesis. The other two subunits of eEF1B have been found not to interact with kinectin in Y2H and coIP experiments (Ong, Lin et al. 2006).

During mitosis of fertilized sea urchin eggs, eEF1Bδ showed a localization change as described earlier in last section. It is found that eEF1Bδ is co-localized with the astral microtubules but not the spindle microtubules at metaphase, anaphase and telophase, and the distribution of eEF1Bδ during mitosis proved to be dependent on microtubules (Boulben, Monnier et al. 2003).

eEF1Bγ is usually considered as a scaffold subunit for the eEF1B complex, as it has no guanine nucleotide exchange activity, and the deletion of eEF1Bγ in S. *cerevisiae* does not affect protein synthesis or translation fidelity *in vivo* (Olarewaju, Ortiz et al. 2004). However, disruption of eEF1Bγ binding to keratin, which is an intermediate filament of the cytoskeleton, leads to decreased protein translation in human epithelial cells (Kim, Wong et al. 2006; Kim, Kellner et al. 2007).

1.4.3 eEF1B and the stress response

Stress conditions include radiation, temperature changes, exposure to drugs or toxins, oxidative stress, hypoxia and nutrient limitation. Cells exposed to stress conditions express stress response genes in order to adapt to the circumstances. Translation factors have been reported to be involved in response to different types of stress conditions, and the roles of initiation factors in stress response is reviewed in Holcik and Sonenberg, 2005.

Proteomic studies identified eEF1Bα and eEF1Bδ as potential candidates that respond to heat shock and may be involved in heat shock signalling pathways in RIF-1 cells whether they are thermotolerant or not (Kim, Song et al. 2002).

eEF1Bα is down regulated in MCF, HCT116 and H460 cell lines exposed to ionizing radiation (IR) (Byun, Han et al. 2009). The down regulation of eEF1Bα has been also observed at both mRNA and protein levels in rice after heat shock (Lin, Chang et al. 2005). The RNA-binding protein TIAR suppresses translation in RKO cells in response to low levels of short-wavelength UV (UVC), by binding to the 3' UTR of the mRNAs of eEF1Bα, as well as eIF4A, eIF4E, but not eEF1Bδ or eEF1Bγ (Mazan-Mamczarz, Lal et al. 2006).

In S. *cerevisiae* exposure to H_2O_2 also causes down regulation of eEF1Bα (Godon, Lagniel et al. 1998). Moreover, H_2O_2 in S. *cerevisiae* leads to protein S-thiolation of eEF1Bα in response to oxidative stress (Shenton and Grant 2003), and loss of eEF1Bα results in great resistance to $CdSO_4$ (Olarewaju, Ortiz et al. 2004).

Unlike eEF1Bα, which is down regulated in response to ionizing radiation, in SCC-35 cells exposed to the same radiation eEF1Bδ has been found upregulated (Jung, Kondratyev et al. 1994). eEF1Bδ is also upregulated in 3T3 cells transformed by cadmium (Joseph, Lei et al. 2002), and in mouse hippocampal HT22 cells treated with ochratoxin A (OTA) (Yoon, Cong et al. 2009). Furthermore, eEF1Bδ is over expressed in human melanoma cell line MeWo exhibiting chemoresistance towards antineoplastic drugs, such as vindesine, cisplatin, fotemstine and etoposide (Sinha, Kohl et al. 2000).

While the significance of a tissue specific isoform of eEF1Bδ is unclear, a recent study (Kaitsuka, Tomizawa et al. 2011) found that tissue-specific alternative splicing is probably a way to coordinate the roles of eEF1Bδ in translation and in heat shock response. Heat shock in Hek293 cells leads to the upregulation of eEF1BδL and downregulation of the shorter eEF1Bδ isoforms, and eEF1BδL has been found to regulate the expression of heat shock element (HSE) containing genes

induced by heat shock transcription factor (HSF) 1. Again as mentioned earlier, it should be pointed out that the cell lines used in this research, HeLa and HEK293 cells, did not show eEF1BδL expression in this thesis although the same antibody was used. Nevertheless, eEF1A1 has been reported to be involved in the activation HSF1 upon heat shock (Kugel and Goodrich 2006; Shamovsky, Ivannikov et al. 2006). HSF1 exists as monomers and is inactive in cells under normal conditions, but is trimerized and activated in response to heat shock. Activated HSF1 is localized in the nucleus and binds to HSEs in the promoters of genes upregulated in heat shock response, inducing the expression of heat-shock proteins (HSPs) and other cytoprotective proteins. The association of eEF1A with HSF1 has been identified in mammalian cell extracts, which was enhanced by heat shock. It is suggested that eEF1A1, together with heat shock RNA (HSR) 1, regulates the trimerization and trigger the activation of HSF1 (Shamovsky, Ivannikov et al. 2006). eEF1A2, the eEF1A isoform in motor neurons, does not have the same function as eEF1A1 in the heat shock response (Lowri Griffiths, PhD thesis, 2011). On the other hand, eEF1BδL, even though its expression may not be restricted in motor neurons only, induces the expression of HSE-containing genes in cooperation with HSF1 but not via the activation of HSF1 (Kaitsuka, Tomizawa et al. 2011). These findings are in line with previous report of the poor heat shock response in motor neurons due to failure of HSF1 activation (Batulan, Shinder et al. 2003).

The third subunit, eEF1Bγ, plays an important role in the oxidative stress response. The N-terminus of eEF1Bγ has a similar structure to the theta-class of GSTs (Koonin, Mushegian et al. 1994), which is important for cellular detoxification of reactive oxygen species (ROS). Whether the GST-like domain of eEF1Bγ contains full GST activity is still to be determined. Rice recombinant eEF1Bγ and the eEF1B complex both show a low GST activity (Kobayashi, Kidou et al. 2001). eEF1B from *Leishmania major* is able to conjugate a variety of electrophilic substrates to trypanothione which is a substrate similar to glutathione (Vickers, Wyllie et al. 2004). Additionally, the GST-like domain is possibly involved in the detoxification of

lipophilic compounds. Overexpression of eEF1Bγ in parasite *Trypanosoma cruzi* leads to the resistance of clomipramine and antidepressant drug (Billaut-Mulot, Fernandez-Gomez et al. 1997).

In S. *cerevisiae* eEF1Bγ is encoded by two genes, TEF3 and TEF4 (Kinzy, Ripmaster et al. 1994). Deletion of both genes does not affect cell viability, but resultes in the resistance to oxidative stress of $CdSO_4$ and H_2O_2 in *S. cerevisiae* (Olarewaju, Ortiz et al. 2004). Further studies found that strains lacking eEF1Bγ show an increased level of oxidized proteins, and defects in protein turnover and the vacuolar functions in response to oxidative damage (Esposito and Kinzy 2010). Moreover, TEF3-encoded protein regulates methionine sulfoxide reductase A (msrA), which plays an important role in the adaptive response of yeast to oxidative stress, by binding to its promoter (Hanbauer, Boja et al. 2003).

1.4.4 eEF1B and diseases

1.4.4.1 eEF1B and cancer

Protein synthesis is crucial for cells to maintain normal activity. Alteration of the expression level of certain proteins, including activation or upregulation of oncogenes and/or inactivation or downregulation of tumour suppressor genes, is a common feature of transformation and tumourigenesis. There are many reports on the changed expression level of the initiation factors (reviewed in Silvera, Formenti et al. 2010) and eEF1A in cancers (reviewed in Lamberti, Caraglia et al. 2004; Lee and Surh 2009). Similarly, the enhanced expression of at least one of eEF1B subunits in various cancers has also been reported.

eEF1Bα

eEF1Bα mRNA is found to be 20 times higher in transformed cultured rat kidney cells than normal rat tissue (Sanders, Maassen et al. 1992). Another report of eEF1Bα overexpression in cancer is in breast cancer. eEF1Bα mRNA in breast cancer cell lines T47D and MDA-MA-231 showed a 2.9-fold increase compared to

non-transformed breast epithelial cell line MCF-10A, demonstrated by Northern blot analysis. The same study also shows by RT-PCR a significant increase of eEF1Bα mRNA in breast cancer tissue over that in normal or fibroadenoma tissues, with a eEF1Bα/GAPDH ratio of 0.45 in cancer tissues and 0.12 in controls, although no difference was observed between different tumour grades (Al-Maghrebi, Anim et al. 2005).

eEF1Bα protein showed 1.33 fold upregulation in the high (PC3M-LN4) over low (PC3M) metastatic prostate cancer cells (Everley, Krijgsveld et al. 2004).

eEF1Bδ

Compared to the other two subunits, the study of eEF1Bδ expression in cancer is more extensive.

A study examining 10 human cancer cell lines derived from different tissues revealed that compared to their corresponding control cell lines, eEF1Bδ mRNA is overexpressed in primary ductal carcinoma cell line HCC1395, breast carcinoma cell lines T-47D, MCF-7, MDA-MB-361 and MDA-MB-453, but not in breast carcinoma cell line DU 4475 (Joseph, O'Kernick et al. 2004). Other studies also reported eEF1Bδ overexpression in cell lines derived from breast cancer (Jacob, Kandpal et al. 1996). Overexpression of eEF1Bδ protein has been identified in medulloblastoma cell line DAOY (Peyrl, Krapfenbauer et al. 2003), as well as in four non-small lung cancer cells lines compared to normal bronchial epithelial cells (Liu, Chen et al. 2004).

Upregulation of eEF1Bδ mRNA has been observed in a number of cancer tissues. eEF1Bδ showed expression change between gastric carcinoma tissues and normal tissues (Zeng, Liao et al. 2007). Overexpression of eEF1Bδ mRNA was found to be significantly associated with worse overall and progression-free survival among all 64 patients with medulloblastoma (De Bortoli, Castellino et al. 2006). Some studies found that a higher expression level of eEF1Bδ mRNA is correlated

with poorer prognosis. In 38 out of 52 cases of oesophageal carcinoma the expression level of eEF1Bδ is significantly associated with lymph node metastases and advanced disease stages (Ogawa, Utsunomiya et al. 2004). In moderately to poorly differentiated hepatocellular carcinoma the overexpression of eEF1Bδ is coordinate with the tumour grading (Shuda, Kondoh et al. 2000). Colon cancer tissues from advanced stages express a higher level of eEF1Bδ compared to normal mucosa (Roblick, Hirschberg et al. 2004).

Further evidence for the involvement of eEF1Bδ in cancer came from the studies on transformation and tumourigenesis of cultured non-carcinoma cells. eEF1Bδ is overexpressed in Balb/c-3T3 cells (Joseph, Lei et al. 2002) and human bronchial epithelial cells (16HBE) (Lei, Wang et al. 2010) transformed by Cadmium, and the carcigenic potential of Cadmium can be reversed by blocking eEF1Bδ with antisense mRNA, suggesting that eEF1Bδ is one of the genes that account for the transformation and carcinogenesis induced by Cadmium. Furthermore, NIH3T3 cells transfected with eEF1Bδ are able to form transformed foci and subcutaneous tumours in nude mice (Joseph, Lei et al. 2002), and blocking eEF1Bδ expression by antisense mRNA also reduces cell transformation (Lei, Chen et al. 2002).

eEF1Bδ is a negative regulator for the ubiquitin ligase SIAH-1, inhibiting the ubiquitation and degradation of its substrates (Wu, Shi et al. 2011). Since some targets of SIAH-1 have proved to be oncogenic and anti-apoptotic (Matsuzawa and Reed 2001; Yoshibayashi, Okabe et al. 2007), this is in line with the tumourigenic potential of eEF1Bδ.

eEF1Bγ

In the breast cancer cell lines T47D and MDA-MA-231 where eEF1Bα is overexpressed, eEF1Bγ mRNA is also 2.9-fold higher than in non-transformed cell line MCF-10A (Al-Maghrebi, Anim et al. 2005). However, while this study found no change of eEF1Bγ in MCF-7 cell line, another group reported eEF1Bγ overexpression (2- to 10-fold) in T47D and MCF-7 cell lines (Joseph, O'Kernick et al.

2004). Similarly, in the same study, eEF1Bγ mRNA expression in breast cancer tissues is about as 3.6 times much as in normal tissues (Joseph, O'Kernick et al. 2004).

Furthermore, eEF1Bγ mRNA overexpression has been observed in other types of cancer tissues. eEF1Bγ mRNA showed an overexpression in 25 out of 29 colorectal carcinomas (Chi, Jones et al. 1992), 13 out of 25 colorectal adenomas (Ender, Lynch et al. 1993), and 7 out of 9 pancreatic adenocarcinomas (Lew, Jones et al. 1992) over their corresponding normal tissues.

Upregulation of eEF1Bγ mRNA was found in 22 of 30 gastric carcinomas compared to corresponding normal tissues, with no relationship between the level of overexpression and tumour grades or the depths of invasion (Mimori, Mori et al. 1995). However, a study in hepatocellular carcinoma found that the overexpression of eEF1Bγ correlated with carcinoma grading (Shuda, Kondoh et al. 2000). Another study in oesophageal carcinoma found that 5 out of 36 cases showed eEF1Bγ mRNA overexpression at a level of two-fold or more than normal tissues. All of the 5 cases were at the most advanced stage IV, and disclosed severe lymph node metastases, showing a relevance between eEF1Bγ overexpression and cancer grade (Mimori, Mori et al. 1996).

On the other hand, overexpression of eEF1Bγ protein in cancers has also been found. A study on tissues from patients with colorectal adenocarcinoma found eEF1Bγ overexpression in 17 of 29 patients. The overexpression was only found in Dukes Stage B, C and D, but not Dukes Stage A cases. However this result should be treated with caution because the Western blot in this study showed only eEF1Bγ, and the subsequent quantification was not corrected to a loading control (Mathur, Cleary et al. 1998).

The mechanism for overexpression of eEF1Bγ is unknown. A study on colorectal carcinoma identified a single base change (L158->S) in one case but not in other cases, and the overexpression of eEF1Bγ in colorectal and pancreatic

carcinomas was not caused by gene amplification or rearrangement (Lew, Jones et al. 1992; Frazier, Inamdar et al. 1998).

1.4.4.2 eEF1B and motor neuron diseases

Motor neuron disease (MND) is a general term used to designate a variety of neurodegenerative diseases, characterized by fatally progressive muscular weakness, atrophy, and paralysis due to the loss of motor neurons. Current studies of translation elongation factors associated with neurodegenerative diseases are mainly focused on initiation factors and eEF1A. Mutations of each of the five subunits of translation initiation factor eIF2B have been identified in patients with leukoencephalopathy with vanishing white matter (VWM) and childhood ataxia with central nervous system hypomyelination (CACH) (reviewed in Scheper, van der Knaap et al. 2007; Pavitt and Proud 2009). Absence of eEF1A2 in mice leads to a wasted phenotype (described in detail in section 1.5).

So far not much is known about whether eEF1B is involved in MND like other translation factors. Information on eEF1B in MND to date is from several studies on amyotrophic lateral sclerosis (ALS), the most common form of MND. A study of the role of copy number variations (CNVs) in ALS reported eEF1Bδ as a potential ALS candidate (Wain, Pedroso et al. 2009). ALS is a fatal disease, characterized by the selective death of motor neurons in the spinal cord, brainstem and cortex. It has been found that CNVs may influence the risk of sporadic ALS (Cronin, Blauw et al. 2008). Both region-based and gene-based association analyses discovered that the gene encoding eEF1Bδ is covered in a CNV region that is associated with ALS. In 575 ALS cases examined, CNV overlapped with the EEF1D gene by at least 1 base pair; in 7 cases there were losses and in 3 gains.

A study of Down syndrome, which is caused by an extra copy of human chromosome 21 (hChr21) that leads to brain developmental dysregulations in neurogenesis, neuronal differentiation, myelinization, and synaptogenesis, has found

that eEF1Bγ, together with several other genes encoding for translational regulators, is likely to participate in the pathway of defective neuron differentiation in the late differentiated stage (Wang, Kadota et al. 2004). Microarray results identified a lower level of eEF1Bγ, but not eEF1Bδ, in ALS patients than controls (Bakay, Wang et al. 2006).

1.5 The wasted mouse, a model for MND

Studies on MND are mostly carried out using mouse models, each carrying specific gene mutation(s) to model a certain type of human MND. Mice are commonly used as models for human diseases because of the advantages including that they share the same mammalian genes with human and the mouse genome is better understood (reviewed in Hafezparast, Ahmad-Annuar et al. 2002). In spite of the fact that it is impossible to replicate all the details of a certain human disease in a mouse model because of the different life span and physiology, and in some cases the mouse model may fail to show the exact phenotype as in human with the same mutations, which could be due to different biochemical pathways (Phaneuf, D., N. Wakamatsu, et al. 1996), the mouse model is an important and useful approach to understand the causes and pathology of MND.

There are two types of MND mouse models for human MND (reviewed in Green and Tolwani 1999): those that develop spontaneously and those that are experimentally induced. The mouse model used in this project, the wasted mutant, occurred spontaneously.

Wasted mutation arose spontaneously in the inbred mouse colony HRS/J at the Jackson laboratory in 1972 (Shultz, Sweet et al. 1982). The mutation has been reported to be a 15kb deletion of the promoter and first noncoding exon of the mouse *Eef1a2* gene and thus abolishes the transcription of the gene (Chambers, Peters et al. 1998).

In wild type mice, eEF1A1 declines in heart, muscle and neurons postnatally, and by 21 days after birth eEF1A1 is shut down and replaced by eEF1A2 in these tissues and cells. In wasted mice, the reduction of eEF1A1 in brain, spinal cord, heart and muscle happens on schedule, regardless of the absence of eEF1A2 in these tissues (Khalyfa, Bourbeau et al. 2001), and causes death to the mice by 27 days. Homozygous wasted mutant mice (*wst/wst*) are characterized by combined

neurologic and immunologic abnormalities, while wild type (+/+) and heterozygote (*wst*/+) littermates are phenotypically normal. At 21 days after birth, wasted mice develop tremors, ataxia, weakness of hind limbs, weight loss, gait abnormalities, spleen and thymus atrophy, and progressive paralysis and die by about 28 days (Shultz, Sweet et al. 1982).

Loss of eEF1A2 in wasted mice causes lesions in central nerve system. Homozygous wasted mice show prominent vacuolar degeneration of motor neurons within anterior horns of the spinal cord and the brainstem (Woloschak, Rodriguez et al. 1987; Lutsep and Rodriguez 1989). In the spinal motor neurons from wasted mice, most of the nuclear envelope (NE) undergoes deformity, and the nuclei are translocated away from the centre (Ueda, Tezuka et al. 2004). The pathology in spinal cord of wasted mice seems to happen in a cascade, first at the cervical level and then progressing caudally. The vacuolation of motor neurons and reactive gliosis in spinal cord from homozygote wasted mice were seen at the cervical but not at the lumbar level (Newbery, Gillingwater et al. 2005). Unlike thymus, motor neurons in wasted mice die by mechanisms other than apoptosis and necrosis (Ueda, Tezuka et al. 2004). Furthermore, wasted mice showed retraction of synapses from motor endplates in muscle (Newbery, Gillingwater et al. 2005), and develop progressive muscle wasting which leads to the loss of body weight, and atrophy of the spleen and thymus due to extensive apoptosis (Potter, Bernstein et al. 1998). Our lab has demonstrated that expression of eEF1A2 in neuronal and muscle tissues in wasted mice corrects the abnormalities.

1.6 Proximity Ligation Assay

In this thesis protein interactions were detected using *in situ* proximity ligation assay (PLA). PLA is a novel technique which is based on the antibody-mediated recognition of target antigens in close proximity (Fredriksson, Gullberg et al. 2002). A pair of oligonucleotide labeled secondary antibodies (PLA probes) generates a signal only when the two PLA probes bind in close proximity, either to the same primary antibody or two primary antibodies that have bound to the sample in close proximity. A schematic diagram of detecting the interaction between two proteins is shown in Figure 1.3. The signal from each detected pair of PLA probes is visualized as an individual fluorescent spot. These PLA signals can be quantified and assigned to a specific subcellular location based on microscopy images.

PLA was first described as a sensitive method for protein measurements in solution (Fredriksson, Gullberg et al. 2002). It was then modified for different biological applications including detection and quantification of protein-protein interactions (Soderberg, Gullberg et al. 2006), protein-DNA or -RNA interactions (Gustafsdottir, Schlingemann et al. 2007), protein expression and protein phosphorylation (Jarvius, Paulsson et al. 2007). Compared to other techniques used to investigate protein-protein interactions, PLA has the advantages of investigating endogenous protein interactions *in situ*, either on tissues or cultured cells directly. It is very sensitive and able to detect transient protein-protein interactions at single-molecule resolution. Finally it is a fast and simple method to visualize protein-protein interactions and could give information on the distribution of interacting proteins between individual cells.

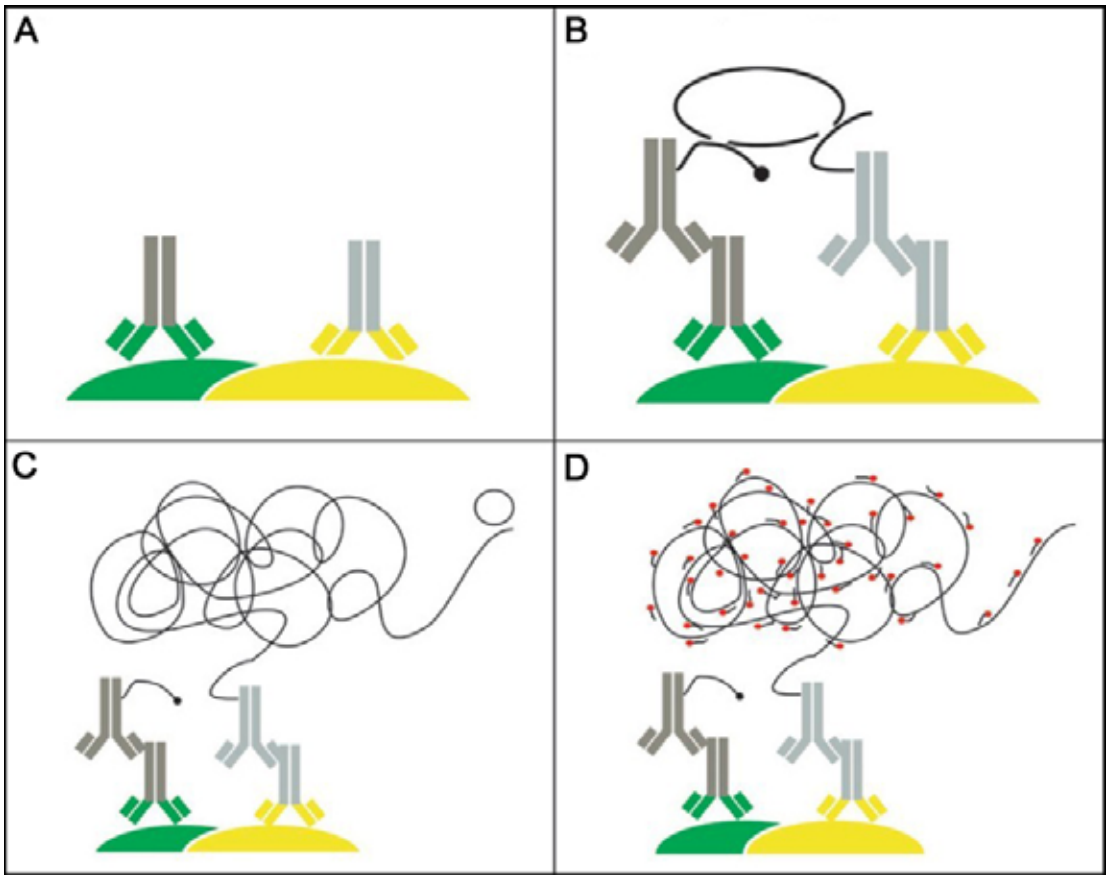

Figure 1.3. Schematic presentation of the principle of PLA. A and B. Target protein 1 (green) and protein 2 (yellow) are recognized by two primary antibodys (dark gray/green and light gray/yellow, respectively), which are then bound by a pair of PLA probes (dark gray and light gray, respectively). The two DNA strands (black line in B) attached to the probes serve to template the hybridization of circularization oligonucleotides, which are joined by ligation into a circular DNA molecule (circular black line in B). C. The circular DNA molecule is amplified by rolling-circle amplification (RCA) primed by one of the PLA probes, producing a long single-stranded DNA molecule (gray line). D. The RCA products are detected by hybridization of fluorescence labeled oligonucleotides (red dots) and can be identified under fluorescent microscope (Figure adapted from Trifilieff, Rives et al. 2011).

1.7 Project aims

eEF1B subunits have been shown in various studies to have multiple functions and to be potentially related to diseases. Most of the studies on the roles of eEF1B in cancer are at mRNA level, and little is known about the potential involvement of eEF1B in motor neurone disease. On the other hand, although the components of eEF1B are identified, further information is needed regarding whether the two GEF in the eEF1B complex have the same function, and whether the two eEF1A isoforms interact with eEF1B in the same way.

The aims of this project are to investigate the roles of eEF1B in cancer, motor neuron diseases, as well as to understand the relationship between eEF1B subunits and eEF1A.

Chapter 2 Materials and Methods

2.1 Materials

2.1.1 Solutions and buffers

The solutions and buffers used in this thesis as well as the recipes are listed in Table 2.1.

Table 2.1. List of solutions and buffers required for performing experiments in the thesis.

Name	Protocol
3,3'-diaminobenzidine (DAB) solution (Vector Laboratories)	5 ml dH_2O 2 drops of buffer Stock Solution 2 drops of DAB Stock Solution 2 drops of the Hydrogen Peroxide Solution
Blocking buffer for Western blots	5% (w/v) Marvel dried skimmed milk 0.2 % (v/v) Tween 20, PBS
Citric acid solution for antigen retrieval in immunohistochemistry	0.1 M citric acid pH 6.0 dH_2O up to 1 liter
Duolink II wash buffer A	One pouch of Duolink II wash Buffer A powder dissolved in 1L dH_2O
Duolink II wash buffer B	One pouch of Duolink II wash Buffer B powder dissolved in 1L dH_2O
Duolink Wash buffer SSC (2x)	1 pouch of Duolink Wash buffer SSC powder dissolved in 1L dH_2O
Duolink Wash buffer TBS-T (2x)	1 pouch of Duolink Wash buffer TBS-T powder dissolved in 1L dH_2O
ECL solution (GE Healthcare)	Detection reagent 1and detection reagent 2 at the 1:1ratio
Freezing medium for liquid nitrogen stocks	10% (v/v) newborn calf serum 90% (v/v) DMSO
Laemmli loading buffer (2x)	60mM Tris.HCl pH 6.8 0.1% Bromophenol blue 10% glycerol 2% SDS dH_2O up to 1L
Laemmli running buffer (10x)	250mM Tris HCl pH 8.3 1.9M Glycine 10% SDS dH_2O up to 1L

Lithium carbonate solution	67.7 mM lithium carbonate in 1L dH_2O
Membranes stripping buffer	10% (v/v) SDS 0.5 M Tris-HCl pH 6.8 0.8 % (v/v) β-mercaptoethanol dH_2O up to 100 ml
4% Neutral buffered formalin (NBF)	108ml 37% formaldehyde 4g monobasic sodium phosphate (NaH_2PO_4) 6.5g disodium hydrogen phosphate (Na_2HPO_4) dH_2O up to 1L
Orange G DNA loading buffer	30% (v/v) glycerol 100 mg Orange G dH_2O up to 50ml
3% Peroxidase blocking solution	40 ml of 30% (v/v) hydrogen peroxide solution dH_2O up to 400 ml Made fresh
Phosphate Buffered Saline (PBS)	1 PBS tablet (Sigma) 100 ml dH_2O Autoclaved, stored at 4^{o}C
PBS-tween-20 (PBS-T)	As above and 0.1% (v/v) Tween-20 (Sigma)
Radioimmuno- precipitation assay (RIPA) buffer	50 mM Tris-HCl pH 7.5 150 mM sodium chloride 1% (v/v) NP-40 0.5 % (w/v) sodium deoxycholate 0.1% (v/v) SDS 1 mini-complete protease tablet (Roche) dH_2O up to 10 ml Stored at -20^{o}C after tablets were added
0.32M Sucrose	10.9g Sucrose in 100ml dH_2O 1 mini-complete protease tablet (Roche) in 10ml
Transfer buffer (10x)	30.3g Tris 144.1g glycine dH_2O up to 1 liter
TBE (Tris-Borate-EDTA)	90 mM Tris-Borate, 2 mM EDTA pH 8.0

2.1.2 Cell lines

All the cell lines used in this study are listed in Table 2.2.

Table 2.2. Panel of cell lines used in different tissue culture applications.

Cell Line	Species	Cell Type	Maintenance Medium	Source
NIH-3T3	Mouse	Embryo fibroblast	DMEM+10% NBCS	ATCC
A1 8.6	Mouse	Fibroblast; Stable cell line overexpressing EEF1A1 coding sequence	DMEM+10% NBCS+ 600µg/ml Geneticin	Dr. Justyna Janikiewicz
A2 9.6	Mouse	Fibroblast; Stable cell line overexpressing EEF1A2 coding sequence	DMEM+10% NBCS+ 450µg/ml zeocin	Dr. Justyna Janikiewicz
A549	Human	Lung carcinoma epithelial	DMEM +10% FBS	ATCC
HCT116	Human	Colon carcinoma epithelial	DMEM+10% NBCS	ATCC
Hek293	Human	Transformed embryonic kidney cells	DMEM +10% FBS	ATCC
HeLa	Human	Cervical cancer epithelial	DMEM+10% FBS	ATCC
MCF-7	Human	Breast adenocarcinoma cells	DMEM +10% FBS	ATCC
MDA-MB-231	Human	Breast carcinoma cells	DMEM +10% FBS	ATCC
MDA-MB-451	Human	Breast carcinoma cells	DMEM +10% FBS	ATCC
NSC34	Mouse	Motor neuron neuroblastoma hybrid	DMEM+10% FBS	ATCC
PC3	Human	Prostate cancer cells	RPMI+10% NBCS	ATCC
Rat 2	Rat	Embryo fibroblast	DMEM +10% FBS	ATCC
T47D	Human	Breast cancer cells	DMEM +10% FBS	ATCC

2.1.3 Animals

All mice were maintained in accordance with Home Office regulations in the small animal Biomedical Research Facility (BRF) at Western General Hospital. The mice were exposed to 12 hour light/12 hour dark cycles with *ad libitum* access to food and water. Wasted mice are on a mixed although predominantly C3H/HeH and C57BL/6J background.

2.1.4 Antibodies

All the antibodies used for the Western blot, IHC and PLA experiments in this thesis, together with their working concentrations for each type of application are listed in Table 2.3.

2.1.5 Slides

For tissues slides, mouse tissues were dissected from mice and immediately transferred to 4% Neutral buffered formalin (NBF) and kept in NBF for 2 days.

Alternatively, for IHC of cultured cells, cells were washed twice with Dulbecco's phosphate buffered saline (DPBS, supplied by Gibco), trypsinized and centrifuged as described in section 2.2.1. The cell pellet was resuspended in 25ml of culture medium and transferred to a 50ml tube. The suspension was incubated at 37°C in a 5% CO_2 incubator for 10 minutes before centrifugation at 400×g and 4°C for 5 minutes. The supernatant was then removed and the cells were resuspended in 50ml of ice cold DPBS. The last two steps were repeated. Finally the cell pellet collected was resuspended in 10ml of 4% NBF for 60 minutes.

Fixed tissues or cells were sent to the Pathology Histology service (University of Edinburgh) for processing. Paraffin embedded tissues or cells were cut using a microtone (Leitz 1512) into 4μm sections and mounted on Superfrost plus slides (Thermo Scientific).

A breast cancer tissue array was obtained from AccuMax Array, containing 12 cancer cases of infiltrating ductal carcinoma, as well as 12 corresponding normal tissues from each patient. MND sections were obtained from the London Neurodegenerative Diseases Brain Bank and the pathological information is listed in Table 2.4.

Table 2.3. List of antibodies and conditions for performing WB, IHC, IF and PLA.

Name/Target	Company	Species	Application And Dilution
Anti-goat biotin	Dako	Rabbit	IHC 1:500
Anti-mouse biotin	Dako	Goat	IHC 1:500
Anti-rabbit biotin	Dako	Goat	IHC 1:500
Anti-goat HRP	Dako	Rabbit	WB 1:2000
Anti-mouse HRP	Dako	Rabbit	WB 1:2000
HRP goat anti-rabbit	Dako	Goat	WB 1:2000
Alexa Fluor anti-rabbit 594 (red)	Invitrogen	Donkey	IF 1:800
Alexa Fluor anti-sheep 488 (green)	Invitrogen	Donkey	IF 1:800
eEF1Bα	Abcam	Rabbit	WB 1:400 IHC 1:200 IF 1:200 PLA 1:40
eEF1Bδ	ProteinTech Group	Rabbit	WB 1:2000 IHC 1: 800 IF/PLA 1:200 PLA 1:200
eEF1Bδ	GeneTex	Rabbit	WB 1:1000
eEF1Bγ	Abcam	Mouse	WB 1:1000
eEF1Bγ	Sigma	Rabbit	WB 1:800
eEF1Bγ	Bethyl	Rabbit	IHC 1:30 PLA 1:40
eEF1A2-1	Custom (Helen Newbery[1])	Sheep	WB 1:200 IHC 1:25 IF 1:25 PLA 1:20
GAPDH	Chemicon	Mouse	WB 1:40000
TK1	Olink	Chicken	PLA 1:10
α-Tubulin	Sigma-Aldrich	Mouse	IF 1:2500
γ-Tubulin	Sigma-Aldrich	Mouse	WB 1:10000
V5	LSBio	Sheep	PLA 1:120

1. Dr Helen Newbery is a Postdoctoral researcher working in Professor Cathy Abbott's group.

Table 2.4. Informations of the MND patients and pathological diagnose as supplied by the London Neurodegenerative Diseases Brain Bank. MN. Motor neuron. AD. Alzheimer's disease. NS. Not specified.

	Age	Sex	Region	Pathological Diagnose
A1	59	F	Thoracic	MND
A2	68	F	Cervical	MND
A3	39	F	Cervical	MND
A4	63	M	Cervical	MND
A5	74	F	Cervical	MND
A6	67	M	Cervical	MND
A7	74	M	NS	MND
A8	62	M	NS	MND
B1	77	M	Cervical	MND
B2	78	F	NS	MND
B3	55	M	Cervical	MND
B4	50	M	Cervical	MND
B5	71	M	Thoracic	MND
B6	45	M	Cervical	MND
B7	63	F	Cervical	MND
B8	70	F	Cervical	MND
C1	55	M	Cervical	MND
C2	84	M	Cervical	MND
C3	49	M	NS	MND
C4	72	M	Thoracic	MND
C5	78	M	NS	MND
C6	81	F	Cervical	MND
C7	80	F	Cervical	MND
C8	81	F	Cervical	MND
D1	68	F	Cervical	MND
D2	61	M	Thoracic	MND
D3	44	F	Cervical	MND
D4	57	F	Thoracic	MND
D5	56	M	Cervical	MND with upper and lower MN damage (possibly familial)

D6	72	M	Cervical	MND with TDP-43 positive glial inclusion in M cervical spine
D7	92	M	Thoracic	MND mild/moderate aging changes
D8	85	F	Cervical	MND and AD
E1	42	M	Cervical	MND mild and focal neurofibrillary tangles
E2	39	M	Cervical	MND with upper and lower MN damage
E3	59	M	Cervical	MND with diffuse inv cervical spine, P62 positive inclusions
E4	71	M	Cervical	MND with extra-motor pathology
E5	62	M	Cervical	MND frontotemporal lobar degeneration AD Braak IV
E6	87	F	Cervical	MND possible AD Braak IV
E7	67	F	Cervical	MND with extra MN inclusions
E8	63	M	Thoracic	MND ubiquitin positive intracytoplasmic inclusions
F1	42	M	Cervical	MND with subcortical ubiquitin inclusions
F2	55	M	Cervical	MND with mild AD changes
F3	83	M	Cervical	MND and AD
F4	70	M	Cervical	MND extramotor p62 positive cytoplasmic neuronal & intranuclear inclusions
F5	87	M	Cervical	MND with upper and lower MN damage
F6	74	M	Cervical	MND AD type neurofibrillary changes Braak I
F7	73	M	Cervical	MND with upper and lower MN damage
F8	68	M	Cervical	MND early AD Braak III
G1	57	M	NS	MND oligodendroglial p62 immunoreactivities
G2	66	M	Thoracic	MND mild tau pathology in limbic Braak I
G3	75	M	Cervical	MND with additional inclusions in hippocampus
G4	66	M	NS	MND evidence of small blood vessel dilation
G5	57	F	Cervical	MND dementia early stage
A	40	M	Lumbar	Control
B	N/A	M	Cervical	Control
C	64	M	NS	Control
D	79	F	NS	Control
E	87	F	Cervical	Control
F	54	M	NS	Control
G	95	M	Cervical	Control
H	61	M	Lumbar	Control

I	55	F	Cervical	Control
J	62	M	Cervical	Control
K	80	M	NS	Control
L	92	F	Cervical	Control (Braak I-II)
M	89	F	Cervical	Control (some hypoxic changes)
N	90	F	Cervical	Control (Mild AD changes Braak II)
O	78	M	NS	Control (metastatic carcinoma deposits)
P	81	M	NS	Control (old cerebral infarct)
Q	68	M	Cervical	Control – hypoxia
R	57	M	NS	Control (mild ischaemia)
S	64	F	Cervical	Control (morphological abnormality)
T	86	F		Control (cerebral infarct)

2.1.6 DNA primers

A list of the primers used throughout this thesis is shown in Table 2.5. Primers were designed with the Primer3 programme (Rozen and Skaletsky 2000) and confirmed by Blasting the sequences with NCBI's BLAST. Primers were all ordered from Sigma-Aldrich.

Upon arrival, all the primers were dissolved in dH_2O to a final concentration of 100μM and stored at -20°C for later experiments. Fresh working solutions of 5μM were made before amplification reactions each time.

2.1.7 siRNAs

siRNAs for eEF1Bα, eEF1Bδ and eEF1Bγ were commercially available from Ambion. Custom siRNAs for eEF1BδL and eEF1A2 were produced by Sigma-Aldrich and Invitrogen respectively. To design specific siRNAs targeting eEF1BδL, the sequence of the exon 3 of eEF1Bδ gene was copied into the BLOCK-iT RNAi designer software (Invitrogen), and the siRNAs were chosen by their ranking given by the software. siRNAs were resuspended to a concentration of 20μM and aliquoted

before storage at -80°C. A non-targeting scrambled siRNA supplied by Invitrogen was used as a negative control for RNAi experiments.

The siRNAs used for RNAi experiments in this thesis are listed in table 2.6.

Table 2.5. Primer sequences used for different PCR applications.

Name	Target	Species	Sequence 5' to 3'
BqPCR5F	eEF1Bα	Mouse	GAAGCCTTGGGATGATGAGA
BqPCR6R	eEF1Bα	Mouse	TATTCCAGCATCCGTTCC
DqPCR3F	eEF1Bδ	Mouse	AGCTTGTGCCTGTTGGCTAT
DqPCR3R	eEF1Bδ	Mouse	CTCTGCACATGCTCCTCAAA
GapdhQPCR2F	GAPDH	Mouse	GGGTGTGAACCACGAGAAAT
GapdhQPCR2F	GAPDH	Mouse	ACTGTGGTCATGAGCCCTTC
GqPCR1F	eEF1Bγ	Mouse	CCTCATCGCTGCTCAGTACA
GqPCR1R	eEF1Bγ	Mouse	ATCACCCTCAAATGCTGGAA

Table 2.6. List of siRNA sequences used in this thesis, as well as their reference names, sources and targets.

Name	Target	Sequence 5'-3'	Source
1A2 siRNA1[1]	Mouse eEF1A2	UUAACGGACACAUUCUUCACAUUGA	Invitrogen
1A2 siRNA2[1]	Mouse eEF1A2	CAAUCUUGUACACAUCCUGCAGAGG	Invitrogen
Bα siRNA1	Mouse eEF1Bα	CCAUCCUACUAGACGUGAAtt	Ambion
Bα siRNA2	Mouse eEF1Bα	CAUCAAGUCGUAUGAAAAtt	Ambion
D siRNA1	Mouse eEF1Bδ	CACCAGCAGAGGACGAUGAtt	Ambion
D siRNA2	Mouse eEF1Bδ	GGACGAUAGUGCUCGUGAAtt	Ambion
DL siRNA1	Mouse eEF1BδL	AUCAAACAGGGCCUCAUAGAAGCCC	Sigma-Aldrich
DL siRNA2	Mouse eEF1BδL	CGUAGGAAACAAGAGAGCUGGGUCA	Sigma-Aldrich
G siRNA1	Mouse eEF1Bγ	GGUGGACUAUGAGUCGUAUtt	Ambion
G siRNA2	Mouse eEF1Bγ	CCUCAUCACUGGGAUGUUUtt	Ambion

1. Designed by Dr Lowri Griffiths.

2.2 Cell culture

2.2.1 Cell culture maintenance

For experiments and maintaining cultures, cell lines were grown in Cell Start T25, T75 or T175 flasks (Greiner Bio-One) unless stated otherwise. Each cell line was grown in the corresponding medium listed in Table 2.2, and kept at 37°C in a 5% CO_2 incubator. When cells reached 80 to 90% confluence, the medium was aspirated and cells were washed twice with prewarmed DPBS and incubated in a 1:1 mix of trypsin:versene (Invitrogen) for about 5 minutes until most cells were detached from the flask. A small amount of prewarmed culture media was added and the suspension was centrifuged at 1200 rpm for 5 minutes. The supernatant was then aspirated and the cell pellet was resuspended in 5 ml of fresh prewarmed culture medium and split into a new flask 1 in 5 or 1 in 10 depending on the volumes of future culture. For T25, T75 or T175 flasks 10 ml, 25 ml or 50 ml of culture medium was added respectively. Cells were usually split approximately every 3 to 7 days and kept until they reached passage number 20 or for NSC34 cells passage number 15.

2.2.2 Cell counting

To count the number of cells, cultured cells were washed with DPBS, trypsinized and the pellet was collected as described in section 2.2.1. The cell pellet was resuspended in 10ml of the culture media, and 100µl of the suspension was mixed with 9.9 ml of Isoton. Cells were then counted automatically using a Coulter Counter Z2 series (Beckman coulter).

Alternatively, cells were counted using a haemocytometer (Weber Scientific International, England). Briefly, cultured cells were collected and resuspended as described in section 2.2.1. 1ml of the cell suspension was diluted in 4ml of culture medium in a 10ml falcon and mixed. The haemocytometer was prepared by placing

the special coverslip properly on the surface of the counting chamber. A drop of the cell suspension was then applied to the edge of the coverslip and sucked into the void so that the chamber was completely filled with the diluted cell suspension. The chamber was then examined under a light microscope (Leica) and the number of cells in the chamber was counted. The cell concentration was calculated by dividing the mean of the numbers from each large square by $10^{-4}cm^2$.

2.2.3 Cryopreservation of cells

To obtain liquid nitrogen stocks of the cells, cultured cells were trypsinised and centrifuged as described in 2.2.1. The pellets were then resuspended in 10ml of 90% FBS or NBS depending on the cell line (Table 2.2) and 10% DMSO. The suspension was transferred into 1ml screw top CryoTube vials (Nunc), and frozen at -20°C overnight, -70°C freezer for three days, and then kept in a liquid nitrogen tank for longer storage.

2.2.4 RNAi

RNAi experiments in this thesis were performed following the standard protocol supplied with the siLentFect Lipid Reagent (Bio-Rad). Cells with no siLentFect reagent, cells with no siRNA and cells with a non-targeting scrambled siRNA were used as negative controls. Each knockdown experiment was performed in triplicate.

An appropriate number of cells were cultured in 12-well plates in corresponding medium so that they reached about 50% confluence overnight. The following day, twenty minutes prior to transfection, the culture medium in each well was replaced by 500µl of fresh medium. For each well to be transfected, 50µl of serum-free medium containing 0.7µl of siRNA was mixed with another 50µl serum-

free medium containing 1.5µl of siLentFect and mixed by pipetting. The mixture was incubated for 20 minutes at room temperature before being added to each well with growing cells. The plate was shaken back and forth to mix the solution and then incubated at 37°C in a 5% CO_2 incubator. The medium was changed 24 hours after transfection, and the cells were cultured for another 48 hours before being subjected to further experiments.

For RNAi in a 96-well plate, each well contained 100µl plating medium, 0.1µl siRNA, 10µl serum-free medium for siRNA and 10µl for siLentFect instead.

2.2.5 MTT assay

The MTT assay was used to determine the viability of cultured cells after RNAi using the MTT Cell Proliferation Assay Kit (Cayman Chemical Company). The reagents were prepared prior to the MTT experiment as follows: the Cell-Based Assay Buffer Tablet was dissolved in 100ml of dH_2O; the 125mg vial of MTT Reagent was dissolved in 25ml of Assay Buffer and made into smaller aliquots.

Cells were seeded in a 96 well plate at a density of $5x10^2$-10^5 cells per well in 100µm of culture medium, and grown at 37°C in a 5% CO_2 incubator for 24 hours before the RNAi procedure described in section 2.2.4. 72 hours after RNAi, the medium was changed, and 10µl of MTT Reagent was added to each well and mixed for one minute on a shaker. The cells were incubated for 3 hours at 37°C in a 5% CO_2 incubator before the formazan produced was visible at the bottom of each well. Subsequently, the culture medium in each well was carefully aspirated avoiding any disruption of the cell monolayer. Next, 100µl of the Crystal Dissolving Solution was added to each well and the formazan crystals were dissolved and the solution in the wells became purple. Finally, the absorbance of each sample was measured at 570nm using a Synergy HT Multi-Mode Microplate Reader (BioTek) and analysed by Gen5 Data Analysis Software (BioTek).

Each knockdown was performed in triplicate. Cells with no siLentFect reagent, cells with no siRNA and cells with a non-targeting scrambled siRNA were used as negative controls for RNAi. Cells with no MTT Reagent and wells with dH_2O only were used as negative controls for the MTT assay.

2.3 Protein-related methods

2.3.1 Protein extraction from cells

Protein extracts were made when cells reached 80 to 90% confluence. To make a cell lysate, the cell culture medium was aspirated off and the cells were washed twice with DPBS, then a small amount of ice cold RIPA buffer was added, just enough to cover the bottom of the flask or the well. Cells were then incubated in RIPA buffer at 4°C for 20 minutes. Subsequently, cells were detached from the flask or the well, and the cells that remained loosely attached were scraped from the wall of the container. Cells were then transferred into a micro-centrifuge tube and centrifuged at 13,000 rpm for 30 minutes at 4°C. The supernatant was collected and stored at -20°C for further study.

The protein concentration of the lysates prepared was measured using a Nano Drop 1000 (Thermo Scientific).

2.3.2 Protein extraction from tissues

Mouse tissues were dissected and flash frozen in liquid nitrogen before storage at -70°C. To produce protein lysates, tissues were placed in 0.32M sucrose solution in tubes from the Precellys ceramic kit or steel kit for heart and muscle tissues, and homogenised in a Precellys 24 Homogeniser. Samples were moved to fresh tubes and stored at -20°C.

2.3.3 Western Blotting

2.3.3.1 Sample preparation

Protein extracts obtained from 2.3.1 or 2.3.2 were mixed at 1:1 with 2× Laemmli loading buffer (Table 2.1) and 1:10 with 1M DTT. The mixtures were then

heated in a boiling water bath at 100°C for 5 min in order to denature the proteins and disrupt protein-protein interactions. Samples were then ready for electrophoresis or stored at -20°C for later examination.

2.3.3.2 SDS-PAGE electrophoresis

Separating gels of 10% or 12% depending on the size of the protein of interest were prepared as follows:

	10%	12%
30% acrylamide	10.4 ml	12.8 ml
1.5 M Tris-HCl pH 8.8	8 ml	8ml
dH_2O	13.4 ml	11ml
20% SDS	160 µl	160µl
25% AMPS	20 µl	20µl
TEMED	80 µl	80µl

The gel solution was well mixed and poured between two glass plates (Bio-Rad) until the gel was 1 to 2cm from the top edge. The remaining space was filled with dH_2O and then the gel was left at room temperature for approximately 30 minutes to set. The water was then removed and replaced with 4% stacking gel prepared as follows:

30% acrylamide	1.45 ml
0.5 M Tris-HCl pH 6.8	2.5 ml
dH_2O	5.95 ml
20% SDS	50µl
25% AMPS	50 µl
TEMED	5 µl

After the stacking gel was poured into the space between the plates, a comb of either 10 or 15 slots (Bio-Rad) was put on the top and the gel was left at room temperature for approximately 15 minutes to set. When the gel was ready, the gel apparatus (Bio-Rad) was assembled and filled up with approximately 500ml of 1x Laemmli running buffer. The combs were then removed and protein samples prepared in Section 2.3.3.1 were loaded into individual wells, as well as a protein size marker (Fullrange rainbow, GE Healthcare) in the first well. The gel was run at 100V long enough to allow the samples to run through the stacking gel, and then run at 120V until the blue dye in the samples reached the bottom edge of the gel.

2.3.3.3 Western blot transfer

After electrophoretic separation, the gel was removed from the plates and placed in 1x transfer buffer together with Whitman filter paper (6cm by 8cm) and sponges. For each gel, a piece of Hybond-P PVDF transfer membrane (Amersham, GE Healthcare) was cut (6cm by 8cm) and pre-wet in methanol before being put in the transfer buffer. A sponge, two pieces of filter paper, the gel, the transfer membrane, another two pieces of filter paper and a sponge were assembled strictly in the above order in a plastic blotter soaked in the transfer buffer. The assembled blot was placed in a tank filled with transfer buffer, a magnetic stirrer and a frozen ice pack. The transfer was run at 100V/400A in a 4°C cold room for 60 minutes and then the blotting apparatus was dissembled and the membrane was placed in blocking buffer. The blocking process was either overnight at 4°C or 1 hour at room temperature.

2.3.3.4 Immunostaining

After blocking, the membrane was probed with a primary antibody diluted in 5% (w/v) powdered milk in PBS-T to an appropriate concentration as described in

Table 2.3. The membrane was then incubated at room temperature for 1.5 hours with gentle shaking, and then washed for 5 minutes ×4 with PBS-T before being probed with an appropriate HRP conjugated secondary antibody for 1 hour at room temperature under gentle shaking. The membrane was washed for 5 minutes ×4 with PBS-T, followed by visualization using the ECL Western blotting detection kit (Amersham, GE Healthcare).

2.3.3.5 Densitometric analysis

Selected pictures of the Western blots were scanned into a computer for quantification. The intensity of the bands on the blot were quantified using the GelQuant.NET software (version 1.6.5) provided by biochemlabsolutions.com.

2.3.3.6 Re-probing the membranes

To re-probe a membrane with a different antibody, the membrane was washed with PBS-T (5 minutes×3) and incubated in stripping buffer for 30 minutes. The membrane was then washed with PBS-T, incubated with blocking buffer and probed with a different antibody following the same procedure described in section 2.3.3.4.

2.3.3.7 Relative quantification of protein expression

To compare the protein expression levels in wild type and wasted mouse tissues, samples for each tissue and genotype were taken from three individual animals. The intensity of the band for the target protein was normalised to that of the loading control (GAPDH or tubulin) in each sample and the mean of the three samples was taken for the comparison.

The standard deviation (SD) and the standard error of the mean (SEM) were calculated and student's t-test was performed in Excel (Microsoft).

2.3.4 Immunohistochemisty (IHC)

2.3.4.1 Antigen retrieval and antibody probing

Slides of cultured cells, human or mouse tissues obtained from section 2.1.5 were deparaffinised twice in xylene for 5 minutes, and rehydrated twice in absolute ethanol, twice in 75% ethanol and finally water. Slides were then immersed in 0.01M citrate buffer (pH 6.0) and microwaved for 15 minutes for antigen retrieval. Slides were cooled and washed with running tap water for 5 minutes, then with PBS for 5 minutes, before being loaded onto Shandon Sequenzas (Thermo Scientific).

Subsequently, slides were immersed in peroxidase blocking solution for 5 minutes and washed with PBS. Slides were then blocked for 30 minutes at room temperature in 100µl serum (diluted 1:5 in PBS) of the same species in which the secondary antibody was raised. Primary antibody diluted to an appropriate concentration in PBS was added onto the slides, and slides were washed 3 times with PBS after 30 minutes incubation of the primary antibody. The slides were then incubated with 100µl of appropriate biotinylated secondary antibody (Dako Cytomation) diluted 1:500 in PBS for 30 minutes. Slides were washed 3 times with PBS afterwards, and 3 drops of Vectastatin R.T.U. Elite® ABC Reagent (Vector Laboratories) were added onto each slide. Slides were incubated at room temperature for 30 minutes, and washed in PBS for 5 minutes.

Slides treated with no primary antibody were used as negative controls.

2.3.4.2 Detection

To visualise the protein expression, slides were treated with pre-mixed DAB solution for approximately one minute. Slides were then counterstained in haematoxylin, washed under running tap water, stained with lithium carbonate, washed again under running tap water, dehydrated twice in 70% ethanol and twice in

absolute ethanol. Finally slides were cleared twice in xylene and mounted using pertex (CellPath).

The slides were viewed under an Olympus BX60 light microscope (Olympus) and pictures were captured using Cell^D software (Olympus). Alternatively, the slides were viewed under a Nikon AZ100 multi-purpose zoom microscope and pictures were captured and analyzed using IPLab software (version 3.9.5 r4 for Mac, BD Biosciences).

2.3.5 Immunofluorescense (IF)

IF was used to visualize the expression of two different proteins in the same sample. The experiment was performed following the same procedure as in IHC described in sections 2.3.4.1 until the step of antigen retrieval was done. The slides were then blocked for 30 minutes with donkey serum (given by Dr Shaun Mackie, MMC, University of Edinburgh), which was diluted 1:10 in PBS. Primary antibodies raised in different species against the two proteins of interest were diluted to an appropriate concentration and added onto the slides. The slides were washed with PBS after 30 minute incubation with primary antibodies. Next, two fluorescent secondary antibodies (HRP conjugated rabbit antibody 594 and HRP conjugated sheep antibody 488, red and green respectively) were added to the slides, and the slides were incubated in the dark at room temperature for 30 minutes before being washed in PBS for 5 minutes. The slides were sealed with coverslips using Vectashield hard set mounting medium with DAPI (Vector).

The IF results were observed under a Zeiss Axioskop 2 fluorescence microscope using appropriate filters, and pictures were captured using Smart Capture 2 software.

2.3.6 Proximity Ligation Assay (PLA) using the Duolink *in situ* PLA Kit

PLA was performed using reagents and directions supplied in the Duolink *in situ* PLA kit, Duolink II Probemaker kit or DuolinkII Fluorescence kit (Olink Bioscience). All the incubation processes were performed in a pre-warmed humidity chamber at 37°C unless stated otherwise.

Negative controls for the PLA experiments included a sample with only one primary antibody to one of the target proteins, and a sample with a pair of primary antibodies raised against one target protein, and a protein that was not expected to interact with the target protein (based on function and/or subcellular localisation).

2.3.6.1 Probing

Slides of fixed mouse tissue or cells obtained from section 2.1.5 were subjected to deparaffinization, rehydration and antigen retrieval as described in section 2.3.4.1. A hydrophobic slide marker, PAP pen (BioGenex), was used to draw a hydrophobic circle around the tissue section on each slide so that the area of reaction was no larger than 1cm^2. The Duolink Blocking stock and the Antibody Diluent stock were diluted 1:5 in dH_2O respectively. 40µl of the Blocking solution was added to each slide. After 30 minutes incubation, the Blocking Solution was tapped off the slides and two primary antibodies diluted in the Antibody Diluent were added onto the slides and the slides were incubated for 30 minutes. Next, the slides were washed in 1x TBST for 5 minutes x 2. The slides were then incubated for 2 hours with two PLA probes (anti-rabbit and anti-sheep) diluted in the Antibody Diluent.

2.3.6.2 Hybridization

Duolink Hybridization stock was diluted 1:5 in dH_2O and mixed well. The slides were washed with 1x TBS-T for 2 x 5 minute under gentle shaking, and 40µl

of the hybridization solution was added on each reaction area. The slides were then incubated for 15 minutes.

2.3.6.3 Ligation

After hybridization, the remaining solution was tapped off the slides and the slides were washed in 1x TBS-T for 1 minute under gentle agitation. The ligation reagent was prepared by diluting the Duolink Ligation stock 1:5 in dH_2O and mixing with the Duolink Ligase. For each reaction 1µl Ligase was added to 39µl Ligation solution. 40µl of the mixture was added to each reaction area, and the slides were incubated for 15 minutes.

2.3.6.3 Amplification

The Ligation-Ligase solution was removed from the slides and the slides were washed using 1x TBS-T for 2x 2 minutes. A solution made by diluted Amplification stock (1:5 in dH_2O) and Polymerase (diluted 1:80 in the Amplification solution and vortexed) was added to the slides (40µl per reaction area). The slides were incubated for 90 minutes.

2.3.6.4 Preparation for imaging

The slides were then washed in 1x TBS-T for 2x 2 minutes under gentle shaking, and 40µl of the Duolink Detection solution 613 (stock diluted 1:5 in dH_2O) was added to each reaction area. Slides were incubated for 60 minutes.

The slides were then washed in the following reagents in a dark room: 2x SSC for 2 minutes, 1x SSC for 2 minutes, 0.2x SSC for 2 minutes, 0.02x SSC for 2 minutes, and 70% ethanol for 1 minute. The slides were left to dry in a dark room.

Finally the slides were mounted with a coverslip using a minimal volume of Duolink Mounting Medium containing DAPI.

2.3.6.5 Imaging

PLA signals were visualized by a Zeiss Axioskop 2 fluorescent microscope with appropriate filters, and pictures were captured using Smart Capture 2 software.

2.3.7 PLA using the Duolink II Probemaker kit

2.3.7.1 Antibody conjugation

Conjugation of the antibody and an oligonucleotide was performed to make a custom PLA probe. The process followed the protocol supplied with Duolink II Probemaker kit (Olink Bioscience). Briefly, 2µl Conjugation Buffer was added to 20µl antibody and then mixed gently with a pipette. The mixture was added to the vial of activated oligonucleotide (Duolink II Plus or Minus for each antibody) and incubated at room temperature overnight. 2µl of the Stop Buffer was added to terminate the reaction, and the solution was incubated at room temperature for 30 minutes. Finally, 24µl of Storage Solution was added to the conjugated probe for storage.

2.3.7.2 Probing

Slides were treated as described in section 2.3.6.1 with conjugated probes instead of PLA probes, but with one drop of the Block Solution from Duolink II Probemaker kit instead of diluted blocking solution.

2.3.7.3 Detection

In this thesis Duolink II Detection Reagents Red was used, which contained reagents for ligation and amplification.

After probing, the solution was tapped off the slides and the slides were washed twice in 1x Wash Buffer for 5 minutes under gentle agitation. 40µl of a solution for the oligo ligation containing the Ligation solution (Ligation stock diluted 1:5 in dH_2O) and the Ligase (diluted 1:40 in the Ligation solution immediately before addition to the samples, and vortexed to mix) was added to each reaction area, and the slides were incubated for 30 minutes.

Subsequently, the Ligation-Ligase solution was removed from the slides and the slides were washed using 1x Wash Buffer A for 2 minutes x 2. A solution made by diluted Amplification stock (1:5 in dH_2O) and Polymerase (diluted 1:80 in the Amplification solution before addition to the samples, and vortexed to mix) was added to the slides (40µl per reaction area). All the diluting steps were performed in dark because of the light sensitivity of the reagents. The slides were incubated for 100 minutes.

2.3.7.4 Preparation for imaging

The slides were then washed twice in 1x Wash Buffer B for 10 minutes under gentle shaking, and then in 0.01x Wash Buffer B for 1 minute. The slides were left to dry in a dark room. Finally the slides were mounted with a coverslip using a minimal volume of Duolink II Mounting Medium with DAPI.

2.3.7.5 Imaging

PLA signals were visualized by a Zeiss Axioskop 2 fluorescent microscope with appropriate filters, and pictures were captured using Smart Capture 2 software.

2.3.8 PLA using the DuoLink II Fluorescence kit

The PLA experiments using this kit were performed with commercially supplied PLA probes, and followed the same steps as described in 2.3.6.1, 2.3.7.3, 2.3.7.4 and finally 2.3.7.5.

2.4 Molecular biology methods

2.4.1 PCR sample preparation

2.4.1.1 RNA extraction

To extract RNA from cultured cells, cell pellets were collected as described in section 2.2.1 and total RNA was extracted following the protocol for cultured cells supplied with the RNeasy Mini Kit (Qiagen).

To extract RNA from frozen tissues, mouse tissue samples of less than 30 mg were used following the protocol for animal tissues supplied with RNeasy Mini Kit (Qiagen).

During extraction, RNA was treated for 15 minutes with DNase I (Qiagen) to minimise any DNA contamination. RNA concentration (ng/µl) in samples was assessed using a NanoDrop 1000 device (Thermo Scientific).

2.4.1.2 cDNA synthesis

In order to synthesize cDNA from mRNA, the High-Capacity cDNA Reverse Transcription Kit (Applied Biosystems) was used following the standard protocol supplied. Each reaction contained the following composition:

10 x Reaction Buffer	2.0µl
25x Deoxynucleotide Mix (100mM)	0.8µl
10x RT Random primers	2.0µl
RNase inhibitor	1.0µl
Reverse transcriptase	1.0µl
RNA sample	10µl
dH_2O	3.2µl

The following condition was used to perform reverse transcription cycles:

Step 1	25°C	10 minutes
Step 2	37°C	120 minutes
Step 3	85°C	5 seconds
Step 4	4°C	5 minutes

The cDNA produced was kept at 4°C for short term or -20°C for long term storage. Samples with no RNA and samples with no reverse transcriptase were used as negative controls and were subjected to the same procedure as the other samples.

2.4.2 PCR reactions

2.4.2.1 PCR with Taq Polymerase

In a regular PCR amplification, each reaction was prepared as follows:

PCR Buffer	1µl
2.5 mM Deoxynucleotide Mix	2µl
Forward primer (0.25µM)	2.5µl
Reverse primer (0.25µM)	2.5µl
Sigma Taq buffer	2.5µl
Taq DNA polymerase	0.5µl
dH_2O	14µl
Template DNA	1µl

The following conditions were programmed on an MJ Research PTC-255 DNA Thermal Cycler (MJ Research, USA) to perform the following DNA amplification cycles:

Step 1	x1	95°C	3 minutes
Step 2	x35	94°C	30 seconds
		54-57°C	30 seconds
		72°C	30 seconds
Step 3	x1	72°C	10 minutes
Step 4	x1	4°C	5 minutes

2.4.2.1 Quantitative PCR (qPCR, Real Time PCR)

qPCR was performed with a standard curve method for the quantification of gene expression. Primers of each gene were designed to amplify a product of 100-180bp with no secondary structure and with low primer dimer formation. To avoid amplification of genomic DNA, primers were designed across splice junctions. The accumulation of PCR product was detected by a fluorescent SYBR Green dye (Finnzymes).

For each reaction, the mixture was made up as follows:

2x DyNAmo Flash Master mix	10µl
Forward primer (0.25µM)	2µl
Reverse primer (0.25µM)	2µl
Template cDNA	2µl
dH_2O	4µl

Samples with no template cDNA, samples with no Reverse Transcriptase sample, as well as a sample of dH_2O only were used as negative controls.

The following programme was used on MyiQ Thermal Cycler (Bio-Rad) to perform DNA amplification cycles:

Step 1	x1	95°C	6 minutes
Step 2	x40	95°C	10 seconds
		60°C	20 seconds
		72°C	20 seconds –data collection
Step 3	x1	95°C	1 minute
Step 4	x1	60°C	1 minute
Step5	x80	60°C	10 seconds –data collection (temperature increased by 0.5°C per cycle to produce the melt curve)

A series of diluted cDNA (1:10, 1:100, 1:1000 and 1:10000 respectively) was used to conduct a standard curve for each pair of primers. Results with efficiencies between 90-105% were used for further analysis. Samples were always in triplicate and the mean was taken for the analysis.

To compare the gene expression in the tissues from wild type and wasted mice, the Ct value of the target gene (Ct_{tgt}) was normalised against the Ct value of the reference gene (Ct_{ref}) using the following fomula:

$$\Delta Ct = Ct_{tgt} - Ct_{ref}$$

The ΔCt values from wild type (ΔCt_{wt}) and wasted (ΔCt_{wst}) mouse samples were then used to calculate the ratio of the gene expression in wasted to wild type mouse samples using the following formula:

$$\text{Comparative expression} = 2^{-(\Delta Ctwst - \Delta Ctwt)}$$

2.4.3 DNA electrophoresis

DNA electrophoresis was performed to confirm the specificity of the PCR products. Agarose gels were made by dissolving the agarose powder in 0.5x TBE buffer to reach a concentration of 1.5 to 2% (w/v) depending on the expected size of the PCR products. Agarose solution was microwaved for at least 2 minutes and cooled under running tap water. SYBR Safe DNA gel stain (Invitrogen) was added to the solution at a final concentration of 1% (v/v). The mixture was then poured into a plastic tray with combs, and left to set at room temperature. Orange G loading buffer at 10% (v/v) of the total sample volume was added to the DNA samples and mixed. The tray with the agarose gel was placed in an electrophoresis tank filled with 0.5x TBE buffer and the comb was removed. The mixed DNA samples were loaded into the wells, with a 100bp-1kb DNA ladder (New England BioLabs) loaded into one well as a molecular weight marker. The gel was run at 100 V for 30 to 90 minutes

until the orange line was approximately 0.5 cm from the edge of the gel. Gels were then removed from the tank and visualized under UVIdoc Gel Documentation System (UVItec).

Chapter 3 Expression of eEF1B subunits in diseases

3.1 Introduction

Protein synthesis is a crucial process in cells tightly controlled by a group of translation factors. Alteration in the expression of specific translation factors in tumourigenesis has been recognised. The roles of initiation factors (eIFs) in tumourigenesis have been extensively studied (reviewed in Silvera, Formenti et al. 2010). eEF1A, especially eEF1A2, has also been found to be oncogenic (reviewed in Lee and Surh 2009).

Increase of eEF1B expression in different cancers was also demonstrated (reviewed in section 1.4.4.1), and most of the studies focused on the change at the mRNA level. A study examining ten human cancer cell lines using real time PCR has observed overexpresson of eEF1Bδ and eEF1Bγ mRNA in breast cancer cell lines compared to normal human primary breast cell lines. eEF1Bδ showed an overexpresson (2- to 10-fold) in cell lines T47D, MCF-7, MDA-MB-361, and MDA-MB-453, while eEF1Bγ showed an overexpresson (2- to 10-fold) in T47D and MCF-7 cells (Joseph, O'Kernick et al. 2004). Another study using Northern blot analysis found increased levels of eEF1Bα and eEF1Bγ mRNA in T47D and MDA-MA-231 cell lines, but not MCF-7 compared to non-transformed breast epithelial cell line MCF-10A. The study also demonstrated a significant increase of eEF1Bα and eEF1Bγ mRNA levels in breast cancer tissues over those in normal or fibroadenoma tissues (Al-Maghrebi, Anim et al. 2005). It is unknown whether the overexpresson of eEF1B subunits happens also at the protein level.

The regulation of translation factors in neuronal cells is associated with neuronal defects. Translational control is important for long-lasting synaptic plasticity and memory by regulating the translation of certain RNAs in response to different synaptic stimulation, including titanic stimulation, treatment with brain-

derived neurotrophic factor (BDNF) (reviewed in Wang and Tiedge 2004; Costa-Mattioli, Sossin et al. 2009). Mutations of each of the five subunits of translation initiation factor eIF2B can cause leukoenocephalopathy with vanishing white matter (VWM) and childhood ataxia with central nervous system hypomyelination (CACH) (reviewed in Scheper, van der Knaap et al. 2007; Pavitt and Proud 2009). Absence of eEF1A2 causes a wasted phenotype in mice (Chambers, Peters et al. 1998; Abbott, Newbery et al. 2009) as described in section 1.5.

So far not much is known about the involvement of eEF1B in MND. A study in the role of copy number variations (CNVs) in amyotrophic lateral sclerosis (ALS) reported eEF1Bδ as a potential ALS candidate (Wain, Pedroso et al. 2009). ALS is a fatal neurodegenerative disease characterized by the selective death of motor neurons in the spinal cord, brainstem and cortex. Using both region-based and gene-based association analyses, Wain and colleagues found that the gene encoding eEF1Bδ was covered in a CNV region that was associated with ALS. In 575 ALS cases examined, CNV overlapped with the EEF1D gene by at least 1 base pair; in 7 cases there were losses and in 3 gains. Microarray results have identified a lower level of eEF1Bγ, but not eEF1Bδ, in ALS patients than controls (Bakay, Wang et al. 2006).

In this study the expression of eEF1B in breast cancer and MND cases were examined in order to further establish the relationship between eEF1B and diseases.

3.2 Result

3.2.1 eEF1B in normal and transformed cell lines

Twelve cell lines were examined for the expression of eEF1B subunits at the protein level. Three of the cell lines are untransformed cell lines, including NIH3T3, Rat2 and Hek293 cell lines. Others are cancer cell lines originating from different human tissues. The species and cell types in detail are shown in Table 2.2.

eEF1Bα was detected in all cell lines except in MCF-7, and showed a lower expression in Rat2, HeLa and T47D cell lines. An extra band lighter than the normal eEF1Bα band (about 20 kD, indicated by Arrow A in Figure 3.1 A) was detected in HeLa, HCT116, PC3, T47D, MDA-MB-231, and MDA-MB-453 cells, but not in others (Figure 3.1 A).

eEF1Bδ appeared as two bands that were very close to each other, representing two isoforms of eEF1Bδ. Like eEF1Bα, there was no visible band in MCF7 cells, but the loading control shows that there was less protein in this track compared with most other cell lines. eEF1Bδ was weaker in Rat2, PC3, T47D cells. Extra bands lighter than normal eEF1Bδ were observed in T47D, HeLa and MDA-MB-453 cells (about 24 kD, indicated by Arrow B in Figure 3.1 B). In MCF7 cells where no eEF1Bα or eEF1Bδ was detected, longer exposure time of the blots also failed to show any band of eEF1Bα or eEF1Bδ (data not shown). Although in the blot shown in Figure 3.1 no eEF1Bδ band of normal size was shown in HeLa cells, in a separate Western blot on the same HeLa cell extract eEF1Bδ showed the normal sized bands as well as the lower band (data not shown).

The expression patterns of eEF1Bγ in all cell lines tested were similar, with no obvious differences observed except that in MCF7 it was weaker (Figure 3.1 C).

Since the cell lines tested are from different tissues and species, the results were not quantified to compare the expression level of eEF1B in cancer cell lines and

in untransformed cell lines, but it can be seen that compared to untransformed cell lines, eEF1Bα and eEF1Bδ have different expression patterns in certain cancer cell lines.

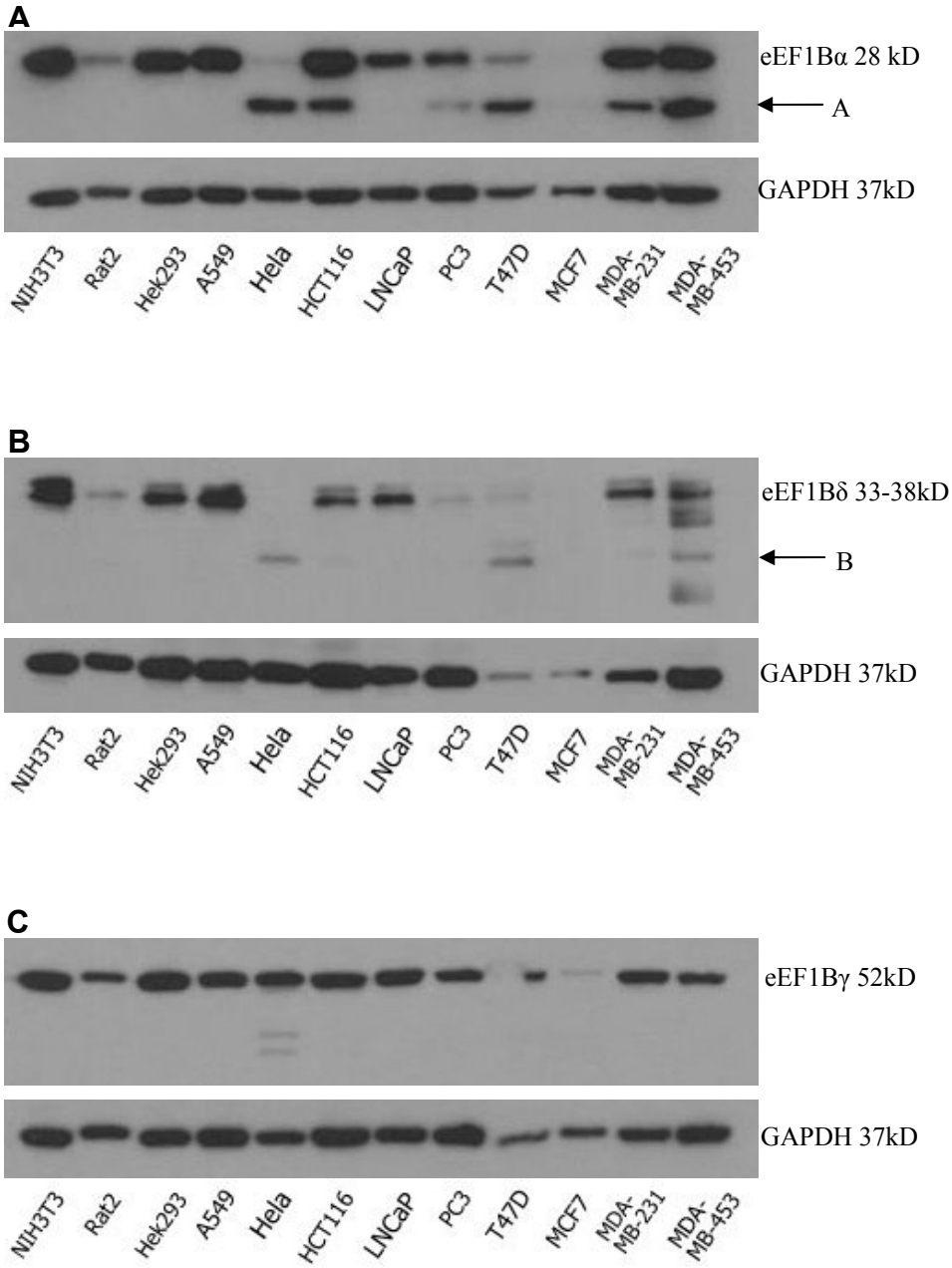

Figure 3.1. WB analysis of eEF1B subunits expression in untransformed cell lines (NIH3T3, Rat2 and Hek 293) and transformed cell lines (A549, HeLa, HCT116, LNCap, PC3, T47D, MCF7, MDA-MB-231 and MDA-MB-453). GAPDH was used as a loading control. Arrow A indicates the lower bands for eEF1Bα. Arrow B indicates the lower band for eEF1Bδ.

3.2.2 eEF1Bα and eEF1Bδ in breast cancer tissues

Since eEF1Bα and eEF1Bδ showed some changes in transformed cell lines, the expression of these two isoforms was then examined in a panel of breast cancer tissues.

The breast consists of branching duct systems extending from the nipple and leading to the terminal duct lobular unit (TDLU), which branches into a cluster of small acini to form a lobule. The ducts and acini are lined by two layers of cells, a luminal layer of epithelial cells and a discontinuous basal layer of myoepithelial cells. The majority of breast stroma is composed of dense fibrous tissues and adipose tissues.

In breast tissue eEF1Bα and eEF1Bδ were present in the cytoplasm of epithelial cells and myoepithelial cells, as well as in stromal cells (Figure 3.2 a-i and Figure 3.3 a-i).

The expression of eEF1Bα in breast cancer tissues showed no prominent difference from normal tissues (Figure 3.2). In all 24 cases, only one (Figure 3.2 F) showed an apparent higher expression of eEF1Bα than normal tissue (Figure 3.2 f). In some cases the overall staining of eEF1Bα appeared stronger in cancer tissues than their corresponding normal tissues, but it was possibly because the sections derived from normal tissues contains mainly adipose tissue or fibrous interlobular tissues (Figure 3.2 b, c, d, e, h and k). In other cases the staining in cancer and normal tissues showed no significant difference.

eEF1Bδ expression in breast cancer tissues (Figure 3.3) was similar to eEF1Bα, showing no significant difference between cancer and normal tissues. Apparent higher expression in cancer tissues was seen only in 2 cases out of 24 (Figure 3.3 A and K). Some cases of normal tissue contained mainly interlobular tissues (Figure 3.3 b, c, d, e, h and k), as with those for eEF1Bα. There were several sections that

showed no staining for eEF1Bδ (Figure 3.3 E, J, i and j), which was most likely an experimental artefact, possibly caused by fixation differences among samples.

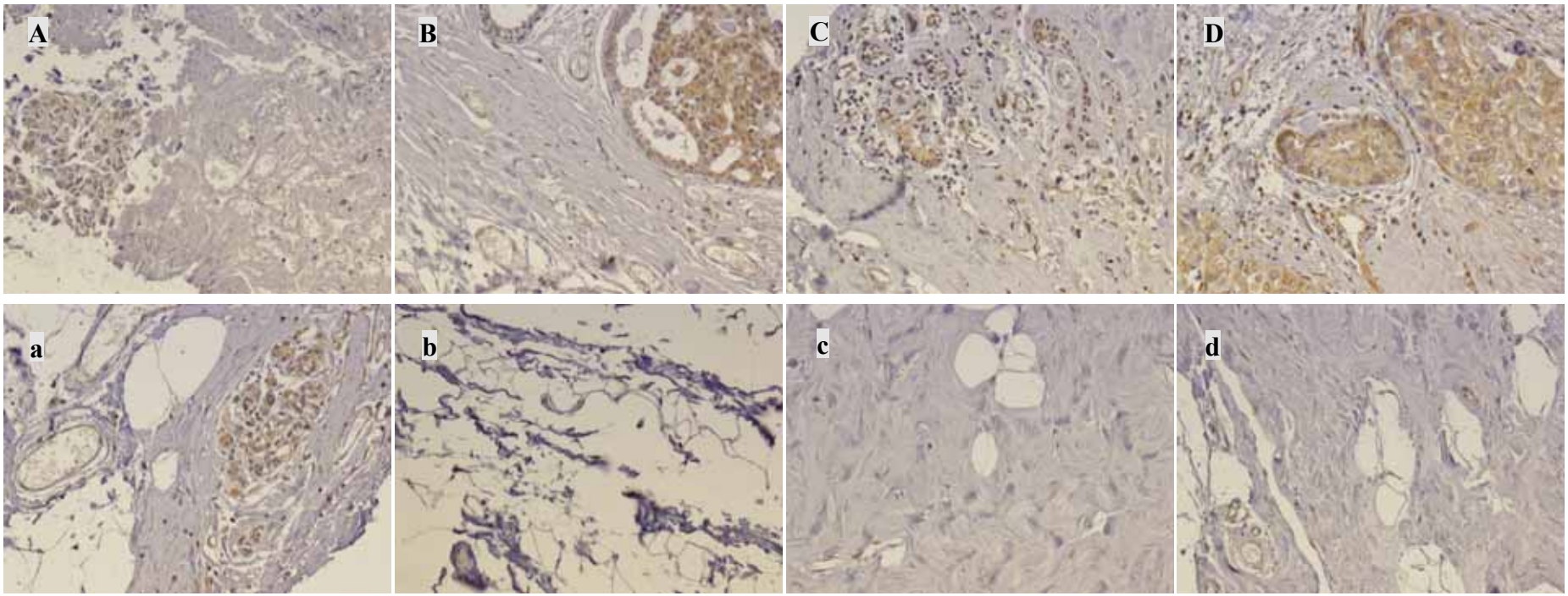

Figure 3.2. Expression of eEF1Bα in breast cancer. A-L. Breast cancer tissues. a-l. corresponding non-neoplastic breast tissues.

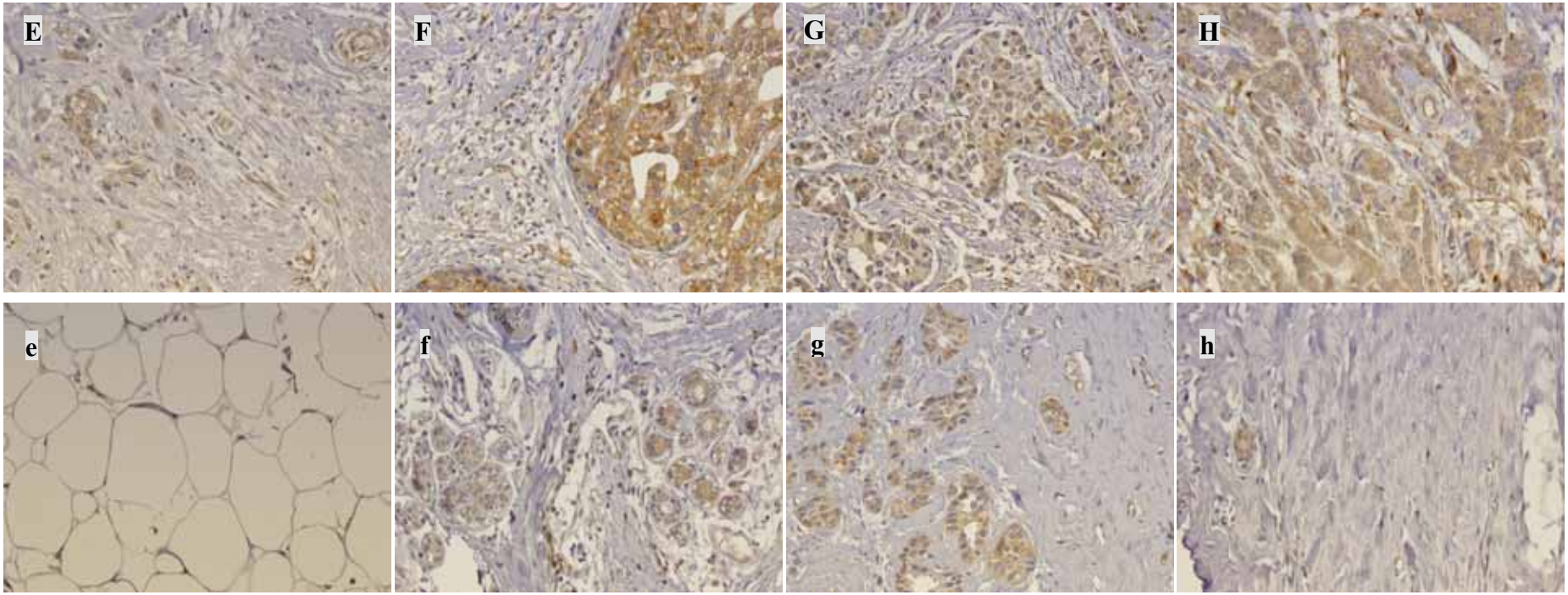

Figure 3.2 continued.

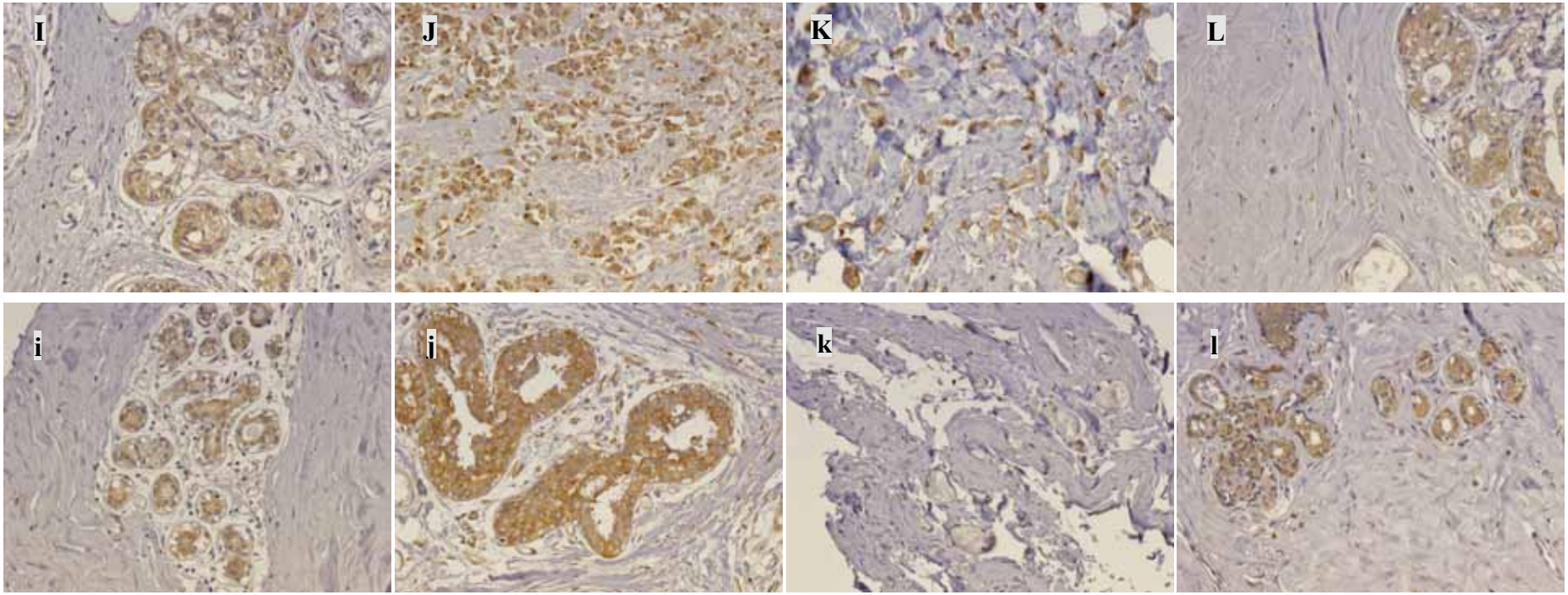

Figure 3.2 continued.

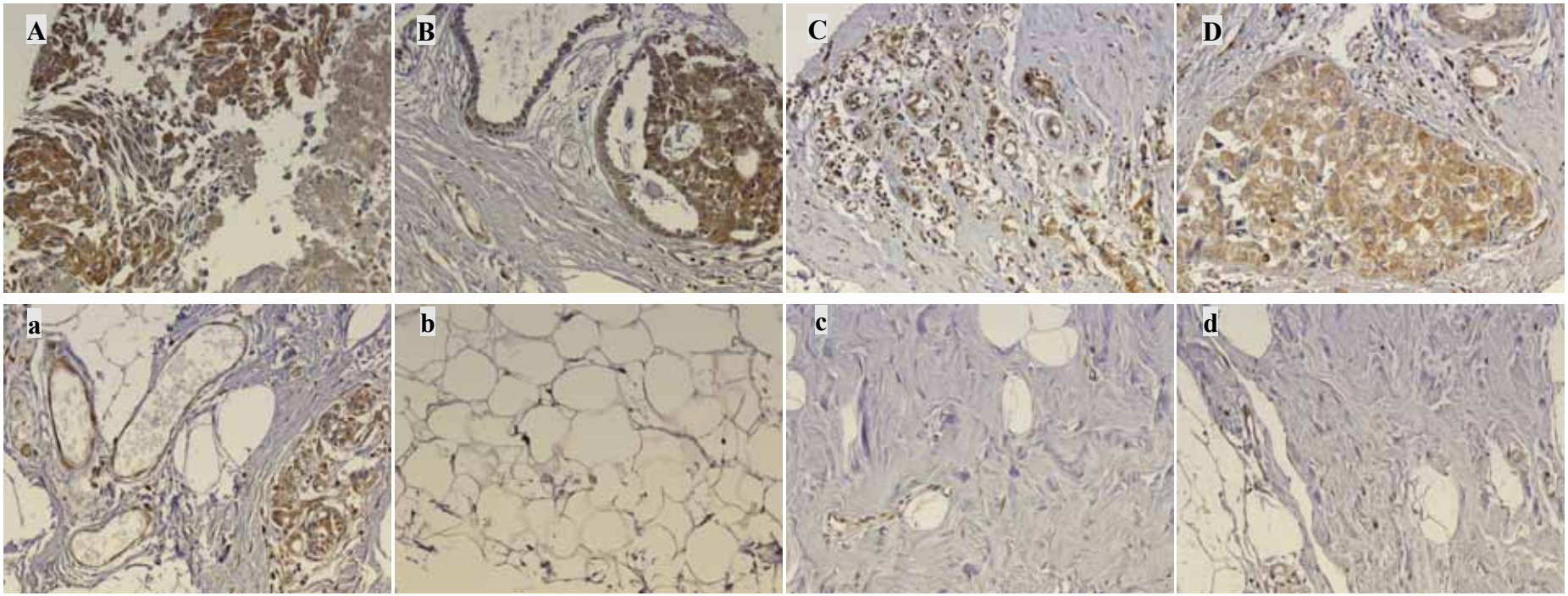

Figure 3.3. Expression of eEF1Bδ in breast cancer. A-L. Breast cancer tissues. a-l. corresponding non-neoplastic breast tissues.

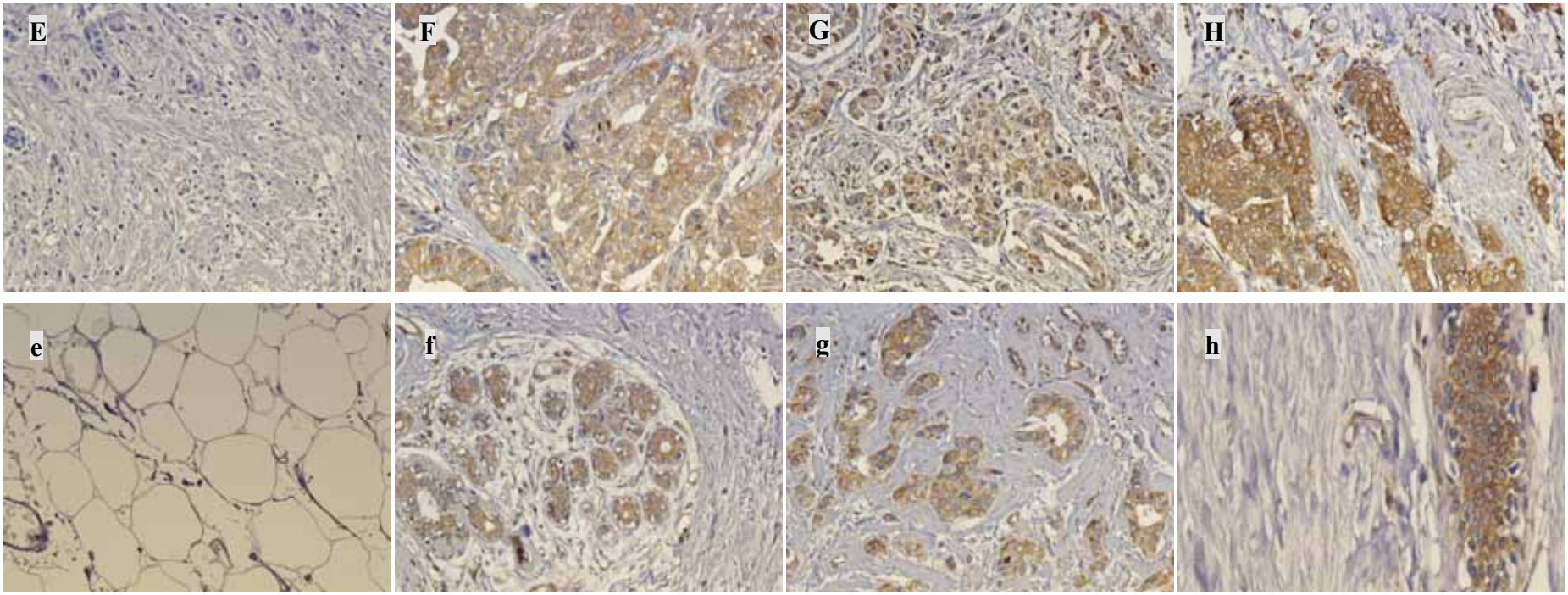

Figure 3.3 continued.

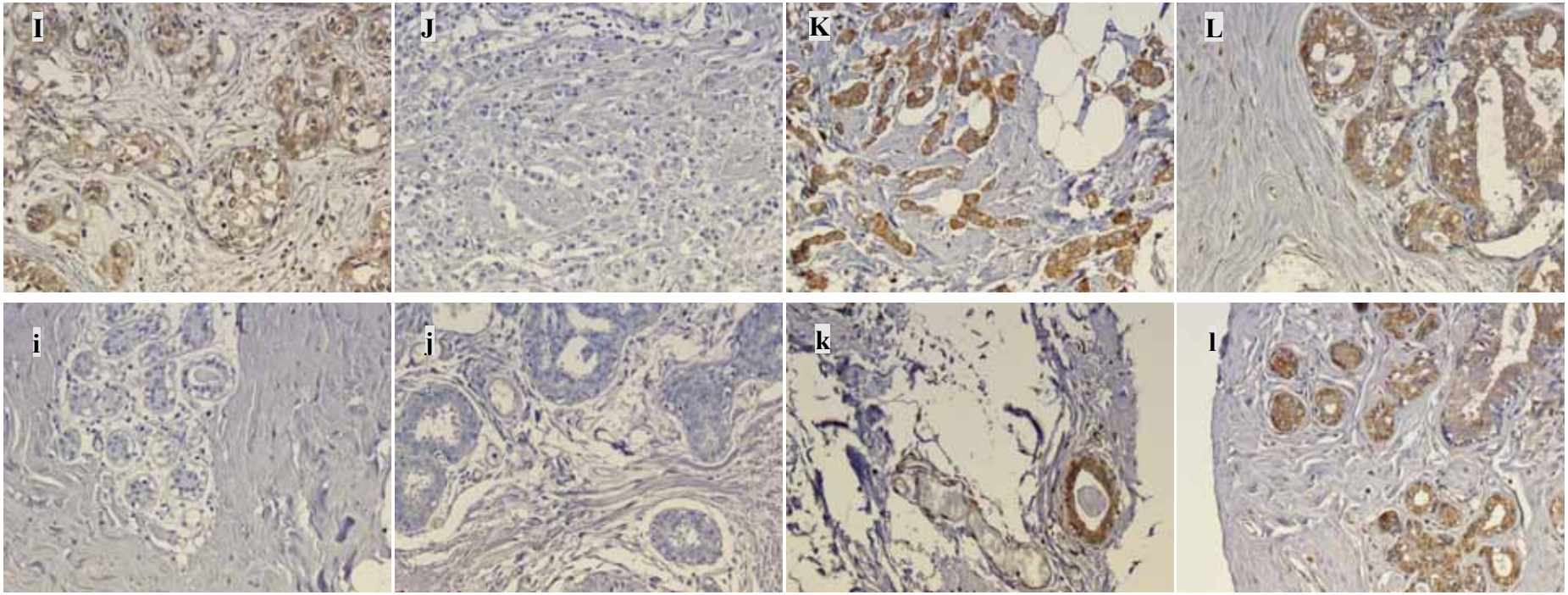

Figure 3.3 continued.

3.2.3 Knockdown of eEF1B in NSC34 cells

All the RNAi experiments in this thesis were carried out in NSC34 cells. NSC34 is a hybrid cell line produced by fusion of motor neuron enriched, embryonic mouse spinal cord cells with mouse neuroblastoma, and expresss motor neuron properties (Cashman, Durham et al. 1992). NSC34 cells express the shorter isoforms as well as the tissue-specific isoform of eEF1Bδ, so the loss of shorter and longer isoforms could be studied respectively.

3.2.3.1 Validation of siRNAs

In order to validate the siRNAs, the cells transfected with each siRNA were collected and expression levels of corresponding proteins were examined using Western blotting. Different siRNA concentrations and cell harvest times after transfection were tested for optimisation (data not shown). In this study cells were harvested 72 hours after transfection using siRNAs at a concentration of 10nM. For each gene, two different siRNAs targeting different sequences were used and each knockdown was performed in triplicate. A non-targeting siRNA was used as a negative control.

Commercial pre-designed siRNAs targeting each eEF1B subunit were shown to be specific and efficient under the experimental condition of this study. Two eEF1Bα siRNAs knocked down eEF1Bα protein in NSC34 cells with similar efficiency, respectively by 51% and 49% on average (Figure 3.4 A2). Similar results were gained by the two eEF1Bγ siRNAs, both of which knocked down eEF1Bγ by 70% on average (Figure 3.4 D2). Both eEF1Bδ siRNAs knocked down eEF1Bδ in NSC34 cells, although siRNAa is more efficient than siRNAb. While eEF1Bδ siRNAa knocked down almost all eEF1Bδ protein, siRNAb knocked down eEF1Bδ proteins by 63% and eEF1BδL by 40% (Figure 3.4 B2).

Since the commercial eEF1Bδ siRNAs knockded down all isoforms, siRNAs targeting eEF1Bδ exon 3, which is only transcribed in eEF1BδL, were designed to knockdown eEF1BδL. As shown in Figure 3.4 C, eEF1BδL siRNAs were also proved to be specific and efficient, which knockded down almost all eEF1BδL expression while other eEF1Bδ isoforms were not affected. However, because the track of negative control on the Western blot seemed to be affected with probably an air bubble since the band shown was slightly smaller than the correct size, the result of this knockdown was not quantified.

3.2.3.2 Decrease of eEF1B did not affect cell viability 72 hours after transfection

To demonstrate the effect of eEF1B knockdown on cell viability, an MTT assay was performed on NSC34 cells 72 hours after transfection. Absorbance at 570nm were recorded and normalised with cells-only control, representing relative cell viability. As shown in Figure 3.5, the viability of cells transfected with each siRNA appeared slightly lower, but showed no statistical difference from controls.

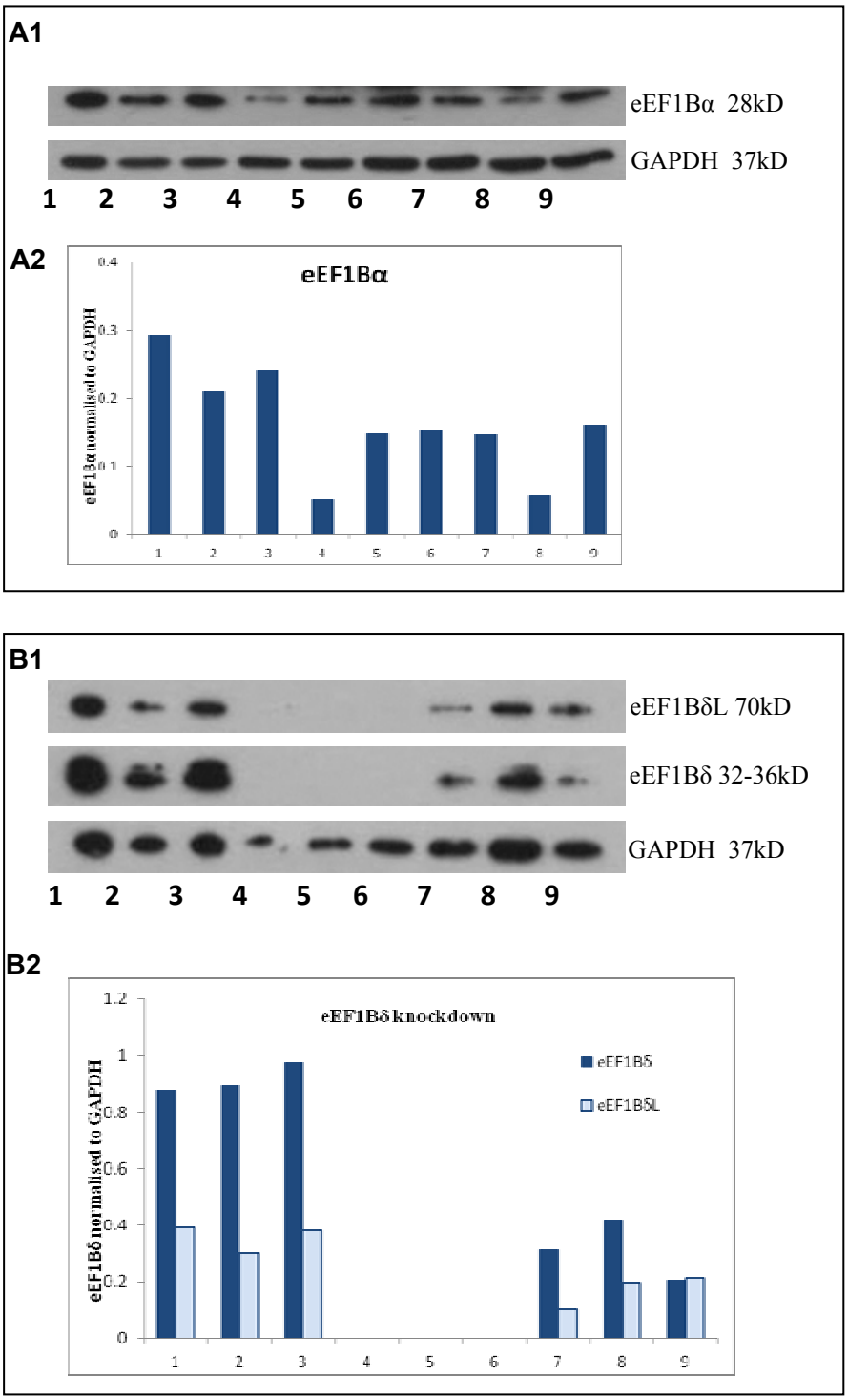

Figure 3.4. siRNAs targeting eEF1B subunits knocked down eEF1Bα (A1), eEF1Bδ (B1), eEF1BδL (C) and eEF1Bγ (D1) in NSC34 cells respectively, with quantifications of the relative expression levels of eEF1Bα (A2) eEF1Bδ (B2) and eEF1Bγ (D2). 1. Cells only. 2. Mock. 3. Non-targeting siRNAs. 4-6. Three samples treated with siRNAa. 7-9. Three samples treated with siRNAb.

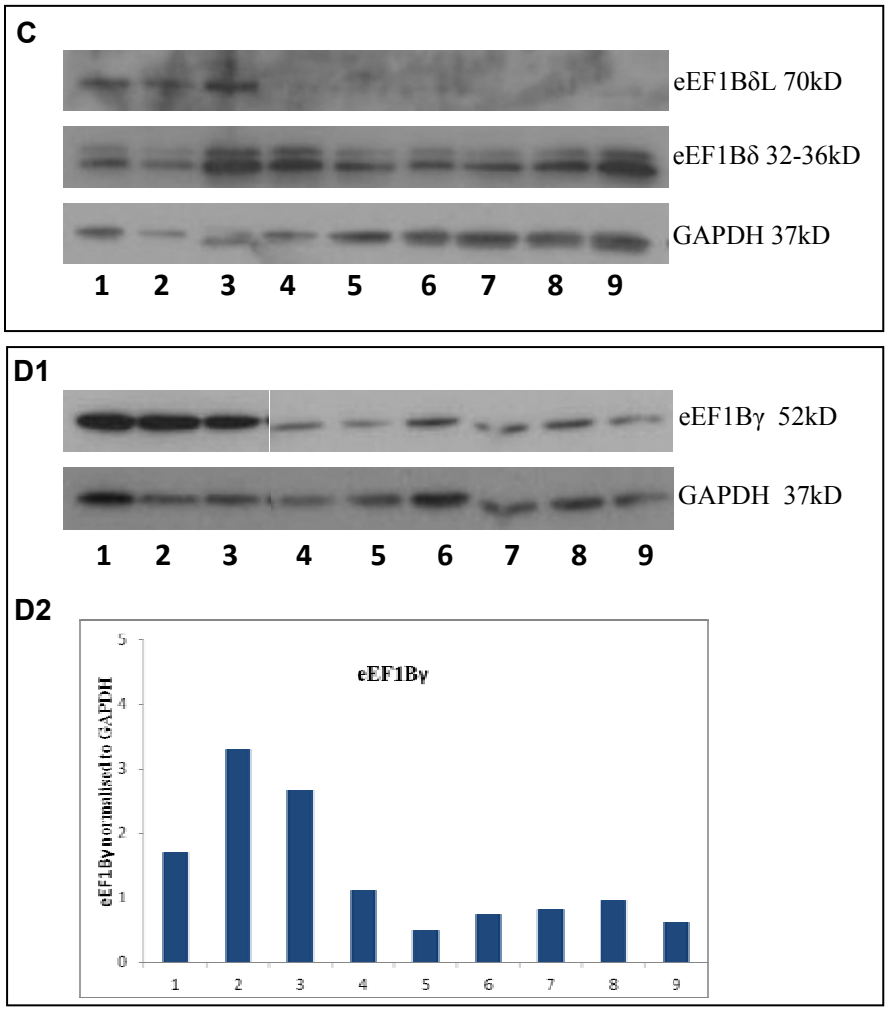

Figure 3.4. continued.

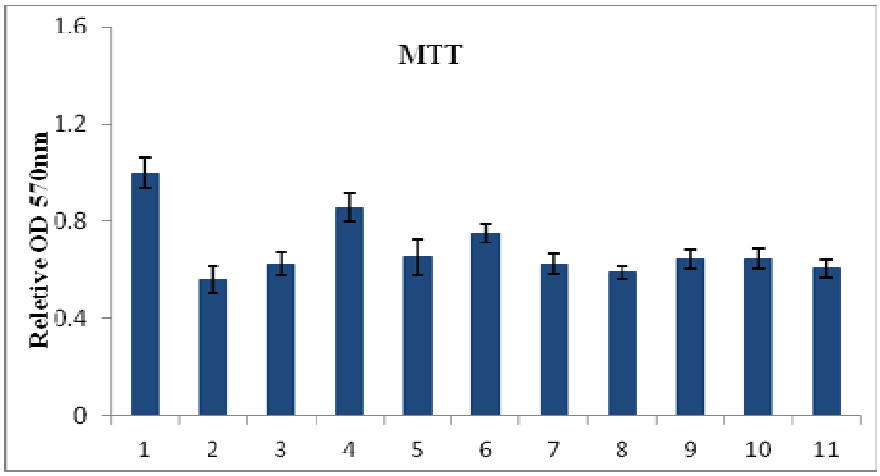

Figure 3.5. NSC34 cell viability after eEF1B subunits knockdown. 1. Cells only. 2. Mock. 3. Non-targetting siRNA. 4. eEF1Bα siRNAa. 5. eEF1Bα siRNAb. 6. eEF1Bδ siRNAa. 7. eEF1Bδ siRNAb. 8. eEF1BδL siRNAa. 9. eEF1BδL siRNAb. 10. eEF1Bγ siRNAa. 11. eEF1Bγ siRNAb. Error bars indicate SEM.

3.2.4 eEF1B in MND

3.2.4.1 eEF1B expression in the spinal cord of wasted mice

In mouse spinal cord sections, eEF1B subunits were almost ubiquitously expressed in the cytoplasm of all types of cell (Figure 3.6 A, B, C1 and C2), except a few cells with no apparent positive staining (solid arrows in Figure 3.6).

Wasted is a mouse model for MND which has no expression of eEF1A2, and is characterized by a wasted phenotype. The expression of eEF1B subunits in spinal cord from wasted mice was examined (Figure 3.6 a, b, c1 and c2) and compared with wild type spinal cord. In wasted mouse spinal cord the expression level of eEF1Bα appeared slightly lower than wild type mouse spinal cord, although there were a few cells that showed strong cytoplasmic staining (hollow arrows in Figure 3.6 a). Compared to wild type spinal cord, wasted mouse spinal cord showed a weaker staining for eEF1Bδ in some neurons and slightly stronger staining in others (Figure 3.6 b). Similarly, compared to wild type, in wasted spinal cord eEF1Bγ was also weaker in motor neurons, and relatively stronger in several cells (hollow arrows in Figure 3.6 c1). When the total eEF1Bγ protein level was examined using Western blotting, however, there was no apparent difference between wild type and wasted type spinal cord (section 5.2.1 and 5.2.2.1 of this thesis). This can be explained by the uneven expression of eEF1Bγ in wasted spinal cord, which was weaker than wild type in some cells but stronger in others (Figure 3.6 C2 and c2) therefore the Western blot experiment did not identify any difference overall. Moreover, the cells with stronger staining also showed nuclear staining, unlike other cells. Some other cells in the wasted mouse spinal cord showed stronger staining of eEF1B than in wild type. The reason for the strong staining is not clear, but might perhaps suggest the existence of intracellular inclusion bodies.

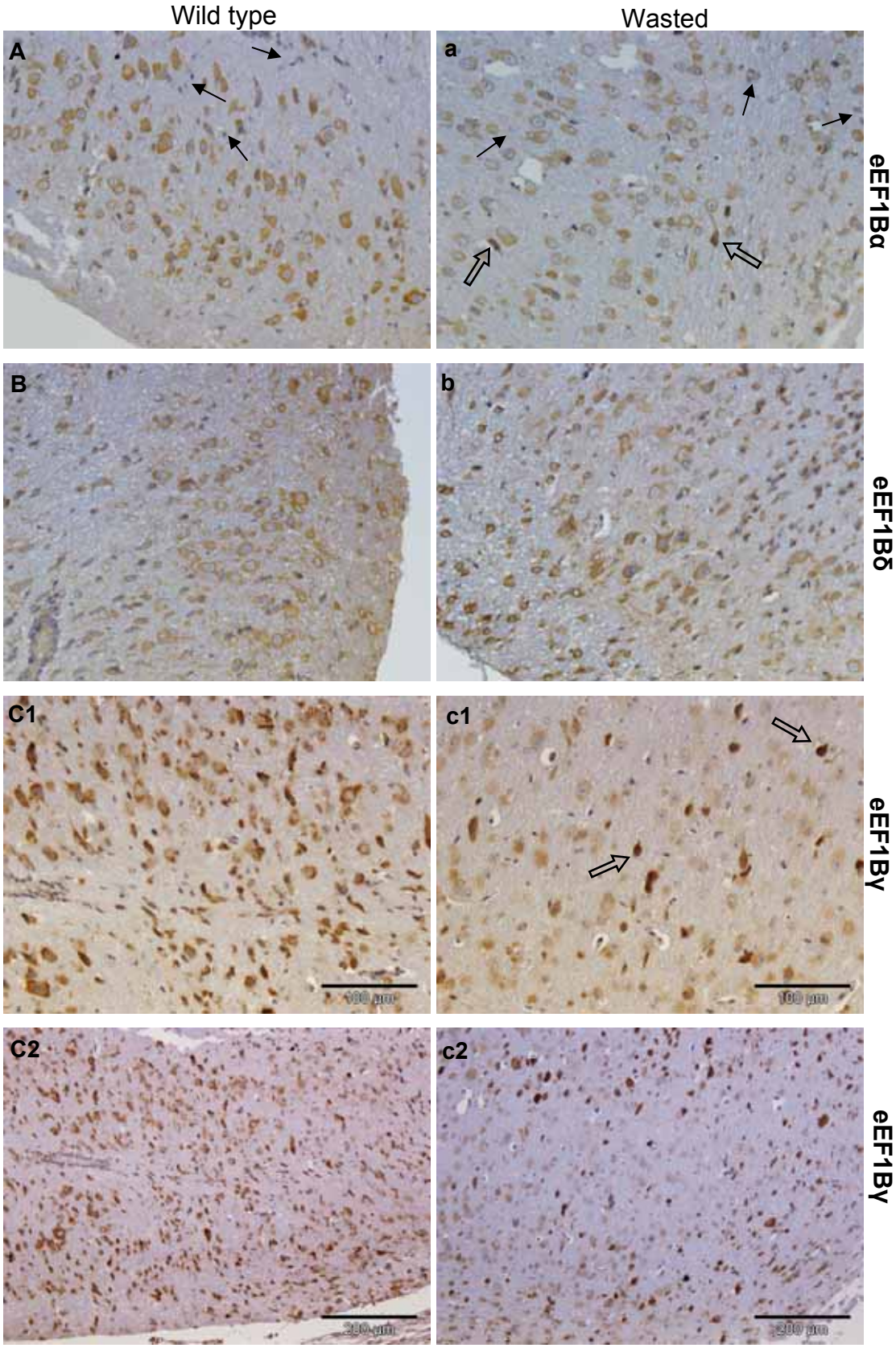

Figure 3.6. IHC analysis of eEF1Bα (A and a), eEF1Bδ (B and b) and eEF1Bγ (C1, C2, c1 and c2) expression in wild type (A to C) and wasted (a to c) mouse spinal cord. Solid arrows indicate cells with no apparent staining. Hollow arrows indicate cells with a stronger staining than others.

3.2.4.2 eEF1B expression in the spinal cord of MND patients

IHC analysis of eEF1B expression was also performed in human spinal cord sections, including 20 controls and 53 MND cases. Due to the restriction of patient sections, only eEF1Bα and eEF1Bδ were examined for this study. Unlike in wasted mice, the change of eEF1B expression in spinal cord sections from MND patients are more complicated.

In the sections from normal spinal cord, eEF1Bα and eEF1Bδ had similar expression patterns, and both were detected in neurons and some of the glial cells (Right panels in Figure 3.7 and 3.8). All neurons showed strong staining, most of which was cytoplasmic while others showed both cytoplasmic and nuclear staining. Axonal staining was also visible in some of the controls. One of the controls presented no motor neurons (Figure 3.7 a5), and eEF1Bα showed weak staining in one control (Figure 3.7 d4) due to a poor section. eEF1Bα and eEF1Bδ were seen only in a subset (1/3 to 1/2) of the glial cells in normal spinal cord.

The staining for eEF1Bα and eEF1Bδ in some spinal cord sections of MND patients showed an apparent difference from the controls (Left panels in Figure 3.7 and 3.8). It can be seen by eye that compared to the control sections, some MND cases showed a weaker staining for eEF1Bα (Figure 3.7 A1, A4 and B3) and/or eEF1Bδ in neurons (Figure 3.8 A1, B2 and C3), while some showed more glial staining (Figure 3.7 B2, Figure 3.8 A2, D1, D3 and D4). Furthermore, MND cases showed less axonal staining than controls, probably because of the loss of MN in some cases, yet since the cases and controls are from different donors it is hard to draw any conclusion at this stage.

Another significance of the results in MND cases is that some of the glial cells with eEF1Bα or eEF1Bδ staining appeared to be star-shaped or have branched processes, especially those in the white matter (Figure 3.7 B2, Figure 3.8 A2, C4, C5, D1, D3 and D4), which was almost absent in the controls. Although specific glial

markers are needed for identification, the distinctive morphology suggests that they were likely to represent certain type(s) of glial cells, such as astrocytes or microglia.

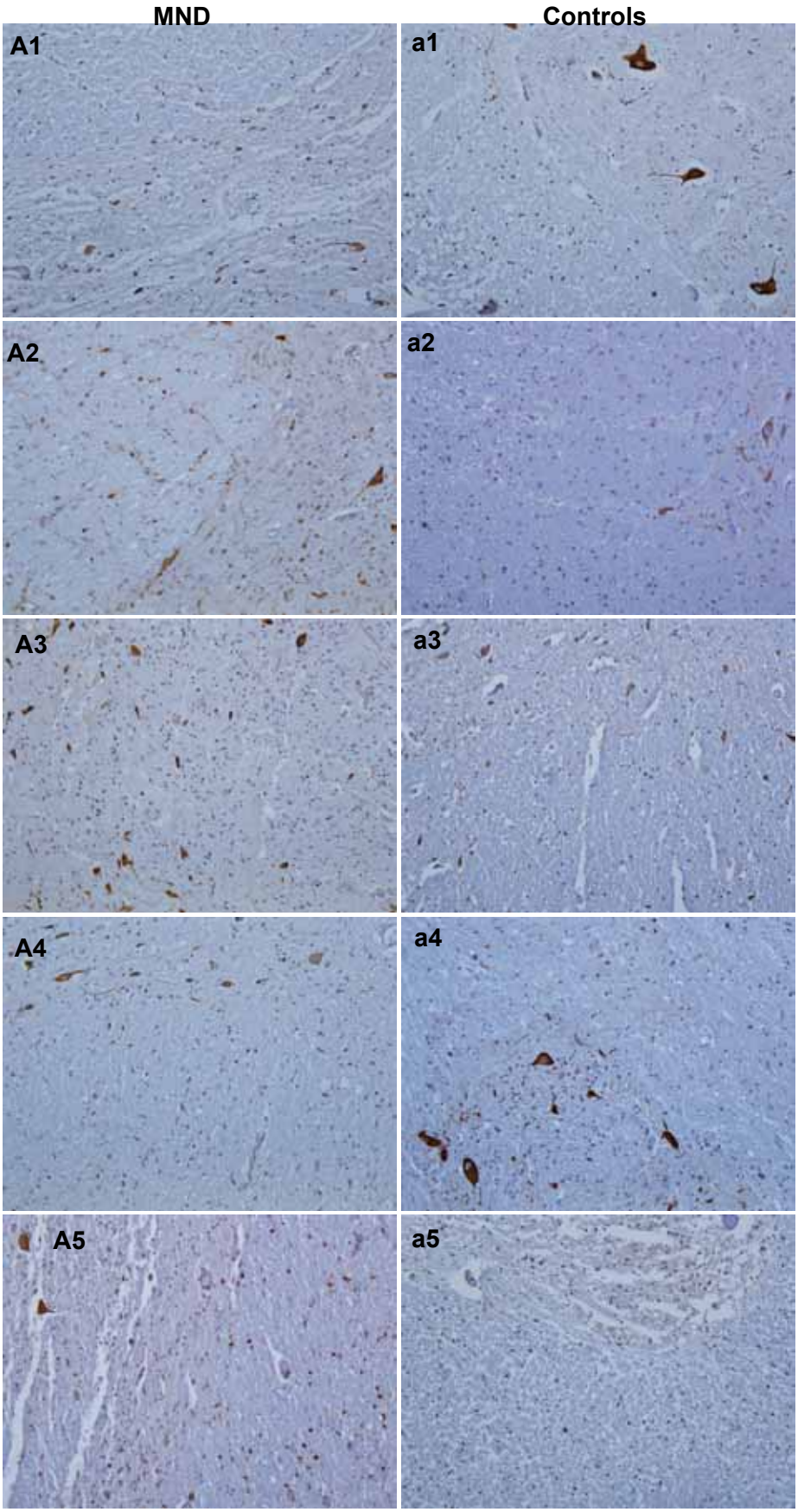

Figure 3.7. eEF1Bα in spinal cord sections from MND patients and controls. Left panel. Representative MND cases. Right panel. Controls. Scale bar, 200μm.

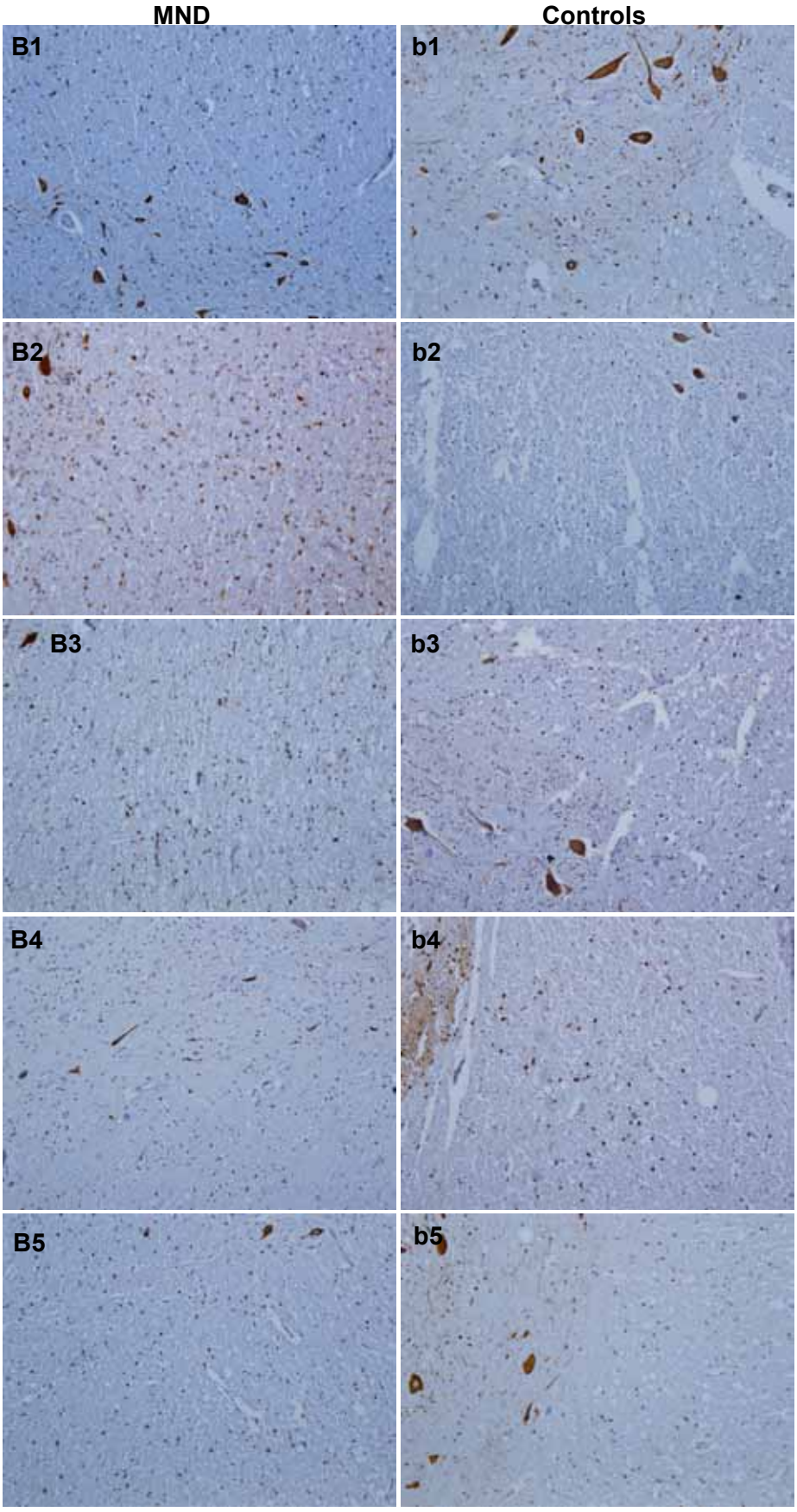

Figure 3.7. continued.

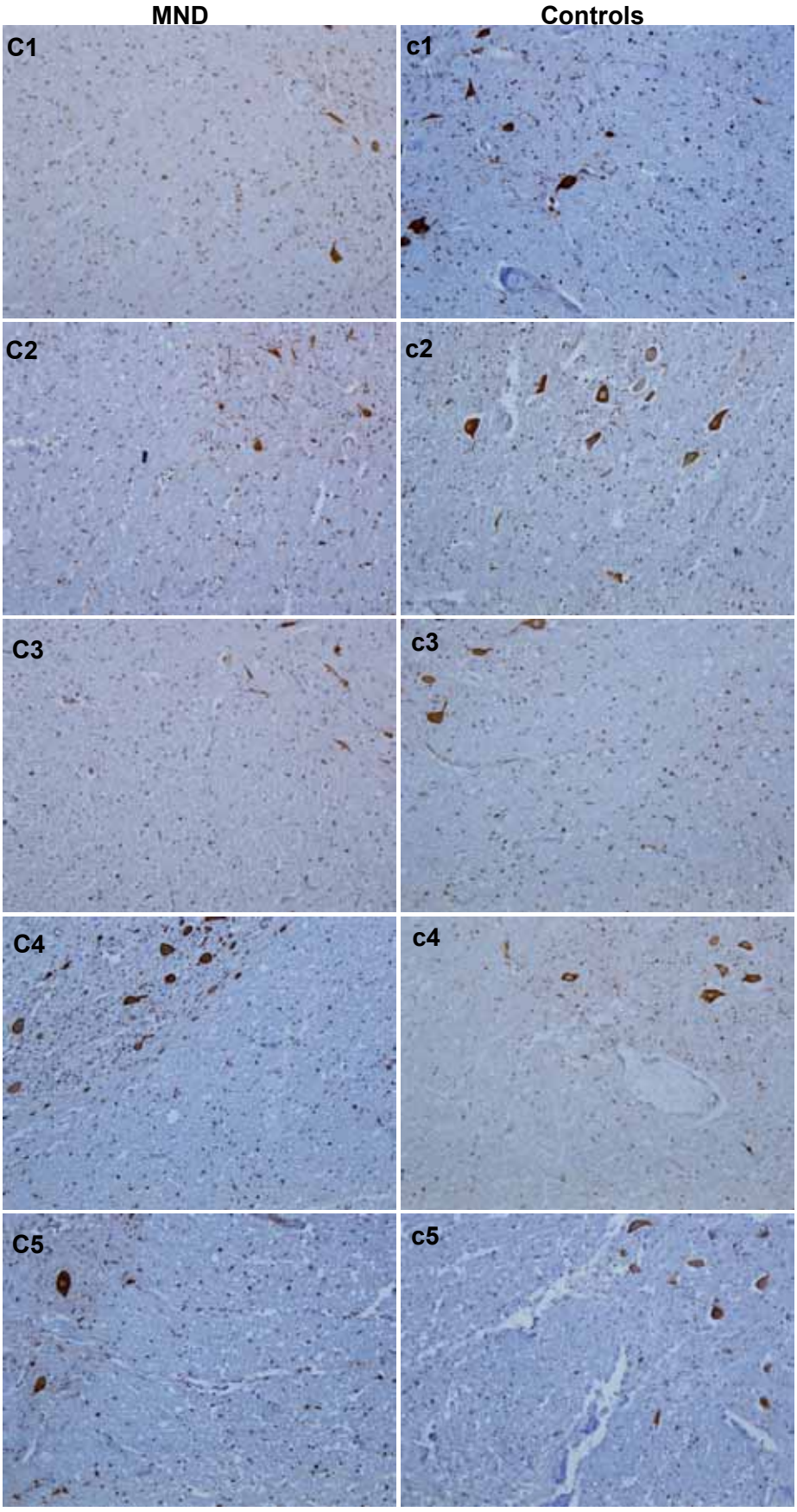

Figure 3.7. continued.

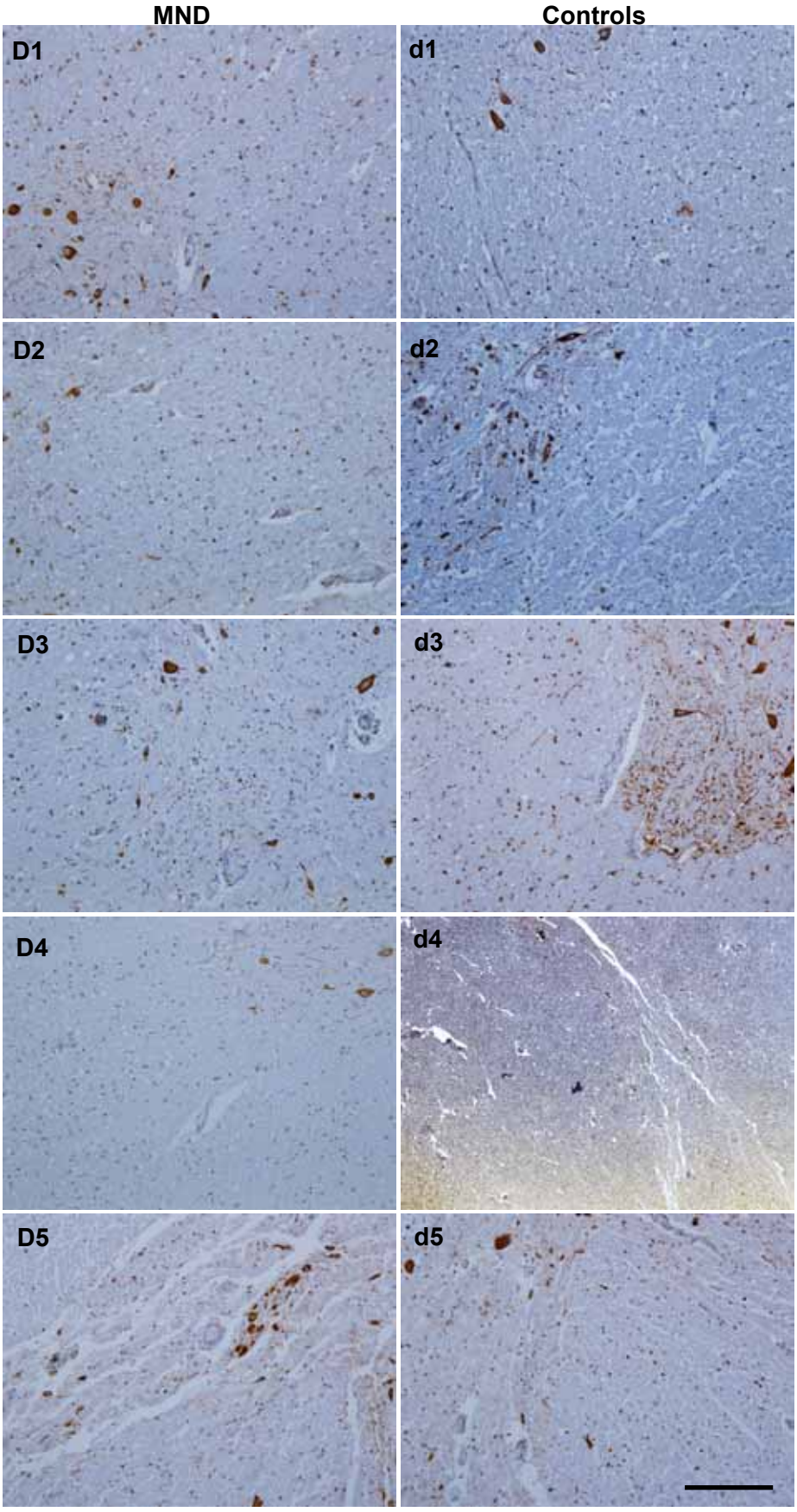

Figure 3.7. continued.

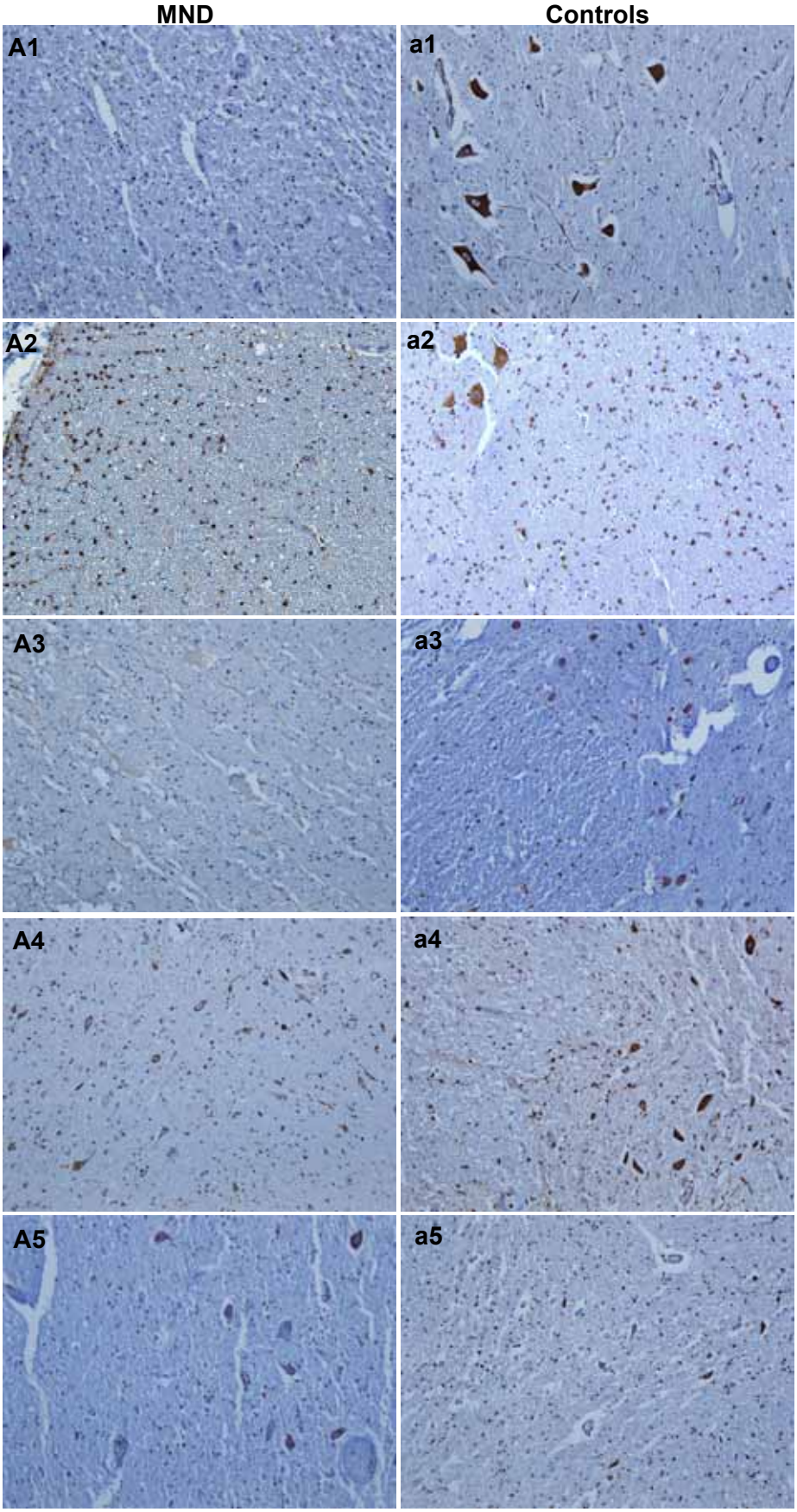

Figure 3.8. eEF1Bδ in spinal cord sections from MND patients and controls. Left panel. Representative MND cases. Right panel. Controls. Scale bar, 200μm.

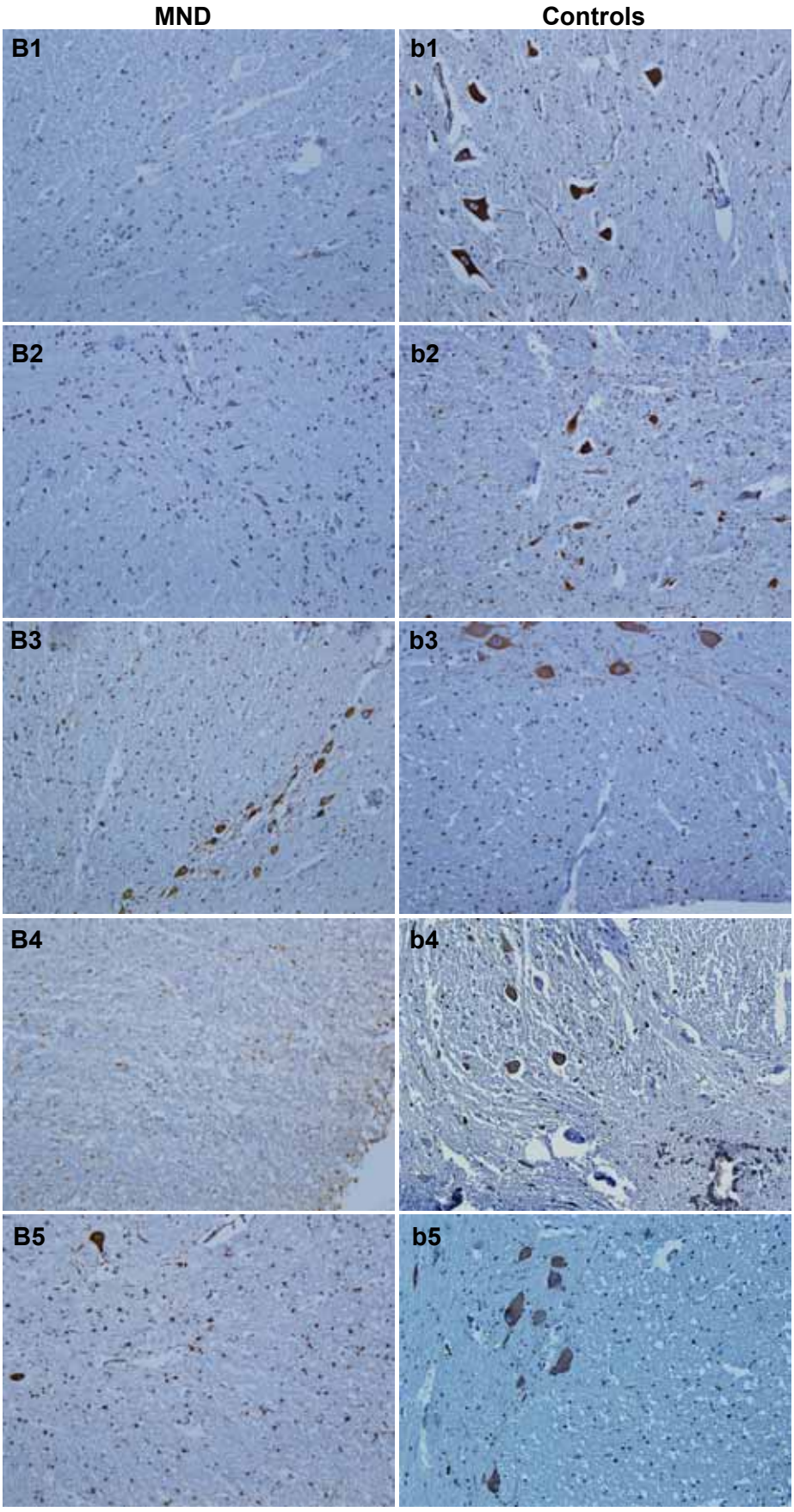

Figure 3.8 continued.

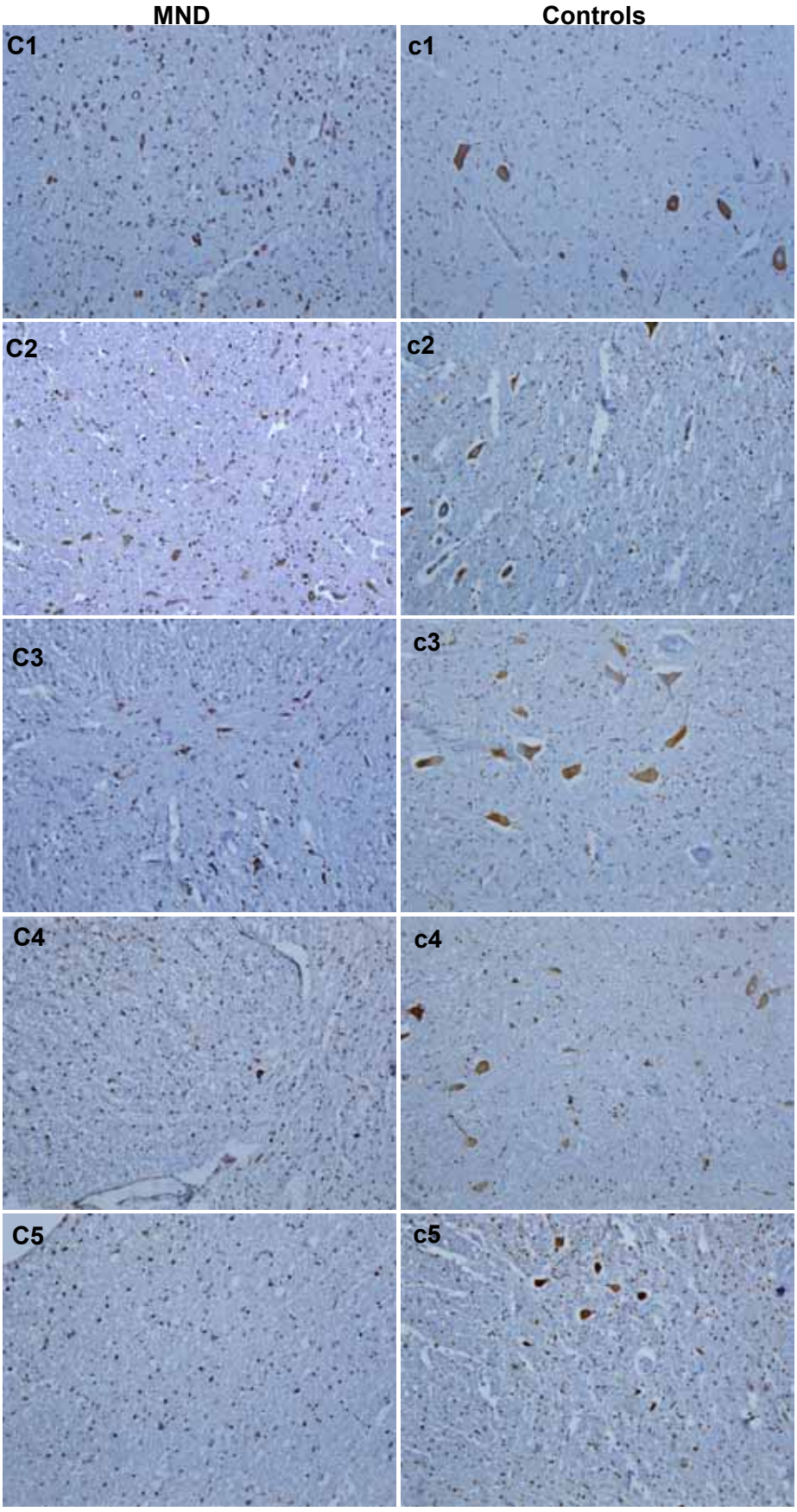

Figure 3.8 continued.

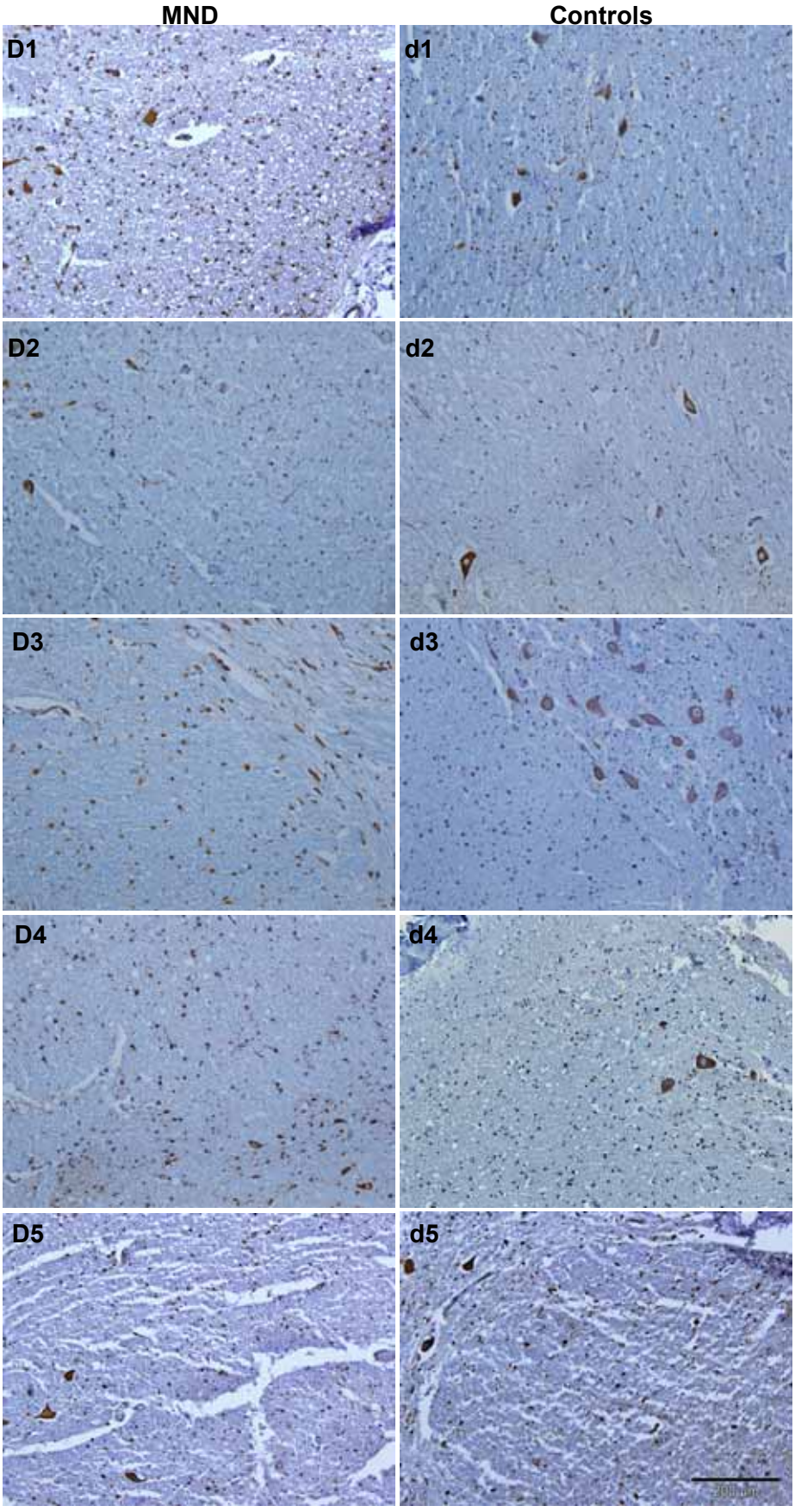

Figure 3.8 continued.

In order to compare the expression between controls and MND patients, quantification of the IHC results was attempted.

At first IPLab (version 3.9.5 r4 for Mac, BD Biosciences) imaging software was used to quantify the intensity of staining and different parameters were calculated and compared. To validate the method, a group of representative sections was examined before applying the method to the entire population. Four sections that showed apparent different expression patterns of eEF1Bδ were chosen for this pilot study, including two controls and two MND cases (Figure 3.9). One of the two controls had strong staining in motor neurons and moderate staining in glia (Figure 3.9 a1), while the other showed moderate staining in neurons and glia (Figure 3.9 a2). In both control sections about one third of the glial cells appeared to be stained. One of the two MND cases chosen showed an apparent weaker staining in neurons (Figure 3.9 A1) and the other showed an increased number of glial cells stained for eEF1Bδ (Figure 3.9 A2).

The result obtained is listed in Table 3.1. Although it can be seen by eye that both control sections showed a stronger staining in motor neurons, the overall intensity quantified (Sum) was not in accordance with this observation, neither was the average intensity per area (Mean). The same situation was found with glial staining. To avoid the variability that was possibly caused by different runs of the IHC experiment procedure, staining intensities of two cell types within one section were also compared. MN/Glia (sum/area) represents the ratio of staining intensity of motor neurons to glial cells per area. The numbers for the two MND cases are slightly lower than controls, meaning a lower intensity in motor neurons and/or higher intensity in glial cells. Yet the numbers were very close and the difference was not significant. Additionally, when the numbers of cells stained in each selected area were counted, the result was not in line with the apparent increase of glial cells stained observed by eye in Figure 3.9 A2. This was likely because the imaging system did not distinguish between brown and blue staining and hence might have counted some unstained cells.

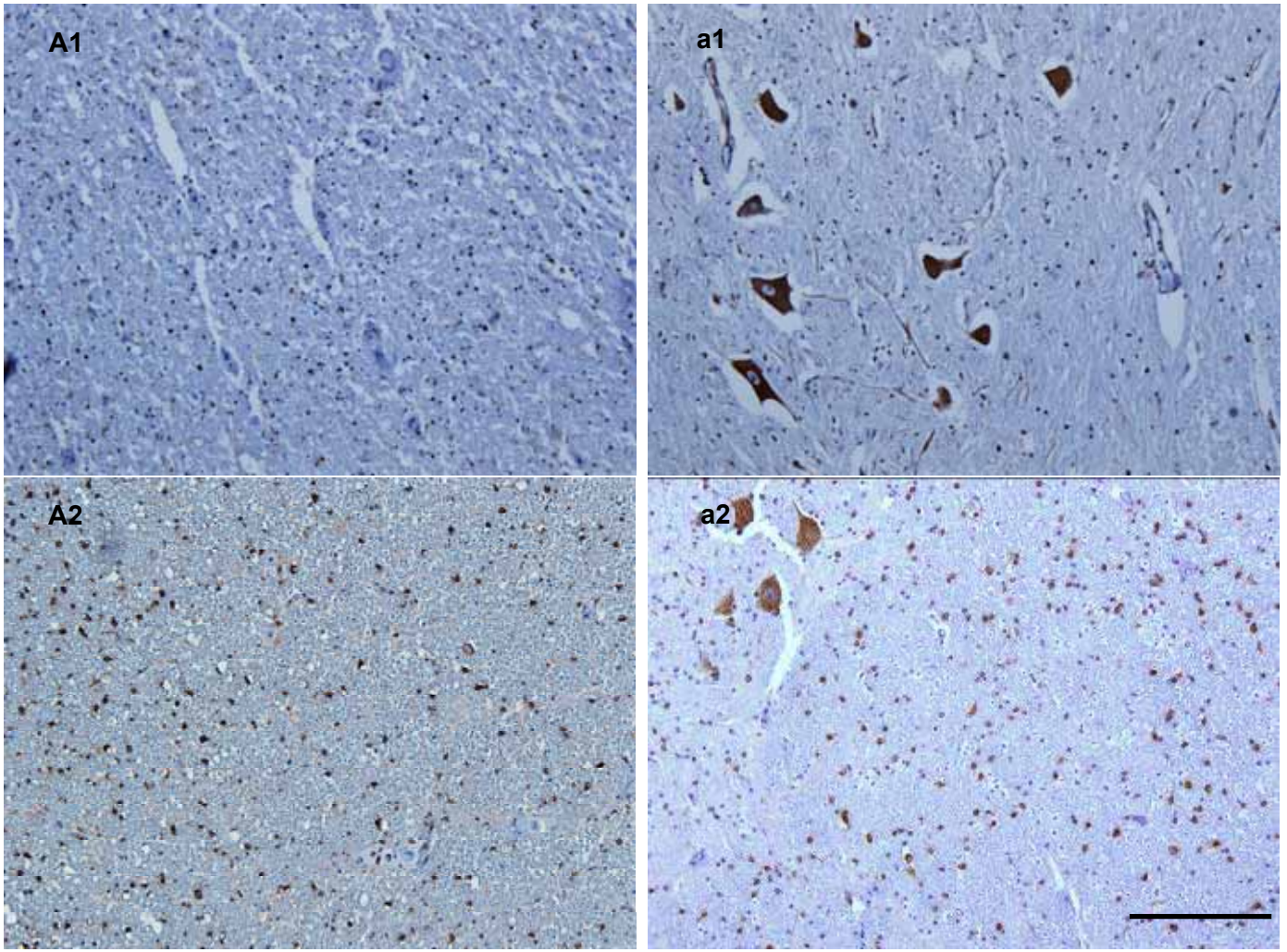

Figure 3.9. Immunohistochemical analysis of eEF1Bδ expression in representative spinal cord sections. A1 and A2. MND cases. a1 and a2. Controls. Scale bar, 200μm.

Table 3.1. Comparison of eEF1Bδ expression in representative spinal cord sections. a1 and a2. control sections. A1 and A2. MND sections. Sum. Overall intensity counted. Area. The total area of brown staining. MN. Motor neuron. The neuron staining was examined in anterior horn. The glia staining was examined in four or five independent areas of same extent in anterior horn and in white matter, and the mean±SEM is shown.

	Cell type	Sum	Area	No of cells stained	Mean (per area)	Mean (per cell)	MN/Glia (sum/area)	MN/Glia (sum/cell)
a1	MN	2208020	10711	32	206	69000	1.036±0.02	16±0.98
	Glia	1.6×10^6±407649	8310±2120	380±96	197±3	4257±255		
a2	MN	4291599	25207	232	170	18498	0.999±0.01	4±0.3
	Glia	3.0×10^6±310541	17342±1681	637±65	170±2	4694±398		
A1	MN	2512142	13316	144	189	17445	0.997±0.004	5±0.4
	Glia	2.7×10^6±515931	14062±2664	764±97	189±1	3454±237		
A2	MN	4031494	23032	213	175	18927	0.966±0.02	5±0.3
	Glia	2.1×10^6±291747	11618±1601	597±73	181±4	3516±175		

Therefore the staining in controls and MND cases was scored by eye (twice), including the staining intensity in motor neurons and glial cells respectively, the approximate ratio of glial cells stained, as well as whether there were branched glial cells stained. A summary is listed in Table 3.2 and original images of each section are listed in Appendix 1 and 2.

Compared to control sections, the staining for eEF1Bα in several MND cases showed certain differences. Some cases showed a lowered level of overall expression (Green in Table 3.2 eEF1Bα). Some showed an increased number of glial cells that were stained (Red in Table 3.2 eEF1Bα), and also in 4 cases some of the glial cells stained for eEF1Bα showed a branched morphology (Blue in Table 3.2 eEF1Bα). The rest of the cases did not show visible difference from control sections.

As to eEF1Bδ expression, the difference between MND and normal spinal cord was more striking. Like eEF1Bα, eEF1Bδ in some cases also showed a lower level in both neurons and glial cells (Green in Table 3.2 eEF1Bδ). However, there were another 10 cases that showed a lower expression in motor neurons but not in glial cells (Purple in Table 3.2 eEF1Bδ). In the rest of the cases, 16 showed more branched glial cells stained with eEF1Bδ antibody (Red in Table 3.2 eEF1Bδ), including 11 cases with more glial cells stained overall (Blue in Table 3.2 eEF1Bδ).

Furthermore, the expression patterns of the two proteins were not coordinated in all the sections examined. For example, some of the control sections showed an apparent low level of eEF1Bδ but a moderate level of eEF1Bα in motor neurons, and a high level of eEF1Bδ and moderate level of eEF1Bα in glial cells (Table 3.2 c3). Another control section had lower expression of eEF1Bα than eEF1Bδ in glial cells (Table 3.2 b2). Similarly in some MND cases the expression patterns of eEF1Bα and eEF1Bδ in the spinal cord from the same patients were different. In some of the cases where eEF1Bδ was increased in glial cells the expression of eEF1Bα showed no apparent difference from control (Table 3.2 C4, C5, C7, D2 and F7), or even lower (Table 3.2 C8, D4 and F6). In some cases of eEF1Bδ staining many branched glial

cells were stained, which were hardly seen in corresponding sections with eEF1Bα staining (Table 3.2 B3, C4, C7, E3, F6, F7 and G4).

Table 3.2. The expression of eEF1Bα and eEF1Bδ in spinal cord from health and MND. a1-d5. Normal spinal cord**. A1-G5.** Spinal cord from MND patients.

		eEF1Bα				eEF1Bδ			
		Staining Intensity		Total glia stained	Branched glia stained	Staining Intensity		Total glia stained	Branched glia stained
		(MN)	(glial)			(MN)	(glial)		
a1	Control	H	M	+	Only a few	H	M/H	+	
a2	Control	M	M	++		M/H	M/H	++	
a3	Control	M	M	+		M	M	+	
a4	Control	***VH***	M	+		***VH***	***H***	++	
a5	Control	No MN	M/H	++		M	M/H	++	
b1	Control	M/H	M	+		M/H	M/H	++	Only a few
b2	Control	M/H	L	+		M/H	M/H	+	
b3	Control	M/H	M	+		M	M	+	
b4	Control	M	M/H	+	Only a few	M/H	M/H	+	
b5	Control	M	M	+		M/H	M	+	
c1	Control	H	H	++		M/H	M/H	++	
c2	Control	M/H	M	++	**Y**	M	M	++	
c3	Control	M	M	++	**Y**	**VL/M**	H	++	**Y**
c4	Control	M	M	++		M	M	+	
c5	Control	M	M/L	+		H	H	++	**Y**
d1	Control	H	M	+		M	M	+	
d2	Control	M/H	M	+		M	M	+	
d3	Control	H	M	++		M	M	+	
d4	Control	M	M	+		M	M	+	
d5	Control	H	M	++		M/H	M/H	++	

Table 3.2 continued

		eEF1Bα				eEF1Bδ			
		Staining Intensity		Total glia stained	Branched glia stained	Staining Intensity		Total glia stained	Branched glia stained
		(MN)	(glial)			(MN)	(glial)		
A1	MND	L	L	+		VL	M	++	
A2	MND	M	M/H	++	Only a few	M/L	Only H in	+++	Y
A3	MND	M/H	L/M	+		Poor section	Poor section	+	
A4	MND	M	L	+		M	M	+	
A5	MND	M/H	H	++	Only a few	VL	VL, some H	+	
A6	MND	M	M	++	Only a few	L	M	++	
A7	MND	M	L/M	++		L/M	L	+	
A8	MND	M	L/M	+		M	L/M	+	
B1	MND	M/H	L/M	+		M/H	L/M	+	
B2	MND	H	M/H	+++	Y	L/M	L/M	+	
B3	MND	H	M	++	Only a few	M	L-M/H	++	Only a few
B4	MND	L/M	L/M	+		M	M/H	++	
B5	MND	H	L/M	+		H	H	++	
B6	MND	L	L	only a few		M/H	M/H	++	
B7	MND	M/H	M	++		M/H	M	++	
B8	MND	H	M/H	+++	Only a few	M	M	++	
C1	MND	M	M	++		M	L	++	
C2	MND	M/H	L, H in some	++		L/M	M	++	Only a few
C3	MND	M	L	++		L	M	++	
C4	MND	H	M	+		M	M/H	++	Y
C5	MND	H	M/H	++		M/H	H	++	Y
C6	MND	M	M	++	Y	M	M	++	Y
C7	MND	M/H	L/M	++	Only a few	M	M/H	++	Y
C8	MND	M/H	L	+		M/H	M/H	+++	Y
D1	MND	M	M	++		M	M	+++	Y
D2	MND	M	M	++		M	M	+	

Table 3.2 continued

		eEF1Bα				eEF1Bδ			
		Staining Intensity		Total glia stained	Branched glia stained	Staining Intensity		Total glia stained	Branched glia stained
		(MN)	(glial)			(MN)	(glial)		
D3	MND	M/H	M	+++	Y	M	M/H	+++	Y
D4	MND	M	L	+		M/H	H	+++	Y
D5	MND	H	M	+		M/H	M	+	
D6	MND	H	M	++		L/M	L/M	+	
D7	MND	M/H	M	++		L/M	L, H in some	+	
D8	MND	M	M/H	++		VL	VL	+	
E1	MND	M	L	+		VL	Few but H	+	
E2	MND	M	L	+		VL	L	+	
E3	MND	H	L/M	+		L/M	H	++	Y
E4	MND	M	L/M	+		M	M	++	
E5	MND	H	M	++	Only a few	M/H	M	++	
E6	MND	M	M	++		M	M	++	
E7	MND	L/M	L	+		M	M	++	
E8	MND	M/H	M/H	+++	Only a few	M(not many	M	++	
F1	MND	M/H	M	++		M/H	M	++	
F2	MND	M	M	++	Only a few	L/M	M	++	
F3	MND	M/H	M/H	++		L/M/H	M	++	
F4	MND	M	L, H in some	++		M	L, H in some	++	Only a few
F5	MND	L	L	a few		L	M	++	
F6	MND	L/M	L	+		H	H	+++	Y
F7	MND	M/H	M/H	++		M/H	H	+++	Y
F8	MND	M/H	M	+		M/H	M/H	++	Only a few
G1	MND	M	M	+		L	M/H	++	
G2	MND	M/H	M	+++	Y	M/H	H	+++	Y
G3	MND	M/H	M	++	Only a few	M	M/H	+++	Y
G4	MND	M/H	L	+		M	H	+++	Y
G5	MND	M	L/M	+	Only a few	M/H	M/H	+++	Y

3.3 Discussion

Considerable evidence suggests that protein synthesis plays an important role in tumourigenesis, and many of the regulatory factors involved in protein translation were found to be potential oncogenes. All three subunits of eEF1B showed overexpression in various cancers respectively, including breast cancer (Al-Maghrebi, Anim et al. 2005), lung cancer (Liu, Chen et al. 2004), oesophageal cancer (Mimori, Mori et al. 1996; Ogawa, Utsunomiya et al. 2004), colon cancer (Chi, Jones et al. 1992; Ender, Lynch et al. 1993; Mathur, Cleary et al. 1998). Overexpression of eEF1Bδ induced transformation of cultured cells and subcutaneous tumours in nude mice (Joseph, Lei et al. 2002).

The studies to date on eEF1B expression in cancer are extensive but not systematic. Previous studies in breast cancer cell lines have identified an increase of all three eEF1B subunits at the mRNA level respectively, although one of the two studies observed eEF1Bγ overexpresson in the MCF-7 cell line while the other one did not. This inconsistency is perhaps a result of different experimental methods (Real Time PCR and Northern blot) and/or cell strains used in different labs. Here in this thesis the expression of eEF1B subunits in different cell lines, including four breast cancer cell lines, was examined at a protein level. Unlike the previous reports comparing the expression levels of eEF1B subunits between cell lines or tissues, the results in this thesis were not quantified due to the lack of a negative control from corresponding tissue and species for each type of cancer cell line.

The two subunits of eEF1B which carry the GEF ability, eEF1Bα and eEF1Bδ, showed an altered expression pattern in some of the cell lines. Extra bands lighter than normal for eEF1Bα and eEF1Bδ were observed in several cancer cell lines while in non-transformed cell lines there was only a single band for eEF1Bα and two for eEF1Bδ representing different variants. Since all cell lysates were prepared in buffer containing protease inhibitors, it seemed unlikely that the shorter bands were

caused by protein degradation. Still more careful characterization will be necessary. These lower bands were seen in some cancer cell lines but not in others, which was probably due to the different origins of the cell lines.

Nevertheless, it seems the lower bands for each subunit existed in different cell lines. eEF1Bα showed the lower band in HeLa, HCT116, PC3, T47D, MDA-MB-231 and MDA-MB-453, while eEF1Bδ, in T47D and MDA-MB-453. In all cell lines tested eEF1Bγ showed one single band. Moreover, compared with other two subunits, eEF1Bδ had a lower expression level in PC3 cell line. The unbalanced expression pattern of eEF1B subunits was also demonstrated at both mRNA and protein levels in human cardioesophageal carcinoma (Veremieva, Khoruzhenko et al. 2010). Although the three subunits are considered to form a complex and each has been reported respectively to show an altered expression in cancer, the non-coordinated changes observed in cancer cells and tissues indicate that the involvement of each subunit in carcinogenesis may be regulated at the level of individual subunits.

Although the reports in breast cancer cell lines and tissues discovered overexpresson of eEF1B mRNA, in this study when the expression of eEF1Bα and eEF1Bδ proteins in breast cancer tissues were examined using IHC and compared with corresponding non-neoplastic tissues, no significant difference was observed. Only a few samples (2 out of 24 cases) showed a stronger staining for eEF1Bα or eEF1Bδ protein. This is likely due to the fact that some tissues contain mainly adipose tissue or fibrous interlobular tissues, and therefore were hardly stained. It is also worth noting that the control tissues were taken from the same patients as of the cancer tissues, and some control tissues showed apparent invasive carcinoma (Figure 3.2 j and 3.3 h), which is possible responsible for the similar staining between breast cancer tissues and corresponding control tissues. Since the sample size in this study is relatively small and some sections contained predominantly adipose tissue, a larger sample size is required for further study, and no conclusion can be drawn at this stage from these preliminary data without suitable negative controls. The research on the other elongation factor eEF1A2 had different findings. While cultured breast

cancer cells showed a higher level of eEF1A2 mRNA, breast cancer tissues also showed apparent overexpression at the protein level of eEF1A2 (Joseph, O'Kernick et al. 2004; Tomlinson, Newbery et al. 2005). This is probably because as a tissue-specific protein, eEF1A2 is normally not expressed in breast, so its high expression level in breast cancer tissues is more significant.

The effect of eEF1B downregulation was also investigated in this thesis. Previous reports on the loss of eEF1B were carried out on yeast strains. Yeast eEF1B consists of two subunits, eEF1Bα (the GEF), and eEF1Bγ with no GTP exchange activity. Therefore it is not surprising that the absence of eEF1Bα is lethal in *S. cerevisiae* as the conversion of GDP to GTP on eEF1A is greatly dependent on its GEF (Hiraga, Suzuki et al. 1993). However, mammalian cells are more complicated. Unlike yeast eEF1B, the mammalian eEF1B complex has two subunits that have GTP exchange activity (van Damme, Amons et al. 1990), which raises the question of whether the two subunits play the same role in translation elongation and other cellular functions. The preliminary study in this thesis examined mammalian cell line NSC34 with knockdown of each eEF1B subunit.

The siRNAs used were all efficient and specific to knock down targeting proteins, although the efficiency may vary. However, the resulting loss of expression seemed not to affect cell viability within the time period of this study. One possible explanation is, as stated above, that eEF1B complex has two subunits that have GTP exchange activity. Although human eEF1Bδ failed to correct the growth defect caused by loss of eEF1Bα in *S. cerevisiae* (Carr-Schmid, Valente et al. 1999), this does not exclude the possibility that in mammalian cells, the effect of one subunit knockdown could be compensated for by the existence of the other and therefore does not significantly reduce cell growth at least in the short term. Furthermore, NSC34 cells express both isoforms of eEF1A. The way the two isoforms function with eEF1Bα and eEF1Bδ is not yet clear, and is in fact rather complicated, as discussed in detail in chapter 5 of this thesis.

eEF1Bγ, the third eEF1B subunit, contains no nucleotide exchange activity. Even though it is often found tightly associated with eEF1Bα, it seems not directly involved in the GTP exchange function of the complex. A study found that knockdown of eEF1Bγ reduced protein synthesis by about 22% in HeLa cells (Kim, Kellner et al. 2007), yet disruption of both genes encoding eEF1Bγ in *S. cerevisiae* did not affect protein translation or cell viability (Kinzy, Ripmaster et al. 1994), the second of which is in line with our observation in NSC34 cells.

The expression of eEF1B was also examined in spinal cord from mice and humans in health and with neuronal disease. Wasted mice are characterised by the deletion of eEF1A2, which is the only form of eEF1A in motor neurons in normal spinal cord. In wasted mice, the expression of eEF1B subunits in some neurons was lower than in wild type, yet to different extents for the different subunits. The down-regulation may reflect the poor condition of motor neurons in wasted mice due to eEF1A absence, or possibly a direct result of eEF1A2 loss in these cells, which is further discussed in the following chapters of this thesis.

On the other hand, eEF1B expression in human spinal cord also showed differences between normal and MND sections, especially eEF1Bδ. The first difference observed was the glial staining in the sections. In the controls only about 1/3 to 1/2 of glial cells showed visible eEF1B staining, while MND cases appeared to show more glial cells which expressed eEF1Bδ. This is in accordance with the pattern of glial activation which happens in response of central nerve system (CNS) injury or disease.

There are mainly two types of glial cells involved in glial activation, microglia and astrocytes. Microglia are small glial cells that are characterised as macrophages in CNS which are considered to serve as innate immune system in CNS monitoring the pathology of neurons (Glezer, Simard et al. 2007). In healthy matured CNS, microglia have a ramified morphology with processes branching off the small soma. Upon activation, microglia undergo morphological change, with processes

withdrawal and an amoeboid appearance (Saijo and Glass 2011). Microglial activation can be identified by the increased expression of marker such as ionized Calcium-binding adapter molecule 1 (Iba1) (Ito, Tanaka et al. 2001) and macrosialin (CD68 or ED-1) (Bauer, Sminia et al. 1994).

Astrocytes have a star-shaped morphology. In gray matter astrocytes have short and highly branched processes, and in white matter, long fibre-like processes. Astrocytes have many roles in the CNS, such as providing trophic support for neurons (Pellerin and Magistretti 2004), maintaining the extracellular ionic environment and pH for neurons, regulating synapses (Slezak and Pfrieger 2003; Santello and Volterra 2009), contacting with blood vessels and mediating CNS blood flow in response to changes of neuronal activity (Schummers, Yu et al. 2008), and involvement in CNS metabolism (Sofroniew and Vinters 2010). Astrocytes are activated in response to CNS injury and diseases, characterised by a significant increase in expression of glial fibrillary acid protein (GFAP) and the marker aldehyde dehydrogenase 1 family, member L1 (ALDH1L1) (Cahoy, Emery et al. 2008). Moreover, astrocytes were found to contribute to microglial activation (Ovanesov, Ayhan et al. 2008).

The branched glial cells that were hardly seen in controls but appeared in some MND cases were likely to be astrocytes or microglia according to their morphology, and presumably most of them were astrocytes since microglia withdraw their branched processes and acquire a round morphology when activated in injured CNS. However, due to the restriction of the spinal cord sections from patients, the sections were not examined for the expression of glial markers, such as CD68 for microglia and GFAP for astrocytes which are overexpressed in microgliosis or astrogliosis respectively. Further study is needed to demonstrate whether the upregulation of eEF1Bδ in MND cases happened in activated glial cells, which can be addressed by double immunofluorescent staining the sections with eEF1Bδ antibody together with a glial marker. Besides, upon CNS injury some of the astrocytes start to proliferate, (Buffo, Rite et al. 2008), which may also contributed to the number increase of

stained astrocytes. Nevertheless the expression of eEF1Bδ protein in glial cells of some MND patients showed a similar pattern to reactive gliosis, with more glial cells showing eEF1Bδ staining.

In addition, in the spinal cord sections which showed more glial staining for eEF1Bδ, a diffuse morphology of glial cells was observed in several cases (Appendix 2 F7, G2, G3, G4 and G5). Reactive astrogliosis is a finely gradated continuum of a progressive process which varies with the severity of the injury or disease in the CNS. According to the classification of reactive astrogliosis proposed by Sofroniew and Vinters, severe diffuse reactive astrogliosis shows upregulation of GFAP and other genes, with hypertrophy of cell body and processes, together with astrocyte proliferation and broader process extension which leads to overlapping of neighbouring astrocyte processes and consequently diffused individual cell domains (Sofroniew and Vinters 2010). Although the pathological diagnosis information is not detailed in the severity of MND for each patient (the information of all the patients is listed in table 2.4), the observation of diffuse star-shaped glial cells that showed eEF1Bδ staining in some MND cases supports the hypothesis that the increase of eEF1Bδ expression could be at least partly explained by reactive astrogliosis. It is important to note that the control case that also showed overlapping glial processes and a stronger expression of eEF1Bα and eEF1Bδ (Figure 3.7 c3 and 3.8 c3) was from a donor without MND but showed some hypoxic change, which triggers reactive astrogliosis as well (Miller, Bartley et al. 2005; Fang, Li et al. 2008).

The other type of change was a lower expression level of eEF1B, mainly for eEF1Bδ, in motor neurons (in about 20% of the cases) instead of much change in glial cells. This downregulation in motor neurons is similar to what was observed in spinal cord sections from wasted mice, which again could have several possible reasons. The expression of eEF1A2 in these cases (IHC performed by Dr. Newbery in our group) was compared with eEF1Bδ. Representative cases with a lower expression of eEF1A2 and/or eEF1Bδ were chosen, including 2 controls and 4 MND cases, and the same regions of each case were compared. It appeared that the

expression patterns of eEF1A2 and eEF1Bδ were not always coordinated (Appendix 3). Some cases showed lower level of both proteins overall, but the expression in each motor neuron was not coordinated (Appendix 3 E1 and G1). However, caution must be applied when comparing the expression in individual cells because the two sections from each case were not necessarily identical. Nevertheless these data suggest that eEF1A2 is unlikely the direct reason for the downregulation of eEF1Bδ in motor neurons of the human MND cases examined.

Interestingly, even though eEF1Bα expression in MND spinal cord showed a similar pattern to eEF1Bδ, in some of the cases where eEF1Bδ is upregulated in glial cells the expression of eEF1Bα showed no apparent difference from controls. This is the same case as in wasted mouse spinal cord sections. Therefore it is likely that the two subunits are regulated through different pathways. More discussion on this issue is in Chapter 5 in this thesis.

These preliminary findings suggest the possible involvement of eEF1B subunits in neuronal diseases. For future investigation of the role of eEF1B in health and diseases, a larger sample size of cancer specimens originating from different tissues will be necessary, and protein overexpresson experiments in cultured cells as a complement of knockdown experiments will be helpful. Probably a different method to demonstrate cell viability after eEF1B knockdown is needed to determine the effect of loss of each eEF1B subunit. Since eEF1B subunits, especially eEF1Bδ, showed potential relevance to reactive gliosis, it would be of interest to perform immunoflourescence experiments staining the spinal cord sections from MND patients with eEF1Bδ and glial markers such as GFAP and CD68 to demonstrate whether the increase of eEF1Bδ expression indeed happened in activated astrocytes and/or microglia.

Chapter 4 eEF1A2 and eEF1B are physically associated

4.1 Introduction

During the process of eukaryotic protein translation elongation, eEF1A delivers aminoacyl-tRNA to the A site of the ribosome, aided by its GTP exchange factor, eEF1B. In mammals eEF1B is composed of three subunits: eEF1Bα, eEF1Bδ and eEF1Bγ, and was shown to form a 'heavy' complex (eEF1H) with eEF1A (Janssen, van Damme et al. 1994). The structure of eEF1H has been broadly studied and several two-dimensional models mapping the structure of eEF1H have been proposed in the last twenty years (reviewed in section1.4 in this thesis). However, while eEF1A has two isoforms in mammals as well as in *Xenopus* (Newbery, Stancheva et al. 2011), one of which, eEF1A2, is tissue-specific and expressed only in certain cells and tissues (Lee, Francoeur et al. 1992; Chambers, Peters et al. 1998; Kahns, Lund et al. 1998; Khalyfa, Bourbeau et al. 2001; Newbery, Loh et al. 2007), most of the models proposed to date did not give information pertaining to eEF1A2.

One of the studies that took eEF1A2 into account was a series of yeast two-hybrid (Y2H) analyses, where the cDNAs of both isoforms of eEF1A and all three eEF1B subunits, were cloned into Y2H expression vectors respectively to map the interaction pattern among the proteins. It was found that in contrast with eEF1A1, eEF1A2 has little or no affinity for eEF1Bα and eEF1Bδ (Mansilla, Friis et al. 2002), the two eEF1B subunits that have GTP exchange activity. It is perplexing as the two isoforms of eEF1A were thought to have similar abilities to bind to eEF1B, particularly eEF1Bα. The amino acid sequences of the two isoforms of human eEF1A are 92% identical. Comparative three-dimensional models of human eEF1A1 and eEF1A2 on the basis of the crystal structure of homologous eEF1A from yeast mapped all the non-identical residues on one side of the molecule, while the binding sites for eEF1Bα were mapped on the other side, as shown in Figure 4.1 (Soares, Barlow et al. 2009). In addition, unlike eEF1A1 which binds GTP more strongly than

GDP, eEF1A2 showed more affinity to GDP than GTP (Kahns, Lund et al. 1998), therefore eEF1A2 was thought to be more dependent on GEF than eEF1A1 was.

One explanation proposed for the different affinities of the two isoforms of eEF1A to eEF1B was the potential existence of a different GEF, other than the eEF1B subunits presented in the Y2H experiments (Mansilla, Friis et al. 2002), for eEF1A2. For instance, multiple chromosomal isoforms of human eEF1Bα have been identified, one of which transcribes a brain- and muscle-specific cDNA (Pizzuti, Gennarelli et al. 1993). This expression pattern is in accordance with that of eEF1A2 and thus might act as the GEF specifically for eEF1A2. Yet this gene was later found to be intronless, absent from mice, and a result of retrotransposition (Chambers, Rouleau et al. 2001). Other than eEF1Bα, eEF1Bδ exists in different isoforms, with the longest isoform, eEF1BδL, expressed in a tissue-specific manner, found in brain, spinal cord and testis only (Kaitsuka, Tomizawa et al. 2011), which is overlapping with the expression pattern of eEF1A2. This tissue-specific isoform of eEF1Bδ was not included in the Y2H experiments mentioned above. Compared to the ubiquitous eEF1Bδ, eEF1BδL has an extra exon that is transcribed and encodes a 367-amino-acid long N-terminus, which contains a putative nuclear localization signal at amino acids 86-93 (Kaitsuka, Tomizawa et al. 2011). So far little is known about this tissue-specific isoform and it is not clear if there is any other binding site in eEF1BδL apart from the leucine zipper motif that exists in both isoforms. The possible interaction of eEF1A2 with eEF1BδL should not be ruled out. The question of whether eEF1A2 is associated with eEF1B as eEF1A1 does remains unanswered; further study of endogenous proteins is required to understand the relationships between eEF1A2 and eEF1B.

Different techniques were involved in previous studies on the structure of eEF1H, including reconstitution of purified subunits (Bec, Kerjan et al. 1994), polyacrylamide gel electrophoresis and limited proteolysis (Janssen, van Damme et al. 1994), analysis of the isolated, native complex (Minella, Mulner-Lorillon et al. 1998), in vitro phosphorylation (Sheu and Traugh 1999), Y2H (Mansilla, Friis et al.

2002), and electron micrographs of protein fractions from gel filtration high-performance liquid chromatography (HPLC) (Jiang, Wolfe et al. 2005). All of the techniques, *in vivo* or *in vitro*, were performed with isolated, pull-down or exogenous proteins, without revealing the transient interactions of endogenous proteins happening within cells. In this study Proximity Ligation Assay (PLA) was used to investigate the interactions among endogenous eEF1H components *in situ*.

PLA is based on dual binding by a pair of probes to the two proteins of interest via two specific antibodies raised in different species, in order to generate DNA strands, which then are amplified and serve as surrogate markers for the detected protein molecules (Fredriksson, Gullberg et al. 2002; Soderberg, Leuchowius et al. 2008) (reviewed in detail in section 1.6). Compared to other techniques listed above, PLA has the advantage of investigating endogenous protein interactions *in situ*, either on tissues or cultured cells directly. It could give information on the distribution of interacting proteins between individual cells. PLA could also be modified to detect interactions between proteins and specific DNA or RNA sequences (Gustafsdottir, Schlingemann et al. 2007), which will not be discussed in this thesis.

The aim of this project is to use *in situ* PLA technique to establish the potential interactions between eEF1A2 isoforms and eEF1B subunits in mammalian cells, and thus to further investigate the structure of eEF1H.

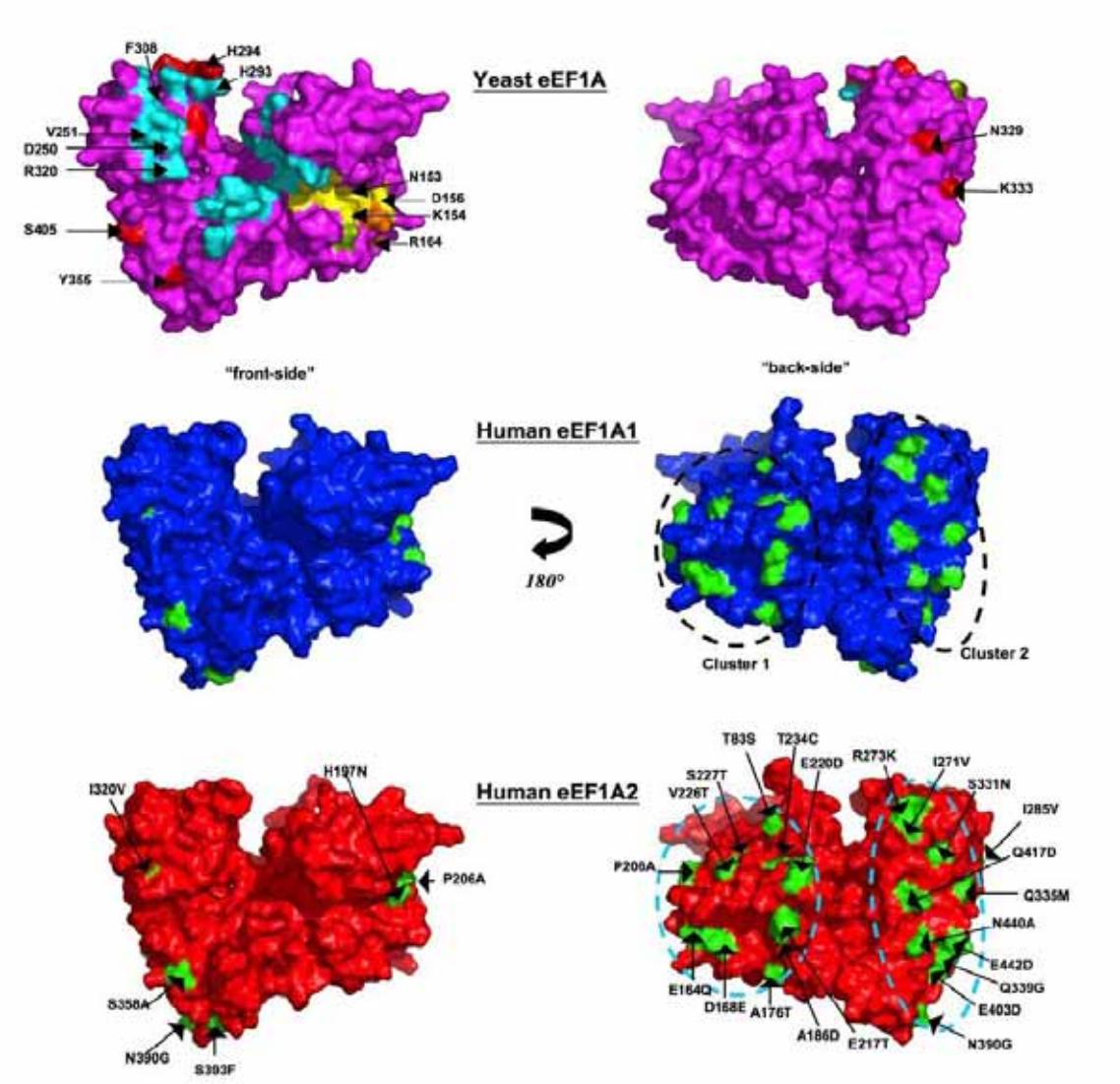

Figure 4.1. Models of human eEF1A1 and eEF1A2 based on yeast eEF1A. Two equivalent views rotated by 180° about the y-axis of the surface representation of the crystal structure of yeast eEF1A (magenta, top panel), and the 3D models of eEF1A1 (blue, middle panel) and eEF1A2 (red, bottom panel). Locations of exposed variant side-chains are mapped onto the surface of the two human eEF1A models (green) and labelled on the eEF1A2 model, with the variant residue from eEF1A1 shown on the right hand side of the label. The C-terminal eEF1Bα-binding site (cyan) and GDP-binding site (yellow) are mapped on the crystal structure of yeast eEF1A. The locations highlighted in red are mutations that inhibit actin-bundling without altering translation *in vivo*. There are no variants in proximity to those residues implicated to be involved in translational fidelity (green). The two variants, Gln164Glu and Glu168Asp, found in close proximity to Arg166, a conservative mutation for the equivalent residue in yeast that was shown to reduce dependence on eEF1B (orange), both retain their main-chain H-bonds with Arg166 (taken from Soares, Barlow et al. 2009).

4.2 Result

4.2.1 Colocalization of eEF1A2 with eEF1Bα and eEF1Bδ in mouse spinal cord

4.2.1.1. Colocalization of eEF1A2, eEF1Bα and eEF1Bδ in spinal cord sections

At the time of this project, commercial eEF1A antibodies available recognized both isoforms, therefore a eEF1A2 specific polyclonal antibody generated in our lab was used in this and all the following studies. The specificity of this antibody has been demonstrated earlier by our lab (Newbery, Loh et al. 2007), and in this study the antibody was also tested in spinal cord sections from healthy mice, as well as wasted mice. Wasted mice have no expression of eEF1A2 (explained in section 1.5), which meant they could be used as a negative control for the antibody. As expected, in wasted spinal cord sections no positive staining was observed (Figure 4.2 A), and in normal spinal cord sections, positive staining was observed only in the motor neurons (Figure 4.2 B). Mouse spinal cord also expresses eEF1Bα and eEF1Bδ almost ubiquitously in all types of cell, although to different extents in different types of cells (Figure 4.2 B and C).

Immunofluorescence results show the same. A direct view of the colocalization of eEF1A2 and eEF1Bα or eEF1Bδ in motor neuron cytoplasm in spinal cord is indicated by the yellow colour. In the cytoplasm of other cells only eEF1B subunits were expressed (Figure 4.3).

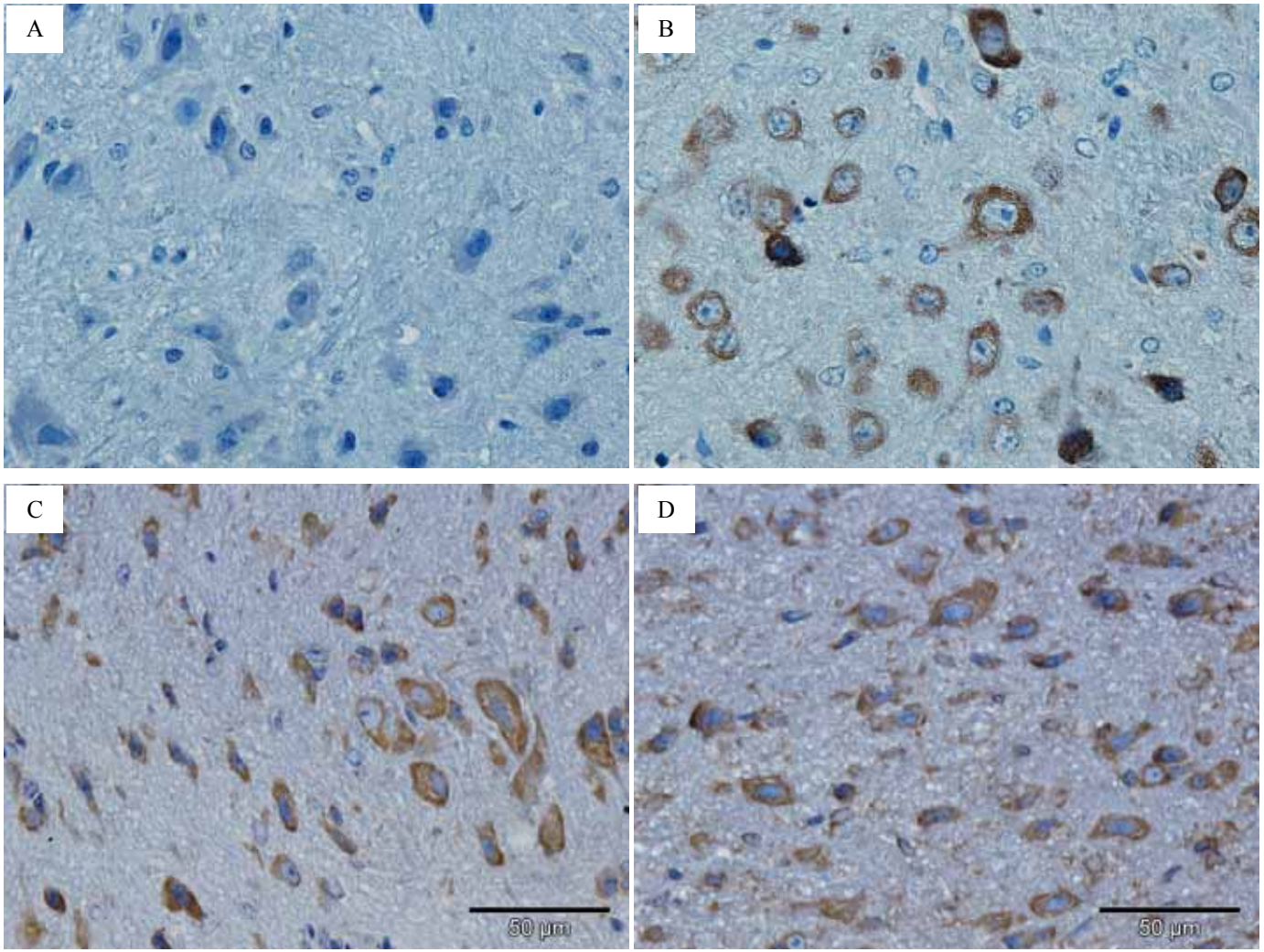

Figure 4.2. The expression of eEF1A2, eEF1Bα and eEF1Bδ in mouse spinal cord. A.eEF1A2 in wasted mouse spinal cord. B. eEF1A2 in normal spinal cord. C. eEF1Bα in normal spinal cord. D. eEF1Bδ in normal spinal cord.

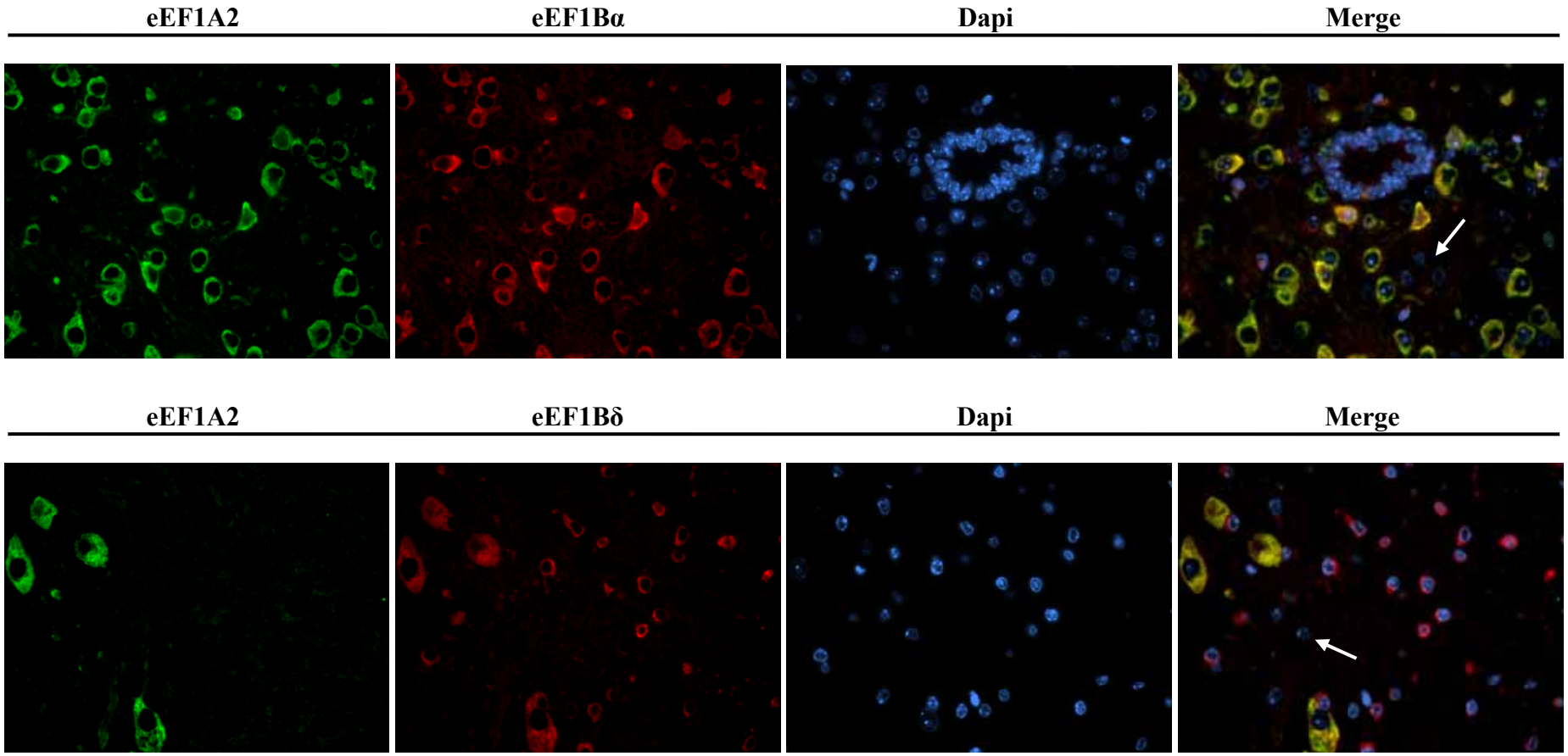

Figure 4.3. IF images of the expression of eEF1A2 and eEF1Bα (top panel) or eEF1Bδ (bottom panel) on mouse spinal cord. Arrows indicate cells without apparent eEF1Bα or eEF1Bδ expression.

4.2.2 PLA of eEF1A and eEF1B

4.2.2.1 PLA on mouse spinal cord sections

The colocalization of eEF1A2 and eEF1B subunits in motor neurons has been confirmed by IHC and IF; therefore the next step is to investigate whether the two proteins are in close proximity to form a complex. As a specific and sensitive technique, PLA enables a direct observation of the interacting endogenous proteins in cells and subcellular compartments.

At first the experiments were performed on mouse spinal cord sections where the IF experiments were carried out. Spinal cord is one of the tissues that express eEF1A2, as well as eEF1BδL. Spinal cord sections from wasted mice where eEF1A2 is absent could be used as a negative control. Unfortunately, despite the fact that spinal cord should have been an ideal object for this study, this experiment encountered many difficulties. As shown in Figure 4.4 B and C, the PLA experiment of eEF1A2 with eEF1Bα and with eEF1Bδ did show PLA signals, recognized as red dots, indicating that eEF1A2 is in close proximity with eEF1Bα and eEF1Bδ. However, and when the spinal cord sections from wasted mice were examined, the same combination of antibodies gave similar positive signals around many nuclei (Figure 4.4. D), although weaker than in wild type spinal cord. As the antibody used in this experiment was proved to be isoform-specific earlier, the false signals are likely to be a result of technical artefact. Nevertheless, the negative control omitting one primary antibody also gave visible positive signals, especially in the white matter. Similar results were observed on mouse brain sections (data not shown).

To address the specificity of the technique became crucial and further proteins were then tested. The three proteins chosen, EF2, PABP and TK1 have not yet been reported to interact with eEF1A and thus were intended to be negative technical controls for PLA. However, the three proteins all gave, to different extents, positive signals with eEF1A2 (Figure 4.4.E-G). Even though the three proteins have not been

reported to be interacting with eEF1A2, it is still possible that they are doing so. The signals of eEF1A2/PABP are dense and in the cytoplasm of motor neurons (Figure 4.4 F), which is similar to the signals given by eEF1A2/eEF1Bα (Figure 4.4 B) and eEF1A2/eEF1Bδ (Figure 4.4 C), while the signals of eEF1A2/EF2 and eEF1A2/TK1 are mostly around nuclei and more spreading (compare Figure 4.4 E, G to B, C), with only a few signals concentrated on certain nuclei (indicated by white arrows). Therefore, it is very likely that most of the red dots are not true PLA signals from the cells displayed, but a general background. This caused difficulties in distinguishing between true PLA signals and random background signals.

Different experimental conditions were used to reduce the false signals, including different combinations of concentrations of primary antibodies and probes. The company (OLink) have also offered technique suggestions, including an improved kit, Duolink II Probemaker (explained in section 2.3.7). However, the background signals from controls could not be removed without depriving signals on other sections at the same time. In a word, in spinal cord and brain sections the background signals could hardly be differentiated from true PLA signals. The false positive signals made it difficult to draw any conclusion from the results above, or to continue the study on spinal cord or brain tissue sections; this led to investigation of other possible objects. The other tissues that express eEF1A2 are heart and muscle. However, sections of these two tissues are difficult to maintain a native morphology for IHC or IF experiments under the experimental conditions in our lab, and give very diffuse staining for eEF1A2. Therefore the following PLA experiments were performed on cultured cells other than animal tissues.

4.2.2.2 PLA on HeLa cells

HeLa cells express both isoforms of eEF1A (Kim, Namkung et al. 2009). In some reports eEF1BδL was found in HeLa cells (Kaitsuka, Tomizawa et al. 2011),

but under the cell culture conditions of our lab the strain used in this study expressed only shorter eEF1Bδ isoforms (Figure 3.1 in chapter 3).

As in spinal cord sections, in HeLa cells eEF1A2 and all eEF1B subunits gave positive PLA signals (Figure 4.5.C, D and E), but with lower density. Cells with eEF1A2 and TK1 antibodies gave neither PLA signals nor dotty background (Figure 4.5 F), showing that the signals given by eEF1A2/eEF1Bα, eEF1A2/eEF1Bδ and eEF1A2/eEF1Bγ are genuine and specific, and that eEF1A2 does co-localise with eEF1Bα, eEF1Bδ, and eEF1Bγ in HeLa cells, at least at the resolution that can be detected by PLA.

4.2.2.3 PLA on transfected NIH-3T3 cells.

In order to further indicate the interactions between eEF1A and eEF1B components, PLA of eEF1A1 with eEF1B was examined. However, due to the lack of an efficient and specific eEF1A1 antibody for IHC/IF and thus PLA, stable NIH-3T3 cell lines expressing tagged eEF1A1 or eEF1A2were used instead.

NIH-3T3 cells express only eEF1A1 and do not express eEF1A2 except in certain conditions, for example serum deprivation (Ann, Moutsatsos et al. 1991). V5-tagged eEF1A1 and eEF1A2 transgenic NIH-3T3 stable cell lines were generated by a former member in our lab, Dr Justyna Janikiewicz. NIH-3T3 cells were transfected with constructs containing human eEF1A1 or eEF1A2 with V5 tag respectively, and were grown in selective cell culture medium containing varying concentrations of Geneticin® (G418) or Zeocin^{TM}. The cell lines with the highest protein level of V5-tagged eEF1A1 or eEF1A2 were chosen for this study (clones A1 8.6 and A2 9.6 in Justyna Janikiewicz's PhD thesis Figure 3.7).

Unlike in HeLa cells, TK1/V5 gave positive signals in V5-eEF1A2 transgenic 3T3 stable cells (data not shown), therefore PLA of TK1 with each of the three eEF1B subunit were tested to demonstrate the reliability of the experiments, and all turned out to be negative (Figure 4.6 and Figure 4.7 D, F, H).

In V5-eEF1A1 transgenic NIH-3T3 cells, V5 gave positive PLA signals with eEF1B subunits, as eEF1A2 with eEF1B in HeLa cells. Signals of V5/eEF1Bγ (Figure 4.6 G) were not as dense as those of V5/eEF1Bα or V5/eEF1Bδ (Figure 4.6 C and E), but still showed a visible difference from all the negative controls. In V5-eEF1A2 transgenic NIH-3T3 cells similar results were observed, except the PLA signals from V5 with all three subunits appeared weaker than in V5-eEF1A1 transgenic cells.

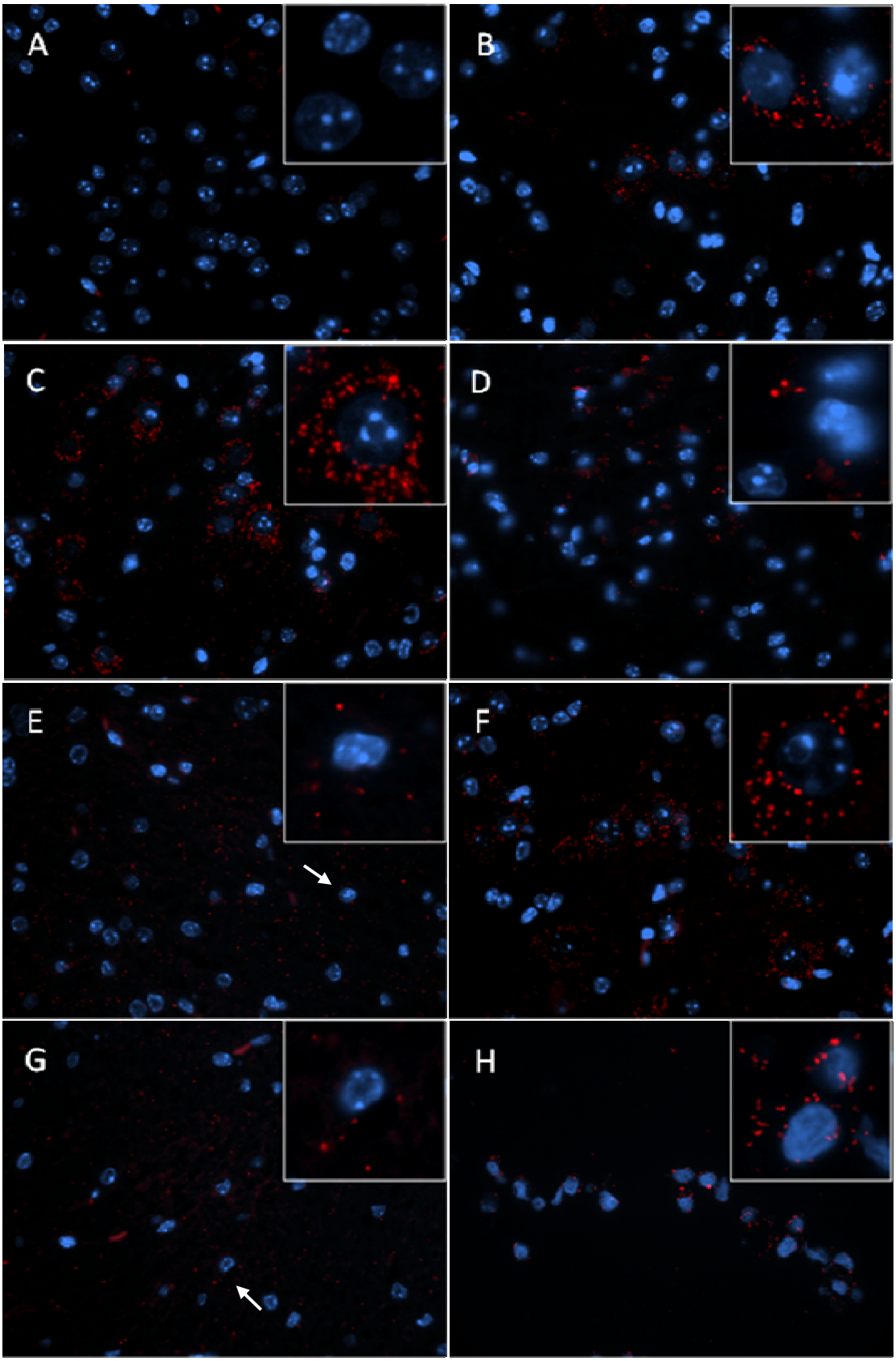

Figure 4.4. PLA on mouse spinal cord. A. both primary antibodies omitted as a negative control. B. eEF1A2 and eEF1Bα. C. eEF1A2 and eEF1Bδ. D. eEF1A2 and eEF11Bδ in wasted spinal cord. E. eEF1A2 and EF2. F. eEF1A2 and PABP. G. eEF1A2 and TK1. H.TK1 positive control in HeLa cells. Images in the squares are higher magnification of selected areas. Arrows indicate PLA signals around nuclei.

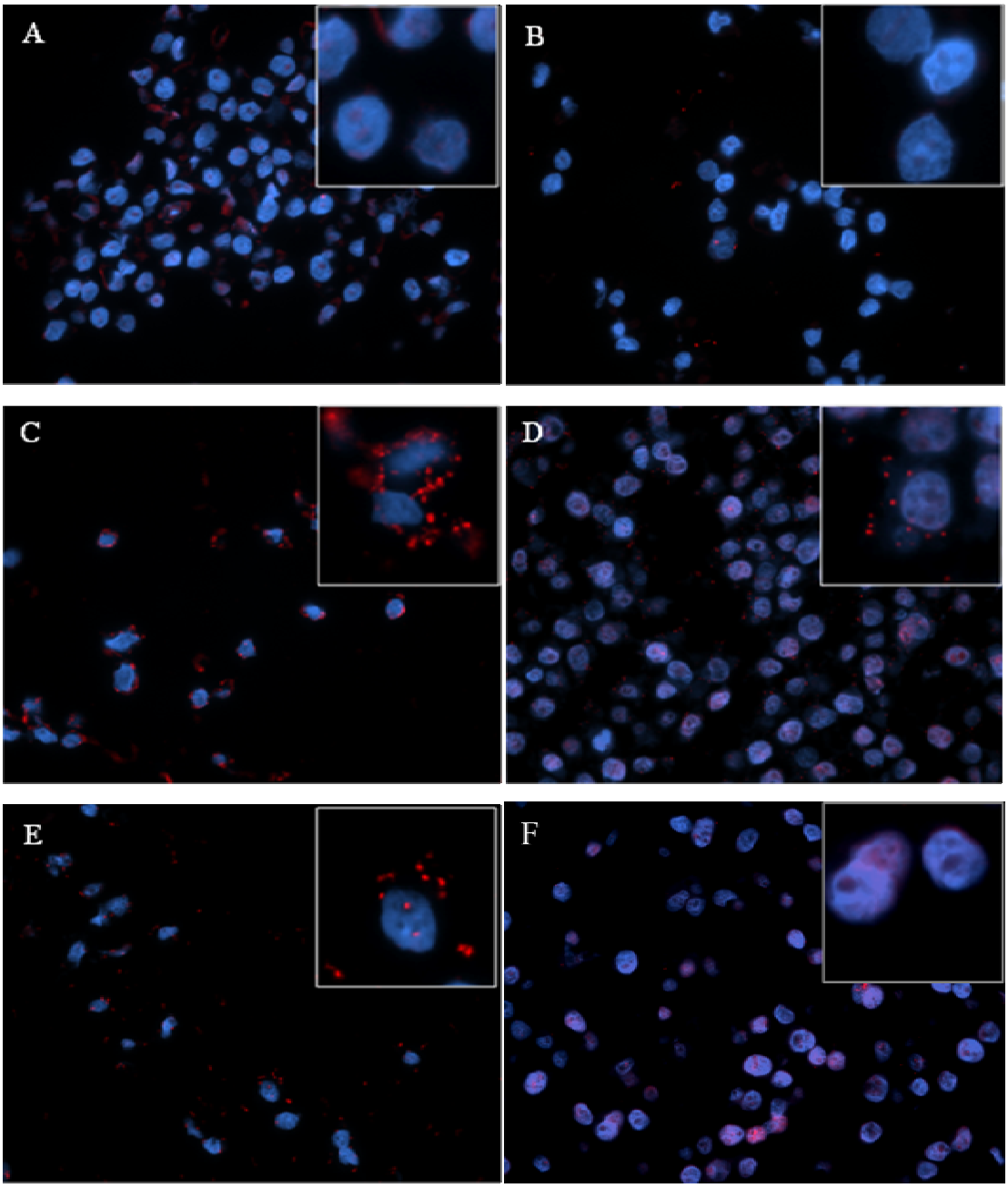

Figure 4.5. PLA on HeLa cells. A. Negative control with both primary antibodies omitted. B. eEF1A2 antibody only. C. PLA of eEF1A2 and eEF1Bα. D. PLA of eEF1A2 and eEF1Bδ. E. PLA of eEF1A2 and eEF1Bγ. F. PLA of eEF1A2 and TK1 as negative control. Images in the squares are higher magnification of selected areas.

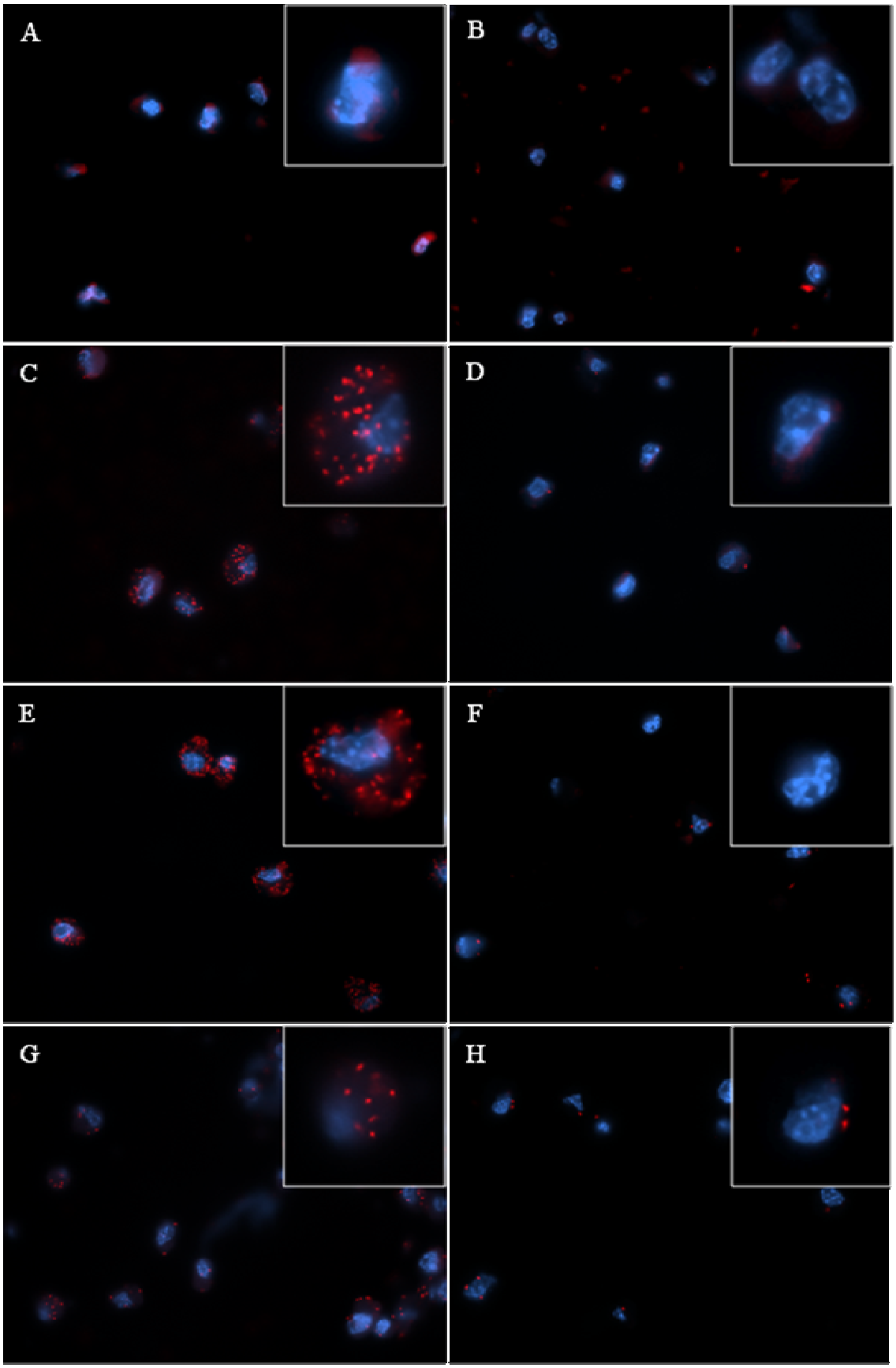

Figure 4.6. PLA on 1A1 transgenic NIH-3T3 cells. A. Negative control with both primary antibodies omitted. B. V5 antibody only. C. PLA of eEF1Bα and V5. D. PLA of eEF1Bα and TK1. E. PLA of eEF1Bδ and V5. F. PLA of eEF1Bδ and TK1. G. PLA of eEF1Bγ and V5. H. PLA of eEF1Bγ and TK1. Images in the squares are higher magnification of selected areas.

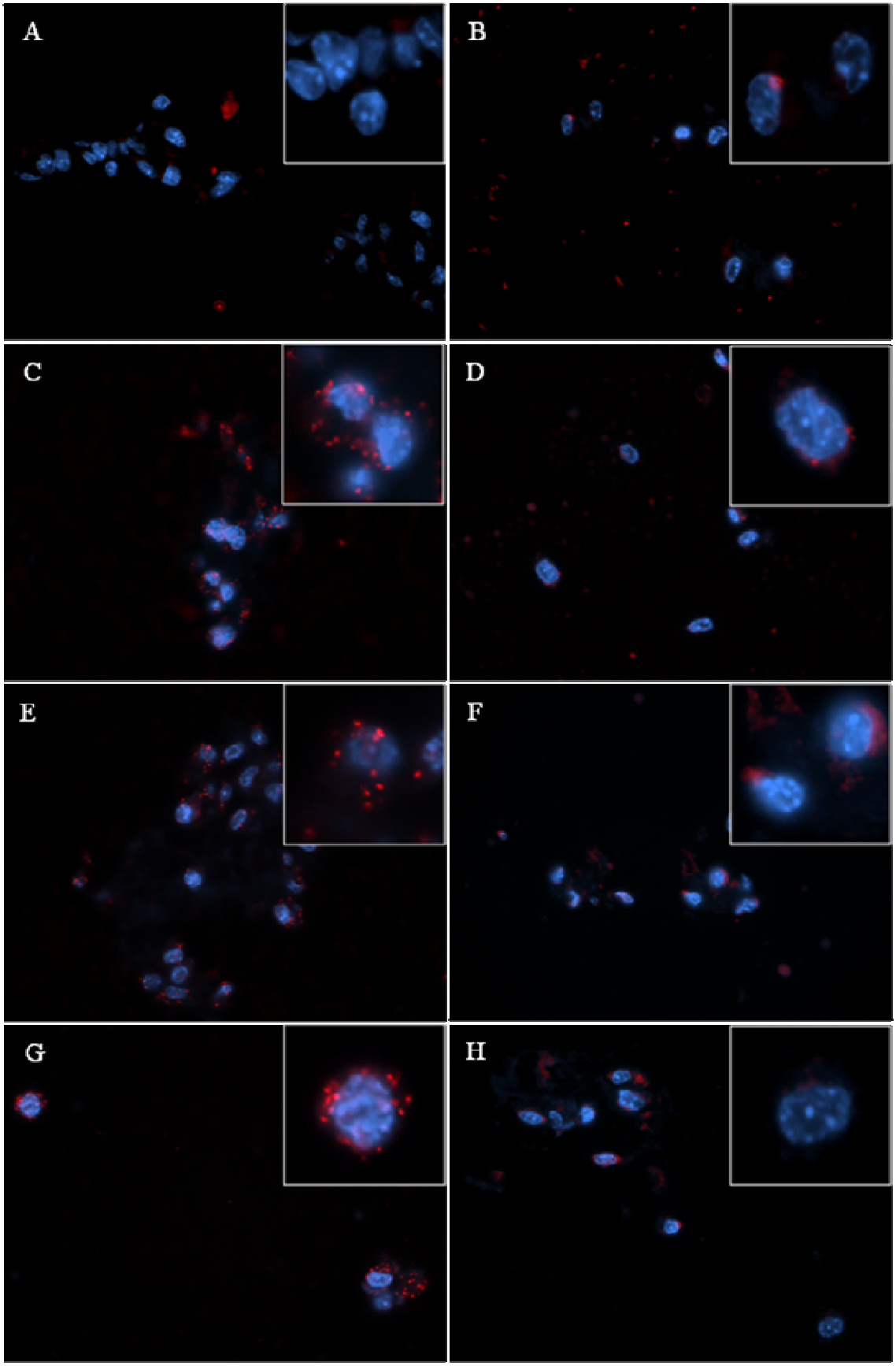

Figure 4.7. PLA on 1A2 transgenic NIH-3T3 cells. A. Negative control with both primary antibodies omitted. B. V5 antibody only. C. PLA of eEF1Bα and V5. D. PLA of eEF1Bα and TK1. E. PLA of eEF1Bδ and V5. F. PLA of eEF1Bδ and TK1. G. PLA of eEF1Bγ and V5. H. PLA of eEF1Bγ and TK1. Images in the squares are higher magnification of selected areas.

4.3 Discussion

As an important part of the cellular machinery that regulates protein translation elongation as well as being involved in other cellular functions, the structure of eEF1H has been broadly studied. eEF1H is composed of eEF1A and eEF1B, and several models have been proposed for relative placement of each component. However, as there is much inconsistency among these models, further studies are required, especially to take different isoforms of the components into account. Besides, while the regions containing sequence differences between eEF1A1 and eEF1A2 proteins do not harbour eEF1B binding sites, suggesting the two isoforms have similar capability of binding to eEF1B, the results from the Y2H experiments that found interactions of eEF1A1/eEF1B but no interactions between eEF1A2 with eEF1B suggest otherwise (Mansilla, Friis et al. 2002).

In IHC and IF experiments on mouse spinal cord eEF1A2 is only observed in motor neurons, which is in accord with the known expression pattern of eEF1A2; eEF1Bα and eEF1Bδ are both expressed almost ubiquitously, with apparent stronger staining in motor neurons, suggesting a higher expression level in these cells. As a result eEF1A2 and eEF1B were found co-localized in the cytoplasm of motor neurons of mouse spinal cord. Both eEF1A2 and eEF1B were expressed in cytoplasm, which is in agreement with their roles as components of protein translation machinery and with previous findings. Unexpectedly, it seems some cells do not express eEF1Bα (indicated by white arrow in Figure 4.3), but it is yet not possible to tell if the absence of eEF1Bα has any specificity for certain type(s) of cell. Two colour immunofluoresence with an antibody that is cell type specific may help to understand if the expression of eEF1Bα is restricted to certain cells. Moreover, since no eEF1Bδ antibody that can distinguish between isoforms is available, it is not possible to demonstrate whether different eEF1Bδ isoforms have different distributions within the spinal cord, i.e. whether there are exclusive expressions among different isoforms, as of eEF1A.

The relationships between eEF1A2 and eEF1B were then studied using *in situ* PLA technique. PLA has been proved to be an efficient and straightforward method to examine endogenous protein-protein interactions *in situ*, avoiding the possible artefacts from experimenting with isolated or exogenous proteins. For example, change of physiological condition may cause inactivation of the protein; techniques like co-Immunoprecipitation (co-IP) performed with proteins from disrupted cells may give false positive results of proteins that actually localize at different subcellular compartments; different post-transcriptional modification is also likely to happen when a protein is expressed in cells from different species. Since spinal cord expresses eEF1A2 and eEF1BδL as well as the ubiquitous isoforms, and the antibodies have already been tested on spinal cord by IHC and IF, mouse spinal cord sections became the first choice for performing PLA. Unfortunately the PLA experiments on mouse spinal cord encountered many problems that it proved impossible to solve. Although PLA signals for eEF1A2/eEF1Bα and eEF1A2/eEF1Bδ were indeed observed, no ideal biological negative control was achieved to validate the results. It was the same with brain tissue sections. In spite of the different experimental conditions tried the situation was not improved.

It was not clear why such false positive signals appeared, and at the time these experiments were performed, no publications on the subject of doing PLA on spinal cord sections were found. One recent study performing PLA on mouse brain sections has observed nonspecific signals that exist in the controls omitting one PLA probe or one primary antibody and are consistent among genotypes (wild type and specific gene knockout mice), which is similar to the situation of our study. The same study also found that nonspecific signals in their study were present in fixed sections but absent in fresh frozen sections. It was therefore presumably caused by the deleterious effect of aldehydes on DNA that might benefit the binding of oligonucleotides to the probes during the PLA reaction (Trifilieff, Rives et al. 2011). This suggestion also explains why the negative control omitting both primary antibodies in our study, which was not present in the study referenced, did not give positive signals. However,

PLA on cultured cells fixed using the same fixation method as for spinal cord or brain sections did not show nonspecific signals. Hence it is possibly because nerve cells are more susceptible to the effect of aldehydes on DNA, and thus showed more intervention in the binding of oligonucleotides to PLA probe.

The same experiments were then carried out on the human HeLa cell line as an alternative, which expresses eEF1A2 (Tomlinson, Newbery et al. 2005). As on spinal cord sections, PLA experiments on HeLa cells have identified co-localisation, consistent with direct interactions of, eEF1A2/eEF1Bα and eEF1A2/eEF1Bδ. In addition, eEF1A2/eEF1Bγ, which was not examined in spinal cord sections, was also found to co-localise. Compared to the results from spinal cord sections, the PLA signals of eEF1A2/eEF1B from HeLa cells have lower density, which could be explained by the apparent higher expression of eEF1A2 in spinal cord than in HeLa cells. TK1, a protein that has not been reported to interact with eEF1A2, was used as a negative control, and no interaction of eEF1A2/TK1 was observed in HeLa cells. Therefore these results seemed more reliable than the ones of spinal cord sections.

The same technique was also used to investigate the interaction between eEF1A1 and eEF1B subunits. However, because at the time of this study there was no antibody that is eEF1A1 specific and suitable for PLA, the PLA of eEF1A1 with eEF1B was carried out on transgenic NIH-3T3 cells instead of HeLa cells. In both V5-tagged 1A1-3T3 cells and 1A2-3T3 cells, PLA of V5 and all three eEF1B subunits gave positive PLA signals. eEF1A1 has previously been found in various researches to be associated with eEF1B subunits (Carvalho, Carvalho et al. 1984; Janssen, van Damme et al. 1994). The results in Figure 4.6 confirmed the binding of the eEF1A1 to eEF1B complex, in accordance with previous reports. On the other hand, as eEF1A2 showed same results in PLA experiments, it indicates that both eEF1A isoforms are likely to be associated with eEF1B in a similar way.

Interestingly, unlike in HeLa cells, transgenic NIH-3T3 cells showed a positive signal suggesting a direct physical link between V5-eEF1A and TK1. This difference

might be the result of the different characters between cell lines; on the other hand, the eEF1A1 and eEF1A2 proteins detected in stable NIH-3T3 cells are exogenous, and although the V5 tag is only 14 amino acids long, the conformation of tagged proteins were probably different from endogenous proteins. The results were hence validated by negative controls of PLA of TK1 and each eEF1B subunit.

It should be kept in mind that neither HeLa nor transgenic NIH-3T3 cells used in this study express eEF1BδL. eEF1BδL is tissue-specific and expressed only in brain, spinal cord and testis (Kaitsuka, Tomizawa et al. 2011), which is overlapping with the tissues that express eEF1A2. Whereas within spinal cord and brain, the expression of eEF1A2 is restricted to certain types of cells, it is not clear if eEF1BδL has a similar pattern, because eEF1BδL has not been extensively studied yet and no eEF1BδL specific antibody is available. As a result, had a cell line that expresses eEF1BδL been used and shown PLA signals of eEF1A2/eEF1Bδ, it would have been impossible to determine which eEF1Bδ isoform interacts with eEF1A2.

In both cell lines used in this study, eEF1A2 appeared to be associated with eEF1Bα, eEF1Bγ and at least the short isoforms of eEF1Bδ, contrary to what the Y2H experiment suggested. Another study of human protein-protein interactions based on mass spectrometry has also identified the interactions of eEF1A2/eEF1Bα and eEF1A2/eEF1Bδ using eEF1A2 as a bait (Ewing, Chu et al. 2007). One explanation for this conflict is that the fusion protein expressed in yeast cells may have failed to keep the native conformation and consequently influenced protein interactions. With the same Y2H system eEF1A2 in fusion with GAL4 DNA-binding domain was competent in interaction with other eEF1A-binding proteins identified in an Y2H screening (Mansilla, Friis et al. 2002; Mansilla, Dominguez et al. 2008), but no positive control was included in the original paper, making it hard to judge the validity of these conclusions. Assuming the results in the follow-up paper to be valid, this has ruled out most potential problems that could cause a false negative result, such as non-functional fusion proteins, toxicity, or fail to localise to the yeast nucleus,

but it is still possible that the fusion protein was modified in a way that masks (part of) the binding sites for eEF1B.

The other major difference between the result in our study and the Y2H experiments is that in transgenic NIH-3T3 cells we also detected an interaction between V5-tagged eEF1A1 and eEF1Bγ, which was not found in the Y2H experiments. This is presumably because that eEF1A and eEF1Bγ are not directly binding each other, but form a complex bridged by another eEF1B subunit, as suggested in most of the eEF1H structure models proposed so far (reviewed in section 1.3.4). In PLA the maximum distance between the two probes that allows DNA hybridization and thus PLA signal is around 16nm (Trifilieff, Rives et al. 2011). Including the two primary antibodies and the two probes, the distance for two proteins to be recognized as being in proximity by PLA is estimated at roughly 30-50nm, depending on the sizes of the antibodies used (Duolink Brochure; Soderberg, Gullberg et al. 2006; Ling, Albuquerque et al. 2010). The question of whether the interactions observed in this study are direct or indirect could be further investigated by complementary techniques such as co-IP.

The two isoforms of eEF1A are 92% identical and 98% similar, and showed equal activity *in vivo* and *in vitro* translation assay, although with different affinities to GTP and GDP respectively: eEF1A1 has about equal affinity to GDP and GTP; eEF1A2 binds to GDP more strongly than GTP, suggesting eEF1A2 has a greater dependence on eEF1B (Kahns, Lund et al. 1998). It is shown herein that both eEF1A1 and eEF1A2 associate with eEF1B subunits, in accordance with their conventional roles in protein translation elongation. It is not yet clear whether eEF1BδL could be included as well and whether eEF1A binds to each eEF1B subunit directly. Based on the hypothesis that eEF1A2 interacts with eEF1B, it would be of much interest to investigate if eEF1A2 is functionally related to eEF1B as eEF1A1 is. For further investigation of the relationships between eEF1A2 and eEF1B, RNAi will be used to knock down the two proteins respectively in cultured cells. In the meantime, a mouse model, wasted mice, where eEF1A2 is abolished will

also be used to examine the influence of absence of eEF1A2 on eEF1B. These questions will be addressed in detail in the next chapter.

Chapter 5 eEF1A2 absence affects eEF1B expression

5.1 Introduction

The two isoforms of eEF1A have similar translation activities, but different affinities for GTP and GDP. eEF1A1 binds GTP more strongly than GDP while eEF1A2 shows the opposite behaviour (Kahns, Lund et al. 1998). In the previous chapter it was found that both eEF1A1 and eEF1A2 interact with eEF1B physically in cells, which is contrary to the Y2H results (Mansilla, Friis et al. 2002). The aim of this chapter is to determine whether they are dependent on each other as well, and the experiments were carried out on both animal model and cultured cells.

The expression patterns of eEF1A isoforms in different mouse tissues have been thoroughly studied and found to be mutually exclusive. eEF1A1 is almost ubiquitously expressed while eEF1A2 is expressed only in brain, spinal cord, heart and muscle. In mouse brain, isoform-specific antibodies picked up eEF1A1 in glial cells and eEF1A2 in Purkinje cells. Similarly, in spinal cord eEF1A1 is found in glial cells, while eEF1A2 is seen in motor neurones only (Lee, Francoeur et al. 1992; Khalyfa, Bourbeau et al. 2001; Newbery, Loh et al. 2007).

Wasted is a spontaneous recessive mutation that arose in HRS/J mice in The Jackson Lab that leads to immuno-deficiency, neural abnormalities and progressive muscular wasting (Shultz, Sweet et al. 1982). The mutation is a deletion in the promoter and first exon of eEF1A2 (Chambers, Peters et al. 1998). In wild type mice, eEF1A1 declines and eEF1A2 is switched on in brain, spinal cord, heart, muscle postnatally. By 21 days after birth eEF1A1 is shut down in heart and muscle and replaced by eEF1A2. In wasted mice, the reduction of eEF1A1 in brain, spinal cord, heart and muscle happens on schedule, regardless of the absence of eEF1A2 in these tissues (Khalyfa, Bourbeau et al. 2001), and causes death to the mice by 27 days. In this study wasted mice are used as a model for investigation of the possible effect of eEF1A2 absence on the expression of eEF1B subunits.

The effect of eEF1A2 and eEF1B absence was also examined respectively in NSC34 cells using RNAi. NSC34 is a hybrid cell line produced by fusion of motor neuron enriched, embryonic mouse spinal cord cells with mouse neuroblastoma. NSC34 cells have a multipolar neuron-like phenotype and express motor neuron properties (Cashman, Durham et al. 1992). Furthermore, NSC34 cells express both eEF1A isoforms, as well as the brain specific isoform of eEF1Bδ, eEF1BδL, which makes it an ideal cell line for this study.

5.2 Result

5.2.1 Pilot study of eEF1B expression in wild type and wasted mouse tissues

Ten tissues were taken from 24-day wild type and wasted mice to compare the expression of eEF1B subunits at the protein level using Western blotting. The experiments were performed in triplicate, i.e. on three wild type and three wasted mice. Figure 5.1 A shows the results from one representative group.

All of the ten tissues tested express eEF1B subunits, and pancreas has the highest expression compared to other tissues (Figure 5.1 A). eEF1Bα is expressed in all ten tissues tested, although relatively in a lower level in brain, spinal cord, heart, lung and muscle. eEF1Bδ shows different variants, with a longer one expressed only in brain and spinal cord (about 72kD), in accord with previous findings (described in section 1.3.2). Other isoforms are around a similar size, between 32 to 38kD, but have different expression patterns (Figure 5.1 B). One of the isoforms, isoform c, is common to all tissues (indicated by arrow c). In heart and muscle there is a heavier isoform a (indicated by arrow a), while spinal cord and brain have a lighter isoform b (indicated by arrow b) although still heavier than isoform c. In kidney, liver, lung, pancreas, spleen and thymus, there is the lightest isoform d (indicated by arrow d), eEF1Bγ is expressed in a similar level in all the tissues tested, except for muscle, where it is weaker, and pancreas, where it is stronger.

Comparing the western blot results of 24 days old mice, it seems eEF1B levels are different between genotypes in some tissues. For example in the tissues from the representative group shown in Figure 5.1 A, heart, lung and spleen appear to have lower level of eEF1B in wasted than in wild type mice. Yet in other groups of mice not all of these tissues show different levels of eEF1B between genotypes (data not shown). Data from quantitative analysis of all three groups show no significant difference (Figure 5.2), probably due to the high variability between individuals. Note that because the shorter isoforms of eEF1Bδ have similar electroporetic

mobility to each other and thus appear very close in Western blot results, it is hard to quantify the bands separately. As a result the quantification of eEF1Bδ refers to the value of total eEF1Bδ. More mice of different ages were then examined for a time course study, in order to understand if the expression pattern of eEF1B during mouse development in wild type and wasted mice reveals any differences.

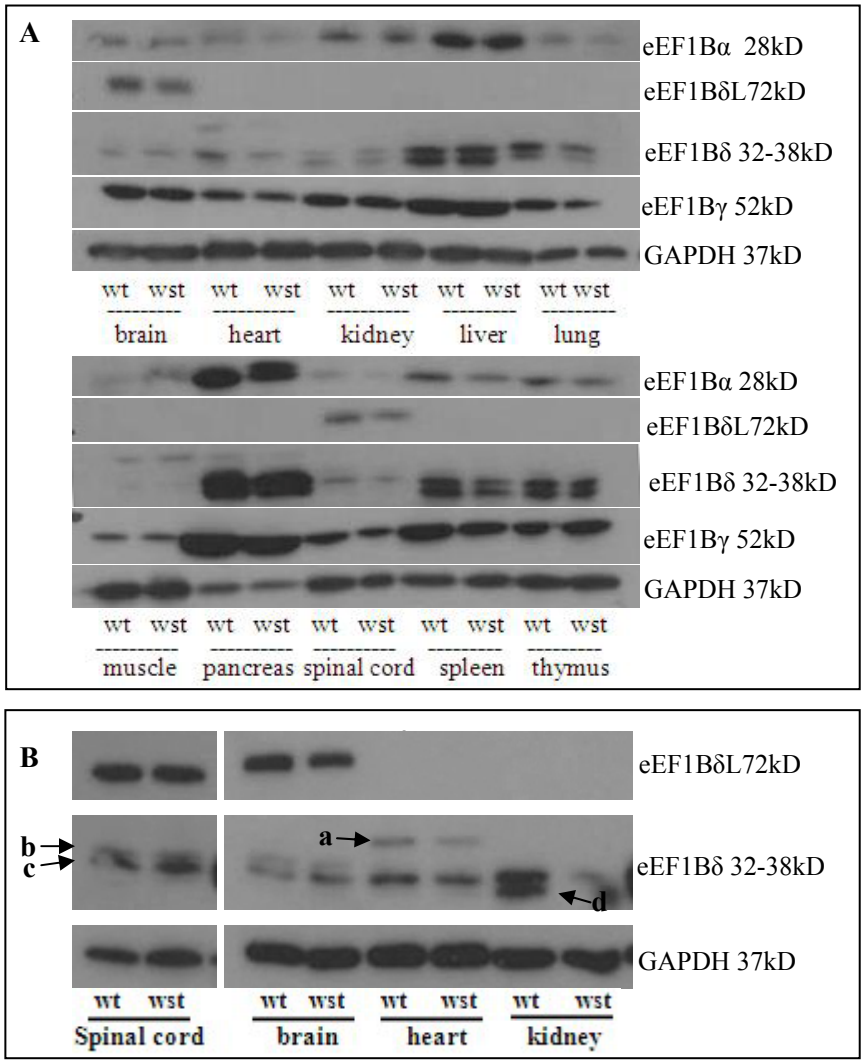

Figure 5.1. The expression of eEF1B subunits in different tissues from wild type (wt) and wasted mice (wst). A. Representative group showing eEF1B expression in mouse tissues. B. Results from another group showing different eEF1Bδ variants.

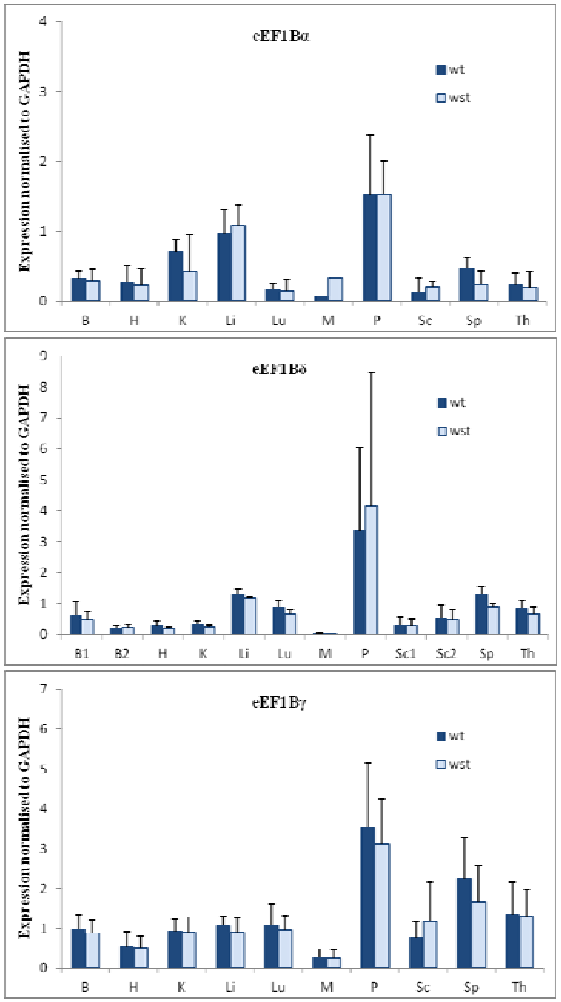

Figure 5.2. Quantitative analysis of eEF1B subunits in 24-day old mice. wt. wild type. wst. wasted. B.Brain. H. Heart. K. Kidney. Li. Liver. Lu. Lung. M. Muscle. P. Pancreas. Sc. Spinal cord. Sp. Spleen. Th. Thymus. B1 and Sc1. eEF1BδL. B2 and Sc2. eEF1Bδ shorter isoforms.

5.2.2 Time course of eEF1B expression in wild type and wasted mouse tissues

In wild type mice, eEF1A2 is expressed mainly in four tissues: spinal cord, brain, heart and muscle. In these tissues the increase of eEF1A2 and decrease of eEF1A1 happen gradually after birth and by 21 days eEF1A1 is undetectable and eEF1A2 takes its place (Khalyfa, Bourbeau et al. 2001). Wasted mice show observable abnormalities from 21 days which coincides with the decline of eEF1A1 in the above tissues, and mice die by 27 days.

For the study of time course of eEF1B expression in mouse tissues during development, the above four tissues taken from 21, 23, 25 and 27 days old wild type and wasted mice were examined.

5.2.2.1 eEF1B expression in mouse spinal cord and brain

From the western blot results on mouse spinal cord, eEF1Bα is apparently weaker in wasted mice of all four ages, while eEF1Bδ expression is more variable. In 21 day old mice, eEF1BδL seems lower in wasted mice spinal cord but other isoforms appear higher in wasted mice. In 23 and 25 day old mice, all eEF1Bδ isoforms are lower in wasted than in wild type mice, while in 27 day old (Figure 5.3 A) and 24 day old (Figure 5.2) mice there is no visible difference of eEF1Bδ expression between wild type and wasted mouse spinal cord. The high variability between samples is probably because the sections were taken from different anatomical levels, which is discussed later in this chapter.

However, the quantitative data show no statistically significant difference in eEF1Bα expression between wild type and wasted mice of all ages. For eEF1Bδ, only 23 day old mice show a lower expression of two isoforms than in wild type (19±3.4% and 46±11% of wild type respectively) (Figure 5.3 B). Unlike eEF1Bα and eEF1Bδ, eEF1Bγ expression in spinal cord is relatively consistent among individuals and between genotypes of all ages.

Brain has the same expression pattern of eEF1A2 as spinal cord. For the experiments on brain mice of two different ages were examined, 21 and 27 days old. All three eEF1B subunits showed no difference between brain from wild type and wasted mice, and quantitation of the data confirmed this (Figure 5.4).

5.2.2.2 eEF1B expression in mouse heart and muscle

Heart and muscle are the two tissues where only eEF1A2 is expressed instead of eEF1A1 after the mice are 21 days old.

In mouse heart eEF1Bα and eEF1Bδ have a similar pattern according to the Western blot results (Figure 5.5 A). In heart from 21 and 23 day old mice the protein is at similar level in wild type and wasted mice, but in 25 and 27 day old mice appears to be lower in wasted mice than in wild type. Quantitative analysis shows that in 27-, but not 25-, day old mice, eEF1Bα is lower in wasted mice than in wild type mice (40±3% of wild type), while the two variants of eEF1Bδ are significantly lower in wasted mice of 25 (34±0.2% and 63±3% of wild type respectively) and 27 days old (34±1.6% and 53±1.5% of wild type respectively) as shown in Western blot results. eEF1Bγ, however, shows no obvious difference between genotypes throughout development.

The other mouse tissue that expresses only eEF1A2 from 21 days is skeletal muscle. In muscle the expression pattern of eEF1B was found to be similar to heart (Figure 5.6 A). eEF1Bα and eEF1Bδ are similar in different genotypes of 21 and 23 day old mice, but are much lower in wasted mice of 25 and 27 days old. eEF1Bγ is the same in genotypes of all ages tested. The quantitative analysis in muscle shows similar results as in heart, except that in muscle from 25 days old mice the expression of eEF1Bα and eEF1Bδ shows no significant difference between genotypes, while in 27 days old mouse muscle, eEF1Bα is 26±5% and the two eEF1Bδ isoforms are 26±0.2% and 18±0.6% of wild type mouse muscle respectively (Figure 5.6 B).

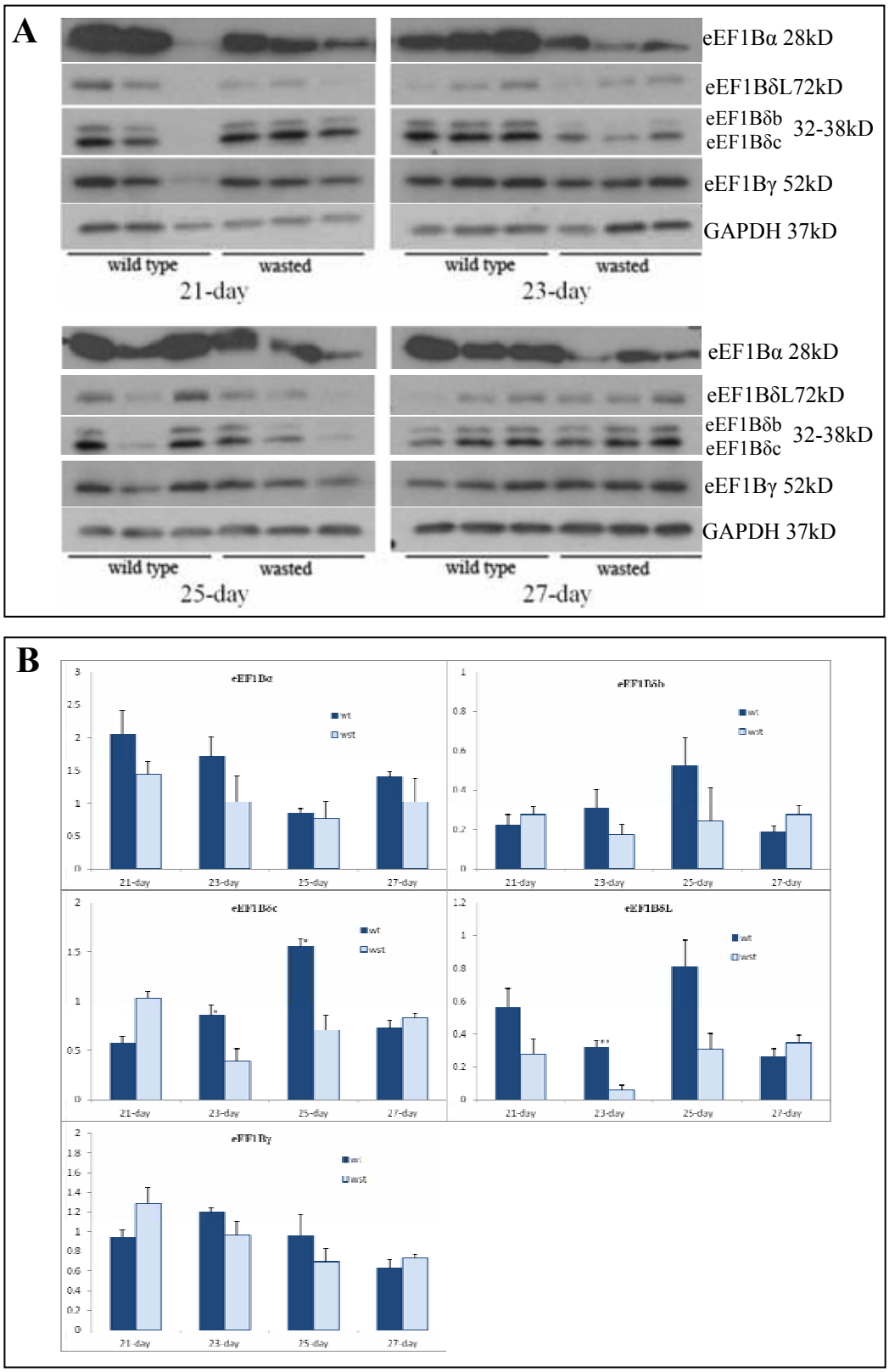

Figure 5.3. Expression of eEF1B in mouse spinal cord. A. Western blot of eEF1Bα, eEF1Bδ and eEF1Bγ in the spinal cord from three wild type (wt) and three wasted (wst) mice of different ages. B. Quantitative analysis of Western blot results normalized to GAPDH. For each age and genotype group the average of three animals were taken and compared between genotypes. The third animal sample of 21-day old wild type mice was excluded due to the lack of visible band. Error bars indicate SEM. *$0.01<p<0.05$. **$p<0.01$

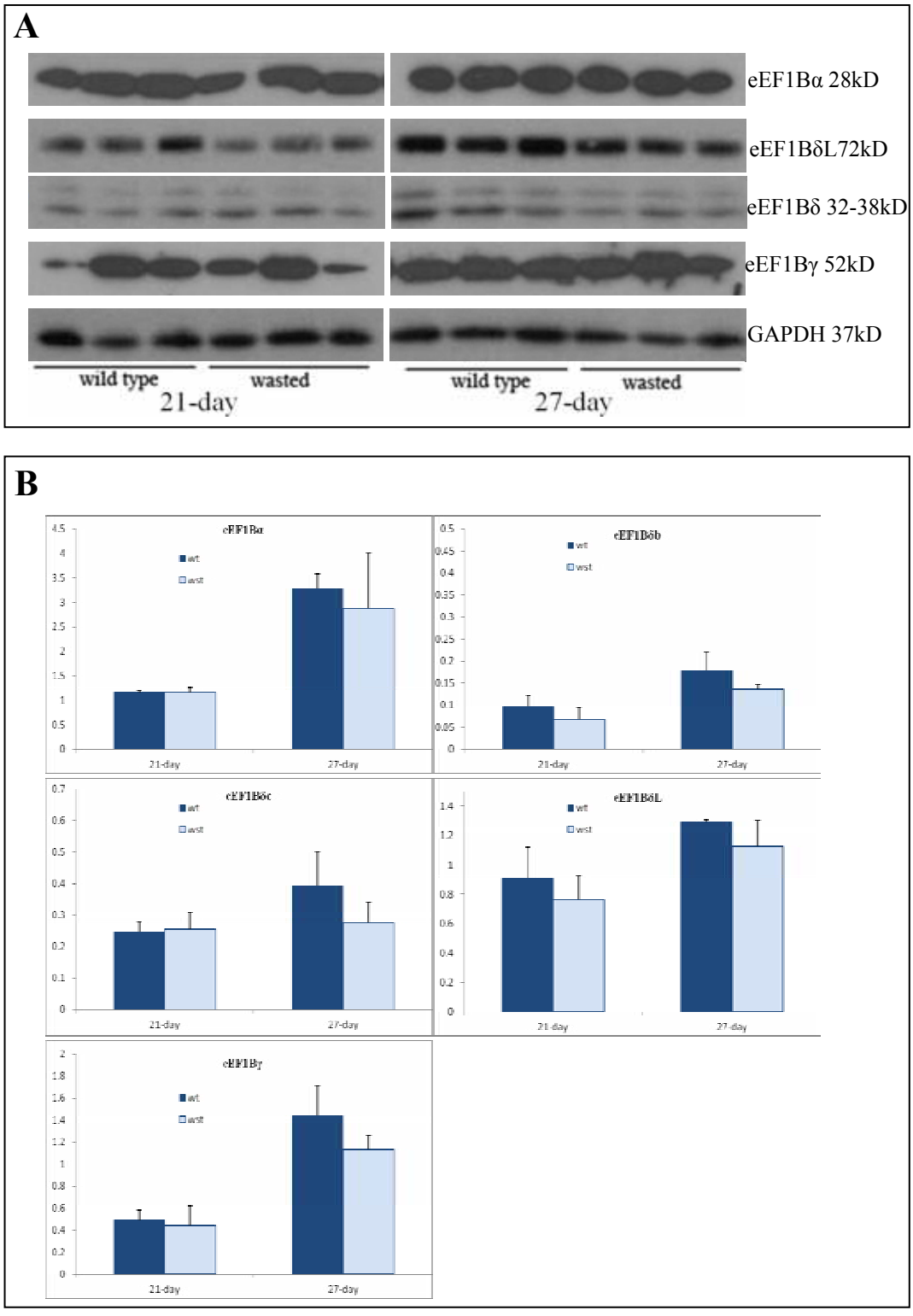

Figure 5.4. Expression of eEF1B in mouse brain. A. Western blot of eEF1Bα, eEF1Bδ and eEF1Bγ in the brain from three wild type (wt) and three wasted (wst) mice of different ages. B. Quantitative analysis of Western blot results normalized to GAPDH. For each age and genotype group the average of three animals were taken and compared between genotypes. Error bars indicate SEM.

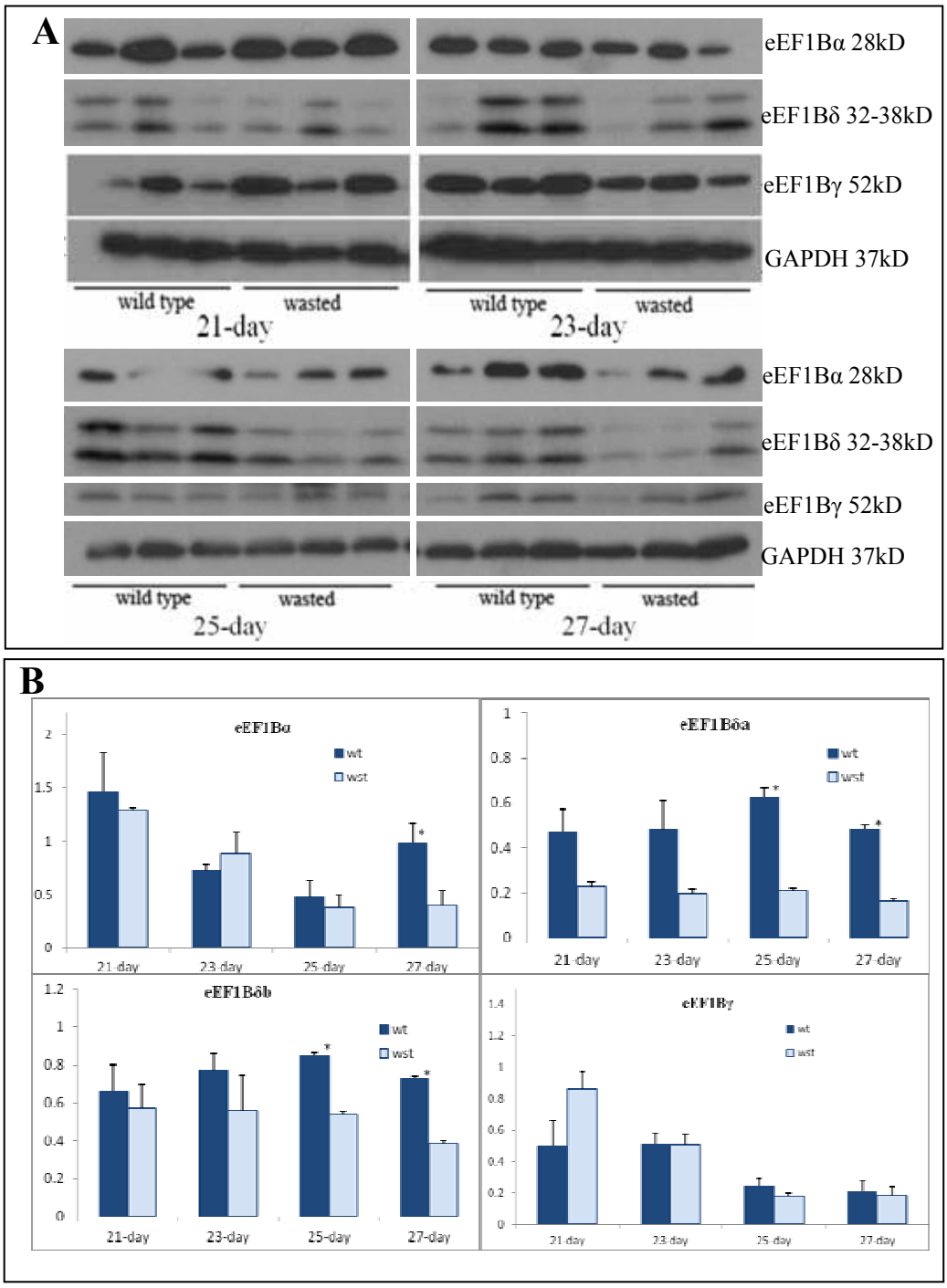

Figure 5.5. **Expression of eEF1Bα and eEF1Bδ in mouse heart.** A.Western blot of eEF1Bα, eEF1Bδ and eEF1Bγ in the heart from three wild type (wt) and three wasted (wst) mice at different ages. B.Quantitative analysis of Western blot results normalized to GAPDH. For each age and genotype group the average of three animals were taken and compared between genotypes. Error bars indicate SEM. *p <0.05

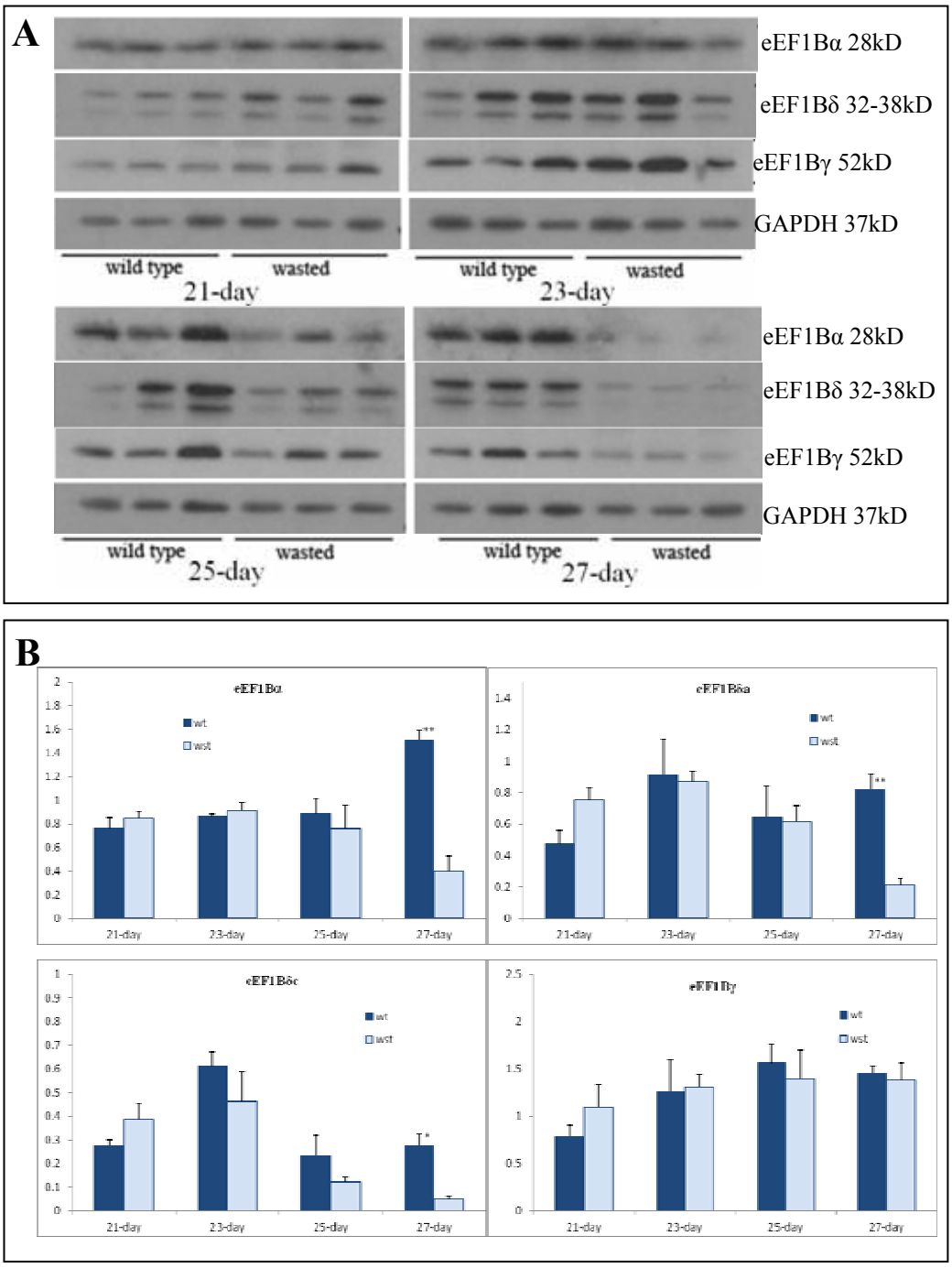

Figure 5.6. Expression of eEF1Bα and eEF1Bδ in mouse muscle. A. Western blot of eEF1Bα, eEF1Bδ and eEF1Bγ in the muscle from three wild type (wt) and three wasted (wst) mice at different ages. B. Quantitative analysis of Western blot results normalized to GAPDH. For each age and genotype group the average of three animals were taken and compared between genotypes. Error bars indicate SEM. *p <0.01

5.2.2.5 eEF1B decreases at the mRNA level

eEF1Bα and eEF1Bδ both declined in heart and muscle from wasted mice where eEF1A2 is absent. In order to examine if this downregulation happens at the protein level only or also at the mRNA level, cDNA from heart tissue of 27 day old wild type and wasted mice were collected to investigate the expression of eEF1B subunits at the mRNA level using quantitative PCR.

As shown in Figure 5.7 the mRNA of both eEF1Bα and eEF1Bδ is lower in wasted mouse heart than in wild type mouse heart (53% of wild type), suggesting that the decrease of eEF1Bα and eEF1Bδ happens at the mRNA level as well as protein level.

eEF1Bγ expression at the mRNA level is similar in wild type and wasted mice, as at the protein level.

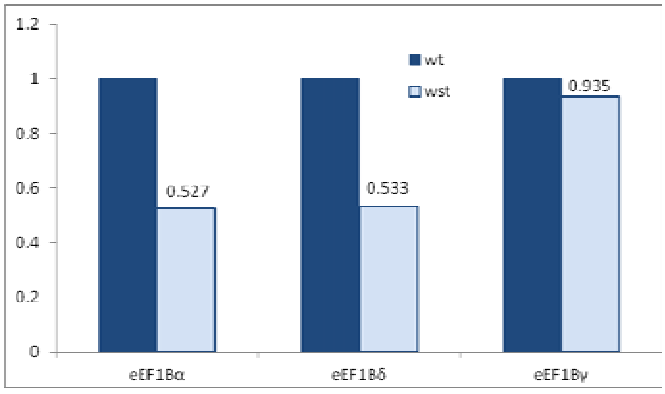

Figure 5.7. Expression of eEF1B mRNA in 27 days mouse heart. Numbers represent the relative value of wst to wt, and each value represents the average of three individual animals of the same genotype.

5.2.3 eEF1Bδ in HSA-EEF1A2 transgenic mice

Transgenic wasted mice that express eEF1A2 under the control of the human specific actin (HSA) promoter were generated in order to investigate the reasons for wasted mice pathology. The transgenic mice, namely HSA-EEF1A2, express eEF1A2 only in heart and muscle, although some transgenic wasted mice express

eEF1A2 in stomach and eyes as well, which is possibly caused by random integration of the transgene.

It was found in our lab that expression of eEF1A2 in neuronal and muscle tissues corrects the abnormalities of wasted mice, but expression of eEF1A2 in heart and muscle alone, as seen in HSA-EEF1A2 transgenic wasted mice, does not, indicating that the wasted phenotype is caused by the loss of eEF1A2 in neurons. HSA-EEF1A2 transgenic wasted mice differ from the wild type mice in the same aspects and with the same ranges of statistic significances as non-transgenic wasted mice do. They have similar phenotypes to non-transgenic wasted mice, including lower body weight, shorter body length, gait abnormality, tremor and muscle pathology. There is no statistical significance in any of the above aspects between HSA-EEF1A2 transgenic and non-transgenic wasted mice. As a result, HSA-EEF1A2 transgenic mice are indistinguishable from non-transgenic wasted mice in sensorimotor function tests and body weight and length. The only difference noticed is that HSA-EEF1A2 transgenic wasted mice survive for one or two days longer than wasted mice according to the result from a relatively small sample number (Permphan Dharmasaroja, PhD thesis, 2007). Unlike non-transgenic wasted mice where there is no eEF1A2 expression at all, the HSA-EEF1A2 transgenic mice used in this study express eEF1A2 in heart and muscle, but no other tissues, and therefore could help to answer the question of whether the downregulation of eEF1Bα and eEF1Bδ in certain tissues from wasted animals is a direct result of the loss of eEF1A2 or whether it is due to other aspects of the wasted phenotype.

Heart tissue proteins extracted from five HSA-EEF1A2 transgenic wasted mice were compared to the proteins of wild type and wasted mice. Although the five transgenic mice were at different ages, number 3 was 25 days old, number 4 was 28 days old, and number 5-7 were 27 days old, they all have a high level of eEF1A2 expression in heart (Figure 5.8 A 3-7), same as or even stronger than in wild type mouse heart (Figure 5.8 A 1), with heart tissue from a wasted mouse used as a negative control (Figure 5.8 A 2).

The heart from the non-transgenic wasted mouse has a lower eEF1Bδ level than wild type, in accordance with the previous observation in section 5.2.2.2, while in HSA-EEF1A2 transgenic wasted mice the level of eEF1Bδ is similar to wild type (Figure 5.8 B). Interestingly, eEF1Bδ in all five transgenic mice is at a similar level to wild type, seemingly not affected by the variable expression level of eEF1A2 (Figure 5.9).

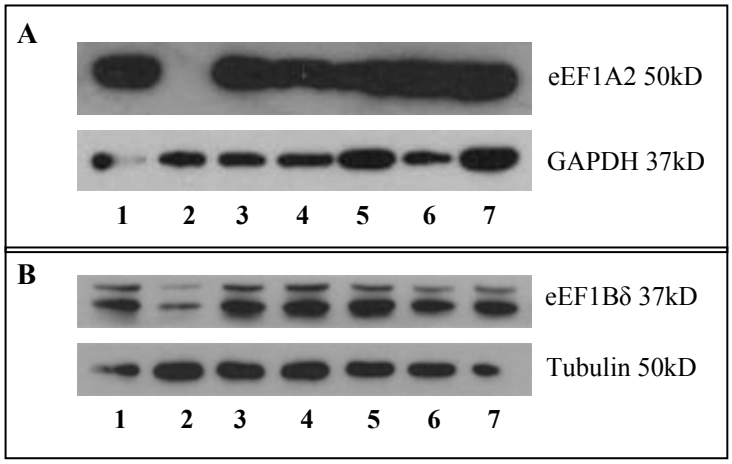

Figure 5.8. Expression of eEF1A2 (A) and eEF1Bδ (B) protein in the heart of HSA-EEF1A2 mice. 1. Wild type mouse. 2. Wasted mouse. 3-7. Five transgenic wasted mice.

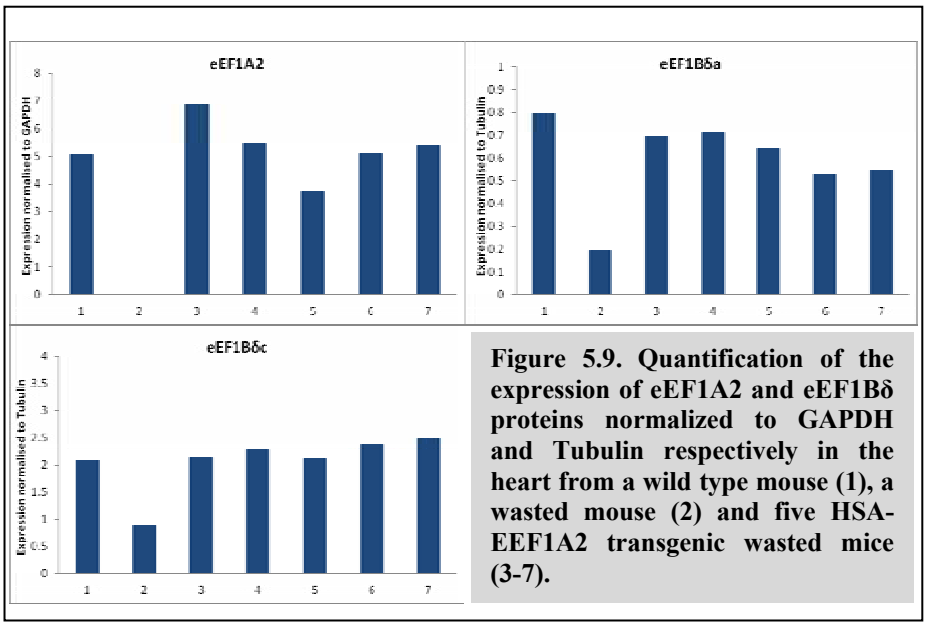

Figure 5.9. Quantification of the expression of eEF1A2 and eEF1Bδ proteins normalized to GAPDH and Tubulin respectively in the heart from a wild type mouse (1), a wasted mouse (2) and five HSA-EEF1A2 transgenic wasted mice (3-7).

5.2.4 RNAi of eEF1A2 and eEF1B subunits in cells

The effect of eEF1A2 absence on eEF1B in cells was investigated using RNAi. eEF1B siRNAs were validated in section 3.2.3.1, and eEF1A2 siRNAs are also specific (Figure 5.10).

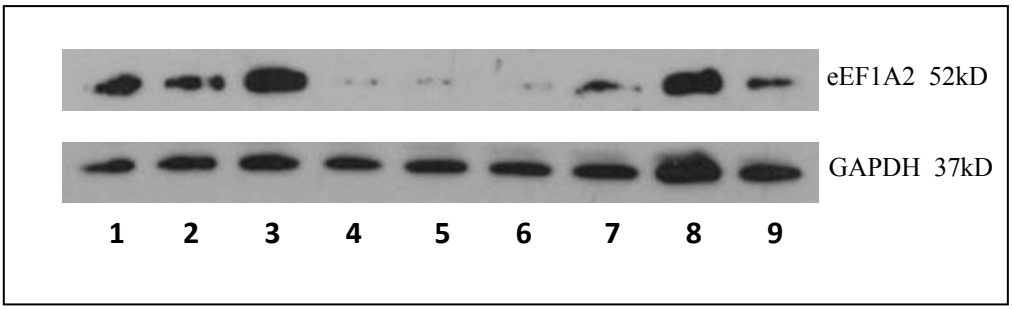

Figure 5.10. Knockdown of eEF1A2 using isoform specific siRNAs. 1. Cells only. 2. Mock. 3. Cells treated with non-targeting siRNAs. 4-6. Three individual samples treated with siRNAa. 7-9. Three individual samples treated with siRNAb.

5.2.4.1Knockdown of eEF1A2 in NSC34 cells

The expression of eEF1B subunits was examined in eEF1A2 knockdown samples.

Unlike the results in mouse tissues, knockdown of eEF1A2 in NSC34 cells did not decrease the level of eEF1Bα (Figure 5.11 A1). In two of the samples of eEF1A2 knockdown, eEF1Bα protein expression was even higher than controls (Figure 5.11 A1 8 and 9), which is possibly due to an artefact. These observations were confirmed when the expression of eEF1Bα was normalised to a loading control, tubulin (Figure 5.11 A2).

eEF1Bδ, on the other hand, showed a lower protein level in samples where eEF1A2 was knocked down (Figure 5.11 B1 and B2), indicating that the knockdown of eEF1A2 causes downregulation of eEF1Bδ in this cellular context. Interestingly in

the three samples where eEF1A2 siRNA was less efficient (Figure 5.10 A7, 8 and 9), the downregulation of eEF1Bδ is less significant than in the other three samples (Figure 5.11 B1 7, 8 and 9). In the Western blot result of eEF1BδL expression the bands representing controls are not clearly visible; it is therefore not possible to quantify eEF1BδL expression.

5.2.4.2 Knockdown of eEF1B in NSC34 cells

The expression of eEF1A2 was examined in cells where eEF1Bα and eEF1Bδ as well as eEF1BδL were knocked down. Surprisingly the three knockdown experiments gave different results.

As shown in Figure 5.12 A1, knockdown of eEF1Bα did not reduce the expression of eEF1A2. In fact it appears that eEF1A2 expression was increased when eEF1Bα was knocked down (Figure 5.12 A2). Knockdown of eEF1Bδ slightly down regulated eEF1A2 expression (Figure 5.12 B1 and B2), while knock down of eEF1BδL showed no effect on eEF1A2 expression (Figure 5.12 C1 and C2), indicating that the decrease of eEF1A2 in Fig 5.12 A1 was caused by the downregulation of the shorter isoforms of eEF1Bδ.

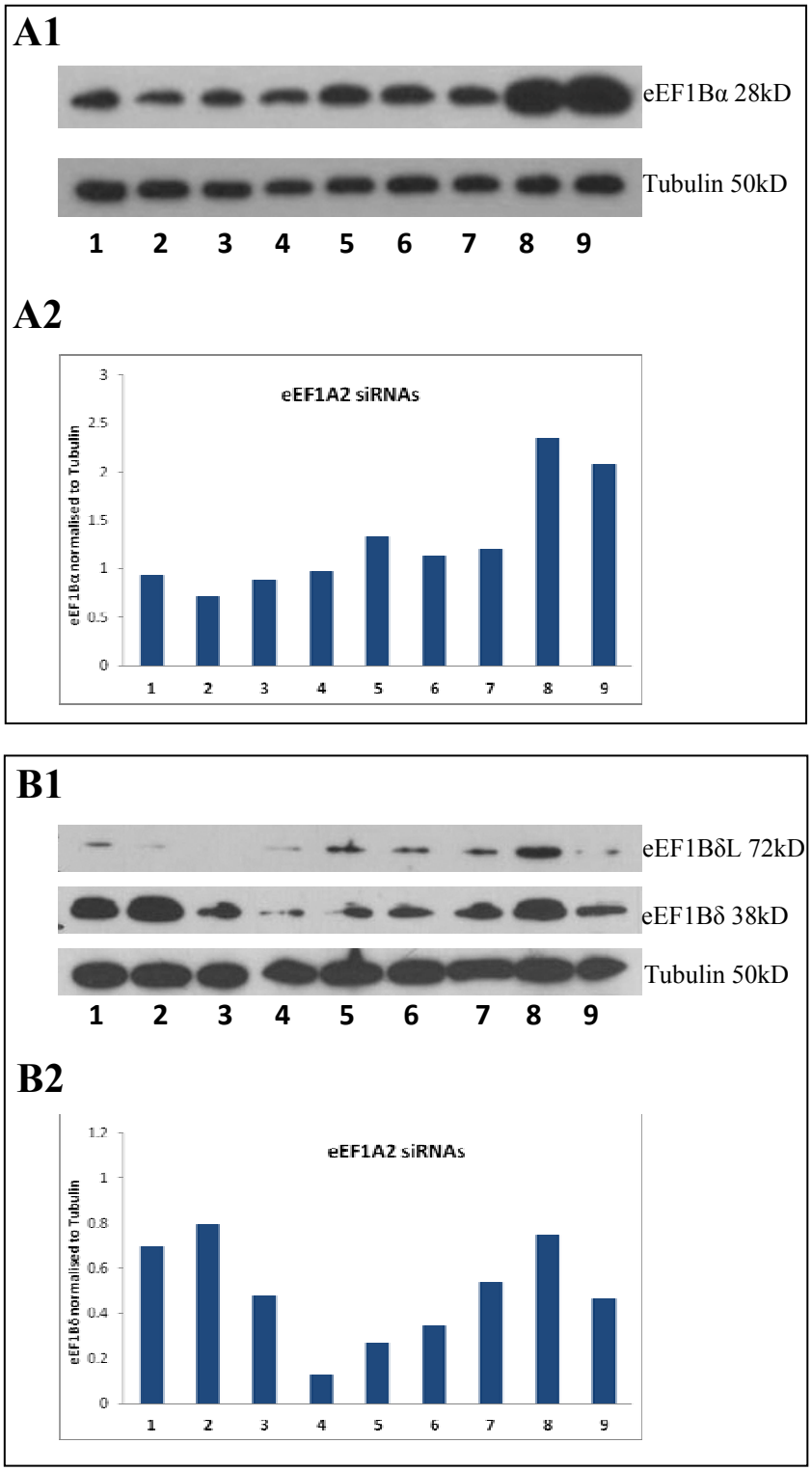

Figure 5.11. Knockdown of eEF1A2 in NSC34 cells. A1. Expression of eEF1Bα. A2. Quantification of eEF1Bα normalized to Tubulin. B1. Expression of eEF1Bδ. B2. Quantification of eEF1Bδ normalized to Tubulin. 1. Cells only. 2. Mock. 3. Cells treated with non-targeting siRNAs. 4-6. Three individual samples treated with eEF1A2 siRNAa. 7-9. Three individual samples treated with eEF1A2 siRNAb.

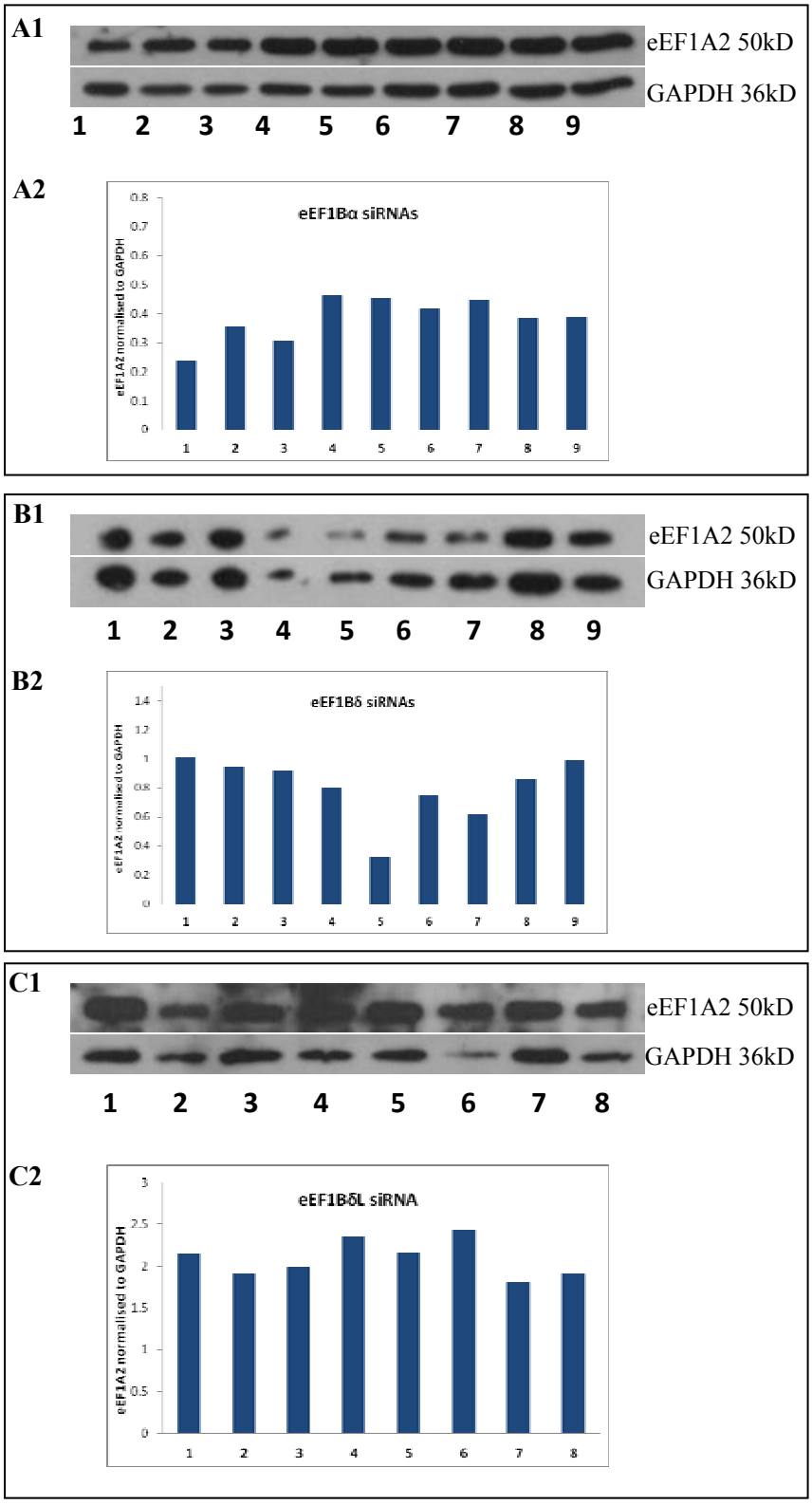

Figure 5.12. eEF1A2 expression in NSC34 cells when eEF1Bα (A1 and A2), eEF1Bδ (B1 and B2), or eEF1BδL (C1 and C2) was knocked down. Quantification of eEF1A2 protein expression normalised to GAPDH. 1. Cells only. 2. Mock. 3. Cells treated with non-targeting siRNAs. 4-6. Three individual samples treated with siRNAa. 7-9. Three individual samples treated with siRNAb.

5.3 Discussion

5.3.1 The absence of eEF1A2 in mice

Following the results achieved in Chapter 4, in this chapter the relationships between expression of eEF1A2 and eEF1B subunits were examined in animals and cultured cells.

In mammals eEF1A2 is expressed in a tissue-specific pattern. It is found to be expressed only in brain, spinal cord, heart and skeletal muscle. In these tissues eEF1A1 expression declines and eEF1A2 increases after birth, and by the age of 21 days eEF1A1 is shut down and taken place by eEF1A2 (Lee, Francoeur et al. 1992; Khalyfa, Bourbeau et al. 2001). Wasted mice do not express eEF1A2 but the decline of eEF1A1 in the above tissues happens on schedule (Khalyfa, Bourbeau et al. 2001). As a result, wasted mice show neurologic and immunologic abnormalities (reviewed in section 1.5) after 21 days and most of them die by 27 days after birth (Lutsep and Rodriguez 1989; Chambers, Peters et al. 1998; Khalyfa, Bourbeau et al. 2001).

In the ten tissues taken from 24 day old mice, it seems that eEF1B is lower in some tissues from wasted mice, but the results are variable. As the decrease of eEF1A1 and increase of eEF1A2 level happens gradually after birth, mice of different ages were then examined in order to demonstrate whether it is the same in mice of other ages.

Four tissues that express eEF1A2 were chosen for the time course study of eEF1B expression: brain, spinal cord, heart and skeletal muscle. The four tissues can be divided into two categories: the first one includes brain and spinal cord, which express both eEF1A1 and eEF1A2 but mutually exclusively in different cells; the second category includes heart and muscle, where only eEF1A2 is expressed instead of eEF1A2 after 21 days. Interestingly the time course of eEF1B expression in these tissues also shows two different patterns: In brain and spinal cord, the expression of eEF1B shows no significant difference between wild type and wasted mice of all

ages tested, whereas in heart and muscle eEF1Bα and eEF1Bδ are much lower in wasted mice than in wild type mice of 25 and 27 years old (summarised in Table 5.1). This difference is likely to be caused by the different expression patterns of eEF1A in these tissues.

In mouse heart and muscle eEF1A1 is present throughout embryonic development but declines postnatally and becomes undetectable by 21 days, while eEF1A2 increases postnatally and takes its place. In wasted mice where eEF1A2 is abolished, there is no eEF1A expressed in heart and muscle by 21 days after birth, which leads to the absence of protein translation in these tissues. However, since the expression level of eEF1B was normalised to a housekeeping protein, it appears that the failure of translation is not responsible for the downregulation of eEF1B. In fact the expression of eEF1Bγ seems fairly stable among genotypes and throughout development, suggesting the downregulation of eEF1Bα and eEF1Bδ is specific and not due to global downregulation. Furthermore, HSA-EEF1A2 transgenic wasted mouse heart expresses eEF1Bδ at a similar level to wild type, without correcting the wasted phenotype and the mice show neuronal and muscular abnormalities as wasted mice do. This result suggests that the downregulation of eEF1Bδ in heart of wasted mice is not a result of the phenotypic abnormalities seen in wasted mice, but is caused specifically by the loss of eEF1A2.

Interestingly, it seems the level of eEF1Bδ is not in accordance with eEF1A2 in transgenic mice, showing that although the transgenic eEF1A2 recovers the expression of eEF1Bδ, excess eEF1A2 does not lead to over expression of eEF1Bδ.

The story is different in brain and spinal cord, where both eEF1A1 and eEF1A2 are expressed mutually exclusively, with eEF1A1 in glial cells and smaller neurons, and eEF1A2 in motor neurons (Khalyfa, Bourbeau et al. 2001; Newbery, Loh et al. 2007). So in wasted mice after 21 days, motor neurons have neither form of eEF1A, yet in other cells eEF1A1 still exists. As a result, while in heart and muscle from wasted mice there is no eEF1A expression, in brain and spinal cord

from the same groups of animal protein translation is still ongoing in certain cells that have eEF1A1, therefore maintaining a relatively stable level of eEF1Bα and eEF1Bδ as the GTP exchange factor. In fact, IHC results on wasted spinal cord do show a weaker staining of eEF1B in some of the motor neurons (section 3.2.4.1). Since the brain and spinal cord extract examined in Western Blotting experiments contains protein from all cell types, further quantitative or semi-quantitative experiments of eEF1B expression in different cell types are needed to support this hypothesis.

Table 5.1. Comparisons of eEF1B expression in four tissues from wild type and wasted mice.

Tissue	eEF1Bα	eEF1Bδ	eEF1Bγ
Spinal cord	Variable	Variable (lower in 23 day old wst)	No difference
Brain	No difference	No difference	No difference
Heart	Lower in 27 day old wst	Lower in 25 and 27 day old wst	No difference
Muscle	Lower in 27 day old wst	Lower in 27 day old wst	No difference

There are a few more points worth noting regarding eEF1B expression in the above four tissues. Firstly, it seems the changes of these two subunits are following slightly different timelines: in heart of all the ages examined the expression of eEF1Bα shows differences between genotype only in 27 days old mice, while for eEF1Bδ the decline starts from the age of 25 days. It should be pointed out that in muscle from 25 days old mice eEF1Bδ shows no significant difference in the quantitative data, which is however more likely to be a result of the variations of eEF1Bδ expression between individuals in wild type mice as shown in Figure 5.6 A. Therefore the possibility of eEF1Bδ also being lower in 25 years old wasted mouse muscle should not be ruled out. Apparently a larger sample size is needed before any conclusion can be drawn. If eEF1Bα and eEF1Bδ indeed show different timecourses in muscle and heart from wasted mice, then it probably means that they are related to eEF1A in different ways, and are affected by time differently.

Secondly, in spinal cord although the overall level of eEF1B shows no significant difference between wild type and wasted mice, the Western blot result is actually highly variable among individuals. The motor neuron pathology in spinal cord of wasted mice varies in different parts, happening first at the cervical level and then progresses caudally, suggesting that eEF1A1 possibly decreases in spinal cord in a cascade. Haematoxylin and eosin staining showed vacuolar degeneration in anterior horn cells at the cervical level but not at the lumbar level of the spinal cord from mice over 24 days (Newbery, Gillingwater et al. 2005).

The motor neurone pathology in wasted mouse spinal cord has added complicity to this study. The spines examined in this study were more or less destroyed when the mice were culled, especially the cervical spine which was easily broken. Although when the spinal cords were taken, they were taken as complete as possible to reduce individual differences, it was still very difficult to make sure that all the samples represented the same level of the spinal cord. Therefore as the expression of eEF1A in spinal cord varies in different samples, the expression of eEF1B may consequently vary between individuals. When the average of eEF1B expression was quantified, none of the ages examined showed statistically significant difference between wild type and wasted mice. Unlike eEF1Bα and eEF1Bδ, although showing no significant difference between wild type and wasted mice as well, the result for eEF1Bγ from spinal cord of different ages is consistent.

In all tissues tested, eEF1Bγ remains at a similar level between genotype despite the age of the mice. Although Western blotting of eEF1Bγ in muscle from 27 days old wasted mice shows a weaker band than in wild type mice, the band of GAPDH which is used as a loading control is also quite faint, probably due to muscle atrophy. When normalised to loading control, the expression of eEF1Bγ in wild type and wasted mice shows no difference. As a subunit of eEF1B, the function of eEF1Bγ in translation is yet not clear. It does not have GTP exchange activity and is considered as a structural subunit for eEF1B that directs the complex to certain cellular components (Janssen and Moller 1988; Le Sourd, Boulben et al. 2006).

eEF1Bγ usually associates tightly with eEF1Bα (Motoyoshi and Iwasaki 1977; Bec, Kerjan et al. 1994), so it is surprising that when eEF1Bα decreases eEF1Bγ seems unaffected. The reason for it is unclear, perhaps related to its non canonical function(s), such as in RNA metabolism (Al-Maghrebi, Brule et al. 2002; Shi, Di Giammartino et al. 2009).

Quantatitive PCR showed that the decline of eEF1Bα and eEF1Bδ in wasted mice happens not only at the protein but also at the mRNA level. However, compared to the differences of eEF1Bα and eEF1Bδ protein levels between wild type and wasted mouse heart, the differences observed at mRNA level appear less significant. Therefore apart from regulation at the mRNA level, the downregulation of eEF1B could also involve post-transcriptional regulation, and/or proteasomal degradation caused by the loss of one subunit of the complex, which can be determined by treating the cells with a proteasome inhibitor. Unfortunately the eEF1Bδ primers used amplify both shorter variants so it is not clear whether the two variants also show different mRNA levels. Besides the Real Time PCR result of muscle cDNA was too variable (data not shown) to compare the expression levels, hence only the results in heart were analysed.

5.3.2 The absence of eEF1A2 in cells

RNAi experiments (results summarized in Table 5.2) in NSC34 cells revealed that when eEF1A2 is knocked down, eEF1Bα stays at a similar level, which is apparently contradictory to the results in wasted mice where the loss of eEF1A2 causes decrease of eEF1Bα. Nevertheless, other research on MCF-7 cells found that eEF1A1 and eEF1Bα siRNAs did not decrease each other's levels (Byun, Han et al. 2009). The MCF-7 cells in this research were harvested 6 days after RNAi, and no other time intervals were investigated, so it is yet unknown whether this result applies to a shorter time interval, for example, 72 hours after transfection as in our study.

Table 5.2. Expression of eEF1A2 and eEF1B in NSC34 cells treated with siRNAs.

Protein	eEF1A2 siRNA	eEF1Bα siRNA	eEF1Bδ siRNA	eEF1BδL siRNA
eEF1A2	-	Increase	Decrease	No change
eEF1Bα	No change	-	-	-
eEF1Bδ	Decrease	-	-	-

One possible explanation for the unchanged eEF1Bα expression after eEF1A2 knockdown is that MCF-7 cells express both eEF1A1 and eEF1A2 (Amiri, Noei et al. 2007), and so do NSC34 cells (data not shown), which means when either eEF1A isoform is knocked down, the other isoform is still present, perhaps maintaining a certain level of translation elongation. Consequently the expression of eEF1Bα is not affected significantly, at least in the short term. More information should be achieved by knocking down both eEF1A isoforms using combined siRNAs. However, since eEF1A is crucial for cell growth, knockdown of both eEF1A isoforms is lethal, making it very difficult to optimize the knockdown conditions to carry out further investigations.

Unexpectedly, when eEF1Bα was knocked down, the level of eEF1A2 was elevated slightly. It has been found that overexpression of eEF1A1 in a eEF1Bα-deficient yeast strain overcomes the lethal phenotype without correcting the growth defect (Ozturk and Kinzy 2008). In cells with eEF1Bα knockdown, the expression of eEF1A1 has not yet been examined, but it is possible that eEF1A2 has similar behaviour to eEF1A1 to complement the loss of eEF1Bα. In this case, perhaps the cells attempt to correct the result of the loss of eEF1Bα, presumably temporarily, by over expressing eEF1A2.

On the other hand, when eEF1A2 was knocked down, eEF1Bδ decreased to a certain extent, and vice versa. The observation that the expression of eEF1A2 is regulated in different ways in the cases of eEF1Bα and eEF1Bδ knockdown indicates

that eEF1Bα and eEF1Bδ may have different physiological functions even though they have similar C-terminal sequences and GDP exchange activity. This was demonstrated earlier in a study with eEF1Bα-deficient yeast which found that human eEF1Bδ failed to complement the conditional growth defects despite the fact that it interacts with yeast eEF1A, as does eEF1Bα (Carr-Schmid, Valente et al. 1999). eEF1Bα and eEF1Bδ bind to eEF1A through different sites, and the binding of eEF1A to eEF1Bα, but not eEF1Bδ, causes masking of the CKII phosphorylation site (Sheu and Traugh 1997). It is unclear whether the CKII phosphorylation could affect the functions of eEF1Bα and eEF1Bδ, or whether the N-terminus difference is also involved, though it is the C-terminus that is considered to interact with eEF1A (van Damme, Amons et al. 1990).

eEF1Bα was not affected by the knockdown of eEF1A2. Whilst eEF1Bδ decreased in the cells where eEF1A2 was knocked down, the decline of eEF1Bδ appeared less significant than in wasted mice. One possible reason is, as stated earlier in this section, the fact that wasted mice have no eEF1A2 and the expression of eEF1A1 also decreases, but the cells with eEF1A2 knockdown still have eEF1A1 and a low level of eEF1A2. The other possibility is the different times when the samples were collected. In fact, the expression of eEF1Bδ in mice did not show a difference between wild type and wasted mice until the age of 25 days, about 4 days after the absence of total eEF1A started, while the RNAi samples were collected 72 hours after transfection. Although mouse tissue and cultured cells cannot be compared directly, it is still possible that the expression of eEF1B changes with time. Hence it would be of much interest to investigate longer time intervals after RNAi, and/or to knock down both eEF1A subunits.

NSC34 cells also express eEF1BδL, which seems not to be affected by changes in eEF1A2 since it shows no change in wasted mice or in cells where eEF1A2 was knocked down, and vice versa, indicating that eEF1BδL, although has a tissue-specific expression pattern that is similar to eEF1A2's, does not affect the expression

of eEF1A2. Clearly a eEF1BδL specific antibody will be helpful to demonstrate whether it is related to eEF1A2 physically or not.

Putting together the above results suggest that eEF1A2 and eEF1B do not only physically interact, but also have a certain dependence on each other, and that the two GEF subunits of eEF1B may have different physiological functions. For future studies more mice should be examined and spinal cord sections need to be processed with particular caution so that different anatomical levels of spinal cord can be investigated for the time course study. Knockdown of combination of eEF1A1 and eEF1A2 siRNAs should be attempted under varying experimental conditions to further establish the effect of eEF1A loss on eEF1B. eEF1A1 should also be examined in cells with eEF1B knockdown to understand whether the two isoforms respond in different ways to loss of eEF1B.

Chapter 6 General Discussion

6.1 Summary

eEF1B is one of the proteins that is believed to have additional functions other than their canonical roles (reviewed in Sasikumar, Perez et al. 2012). In this thesis the involvement of eEF1B in cancer and MND, as well as the relationships between eEF1B subunits and eEF1A were studied.

The cell lines derived from different cancers showed an altered expression pattern of eEF1B subunits compared to untransformed cell lines. However, when the expression of eEF1B protein was examined in tissues, no significant difference was observed between breast cancer tissues and corresponding normal tissues, indicating that the previous reports of an upregulated eEF1B mRNA in breast cancer tissues may not necessarily reflect the expression pattern of eEF1B protein.

A couple of reports suggest that eEF1B subunits may play a role in MND (Bakay, Wang et al. 2006; Wain, Pedroso et al. 2009). The results in this thesis showed that eEF1Bδ had a different expression pattern in the spinal cord from MND patients compared to the controls. Although further evidence is needed, it seems likely that eEF1Bδ is involved in the reactive gliosis that happens in response to CNS injury or diseases. Another proportion of the MND cases showed a lower expression of eEF1Bδ in motor neurons, the reason for which is yet to be elucidated. Unlike the observation in wasted mice, in the MND cases eEF1A2 seems unlikely to be the direct reason for the downregulation of eEF1Bδ, since the motor neurons with a lower expression of eEF1Bδ in MND patients did not always show a lower level of eEF1A2 compared to the controls, suggesting the possibility of other pathways.

The other aspect of this thesis is to investigate the relationship between eEF1B and eEF1A. Previous studies of the structure of eEF1H did not take eEF1A2 into account, except one Y2H experiment which identified no interaction between

eEF1A2 and any of the eEF1B subunits, which is very surprising because eEF1A2 in fact is likely to be more dependent on a GEF than eEF1A1 since it showed more affinity to GDP than GTP (Kahns, Lund et al. 1998). It is important to determine whether eEF1A2 uses eEF1B as its GEF or whether there exist other proteins that function as a GEF for eEF1A2. Using the PLA technique both eEF1A1 and eEF1A2 were found to be associated with eEF1B subunits as a complex. Furthermore, experiments on wasted mice and in cells using RNAi showed that eEF1A2 and eEF1B are not only physically associated, but also have a certain dependence on each other, which supports the possibility that eEF1A2 does use eEF1B as its GEF. Due to the lack of isoform specific antibody, it is yet to know which eEF1Bδ isoform is responsible for the interaction observed between eEF1Bδ and eEF1A, and whether both eEF1A1 and eEF1A2 interact with the same eEF1Bδ isoform(s).

Interestingly, the results of eEF1B expression in cells and tissues showed an unbalanced expression of the three subunits. In the breast cancer cell lines and spinal cord sections from MND patients examined, the expression of eEF1Bα and eEF1Bδ were not always coordinate. The cell lines that showed an altered expression pattern of eEF1Bα did not necessarily show a similar change of eEF1Bδ. Similarly, in wasted mouse spinal cord sections, the two proteins showed different expression patterns especially in motor neurons. The difference is more significant in the spinal cord sections from MND patients, as in some of the MND cases where eEF1Bδ was upregulated in glial cells the expression of eEF1Bα showed no apparent difference from controls. Moreover, the RNAi experiments in cultured cells also revealed that the knockdown of eEF1A2 has different effects on eEF1Bα and eEF1Bδ expression, and vice versa. Although the three eEF1B subunits are considered to function as a complex in protein translation, the observations above indicate that they are very likely to be regulated as individual proteins rather than an integrate complex, which supports the possibility of different physiological functions of eEF1Bα and eEF1Bδ, and could explain in part the significance of the existence of two GEFs that could not supplement nucleotide exchange deficient yeast.

6.2 Future studies

6.2.1 eEF1B subunits expression

As seen in the Western blot results of cell lines and mouse tissues, eEF1Bδ exists as different variants, and the expression of some of the variants showed a tissue specific pattern. These variants should be further examined at the mRNA level to investigate the different eEF1Bδ transcripts. Antibodies against each eEF1Bδ isoform should be produced to detect the sub-cellular localisation and possible cell type specificity of each isoform. Since the two isoforms of eEF1A have different expression patterns through development, it would be interesting to examine whether eEF1Bδ isoforms also show specific expression patterns in different developmental stages and different tissues of mice.

Current studies showed certain inconsistencies regarding the effect of the loss of eEF1B subunits on cell viability. In this thesis an MTT essay did not detect any viability change in NSC34 cells 72 hours after eEF1B knockdown, which needs to be validated using other different methods. Other aspects of the effects of eEF1B knockdown on cultured cells should also be examined, including morphology, cell cycle and apoptosis, in order to fully understand the functions of eEF1B subunits in different cellular activities. Protein overexpression experiment should be used as a complementary approach to attempt to rescue the possible phenotype caused by the knockdown of eEF1B subunits.

6.2.2 The involvement of eEF1B in cancer and MND

More transformed cell lines should be examined for the expression of eEF1B subunits, and corresponding control cell lines would be helpful to compare the expression levels of eEF1B subunits. The expression of eEF1B subunits should be examined at both protein and mRNA levels to investigate whether the lower bands

for eEF1Bα and eEF1Bδ observed in this thesis are caused by alternative splicing or merely products of protein degradation, and whether there is a change of expression levels in transformed cells. On the other hand, protein overexpression experiments coupled with transformation assays such as soft agar assay could be performed in untransformed cell lines to examine whether the overexpression of eEF1B subunits is able to cause transformation in cultured cells, in order to further understand the tumourigenesis potential of eEF1B subunits.

In the breast cancer tissues investigated in this thesis, the expression of eEF1Bα and eEF1Bδ proteins in cancer tissues showed no significant difference from that in corresponding control tissues. A larger sample size of cancer specimens originating from different tissues, as well as suitable controls of corresponding normal tissues would be helpful to understand whether the upregulation of eEF1B subunits is common in different cancers. Furthermore, the expression levels of eEF1B mRNA in cancer tissues can be also examined using microarray and real-time quantitative PCR.

For the study of eEF1B expression in MND, more specimens would be used and all the three subunits would be examined in the spinal cord from MND patients and the controls, for both the expression level and the distribution of eEF1B in different cell types of spinal cord. A relatively larger sample size and detailed pathological information would be necessary to demonstrate whether there is any correlation between the expression patterns of eEF1B and the pathological background as well as the age and sex of the patients.

Nevertheless, the preliminary data in this thesis indicate a possible involvement of eEF1Bδ in neuronal diseases, which is worth further investigation and could be studied in two areas. Firstly, immunofluorescence experiments staining the spinal cord sections from MND patients with both eEF1Bδ and a glial marker such as GFAP and CD68 would be very helpful to demonstrate whether the increase of eEF1Bδ expression indeed happened in activated astrocytes and/or microglia to

examine whether eEF1Bδ showed potential relevance to reactive gliosis. Furthermore, the previous report of the involvement of EEF1D gene in a CNV region associated with ALS (Wain, Pedroso et al. 2009) also needs further verification. The copy number of EEF1D gene in ALS cases can be determined by Real Time PCR; genomic DNA sequencing can be performed to identify potential gene mutation(s) in the EEF1D gene in ALS cases.

The other aspect is related to the isoforms of eEF1Bδ. Since the longest isoform, eEF1BδL, is tissue specific, and has been found only in brain, spinal cord and testis, it is of great interest to determine whether it is this isoform that is involved in MND. If this is confirmed, the next step is to investigate whether the loss of eEF1BδL in neurons causes any phenotype. This can be approached in cultured neuronal cells using siRNAs targeting different eEF1Bδ isoforms, as well as mouse strains with deletion of a specific isoform.

Knockout mice produced by inactivating a specific eEF1B subunit could also be used to investigate the loss of each eEF1B subunit in animals to extend the studies proposed in section 6.2.1. Conditional knockout mice with deletion of each eEF1B subunit in a tissue specific manner would be helpful to interpret the effect of eEF1B loss more specifically, especially if the deletion of any eEF1B subunit leads to embryonic lethality. For example, the inactivation of eEF1B subunits in brain and spinal cord can be used to investigate the loss of eEF1B in CNS and to understand its potential roles in neuronal disease.

6.2.3 The relationship between eEF1B and eEF1A

PLA experiments in this study have detected a physical interaction between eEF1B subunits and both eEF1A isoforms. Since the PLA with eEF1A1 was performed in stable cell lines, in the future study if a eEF1A1 antibody for PLA is available, the interaction of eEF1B and the endogenous eEF1A1 should be examined.

The physical interaction between eEF1B and eEF1A should be further confirmed using techniques such as coIP.

The expression of eEF1B in different tissues from wild type and wasted mice has established a certain expression pattern of eEF1B in the absence of eEF1A, but the expression of eEF1B in spinal cord needs more analysis. In the future study the spinal cord sections need to be processed with particular caution so that different anatomical levels of spinal cord can be investigated for the time course study and to determine whether there is any correlation between eEF1B expression change and the anatomical level. In addition, the Western blot experiments should be combined with IHC to examine whether the downregulation of protein expression happens in a cell type specific manner.

From the results of wasted mouse tissues and the RNAi experiments, it seems that eEF1Bα and eEF1Bδ showed different dependencies on the two eEF1A isoforms. In order to further establish the relationships between eEF1B subunits and eEF1A, combinations of eEF1A1 and eEF1A2 siRNAs should be used under varying experimental conditions to knockdown both eEF1A isoforms at the same time, and cell lines expressing only eEF1A1 should be also examined for eEF1A or eEF1B knockdown. These experiments would be helpful to answer the question of whether the expression of eEF1Bα and eEF1Bδ is dependent on the existence of a specific eEF1A isoform or not.

The details of how the two GEF and the two eEF1A isoforms associate are not clear, yet they did show dependence on each other although to different extents. The next step is to determine whether this dependence is functional. Protein synthesis assay should be combined with RNAi experiments to investigate whether the loss of each subunit or isoform affects the function of others in protein synthesis.

6.2.4 The tissue specific isoform of eEF1Bδ

So far little is known about eEF1BδL, but it is obviously of great interest to understand the significance of a tissue specific isoform of eEF1Bδ. As mentioned earlier, a eEF1BδL specific antibody would be helpful for further investigations. Since there is no commercial eEF1BδL antibody available at the moment, it would be necessary to generate a eEF1BδL specific antibody that can be used to investigate the whether eEF1BδL is specifically expressed in certain cell types, and whether it coexists with eEF1A2 in brain and spinal cord.

eEF1BδL has an expression pattern that overlaps with that of eEF1A2, which leads to a hypothesis that eEF1BδL might be the GEF specifically for eEF1A2. The results in this thesis showed that the expression of eEF1BδL and eEF1A2 is not necessarily dependent on each other, but it does not exclude the possibility of eEF1BδL and eEF1A2 do form a complex in protein translation or that they are functionally related, similar to the relationship between eEF1Bγ and eEF1A2. A PLA experiment of eEF1A2 and eEF1BδL would be helpful to determine whether eEF1BδL is included in eEF1H complex to function in protein translation elongation.

The potential involvement of eEF1BδL in the heat shock response by inducing the expression of HSE-containing genes in cooperation with HSF1 is also worth further investigation. Because there is some inconsistency between my results and the report of eEF1BδL in the heat shock response, different cell lines should be examined in further studies to establish the expression profile of eEF1BδL in cells, and the heat shock dependent alternative splicing of eEF1BδL needs to be confirmed at both protein and mRNA levels.

Once the involvement of eEF1BδL in heat shock response is established, the next question would be whether it is related to the role of eEF1A as one of the co-activators for HSF1 in response to heat shock, which, if eEF1BδL is not exclusively expressed in motor neurons, could be addressed by a series of knockdown

experiment followed by heat shock in cultured cells. Since cultured cells expressing eEF1BδL usually express both eEF1A1 and eEF1A2, it is worth performing the above knockdown experiments both in cells with endogenous eEF1δL and in cells that do not express eEF1A2 but are transfected with exogenous eEF1BδL, even though eEF1A2 is likely not able to complement the loss of eEF1A1 in heat shock.

6.3 Conclusion

The data presented in this thesis demonstrated the involvement of eEF1B in diseases and its relationship with eEF1A *in vivo* and further supports the theory that the eEF1B subunits can be regulated separately from the complex, providing insight into the non-canonical functions of eEF1B subunits and the composition of the eEF1H complex. Further studies are needed to investigate of the roles of each eEF1B subunit other than in protein translation, such as tumourigenesis, motor neuron diseases, cell cycle regulation and stress response, and the underlying mechanisms, as well as to understand in detail the structure of eEF1H and the significance of different isoforms of eEF1B.

Conference Presentations

Translation Elongation Factor 1B in Normal and Cancer Cells. 2009, Western General Hospital, The University of Edinburgh, UK

The Roles of Translation Elongation Factor 1B. 2010, Western General Hospital, The University of Edinburgh, UK

The Interaction between Eukaryotic Translation Elongation Factor 1A and 1B Subunits. Posted on Translation UK conference, 2011, Cambridge, UK

Investigating the Role of Translation Elongation Factor 1B. 2011, Western General Hospital, The University of Edinburgh, UK

References

Abbott, C. M., H. J. Newbery, et al. (2009). "eEF1A2 and neuronal degeneration." Biochem Soc Trans 37(Pt 6): 1293-7.

Al-Maghrebi, M., J. T. Anim, et al. (2005). "Up-regulation of eukaryotic elongation factor-1 subunits in breast carcinoma." Anticancer Res 25(3c): 2573-7.

Al-Maghrebi, M., H. Brule, et al. (2002). "The 3' untranslated region of human vimentin mRNA interacts with protein complexes containing eEF-1gamma and HAX-1." Nucleic Acids Res 30(23): 5017-28.

Amiri, A., F. Noei, et al. (2007). "eEF1A2 activates Akt and stimulates Akt-dependent actin remodeling, invasion and migration." Oncogene 26(21): 3027-40.

Amons, R., W. Pluijms, et al. (1983). "Sequence homology between EF-1 alpha, the alpha-chain of elongation factor 1 from Artemia salina and elongation factor EF-Tu from Escherichia coli." FEBS Lett 153(1): 37-42.

Ann, D. K., I. K. Moutsatsos, et al. (1991). "Isolation and characterization of the rat chromosomal gene for a polypeptide (pS1) antigenically related to statin." J Biol Chem 266(16): 10429-37.

Bakay, M., Z. Wang, et al. (2006). "Nuclear envelope dystrophies show a transcriptional fingerprint suggesting disruption of Rb-MyoD pathways in muscle regeneration." Brain 129(Pt 4): 996-1013.

Batulan, Z., G. A. Shinder, et al. (2003). "High threshold for induction of the stress response in motor neurons is associated with failure to activate HSF1." J Neurosci 23(13): 5789-98.

Bauer, J., T. Sminia, et al. (1994). "Phagocytic activity of macrophages and microglial cells during the course of acute and chronic relapsing experimental autoimmune encephalomyelitis." J Neurosci Res 38(4): 365-75.

Bec, G., P. Kerjan, et al. (1994). "Reconstitution in vitro of the valyl-tRNA synthetase-elongation factor (EF) 1 beta gamma delta complex. Essential roles of the NH2-terminal extension of valyl-tRNA synthetase and of the EF-1 delta subunit in complex formation." J Biol Chem 269(3): 2086-92.

Bec, G. and J. P. Waller (1989). "Valyl-tRNA synthetase from rabbit liver. II. The enzyme derived from the high-Mr complex displays hydrophobic as well as polyanion-binding properties." J Biol Chem 264(35): 21138-43.

Belle, R., J. Derancourt, et al. (1989). "A purified complex from Xenopus oocytes contains a p47 protein, an in vivo substrate of MPF, and a p30 protein respectively homologous to elongation factors EF-1 gamma and EF-1 beta." FEBS Lett 255(1): 101-4.

Billaut-Mulot, O., R. Fernandez-Gomez, et al. (1997). "Phenotype of recombinant Trypanosoma cruzi which overexpress elongation factor 1-gamma: possible involvement of EF-1gamma GST-like domain in the resistance to clomipramine." Gene 198(1-2): 259-67.

Boulben, S., A. Monnier, et al. (2003). "Sea urchin elongation factor 1delta (EF1delta) and evidence for cell cycle-directed localization changes of a sub-fraction of the protein at M phase." Cell Mol Life Sci 60(10): 2178-88.

Buffo, A., I. Rite, et al. (2008). "Origin and progeny of reactive gliosis: A source of multipotent cells in the injured brain." Proc Natl Acad Sci U S A **105**(9): 3581-6.

Byun, H. O., N. K. Han, et al. (2009). "Cathepsin D and eukaryotic translation elongation factor 1 as promising markers of cellular senescence." Cancer Res 69(11): 4638-47.

Cahoy, J. D., B. Emery, et al. (2008). "A transcriptome database for astrocytes, neurons, and oligodendrocytes: a new resource for understanding brain development and function." J Neurosci 28(1): 264-78.

Carr-Schmid, A., L. Valente, et al. (1999). "Mutations in elongation factor 1beta, a guanine nucleotide exchange factor, enhance translational fidelity." Mol Cell Biol 19(8): 5257-66.

Carvalho, J. F., M. D. Carvalho, et al. (1984). "Purification of various forms of elongation factor 1 from rabbit reticulocytes." Arch Biochem Biophys 234(2): 591-602.

Cashman, N. R., H. D. Durham, et al. (1992). "Neuroblastoma x spinal cord (NSC) hybrid cell lines resemble developing motor neurons." Dev Dyn 194(3): 209-21.

Chambers, D. M., J. Peters, et al. (1998). "The lethal mutation of the mouse wasted (wst) is a deletion that abolishes expression of a tissue-specific isoform of translation elongation factor 1alpha, encoded by the Eef1a2 gene." Proc Natl Acad Sci U S A 95(8): 4463-8.

Chambers, D. M., G. A. Rouleau, et al. (2001). "Comparative genomic analysis of genes encoding translation elongation factor 1B(alpha) in human and mouse shows EEF1B1 to be a recent retrotransposition event." Genomics 77(3): 145-8.

Chang, Y. W. and J. A. Traugh (1997). "Phosphorylation of elongation factor 1 and ribosomal protein S6 by multipotential S6 kinase and insulin stimulation of translational elongation." J Biol Chem 272(45): 28252-7.

Chang, Y. W. and J. A. Traugh (1998). "Insulin stimulation of phosphorylation of elongation factor 1 (eEF-1) enhances elongation activity." Eur J Biochem 251(1-2): 201-7.

Chen, C. J. and J. A. Traugh (1995). "Expression of recombinant elongation factor 1 beta from rabbit in Escherichia coli. Phosphorylation by casein kinase II." Biochim Biophys Acta 1264(3): 303-11.

Chi, K., D. V. Jones, et al. (1992). "Expression of an elongation factor 1 gamma-related sequence in adenocarcinomas of the colon." Gastroenterology 103(1): 98-102.

Costa-Mattioli, M., W. S. Sossin, et al. (2009). "Translational control of long-lasting synaptic plasticity and memory." Neuron 61(1): 10-26.

Cronin, S., H. M. Blauw, et al. (2008). "Analysis of genome-wide copy number variation in Irish and Dutch ALS populations." Hum Mol Genet 17(21): 3392-8.

De Benedetti A and Graff J R (2004). "eIF-4E expression and its role in malignancies and metastases." Oncogene 23: 3189–99.

De Bortoli, M., R. C. Castellino, et al. (2006). "Medulloblastoma outcome is adversely associated with overexpression of EEF1D, RPL30, and RPS20 on the long arm of chromosome 8." BMC Cancer 6: 223.

Ender, B., P. Lynch, et al. (1993). "Overexpression of an elongation factor-1 gamma-hybridizing RNA in colorectal adenomas." Mol Carcinog 7(1): 18-20.

Esposito, A. M. and T. G. Kinzy (2010). "The eukaryotic translation elongation Factor 1Bgamma has a non-guanine nucleotide exchange factor role in protein metabolism." J Biol Chem 285(49): 37995-8004.

Everley, P. A., J. Krijgsveld, et al. (2004). "Quantitative cancer proteomics: stable isotope labeling with amino acids in cell culture (SILAC) as a tool for prostate cancer research." Mol Cell Proteomics 3(7): 729-35.

Ewing, R. M., P. Chu, et al. (2007). "Large-scale mapping of human protein-protein interactions by mass spectrometry." Mol Syst Biol 3: 89.

Fabian, M. R., N. Sonenberg, et al. (2010). "Regulation of mRNA translation and stability by microRNAs." Annu Rev Biochem 79: 351-79.

Fan, Y., M. Schlierf, et al. (2010). "Drosophila translational elongation factor-1gamma is modified in response to DOA kinase activity and is essential for cellular viability." Genetics 184(1): 141-54.

Fang, D., Z. Li, et al. (2008). "Expression of bystin in reactive astrocytes induced by ischemia/reperfusion and chemical hypoxia in vitro." Biochim Biophys Acta 1782(11): 658-63.

Frazier, M. L., N. Inamdar, et al. (1998). "Few point mutations in elongation factor-1gamma gene in gastrointestinal carcinoma." Mol Carcinog 22(1): 9-15.

Fredriksson, S., M. Gullberg, et al. (2002). "Protein detection using proximity-dependent DNA ligation assays." Nat Biotechnol 20(5): 473-7.

Fujimoto, H. and I. Mabuchi (2010). "Elongation factors are involved in cytokinesis of sea urchin eggs." Genes Cells 15(2): 123-35.

Furukawa, R., T. M. Jinks, et al. (2001). "Elongation factor 1beta is an actin-binding protein." Biochim Biophys Acta 1527(3): 130-40.

Glezer, I., A. R. Simard, et al. (2007). "Neuroprotective role of the innate immune system by microglia." Neuroscience 147(4): 867-83.

Godon, C., G. Lagniel, et al. (1998). "The H2O2 stimulon in Saccharomyces cerevisiae." J Biol Chem 273(35): 22480-9.

Green, S. L. and R. J. Tolwani (1999). "Animal models for motor neuron disease." Lab Anim Sci 49(5): 480-7.

Guerrucci, M. A., A. Monnier, et al. (1999). "The elongation factor-1delta (EF-1delta) originates from gene duplication of an EF-1beta ancestor and fusion with a protein-binding domain." Gene 233(1-2): 83-7.

Gustafsdottir, S. M., J. Schlingemann, et al. (2007). "In vitro analysis of DNA-protein interactions by proximity ligation." Proc Natl Acad Sci U S A 104(9): 3067-72.

Gyenis, L., J. S. Duncan, et al. (2011). "Unbiased functional proteomics strategy for protein kinase inhibitor validation and identification of bona fide protein kinase substrates: application to identification of as a substrate for CK2." J Proteome Res 10(11): 4887-901.

Hafezparast, M., A. Ahmad-Annuar, et al. (2002). "Mouse models for neurological disease." Lancet Neurol 1(4): 215-24.

Hanbauer, I., E. S. Boja, et al. (2003). "A homologue of elongation factor 1 gamma regulates methionine sulfoxide reductase A gene expression in Saccharomyces cerevisiae." Proc Natl Acad Sci U S A 100(14): 8199-204.

Hiraga, K., K. Suzuki, et al. (1993). "Cloning and characterization of the elongation factor EF-1 beta homologue of Saccharomyces cerevisiae. EF-1 beta is essential for growth." FEBS Lett 316(2): 165-9.

Holcik, M. and N. Sonenberg (2005). "Translational control in stress and apoptosis." Nat Rev Mol Cell Biol 6(4): 318-27.

Ito, D., K. Tanaka, et al. (2001). "Enhanced expression of Iba1, ionized calcium-binding adapter molecule 1, after transient focal cerebral ischemia in rat brain." Stroke 32(5): 1208-15.

Jacob, A. N., G. Kandpal, et al. (1996). "Isolation of expressed sequences that include a gene for familial breast cancer (BRCA2) and other novel transcripts from a five megabase region on chromosome 13q12." Oncogene 13(1): 213-21.

Janssen, G. M., G. D. Maessen, et al. (1988). "Phosphorylation of elongation factor 1 beta by an endogenous kinase affects its catalytic nucleotide exchange activity." J Biol Chem 263(23): 11063-6.

Janssen, G. M. and W. Moller (1988). "Elongation factor 1 beta gamma from Artemia. Purification and properties of its subunits." Eur J Biochem 171(1-2): 119-29.

Janssen, G. M., J. Morales, et al. (1991). "A major substrate of maturation promoting factor identified as elongation factor 1 beta gamma delta in Xenopus laevis." J Biol Chem 266(23): 14885-8.

Janssen, G. M., H. T. van Damme, et al. (1994). "The subunit structure of elongation factor 1 from Artemia. Why two alpha-chains in this complex?" J Biol Chem 269(50): 31410-7.

Jarvius, M., J. Paulsson, et al. (2007). "In situ detection of phosphorylated platelet-derived growth factor receptor beta using a generalized proximity ligation method." Mol Cell Proteomics 6(9): 1500-9.

Jeppesen, M. G., P. Ortiz, et al. (2003). "The crystal structure of the glutathione S-transferase-like domain of elongation factor 1Bgamma from Saccharomyces cerevisiae." J Biol Chem 278(47): 47190-8.

Jiang, S., C. L. Wolfe, et al. (2005). "Three-dimensional reconstruction of the valyl-tRNA synthetase/elongation factor-1H complex and localization of the delta subunit." FEBS Lett 579(27): 6049-54.

Joseph, P., Y. X. Lei, et al. (2002). "Oncogenic potential of mouse translation elongation factor-1 delta, a novel cadmium-responsive proto-oncogene." J Biol Chem 277(8): 6131-6.

Joseph, P., C. M. O'Kernick, et al. (2004). "Expression profile of eukaryotic translation factors in human cancer tissues and cell lines." Mol Carcinog 40(3): 171-9.

Jung, M., A. D. Kondratyev, et al. (1994). "Elongation factor 1 delta is enhanced following exposure to ionizing radiation." Cancer Res 54(10): 2541-3.

Kahns, S., A. Lund, et al. (1998). "The elongation factor 1 A-2 isoform from rabbit: cloning of the cDNA and characterization of the protein." Nucleic Acids Res 26(8): 1884-90.

Kaitsuka, T., K. Tomizawa, et al. (2011). "Transformation of eEF1Bdelta into heat-shock response transcription factor by alternative splicing." EMBO Rep 12(7): 673-81.

Kato, K., Y. Kawaguchi, et al. (2001). "Epstein-Barr virus-encoded protein kinase BGLF4 mediates hyperphosphorylation of cellular elongation factor 1delta (EF-1delta): EF-1delta is

universally modified by conserved protein kinases of herpesviruses in mammalian cells." J Gen Virol 82(Pt 6): 1457-63.

Kawaguchi, Y. and K. Kato (2003). "Protein kinases conserved in herpesviruses potentially share a function mimicking the cellular protein kinase cdc2." Rev Med Virol 13(5): 331-40.

Kawaguchi, Y., K. Kato, et al. (2003). "Conserved protein kinases encoded by herpesviruses and cellular protein kinase cdc2 target the same phosphorylation site in eukaryotic elongation factor 1delta." J Virol 77(4): 2359-68.

Kawaguchi, Y., T. Matsumura, et al. (1999). "Cellular elongation factor 1delta is modified in cells infected with representative alpha-, beta-, or gammaherpesviruses." J Virol 73(5): 4456-60.

Kawaguchi, Y., C. Van Sant, et al. (1998). "Eukaryotic elongation factor 1delta is hyperphosphorylated by the protein kinase encoded by the U(L)13 gene of herpes simplex virus 1." J Virol 72(3): 1731-6.

Khalyfa, A., D. Bourbeau, et al. (2001). "Characterization of elongation factor-1A (eEF1A-1) and eEF1A-2/S1 protein expression in normal and wasted mice." J Biol Chem 276(25): 22915-22.

Kim, H. J., E. J. Song, et al. (2002). "Proteomic analysis of protein phosphorylations in heat shock response and thermotolerance." J Biol Chem 277(26): 23193-207.

Kim, J., W. Namkung, et al. (2009). "The role of translation elongation factor eEF1A in intracellular alkalinization-induced tumor cell growth." Lab Invest 89(8): 867-74.

Kim, S., J. Kellner, et al. (2007). "Interaction between the keratin cytoskeleton and eEF1Bgamma affects protein synthesis in epithelial cells." Nat Struct Mol Biol 14(10): 982-3.

Kim, S., P. Wong, et al. (2006). "A keratin cytoskeletal protein regulates protein synthesis and epithelial cell growth." Nature 441(7091): 362-5.

Kinzy, T. G., T. L. Ripmaster, et al. (1994). "Multiple genes encode the translation elongation factor EF-1 gamma in Saccharomyces cerevisiae." Nucleic Acids Res 22(13): 2703-7.

Kobayashi, S., S. Kidou, et al. (2001). "Detection and characterization of glutathione S-transferase activity in rice EF-1betabeta'gamma and EF-1gamma expressed in Escherichia coli." Biochem Biophys Res Commun 288(3): 509-14.

Koonin, E. V., A. R. Mushegian, et al. (1994). "Eukaryotic translation elongation factor 1 gamma contains a glutathione transferase domain--study of a diverse, ancient protein superfamily using motif search and structural modeling." Protein Sci 3(11): 2045-54.

Kugel, J. F. and J. A. Goodrich (2006). "Beating the heat: A translation factor and an RNA mobilize the heat shock transcription factor HSF1." Mol Cell 22(2): 153-4.

Lamberti, A., M. Caraglia, et al. (2004). "The translation elongation factor 1A in tumorigenesis, signal transduction and apoptosis: review article." Amino Acids 26(4): 443-8.

Le Sourd, F., S. Boulben, et al. (2006). "eEF1B: At the dawn of the 21st century." Biochim Biophys Acta 1759(1-2): 13-31.

Lee, M. H. and Y. J. Surh (2009). "eEF1A2 as a putative oncogene." Ann N Y Acad Sci 1171: 87-93.

Lee, S., A. M. Francoeur, et al. (1992). "Tissue-specific expression in mammalian brain, heart, and muscle of S1, a member of the elongation factor-1 alpha gene family." J Biol Chem 267(33): 24064-8.

Lei, Y. X., J. K. Chen, et al. (2002). "Blocking the translation elongation factor-1 delta with its antisense mRNA results in a significant reversal of its oncogenic potential." Teratog Carcinog Mutagen 22(5): 377-83.

Lei, Y. X., M. Wang, et al. (2010). "Alternative expression and sequence of human elongation factor-1 delta during malignant transformation of human bronchial epithelial cells induced by cadmium chloride." Biomed Environ Sci 23(2): 151-7.

Lew, Y., D. V. Jones, et al. (1992). "Expression of elongation factor-1 gamma-related sequence in human pancreatic cancer." Pancreas 7(2): 144-52.

Lin, S. K., M. C. Chang, et al. (2005). "Proteomic analysis of the expression of proteins related to rice quality during caryopsis development and the effect of high temperature on expression." Proteomics 5(8): 2140-56.

Ling, S. C., C. P. Albuquerque, et al. (2010). "ALS-associated mutations in TDP-43 increase its stability and promote TDP-43 complexes with FUS/TLS." Proc Natl Acad Sci U S A 107(30): 13318-23.

Liu, Y., Q. Chen, et al. (2004). "Tumor suppressor gene 14-3-3sigma is down-regulated whereas the proto-oncogene translation elongation factor 1delta is up-regulated in non-small cell lung cancers as identified by proteomic profiling." J Proteome Res 3(4): 728-35.

Lutsep, H. L. and M. Rodriguez (1989). "Ultrastructural, morphometric, and immunocytochemical study of anterior horn cells in mice with "wasted" mutation." J Neuropathol Exp Neurol 48(5): 519-33.

Mansilla, F., C. A. Dominguez, et al. (2008). "Translation elongation factor eEF1A binds to a novel myosin binding protein-C-like protein." J Cell Biochem 105(3): 847-58.

Mansilla, F., I. Friis, et al. (2002). "Mapping the human translation elongation factor eEF1H complex using the yeast two-hybrid system." Biochem J 365(Pt 3): 669-76.

Mateyak, M. K. and T. G. Kinzy (2010). "eEF1A: thinking outside the ribosome." J Biol Chem 285(28): 21209-13.

Mathur, S., K. R. Cleary, et al. (1998). "Overexpression of elongation factor-1gamma protein in colorectal carcinoma." Cancer 82(5): 816-21.

Matsuzawa, S. I. and J. C. Reed (2001). "Siah-1, SIP, and Ebi collaborate in a novel pathway for beta-catenin degradation linked to p53 responses." Mol Cell 7(5): 915-26.

Mazan-Mamczarz, K., A. Lal, et al. (2006). "Translational repression by RNA-binding protein TIAR." Mol Cell Biol 26(7): 2716-27.

Miller, J. T., J. H. Bartley, et al. (2005). "The neuroblast and angioblast chemotaxic factor SDF-1 (CXCL12) expression is briefly up regulated by reactive astrocytes in brain following neonatal hypoxic-ischemic injury." BMC Neurosci 6: 63.

Mimori, K., M. Mori, et al. (1996). "Elongation factor 1 gamma mRNA expression in oesophageal carcinoma." Gut 38(1): 66-70.

Mimori, K., M. Mori, et al. (1995). "The overexpression of elongation factor 1 gamma mRNA in gastric carcinoma." Cancer 75(6 Suppl): 1446-9.

Minella, O., O. Mulner-Lorillon, et al. (1998). "Multiple phosphorylation sites and quaternary organization of guanine-nucleotide exchange complex of elongation factor-1 (EF-1betagammadelta/ValRS) control the various functions of EF-1alpha." Biosci Rep 18(3): 119-27.

Minella, O., O. Mulner-Lorillon, et al. (1996). "The guanine-nucleotide-exchange complex (EF-1 beta gamma delta) of elongation factor-1 contains two similar leucine-zipper proteins EF-1 delta, p34 encoded by EF-1 delta 1 and p36 encoded by EF-1 delta 2." Eur J Biochem 237(3): 685-90.

Monnier, A., R. Belle, et al. (2001). "Evidence for regulation of protein synthesis at the elongation step by CDK1/cyclin B phosphorylation." Nucleic Acids Res 29(7): 1453-7.

Morales, J., P. Cormier, et al. (1992). "Molecular cloning of a new guanine nucleotide-exchange protein, EF1 delta." Nucleic Acids Res. 20(15): 4091.

Motoyoshi, K. and K. Iwasaki (1977). "Resolution of the polypeptide chain elongation factor-1 beta gamma into subunits and some properties of the subunits." J Biochem 82(3): 703-8.

Mulner-Lorillon, O., P. Cormier, et al. (1992). "Phosphorylation of Xenopus elongation factor-1 gamma by cdc2 protein kinase: identification of the phosphorylation site." Exp Cell Res 202(2): 549-51.

Mulner-Lorillon, O., O. Minella, et al. (1994). "Elongation factor EF-1 delta, a new target for maturation-promoting factor in Xenopus oocytes." J Biol Chem 269(31): 20201-7.

Mulner-Lorillon, O., R. Poulhe, et al. (1989). "Purification of a p47 phosphoprotein from Xenopus laevis oocytes and identification as an in vivo and in vitro p34cdc2 substrate." FEBS Lett 251(1-2): 219-24.

Murray, A. W. (2004). "Recycling the cell cycle: cyclins revisited." Cell 116(2): 221-34.

Newbery, H. J., T. H. Gillingwater, et al. (2005). "Progressive loss of motor neuron function in wasted mice: effects of a spontaneous null mutation in the gene for the eEF1 A2 translation factor." J Neuropathol Exp Neurol 64(4): 295-303.

Newbery, H. J., D. H. Loh, et al. (2007). "Translation elongation factor eEF1A2 is essential for post-weaning survival in mice." J Biol Chem 282(39): 28951-9.

Newbery, H. J., I. Stancheva, et al. (2011). "Evolutionary importance of translation elongation factor eEF1A variant switching: eEF1A1 down-regulation in muscle is conserved in Xenopus but is controlled at a post-transcriptional level." Biochem Biophys Res Commun 411(1): 19-24.

Ogawa, K., T. Utsunomiya, et al. (2004). "Clinical significance of elongation factor-1 delta mRNA expression in oesophageal carcinoma." Br J Cancer 91(2): 282-6.

Olarewaju, O., P. A. Ortiz, et al. (2004). "The translation elongation factor eEF1B plays a role in the oxidative stress response pathway." RNA Biol 1(2): 89-94.

Ong, L. L., C. P. Er, et al. (2003). "Kinectin anchors the translation elongation factor-1 delta to the endoplasmic reticulum." J Biol Chem 278(34): 32115-23.

Ong, L. L., P. C. Lin, et al. (2006). "Kinectin-dependent assembly of translation elongation factor-1 complex on endoplasmic reticulum regulates protein synthesis." J Biol Chem 281(44): 33621-34.

Ovanesov, M. V., Y. Ayhan, et al. (2008). "Astrocytes play a key role in activation of microglia by persistent Borna disease virus infection." J Neuroinflammation 5: 50.

Ozturk, S. B. and T. G. Kinzy (2008). "Guanine nucleotide exchange factor independence of the G-protein eEF1A through novel mutant forms and biochemical properties." J Biol Chem 283(34): 23244-53.

Palen, E., T. T. Huang, et al. (1990). "Comparison of phosphorylation of elongation factor 1 from different species by casein kinase II." FEBS Lett 274(1-2): 12-4.

Palen, E., R. C. Venema, et al. (1994). "GDP as a regulator of phosphorylation of elongation factor 1 by casein kinase II." Biochemistry 33(28): 8515-20.

Pavitt, G. D. and C. G. Proud (2009). "Protein synthesis and its control in neuronal cells with a focus on vanishing white matter disease." Biochem Soc Trans 37(Pt 6): 1298-310.

Pellerin, L. and P. J. Magistretti (2004). "Neuroenergetics: calling upon astrocytes to satisfy hungry neurons." Neuroscientist 10(1): 53-62.

Perez, J. M., J. Kriek, et al. (1998). "Expression, purification, and spectroscopic studies of the guanine nucleotide exchange domain of human elongation factor, EF-1beta." Protein Expr Purif 13(2): 259-67.

Pestova, T. V. and V. G. Kolupaeva (2002). "The roles of individual eukaryotic translation initiation factors in ribosomal scanning and initiation codon selection." Genes Dev 16(22): 2906-22.

Peters, H. I., Y. W. Chang, et al. (1995). "Phosphorylation of elongation factor 1 (EF-1) by protein kinase C stimulates GDP/GTP-exchange activity." Eur J Biochem 234(2): 550-6.

Peyrl, A., K. Krapfenbauer, et al. (2003). "Protein profiles of medulloblastoma cell lines DAOY and D283: identification of tumor-related proteins and principles." Proteomics 3(9): 1781-800.

Phaneuf, D., N. Wakamatsu, et al. (1996). "Dramatically different phenotypes in mouse models of human Tay-Sachs and Sandhoff diseases." Hum Mol Genet 5(1): 1-14.

Pittman, Y. R., K. Kandl, et al. (2009). "Coordination of eukaryotic translation elongation factor 1A (eEF1A) function in actin organization and translation elongation by the guanine nucleotide exchange factor eEF1Balpha." J Biol Chem 284(7): 4739-47.

Pittman, Y. R., L. Valente, et al. (2006). "Mg2+ and a key lysine modulate exchange activity of eukaryotic translation elongation factor 1B alpha." J Biol Chem 281(28): 19457-68.

Pizzuti, A., M. Gennarelli, et al. (1993). "Human elongation factor EF-1 beta: cloning and characterization of the EF1 beta 5a gene and assignment of EF-1 beta isoforms to chromosomes 2,5,15 and X." Biochem Biophys Res Commun 197(1): 154-62.

Potter, M., A. Bernstein, et al. (1998). "The wst gene regulates multiple forms of thymocyte apoptosis." Cell Immunol 188(2): 111-7.

Prado, M. A., P. Casado, et al. (2007). "Phosphorylation of human eukaryotic elongation factor 1Bgamma is regulated by paclitaxel." Proteomics 7(18): 3299-304.

Roblick, U. J., D. Hirschberg, et al. (2004). "Sequential proteome alterations during genesis and progression of colon cancer." Cell Mol Life Sci 61(10): 1246-55.

Rozen, S. and H. Skaletsky (2000). "Primer3 on the WWW for general users and for biologist programmers." Methods Mol Biol 132: 365-86.

Saijo, K. and C. K. Glass (2011). "Microglial cell origin and phenotypes in health and disease." Nat Rev Immunol 11(11): 775-87.

Sanders, J., J. A. Maassen, et al. (1992). "Elongation factor-1 messenger-RNA levels in cultured cells are high compared to tissue and are not drastically affected further by oncogenic transformation." Nucleic Acids Res 20(22): 5907-10.

Santello, M. and A. Volterra (2009). "Synaptic modulation by astrocytes via Ca2+-dependent glutamate release." Neuroscience 158(1): 253-9.

Sasikumar, A. N., W. B. Perez, et al. (2012). "The many roles of the eukaryotic elongation factor 1 complex." WIREs RNA 2012. doi: 10.1002/wrna.1118.

Savaldi-Goldstein, S., G. Sessa, et al. (2000). "The ethylene-inducible PK12 kinase mediates the phosphorylation of SR splicing factors." Plant J 21(1): 91-6.

Scheper, G. C., M. S. van der Knaap, et al. (2007). "Translation matters: protein synthesis defects in inherited disease." Nat Rev Genet 8(9): 711-23.

Schneider-Poetsch, T., T. Usui, et al. (2010). "Garbled messages and corrupted translations." Nat Chem Biol 6(3): 189-198.

Schummers, J., H. Yu, et al. (2008). "Tuned responses of astrocytes and their influence on hemodynamic signals in the visual cortex." Science 320(5883): 1638-43.

Shamovsky, I., M. Ivannikov, et al. (2006). "RNA-mediated response to heat shock in mammalian cells." Nature 440(7083): 556-60.

Shenton, D. and C. M. Grant (2003). "Protein S-thiolation targets glycolysis and protein synthesis in response to oxidative stress in the yeast Saccharomyces cerevisiae." Biochem J 374(Pt 2): 513-9.

Sheu, G. T. and J. A. Traugh (1997). "Recombinant subunits of mammalian elongation factor 1 expressed in Escherichia coli. Subunit interactions, elongation activity, and phosphorylation by protein kinase CKII." J Biol Chem 272(52): 33290-7.

Sheu, G. T. and J. A. Traugh (1999). "A structural model for elongation factor 1 (EF-1) and phosphorylation by protein kinase CKII." Mol Cell Biochem 191(1-2): 181-6.

Shi, Y., D. C. Di Giammartino, et al. (2009). "Molecular architecture of the human pre-mRNA 3' processing complex." Mol Cell 33(3): 365-76.

Shuda, M., N. Kondoh, et al. (2000). "Enhanced expression of translation factor mRNAs in hepatocellular carcinoma." Anticancer Res 20(4): 2489-94.

Shultz, L. D., H. O. Sweet, et al. (1982). "'Wasted', a new mutant of the mouse with abnormalities characteristic to ataxia telangiectasia." Nature 297(5865): 402-4.

Silvera, D., S. C. Formenti, et al. (2010). "Translational control in cancer." Nat Rev Cancer 10(4): 254-66.

Sinha, P., S. Kohl, et al. (2000). "Identification of novel proteins associated with the development of chemoresistance in malignant melanoma using two-dimensional electrophoresis." Electrophoresis 21(14): 3048-57.

Sivan, G., N. Kedersha, et al. (2007). "Ribosomal slowdown mediates translational arrest during cellular division." Mol Cell Biol 27(19): 6639-46.

Sivan, G., R. Aviner, et al. (2011). "Mitotic modulation of translation elongation factor 1 leads to hindered tRNA delivery to ribosomes." J Biol Chem.

Slezak, M. and F. W. Pfrieger (2003). "New roles for astrocytes: regulation of CNS synaptogenesis." Trends Neurosci 26(10): 531-5.

Soares, D. C., P. N. Barlow, et al. (2009). "Structural models of human eEF1A1 and eEF1A2 reveal two distinct surface clusters of sequence variation and potential differences in phosphorylation." PLoS One 4(7): e6315.

Soderberg, O., M. Gullberg, et al. (2006). "Direct observation of individual endogenous protein complexes in situ by proximity ligation." Nat Methods 3(12): 995-1000.

Soderberg, O., K. J. Leuchowius, et al. (2008). "Characterizing proteins and their interactions in cells and tissues using the in situ proximity ligation assay." Methods 45(3): 227-32.

Sofroniew, M. V. and H. V. Vinters (2010). "Astrocytes: biology and pathology." Acta Neuropathol 119(1): 7-35.

Tomlinson, V. A., H. J. Newbery, et al. (2005). "Translation elongation factor eEF1A2 is a potential oncoprotein that is overexpressed in two-thirds of breast tumours." BMC Cancer 5: 113.

Trifilieff, P., M. L. Rives, et al. (2011). "Detection of antigen interactions ex vivo by proximity ligation assay: endogenous dopamine D2-adenosine A2A receptor complexes in the striatum." Biotechniques 51(2): 111-8.

Ueda, H., H. Tezuka, et al. (2004). "Nuclear Envelope Breakdown Is a Prominent Feature in Spinal Motor Neurons of Wasted Mice." ACTA HISTOCHEMICA ET CYTOCHEMICA 37(3): 159-162.

van Damme, H., R. Amons, et al. (1991). "Mapping the functional domains of the eukaryotic elongation factor 1 beta gamma." Eur J Biochem 197(2): 505-11.

van Damme, H. T., R. Amons, et al. (1990). "Elongation factor 1 beta of artemia: localization of functional sites and homology to elongation factor 1 delta." Biochim Biophys Acta 1050(1-3): 241-7.

Venema, R. C., H. I. Peters, et al. (1991). "Phosphorylation of elongation factor 1 (EF-1) and valyl-tRNA synthetase by protein kinase C and stimulation of EF-1 activity." J Biol Chem 266(19): 12574-80.

Veremieva, M., A. Khoruzhenko, et al. (2010). "Unbalanced expression of the translation complex eEF1 subunits in human cardioesophageal carcinoma." Eur J Clin Invest 41(3): 269-76.

Vickers, T. J., S. Wyllie, et al. (2004). "Leishmania major elongation factor 1B complex has trypanothione S-transferase and peroxidase activity." J Biol Chem 279(47): 49003-9.

Wain, L. V., I. Pedroso, et al. (2009). "The role of copy number variation in susceptibility to amyotrophic lateral sclerosis: genome-wide association study and comparison with published loci." PLoS One 4(12): e8175.

Wang, C. C., M. Kadota, et al. (2004). "Molecular hierarchy in neurons differentiated from mouse ES cells containing a single human chromosome 21." Biochem Biophys Res Commun 314(2): 335-50.

Wang, H. and H. Tiedge (2004). "Translational control at the synapse." Neuroscientist 10(5): 456-66.

Woloschak, G. E., M. Rodriguez, et al. (1987). "Characterization of immunologic and neuropathologic abnormalities in wasted mice." J Immunol 138(8): 2493-9.

Wu, H., Y. Shi, et al. (2011). "Eukaryotic translation elongation factor 1 delta inhibits the ubiquitin ligase activity of SIAH-1." Mol Cell Biochem.

Yoon, S., W. T. Cong, et al. (2009). "Proteome response to ochratoxin A-induced apoptotic cell death in mouse hippocampal HT22 cells." Neurotoxicology 30(4): 666-76.

Yoshibayashi, H., H. Okabe, et al. (2007). "SIAH1 causes growth arrest and apoptosis in hepatoma cells through beta-catenin degradation-dependent and -independent mechanisms." Oncol Rep 17(3): 549-56.

Yun, B., R. Farkas, et al. (1994). "The Doa locus encodes a member of a new protein kinase family and is essential for eye and embryonic development in Drosophila melanogaster." Genes Dev 8(10): 1160-73.

Zeng, X., A. J. Liao, et al. (2007). "[Screening human gastric carcinoma-associated antigens by serologic proteome analysis]." Ai Zheng 26(10): 1080-4.

Appendix 1. eEF1B2 in spinal cord from MND cases. Scale bar, 200µm.

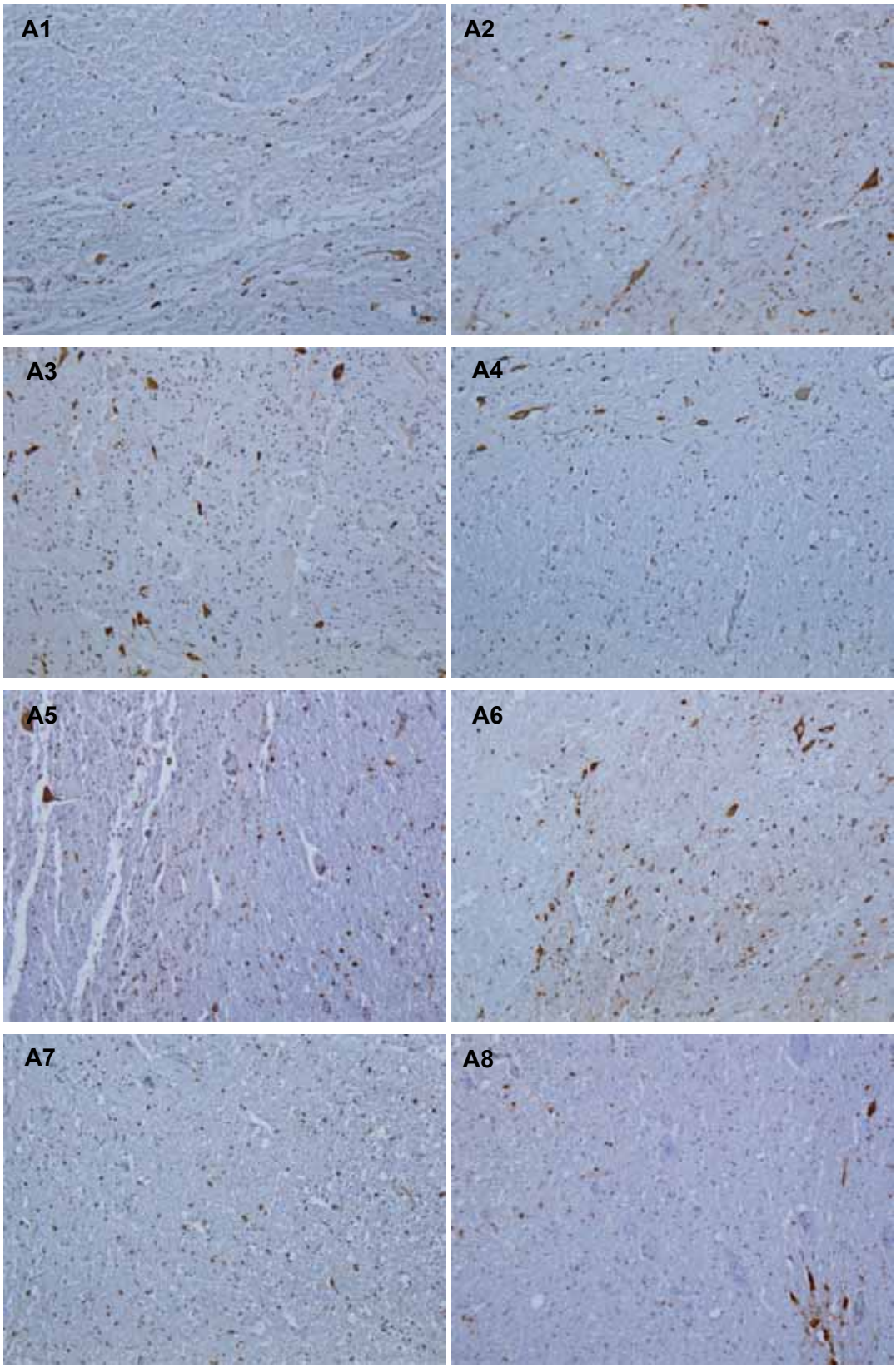

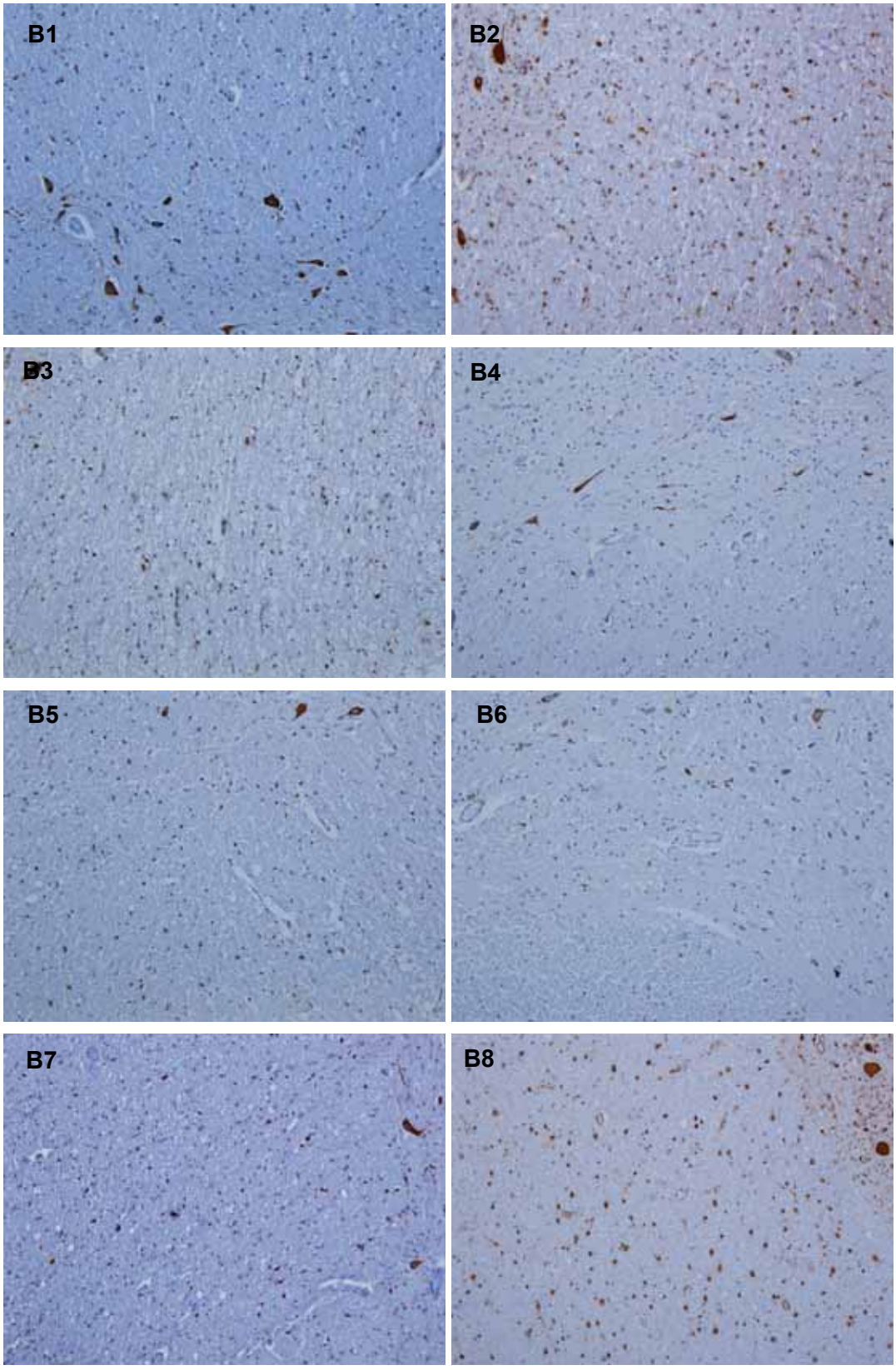
B1
B2
B3
B4
B5
B6
B7
B8

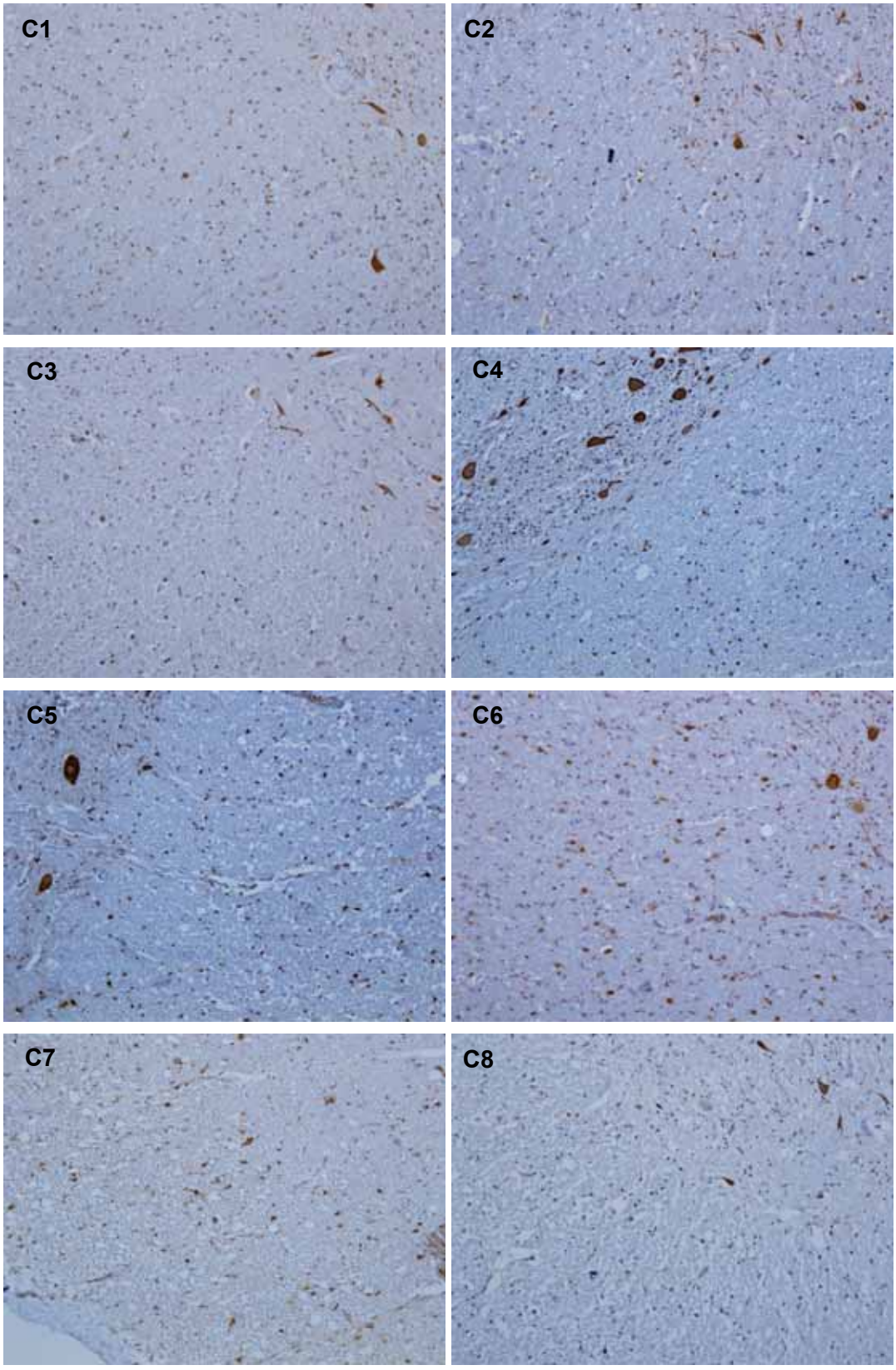
C1
C2
C3
C4
C5
C6
C7
C8

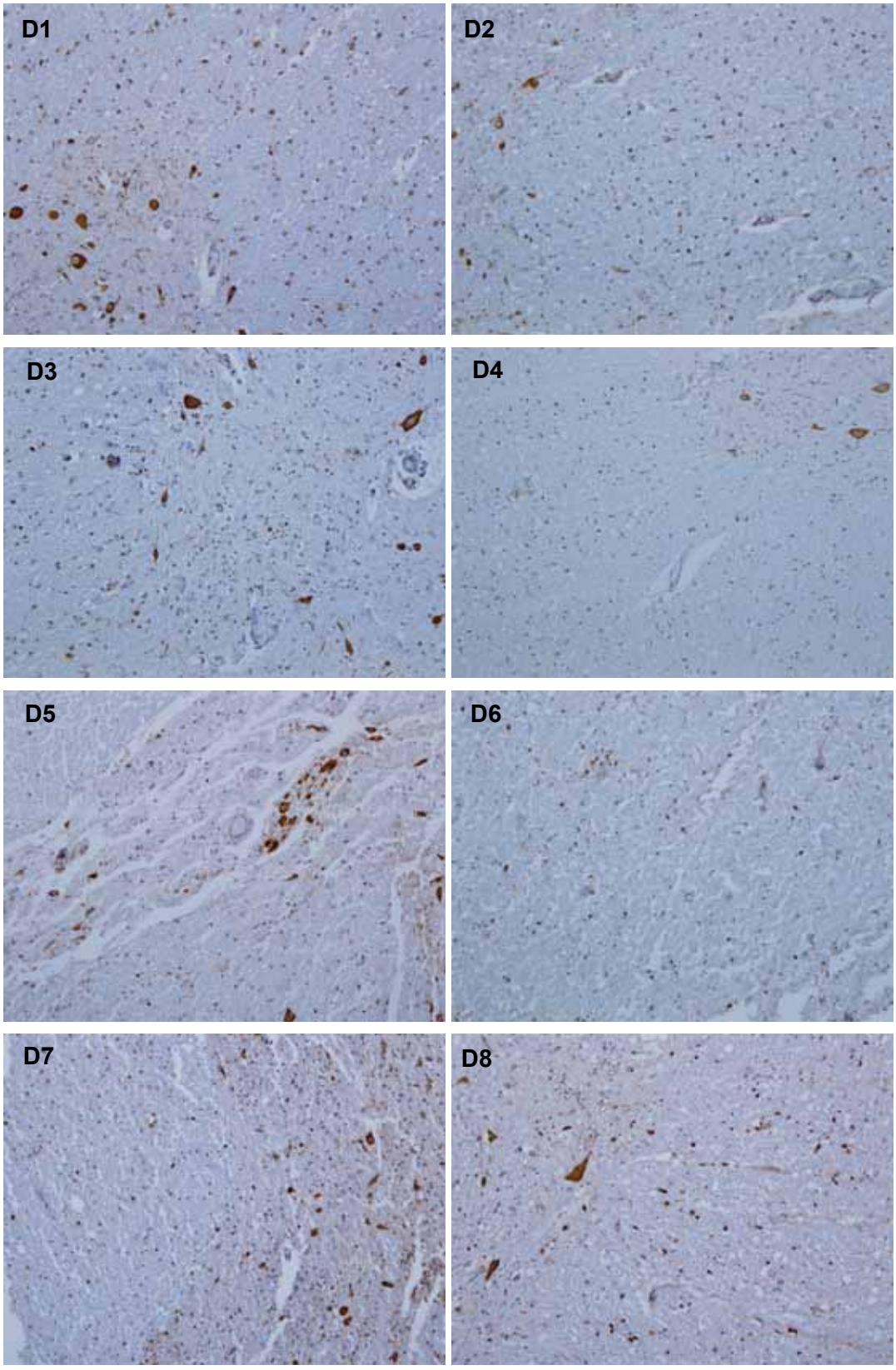
D1
D2
D3
D4
D5
D6
D7
D8

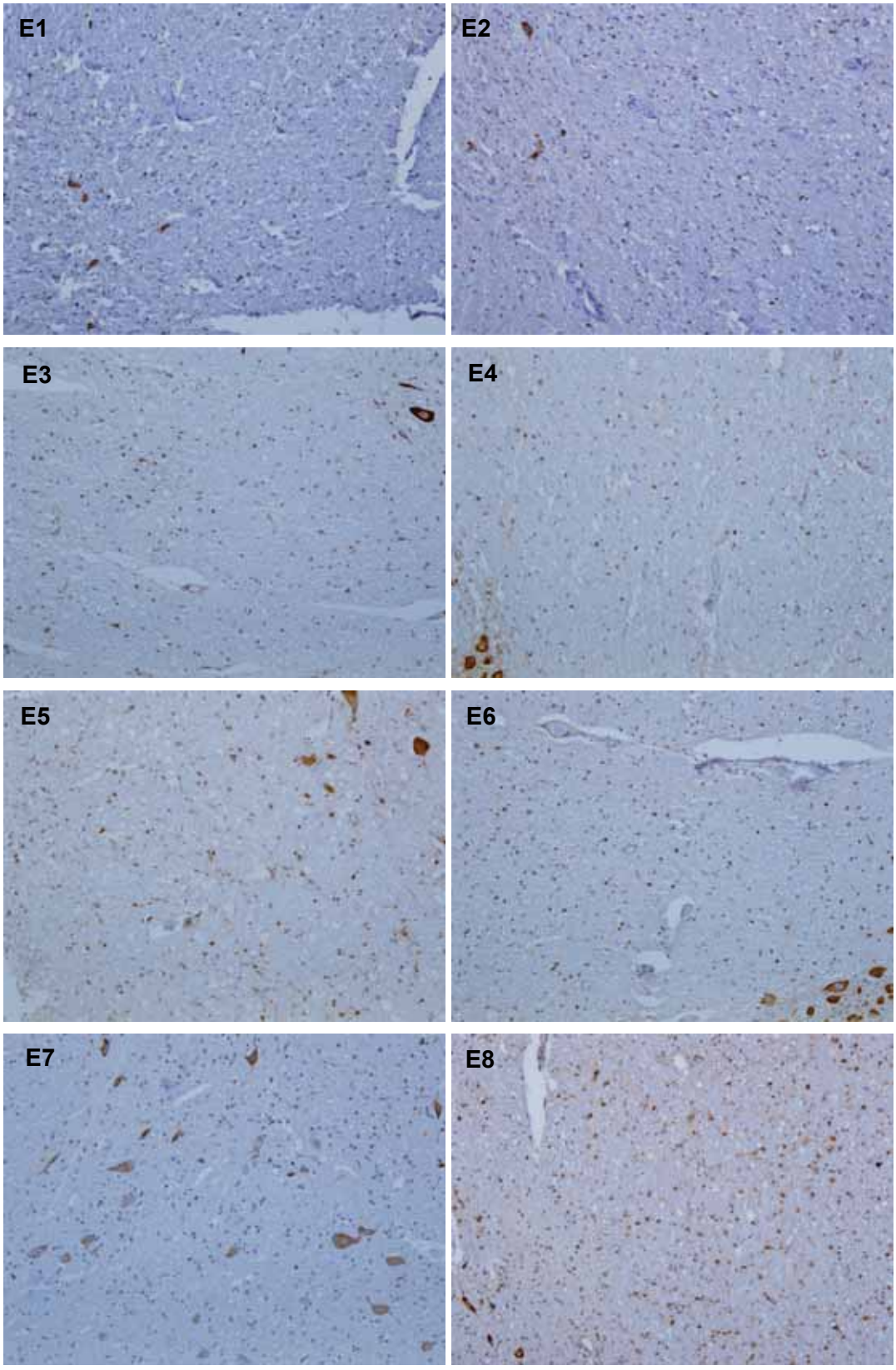
E1
E2
E3
E4
E5
E6
E7
E8

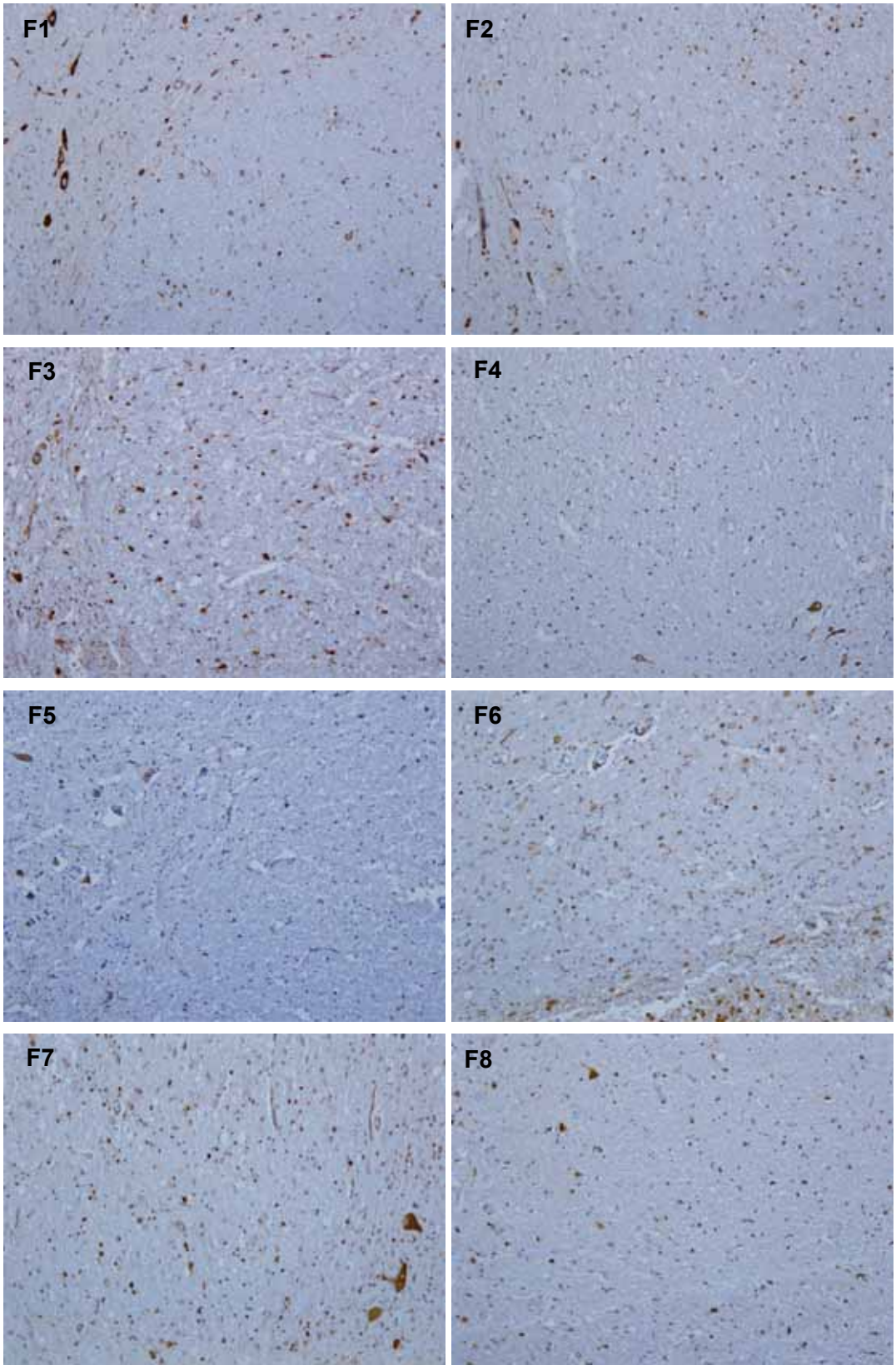
F1
F2
F3
F4
F5
F6
F7
F8

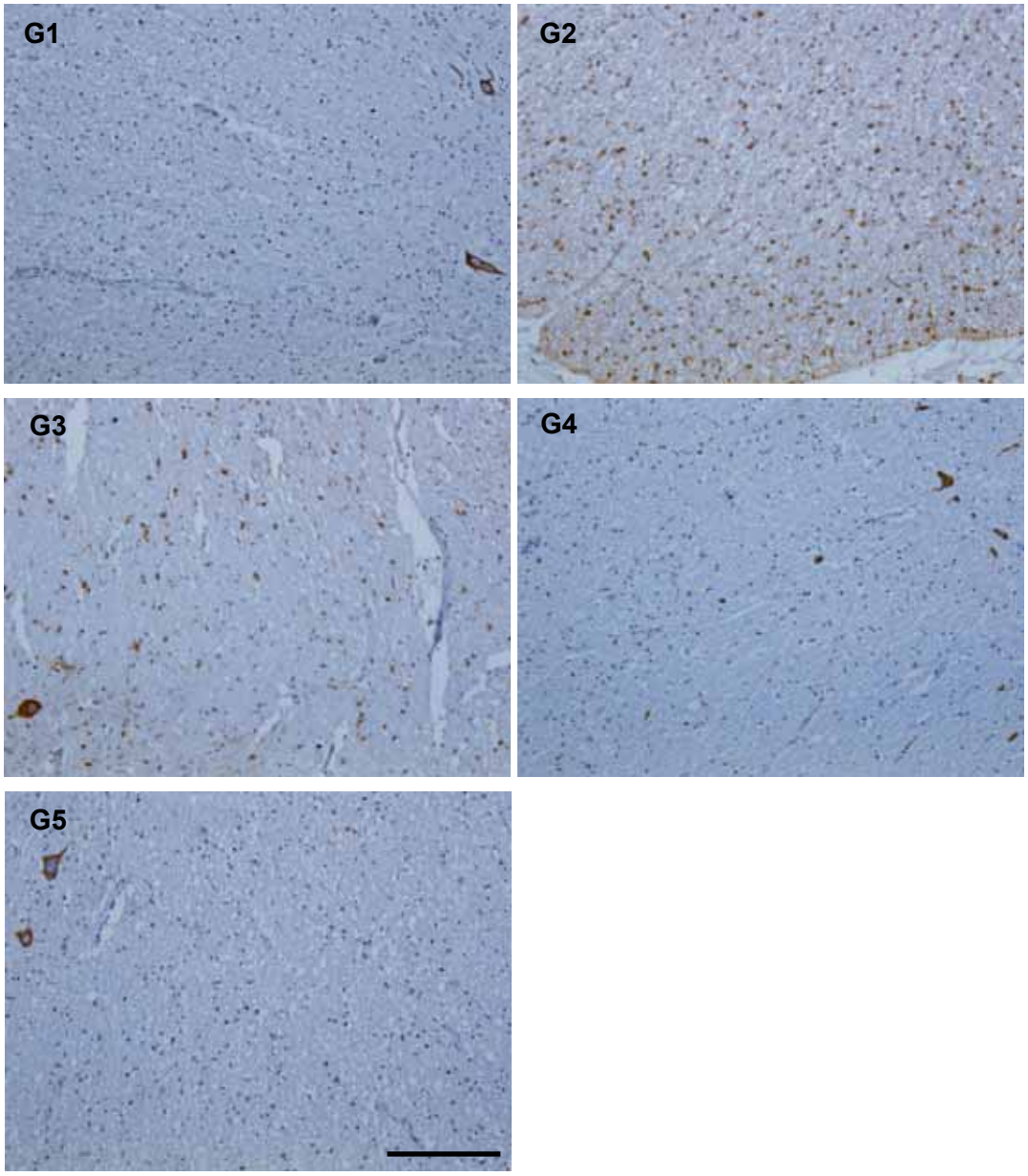
G1
G2
G3
G4
G5

Appendix 2. eEF1D in spinal cord from MND cases. Scale bar, 200µm.

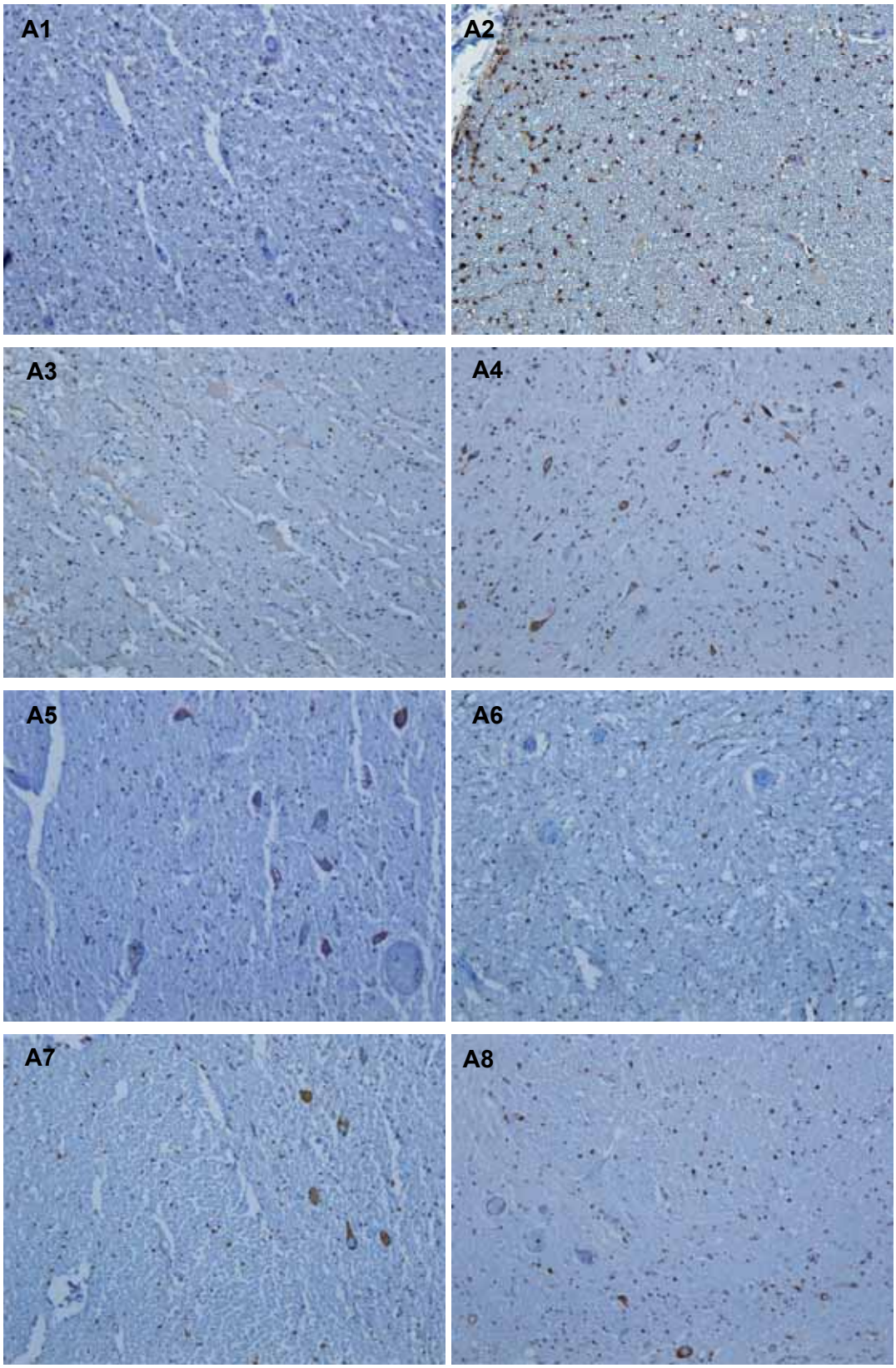

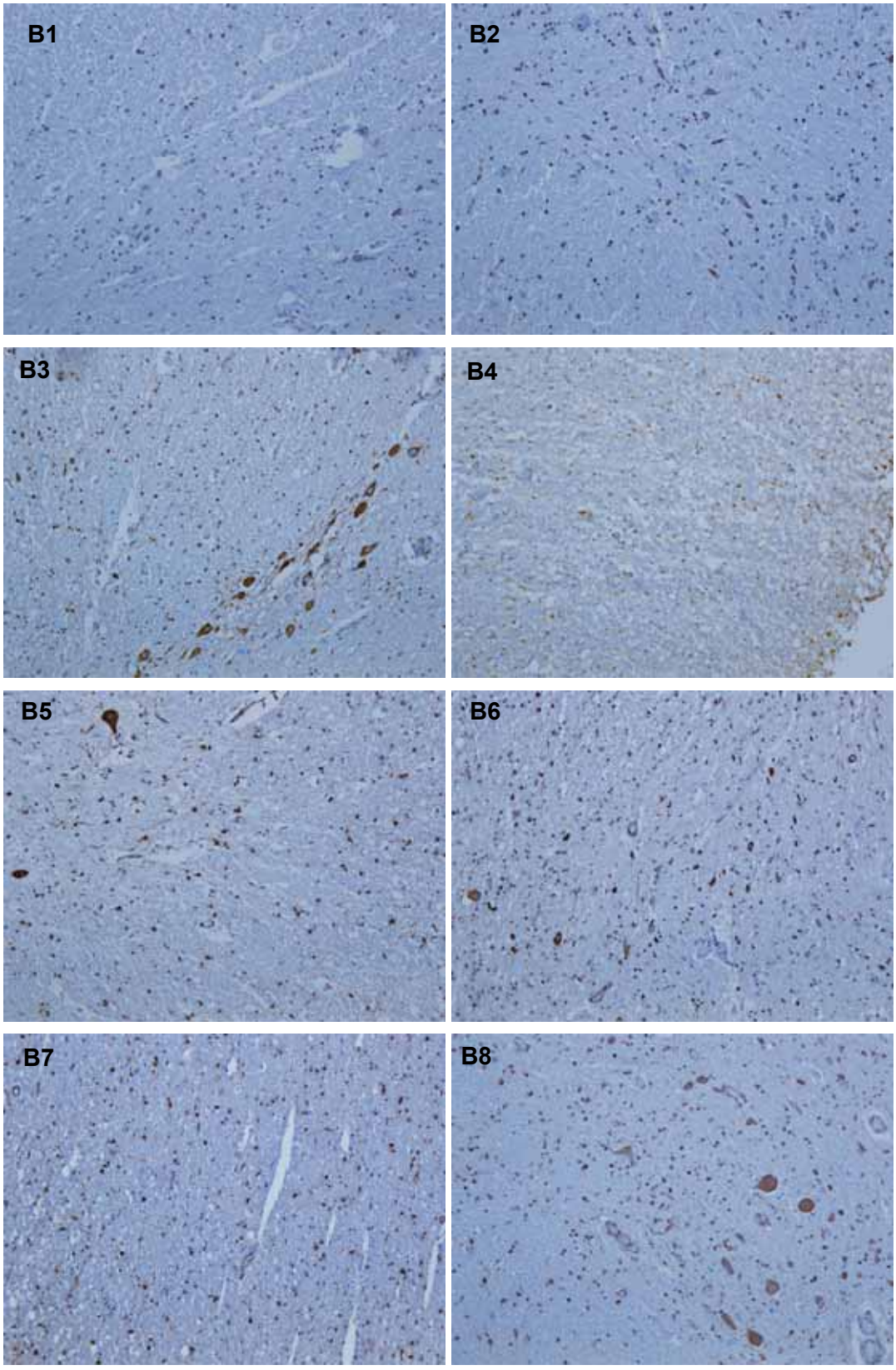
B1
B2
B3
B4
B5
B6
B7
B8

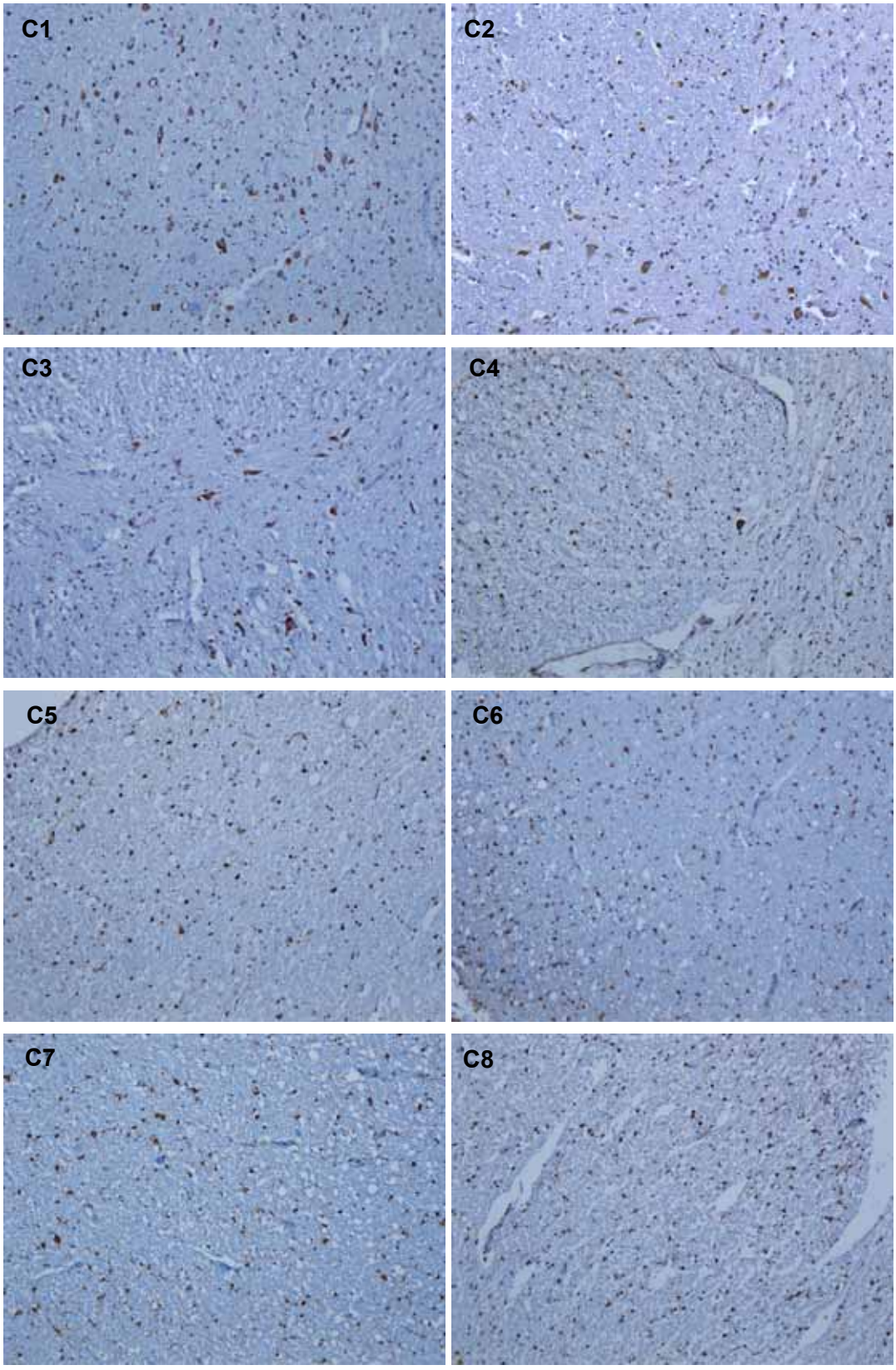
C1
C2
C3
C4
C5
C6
C7
C8

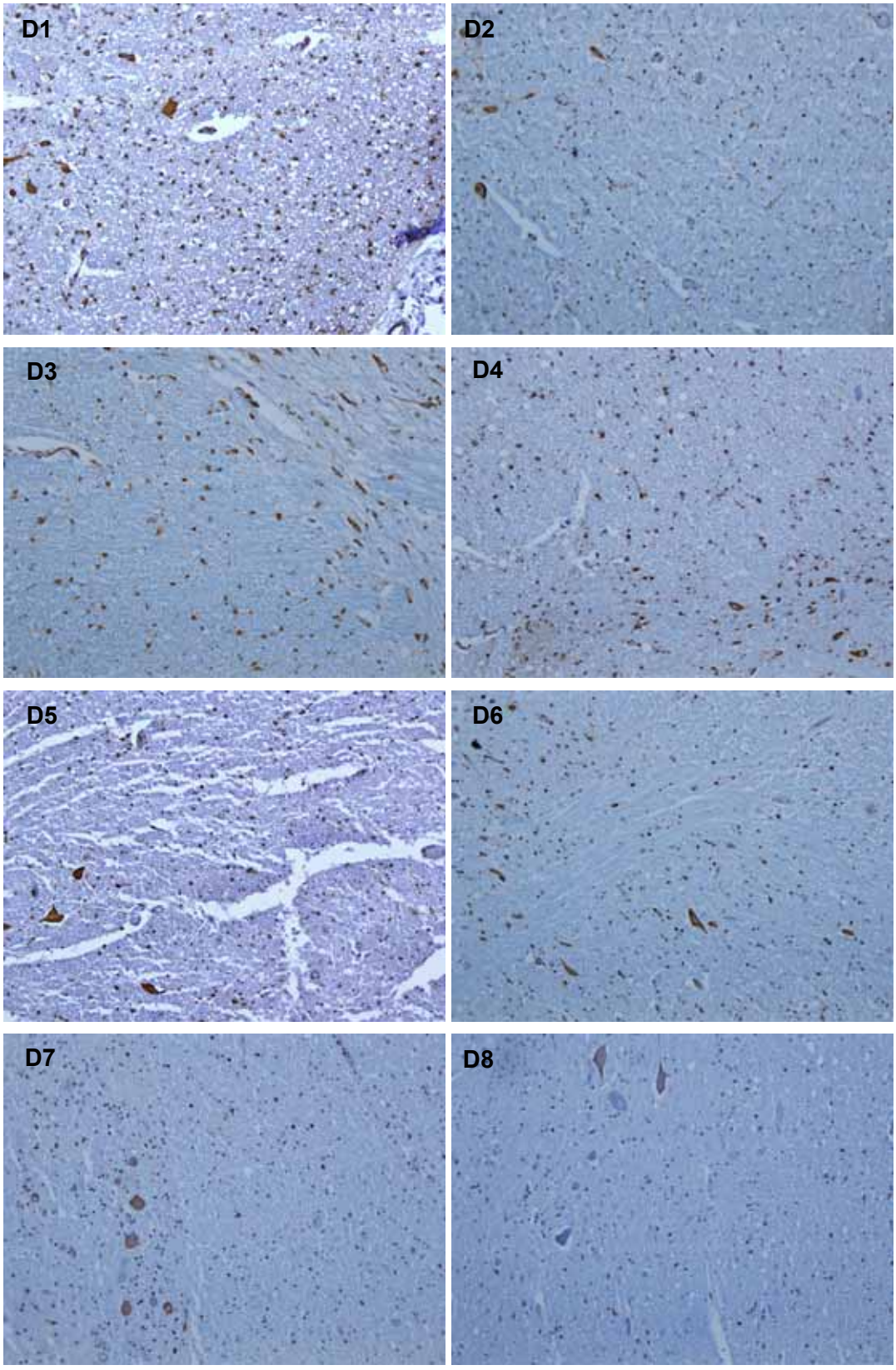
D1
D2
D3
D4
D5
D6
D7
D8

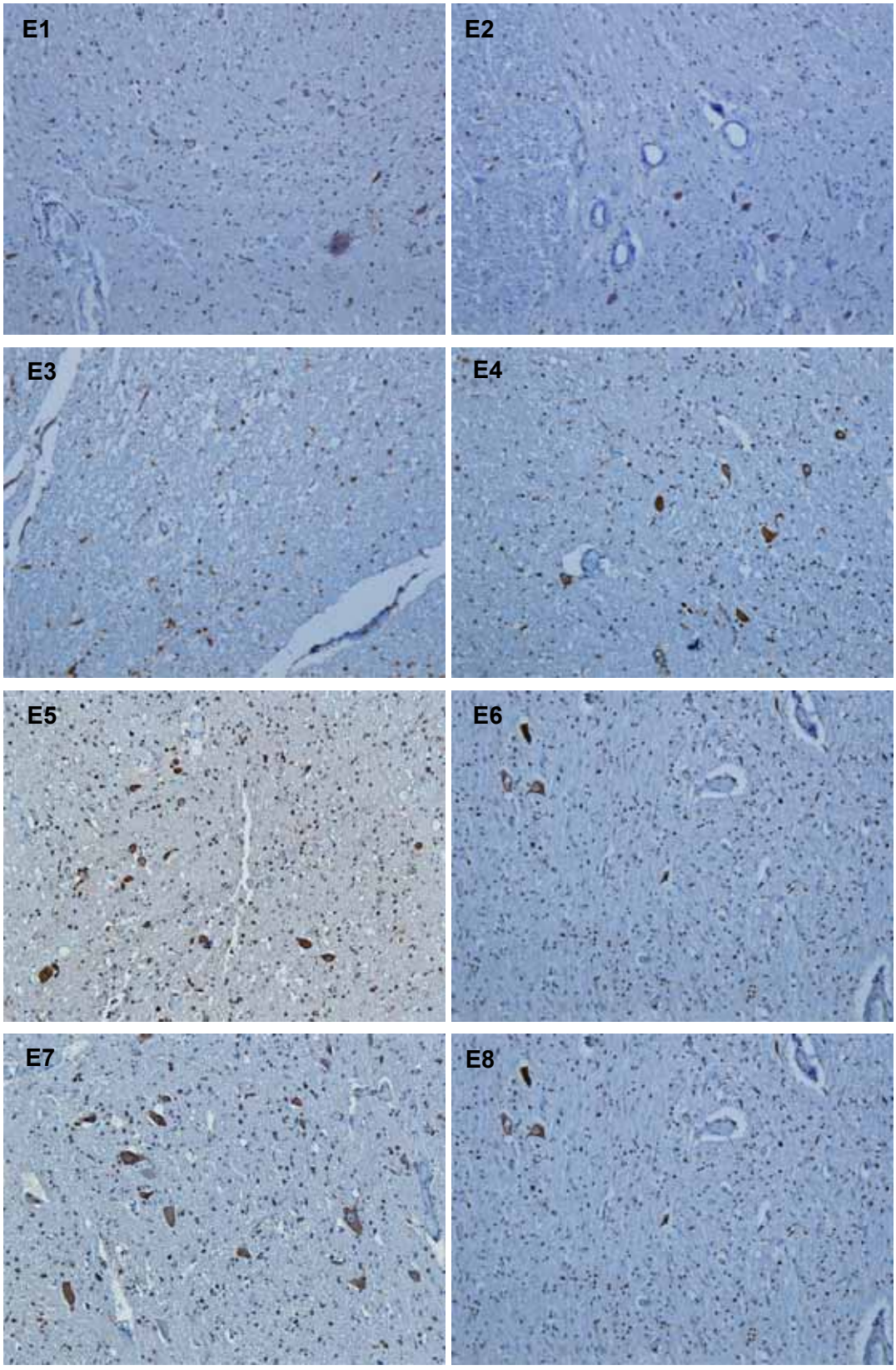
E1
E2
E3
E4
E5
E6
E7
E8

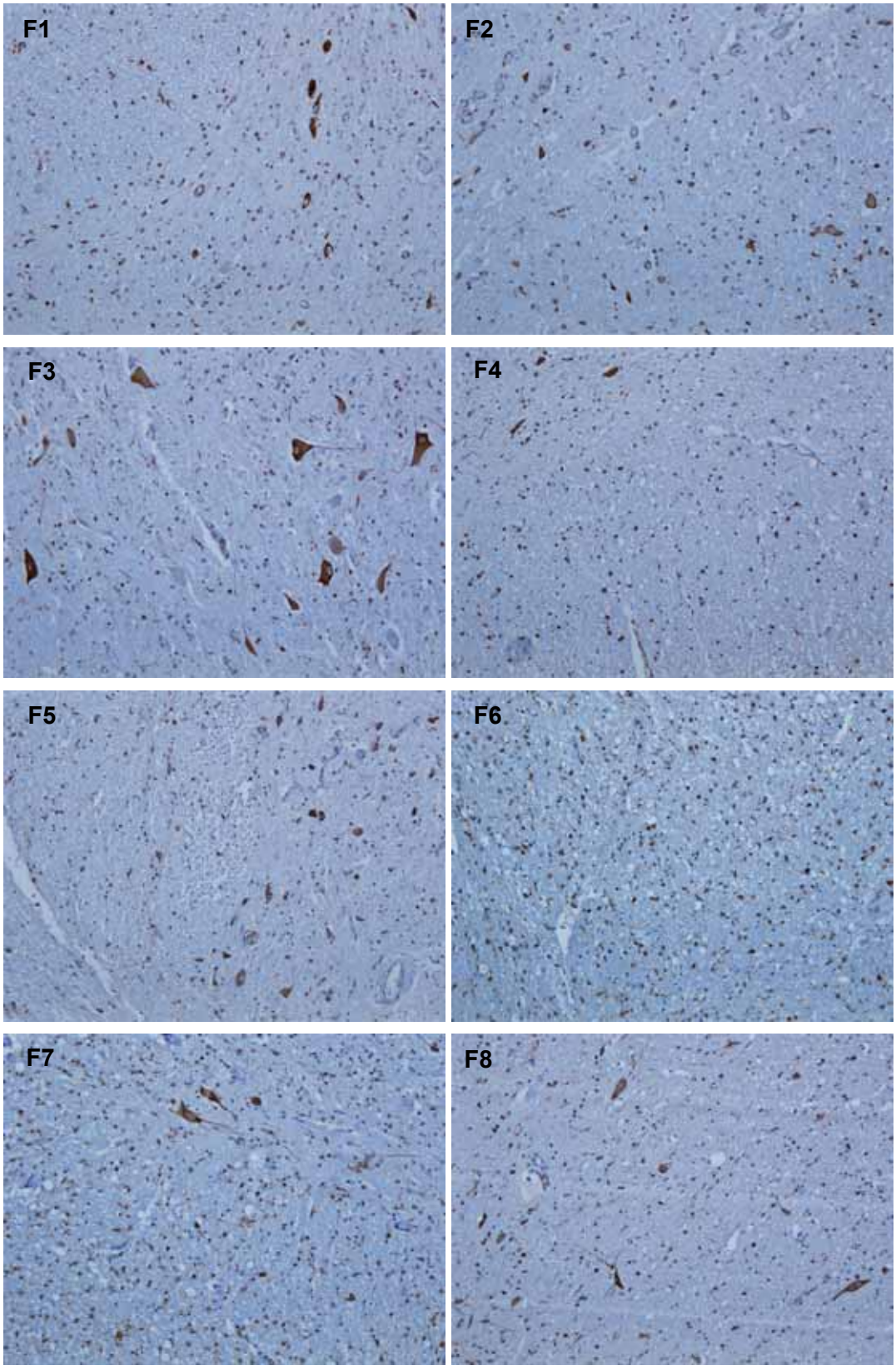
F1
F2
F3
F4
F5
F6
F7
F8

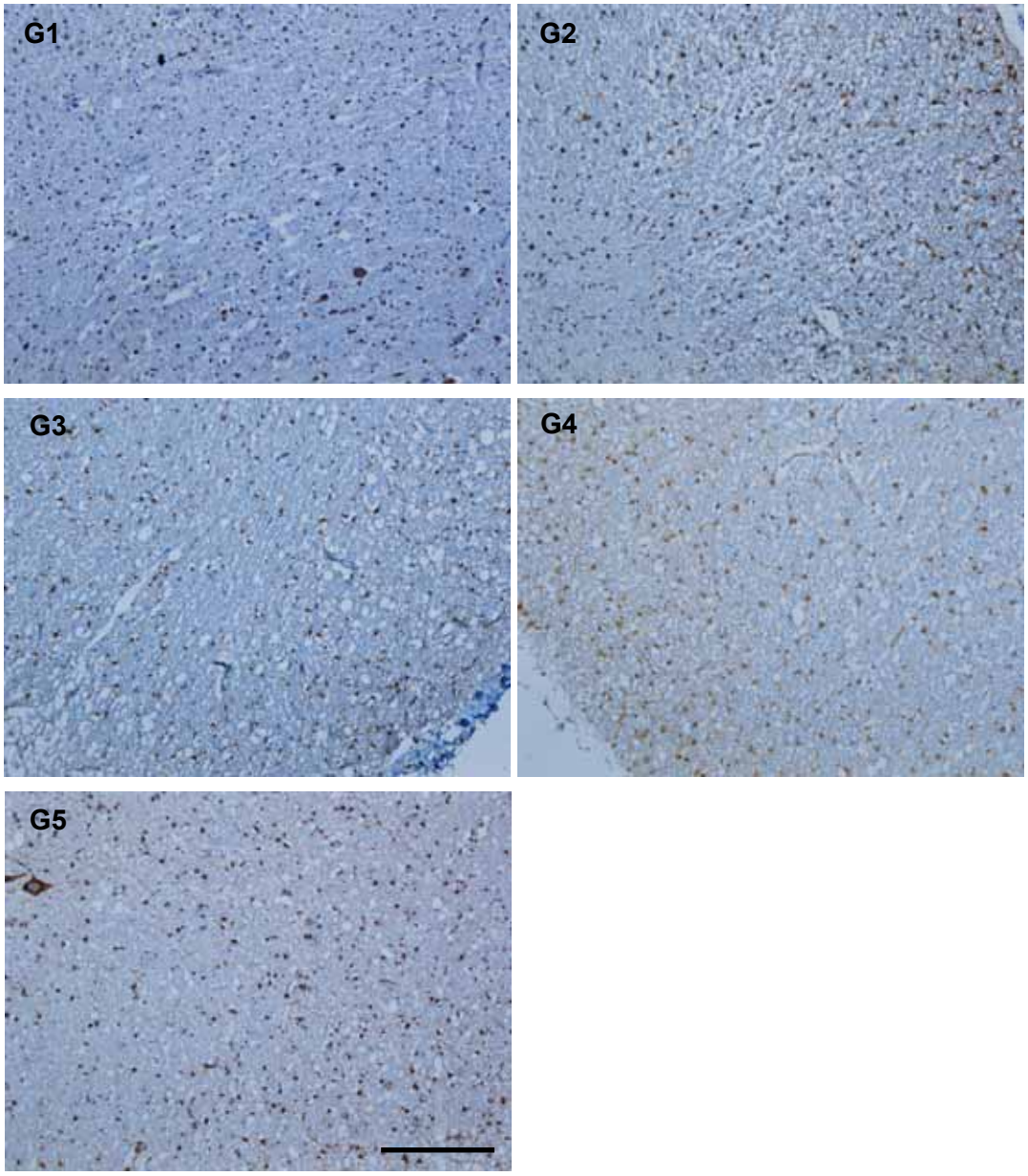
G1
G2
G3
G4
G5

Appendix 3. Comparision of eEF1A2 (Left panel) and eEF1D (Right panel) expression in spinal cord from control (B and M) and MND cases (A5, E1, F2 and G1). Scale bar, 200µm.

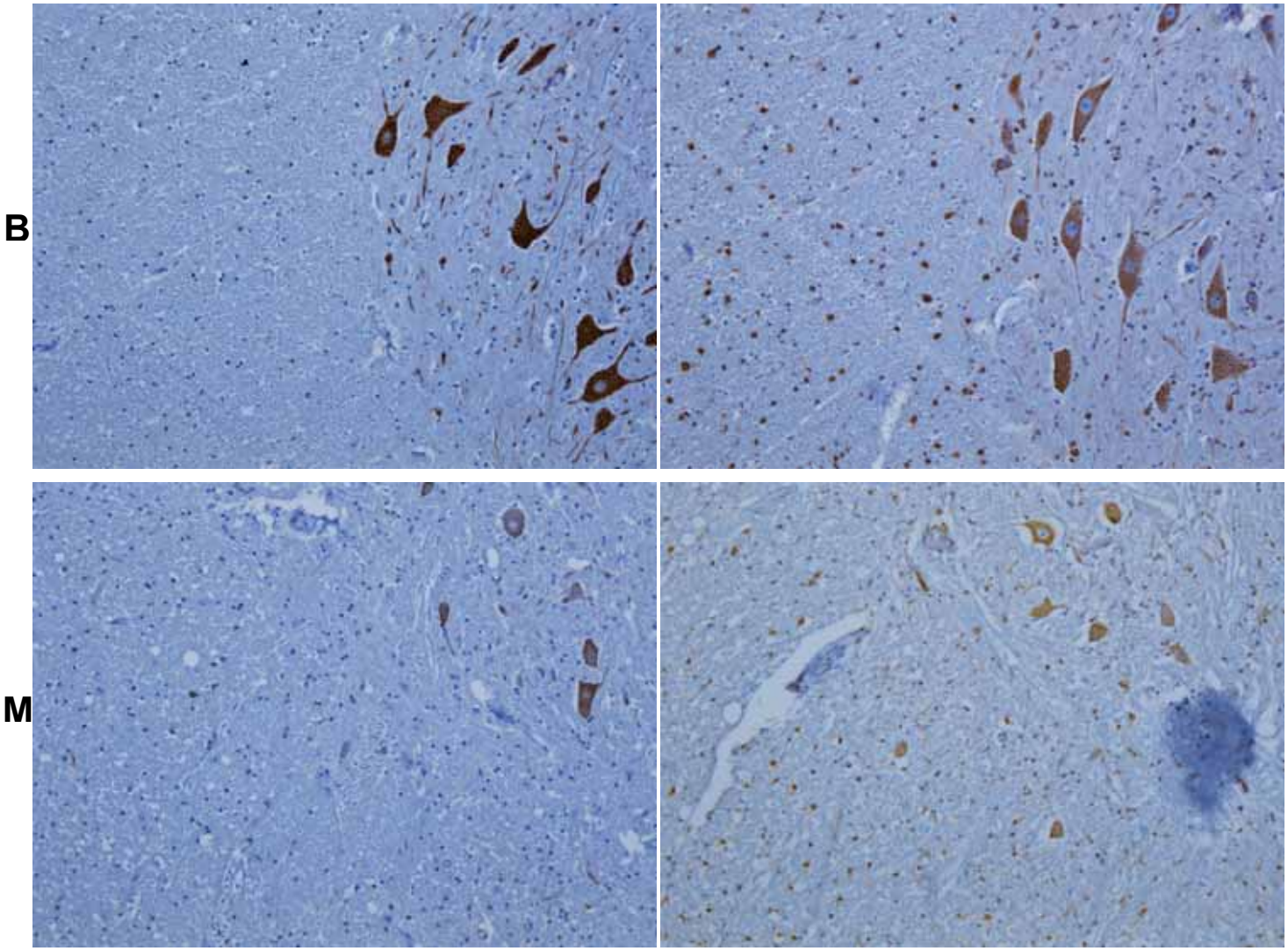

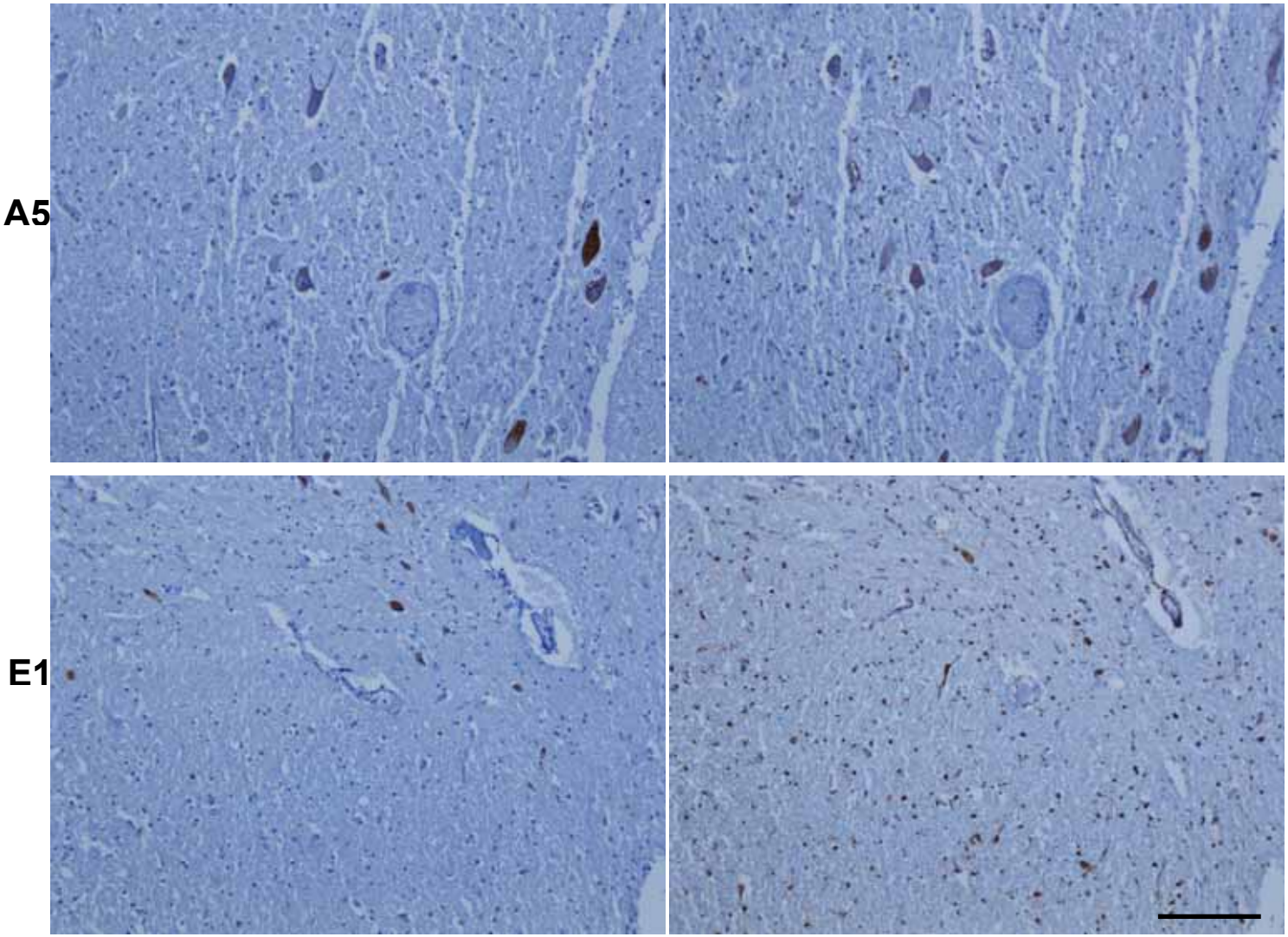
A5
E1

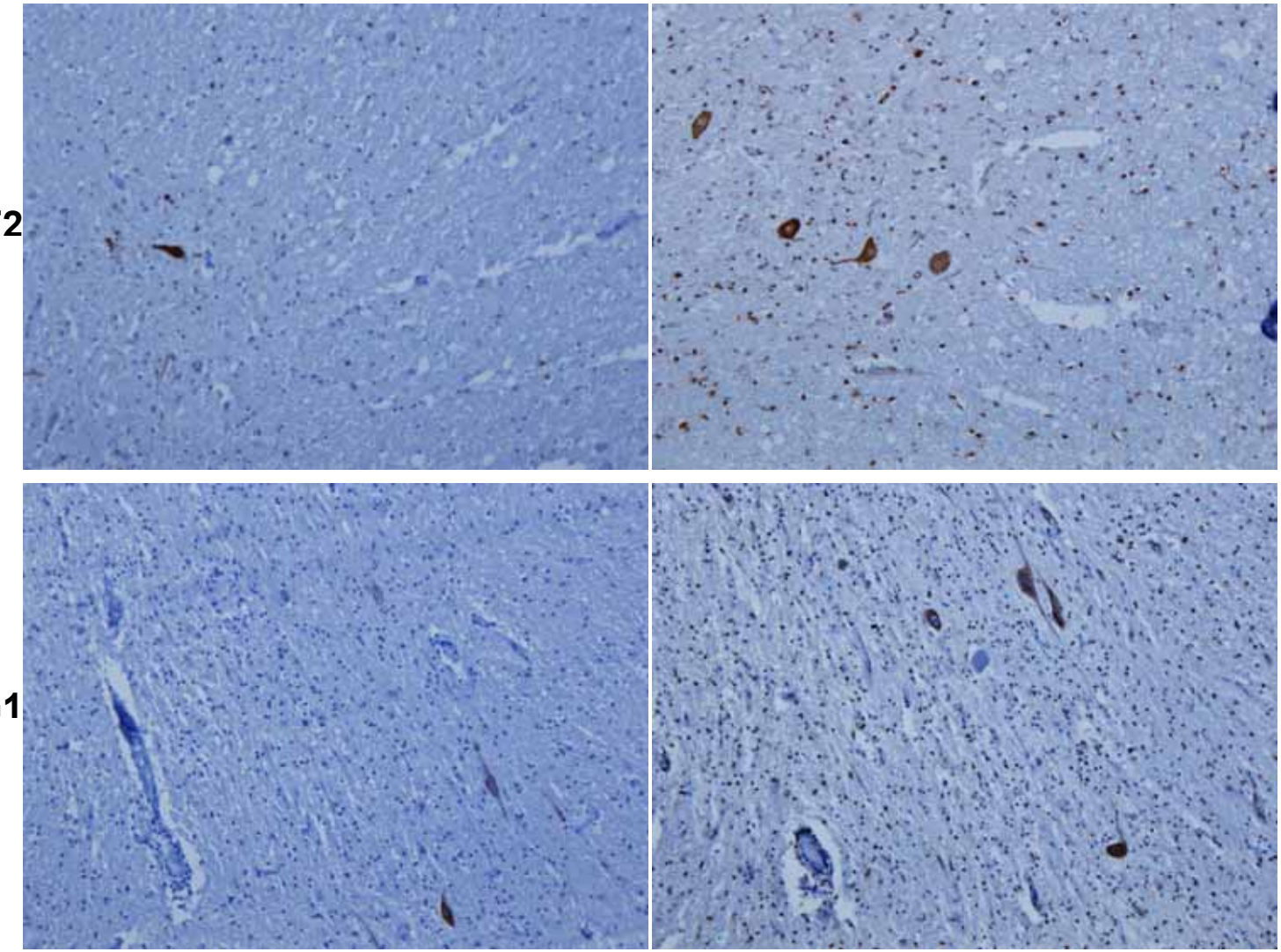
F2
G1